Technische Universität Braunschweig

iBMB MPA TU BRAUNSCHWEIG

A risk-informed and performance-based life safety concept in case of fire

Cornelius Albrecht

Institut für Baustoffe, Massivbau und Brandschutz (iBMB)
Materialprüfanstalt für das Bauwesen (MPA) Braunschweig

Heft 217 **Braunschweig** **2012**

ISBN 978-3-89288-202-2

ISSN 1439-3875

Von der Fakultät Architektur, Bauingenieurwesen und Umweltwissenschaften der Technische Universität Carolo-Wilhelmina zu Brauschweig zur Erlangung des Grades eines Doktoringenieurs (Dr.-Ing.) genehmigte Dissertation

Eingereicht am 9. Dezember 2011

Disputation am 4. Mai 2012

Berichterstatter: Prof. Dr.-Ing. D. Hosser
Prof. Dr. M. Fontana

Abstract

A risk-informed and performance-based life safety concept in case of fire

Protection of the health and life of the occupants in case of a hostile fire is the main safety objective of Fire Protection Engineering. This is usually achieved by providing for the possibility of a safe evacuation from the building before the various effects of the fire inflict casualties on the occupants. The requirement of successful evacuation of buildings is manifested in nearly all of today's building fire codes in countries all over the world and is traditionally achieved by complying with so-called "deemed-to-satisfy" codes and regulations, implying that a building is safe if the so-called prescriptive requirements for the design of the escape routes from the codes are followed. Yet architecture has become increasingly complex during the last decades. On many occasions, these advancements have outrun the prescriptive requirements since atria or multi-functional assembly buildings cannot be realized in accordance with the codes. In such cases, shortcomings to the requirements are compensated for with so-called performance-based engineering methods as part of a holistic fire safety concept on an individual basis in order to maintain the required safety level. Yet the latter is usually unknown and various numerical simulations are carried out using (usually conservatively chosen) deterministic values as input parameters even though they are subjected to major uncertainties.

Within this thesis a probabilistic methodology is developed in order to quantify the safety levels implied by the prescriptive codes. The definition of risk and its relation to reliability and probabilistic design procedures is discussed and structured under various aspects. To achieve the most accurate solutions, various aspects of the current procedural methods of life safety analysis are analyzed, discussed, and improved. Based on the findings, stochastic models are found for the various uncertain parameters. After an introduction to reliability theory, an adaptive response surface method based on interpolating moving least squares (IMLS) is developed, validated and benchmarked. This allows for

a fast and efficient calculation of failure probabilities of life safety design solution using state-of-the-art numerical fire protection engineering tools. The method is applied to a typical building and the current reliability levels are (quantitatively) derived considering various possible scenarios. A subsequent inclusion of various fire protection barriers (i.e. sprinklers etc.) shows their quantitative effect and how they can be considered within a probabilistic safety format. Thus a way for a risk-informed and performance-based life safety design is paved.

Zusammenfassung

Ein risikogerechtes und leistungsorientiertes Personensicherheitskonzept im Brandfall

Der Schutz von Gesundheit und Leben der Gebäudenutzer im Falle eines Schadenfeuers ist die Kernaufgabe des Brandschutzingenieurwesens. Diese wird meistens dadurch gelöst, dass eine sichere Entfluchtung möglich sein muss, bevor die verschiedenen schädlichen Auswirkungen des Feuers Verletzungen verursachen oder sogar Todesopfer fordern. Die Anforderung an die sichere Entfluchtung von Gebäuden ist weltweit im Baurecht verankert und wird meist nachgewiesen, indem bestimmte, so genannte präskriptive Anforderungen an die Gestaltung und Dimensionierung der Rettungswege erfüllt werden. Das Gebäude gilt dann als „sicher per Definition“. Allerdings hat sich die Architektur in den letzten Jahrzehnten verändert und ist teilweise sehr filigran und weiträumig geworden, sodass in vielen Fällen die Fortschritte hier die präskriptiven Anforderungen überholt haben. Vor allem offene Bauweisen wie Atrien und multifunktionale Versammlungsstätten lassen sich nicht mehr mit den traditionellen Anforderungen in Einklang bringen. Wo Abweichungen von baurechtlichen Anforderungen unvermeidbar sind, wird dann auf individueller Basis mit leistungsorientierten Nachweisen im Rahmen eines Brandschutzkonzeptes gearbeitet, um das gewohnte Sicherheitsniveau mindestens zu erhalten oder zu übertreffen. Allerdings ist genau dieses in der Regel unbekannt, sodass eine Vielzahl von numerischen Simulationen mit (meist konservativ) gewählten, deterministischen Eingangswerten ausgeführt wird, obwohl hier bekanntlich große Unsicherheiten bestehen.

In dieser Arbeit wird ein probabilistischer Ansatz entwickelt, der es erlaubt, das implizite Sicherheitsniveau gemäß den baurechtlichen Anforderungen zu quantifizieren. Eine Definition des Risikos und dessen Verhältnis zur Zuverlässigkeit und zu probabilistischen Nachweisverfahren werden diskutiert und unter verschiedenen Aspekten strukturiert dar-gestellt. Um möglichst genaue Ergebnisse zu erzielen, werden außerdem die Verfahrensweisen beim Nachweis der Personensicherheit nach dem derzeitigen Stand der

Technik analysiert, diskutiert und nach Möglichkeit verbessert oder erweitert. Darauf aufbauend werden stochastische Modelle für die wichtigsten Eingangsparameter abgeleitet. Desweiteren wird nach einer kurzen Einführung in die Zuverlässigkeitstheorie ein adaptives Antwort-flächenverfahren auf Basis einer Methode der kleinsten, interpolierenden und gleitenden Fehlerquadrate (IMLS) entwickelt, verifiziert und getestet. Damit ist es möglich, schnell und effizient die Versagenswahrscheinlichkeiten von Personensicherheitsnachweisen zu berechnen, welche mit numerischen Methoden nach dem neuesten Stand der Forschung im Brandschutzingenieurwesen durchgeführt werden. Das Verfahren wird auf ein typisches Beispielgebäude angewendet, dessen momentanes Sicherheitsniveau anhand diverser möglicher Szenarien (quantitativ) ermittelt wird. Anschließend wird gezeigt, wie anlagentechnische Brandschutzmaßnahmen (z. B. Sprinkleranlagen) in die Zuverlässigkeitsanalysen einbezogen werden können, welchen quantitativen Einfluss sie auf die Zuverlässigkeit haben und wie sie in einem Sicherheitsformat berücksichtigt werden können. Somit wird der Weg zu einer risikogerechten und leistungsorientierten Auslegung der Personensicherheit geebnet.

Vorwort

Diese Arbeit entstand während meiner Tätigkeit als wissenschaftlicher Mitarbeiter am Institut für Baustoffe, Massivbau und Brandschutz (iBMB) an der Technischen Universität Braunschweig.

Mein besonderer Dank gilt meinem Doktorvater, Herrn Prof. Dr.-Ing. *Dietmar Hosser*, der mir nicht nur die Möglichkeit zur Promotion gegeben hat, sondern mich auch für das spannende Thema Probabilistik begeistert hat. Sein großes Vertrauen, seine guten Ratschläge und die Möglichkeit zum freien wissenschaftlichen Arbeiten haben letztlich diese Arbeit überhaupt erst möglich gemacht.

Bei Herrn Prof. Dr. *Mario Fontana* möchte ich mich ganz herzlich für die Übernahme des Korreferats und die damit verbundenen Mühen (inklusive der weiten Anreise für die Disputation) bedanken.

Ebenso bedanken möchte ich mich bei Herrn PD Dr.-Ing. habil. *Volker Berkhahn* für die Mitwirkung als Prüfer und bei Herrn Prof. Dr.-Ing. *Harald Budelmann* für die Übernahme des Prüfungsvorsitzes.

Für die kritische Durchsicht und die fachlichen Anmerkungen möchte ich mich bei Herrn Dr.-Ing. *Christoph Klinzmann* und bei Herrn Dipl.-Ing. *Matthias Siemon* bedanken.

Meiner Freundin *Wendy Costa* danke ich nicht nur für ihre sprachlichen Korrekturen, sondern vor allem für ihre fortwährende Unterstützung aus der ich meine Motivation schöpfen konnte.

Meinen Kollegen am Fachgebiet Brandschutz danke ich für die interessanten und kurzweiligen Diskussionen, die mitunter weit über das Thema Brandschutz hinausgingen. Die Zusammenarbeit hat mir viel Freude gemacht und ich werde gerne daran zurückdenken.

Meiner Familie und *meinen Freunden* danke ich für den Rückhalt und die Unterstützung, die sie mir entgegen gebracht haben.

VIELEN DANK.

Braunschweig, im Mai 2012 Cornelius Albrecht

Contents

Nomenclature

Greek letters

α	Sensitivity Factor
β	Reliability Index
Δm	Mass difference
Δt	Time-step length
δx	Grid size
γ	Semi-Probabilistic Safety Factor
κ	Empirical Safety Factor
Λ	Matrix of Eigenvalues
λ	Multiplier or Eigenvalue
μ	Mean
Ω	Domain
Φ	Global Equivalence Ratio
ρ	Density or Correlation Coefficient
σ	Standard Deviation
σ^2	Variance
ε	Error Component
ε_{reg}	Regularization parameter

Latin letters

c_p	Specific Heat
D^*	Characteristic Fire Diameter
E	Energy
$F_{I,a}$	Incapacitation dose of a
g	Gravity
m	Mass or Arbitrary Natural Number
n	Arbitrary Natural Number
p_f	Probability of Failure
p_s	Probability of Success ($p_s = 1 - p_f$)

T ..... Temperature
t, t_i ..... Time (at time-step i)
t_g ..... Time to reach 1 MW
$t_{I,a}$ ..... Time to incapacitation due to a

Acronyms

AFFE ..... Advanced Fast-Forward Evaluation
AHJ ..... Authorities Having Jurisdiction
AIS ..... Adaptive Importance Sampling
ALARP ..... As Low As Reasonably Practicable
ASET ..... Available Safe Egress Time
BS ..... British Standard
CDF ..... Cumulative Distribution Function
CFAST ..... Consolidated Model of Fire Growth and Smoke Transport
CFD ..... Computational Fluid Dynamics
CPU ..... Central Processing Unit
DALY ..... Disability-Adjusted Life Years
DIN ..... Deutsches Institut für Normung (German Institute for Standardization)
DNS ..... Direct Numerical Simulation
DoE ..... Design of Experiments
FDM ..... Finite Differences Method
FDS ..... Fire Dynamics Simulator (CFD Fire Simulation)
FEC ..... Fractional Effective Concentration
FED ..... Fractional Effective Dose
FID ..... Fractional Incapacitation Dose
FLD ..... Fractional Lethal Dose
FORM/SORM ..... First/Second Order Reliability Method
FPE ..... Fire Protection Engineering
GDP ..... Gross Domestic Product
HPC ..... High Performance Computing
HRR ..... Heat Release Rate
HTC ..... High Throughput Computing
HVAC ..... Heat, Ventilation, and Air Conditioning
ICC ..... International Code Council
IMLS ..... Interpolating Moving Least Squares
ISO ..... International Standardization Organization
ISPUD ..... Importance Sampling Using Design Point
LES ..... Large Eddy Simulation
LHS ..... Latin Hypercube Sampling

LQI ..... Life Quality Index
MBO ..... Musterbauordnung (Exemplary Building Code)
MC ..... Monte Carlo Simulation
MLS ..... Moving Least Squares
MVStättV ..... Musterversammlungsstättenverordnung (Exemplary Assembly Building Code)
NFPA ..... National Fire Protection Association
OD ..... Optical Density
PC ..... Principal Component
PDF ..... Probability Density Function
ppm ..... Parts Per Million
QALY ..... Quality-Adjusted Life Years
RANS ..... Reynolds-Averaged Navier-Stokes
RMV ..... Respiratory Mean Volume
RSET ..... Required Safe Egress Time
RSM ..... Response Surface Method
RTI ..... Response Time Index (Sprinkler)
SFPE ..... Society of Fire Protection Engineers
SHE ..... Smoke and Heat Exhaustion System
US(A) ..... United States of America
vfdb ..... Verein zur Förderung des Deutschen Brandschutzes (German Fire Protection Association)

Mathematical terms, exponents, and indices

$\bar{x}$ ..... (Empirical) Mean of x
χ^2 ..... χ^2-distribution
$\dot{Q}$ ..... Deviation in time of the fire load (Heat Release Rate)
$\hat{F}_n(x)$ ..... Empirical Cumulative Distribution Function of x, based on n samples
∞ ..... Infinity
$\int u\,du$ ..... Temporary variable used in integrals
$\mathbb{N}$ ..... Natural Numbers
$\mathbb{R}$ ..... Real Numbers
∇ ..... Nabla-Operator (Vector of partial derivatives $\frac{\partial}{\partial x_i}$)
$\Phi(z)$ ..... Gaussian standard normal distribution function
$\phi(z)$ ..... Gaussian probability density function
$\zeta_{\mathbf{X}}$ ..... Likelihood Ratio
$E(x)$ ..... Expected Value of the distribution f_X
$F(x)$ ..... Primitive function of x
$f(x)$ ..... Function of x

i, j, k	Control Variables
$P(x)$	Probability of the event x
R^2_{adj}	Adjusted Coefficient of Determination
s^2	(Empirical) Variance
CoV	Covariance
df	Degrees of freedom
SS	Empirical variance of a sample dataset
x	Variable x
$\mathbf{x}$	Vector of n elements
$\mathbf{X}$	Matrix of $[n \times m]$ elements
$\mathbf{X}^T$	Transpose of the matrix $\mathbf{X}$
$\mathbf{X}^{-1}$	Inverse of the matrix $\mathbf{X}$

Chapter 1

Introduction

Protection of the health and life of the occupants in case of a hostile fire is the main safety objective of Fire Protection Engineering and is manifested in nearly all current fire codes in countries all over the world. This objective is usually achieved by providing the possibility of safe egress from a building before the various effects of the fire inflict serious injuries or casualties among the occupants.

Traditionally, life safety is implicitly achieved by complying with "prescriptive" building codes and standards which contain basic design as well as material and constructional requirements. These requirements include, but are not limited to, restriction of the maximum lengths of escape routes, material requirements for hallways and stairwells, and minimum widths of escape ways and exit doors. This is usually referred to as "deemed-to-satisfy" design as the compliance with the codes and standards make the building safe by definition. For buildings with a particular occupancy, such as theaters, high-rise or assembly buildings, etc. specific supplementary codes, standards and guidelines exist which include further requirements for fire system installations or organizational measures in order to address the specific risk emanating from the particular occupancy. These can be requirements and specifications for the installation of automatic fire detection systems, sprinkler systems or smoke and heat exhaustion systems (so-called fire protection barriers) as well as the request for fire safety regulations and escape plans (organizational fire protection). Examples are the assembly building code in Germany (MVStättV, 2005) or the NFPA 101 (2008) for various occupancies in the United States.

Yet architecture has become increasingly complex during the last decades and advancements in structural engineering and in material sciences allow for extravagant constructions, e.g. multi-purpose buildings with large open spaces. On many occasions these constructions outrun these prescriptive fire codes, and large atria, multi-purpose assembly buildings and other complex geometries could not be realized by strictly complying with the codes. In these cases, shortcomings to the prescriptive requirements are

addressed in a holistic fire safety concept on an individual basis in order to achieve the same level of safety as implied in the codes by using so-called performance-based methods to find particular solutions to the identified risk. Another motivation to use performance-based methods is the optimization of the cost-benefit ratio of the fire protection design which can cost as much as 10 % of the total building costs (Ramachandran, 1998, p.12).

Despite the obvious benefits of performance-based methods, they can be—and have been—misused due to a lack of understanding or even intentionally as Fleischmann (2011) outlines in a recent paper. Also, many other points remain unclear such as the quantitative and objective required safety level of the current codes and the safety level achieved by the performance-based design, the scenarios, design fires, parameters and performance criteria to be used and the uncertainty within the methods and safety factors to be added. This has led to limited acceptance of the performance-based methods, especially by the authorities having jurisdiction (AHJs).

1.1. Motivation

The motivation to this thesis is to analyze, improve, and restructure recent state-of-the-art performance-based life safety design methods in order to develop a risk-informed framework which allows for the objective and quantitative assessment of life safety design. As regulatory frameworks usually consist of various different aspects as shown in Figure 1.1, the main focus herein is on the quantification of the current safety level implied by the prescriptive codes. To achieve this in a most neutral way, an in-depth analysis of the current state-of-the-art is as necessary as the derivation of a hierarchy for the various methods as highlighted in the Figure. A subsequent probabilistic quantification or calibration, respectively, gives valuable information about the uncertainties and safety level of the current prescriptive design which can be used as a target reliability in future risk-informed codes. A probabilistic consideration of the various fire protection systems can also lead to more efficient and cost-benefit-optimized designs, as the effect on the safety level of each barrier can be quantified at known costs.

Yet as a probabilistic analysis using state-of-the-art numerical fire tools is not possible using the conventional methods of reliability analysis due to the high computation times, a more efficient is needed. Such a methodology is developed, validated, benchmarked, applied, and discussed herein to allow for a *state-of-the-art risk quantification of fire life safety analysis*.

All the aforementioned aspects can not only lead to the addressed cost-benefit optimization but also to a general acceptance of performance-based life safety design methods as the competencies are clear and the design is logically and comprehensibly assessable and verifiable by a third party, i.e. the AHJs.

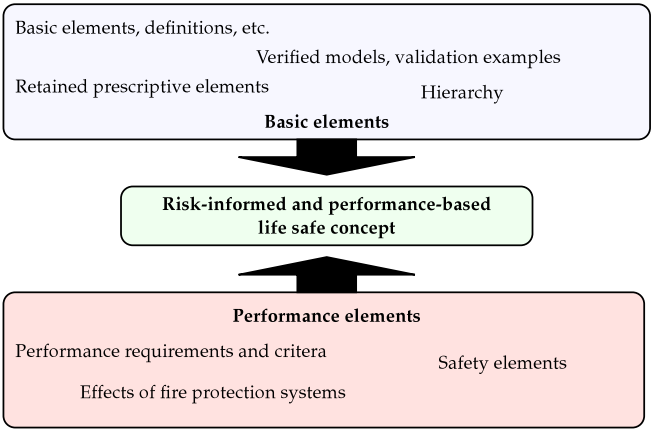

Figure 1.1.: Different aspects of a framework for a life safety code. It can be categorized into basic elements and performance elements with their respective considerations.

1.2. Outline of this thesis

After a general introduction to the definition of risk and the various aspects thereof in Chapter 2, approaches to consequence modeling and the derivation of acceptable risk criteria are outlined. A closer look is taken at some aspects of probabilities, their origin, and their use within probabilistic design. Additionally, an overview over risk-informed approaches in Fire Protection Engineering is given along with the essential conclusions for a risk-informed life safety design.

Chapter 3 provides an introduction in the current life safety design process, comparing the traditional prescriptive and the new performance-based approach along with a commonly used empirical safety concept. As the performance-based methods are manifold with varying levels of complexity, a hierarchy similar to the Eurocodes is proposed to provide a basic structure of methods and to define levels of recommended competencies for each complexity level defined. Further details of the particular methods, parameters, performance-criteria, and limitations are provided in Chapter 4. After a general introduction to numerical fire and evacuation modeling, the performance-criteria and their determination are analyzed and improvements are proposed. In the second part of the Chapter essential design fire scenarios are introduced and the corresponding design fires are shown and adjusted for the particular life safety case.

Usually probabilistic methods and reliability analyses are employed to quantify risk and safety. In Chapter 5, a general introduction to various aspects of reliability analysis is given along with the mathematical formulations and improvements of the methods to increase the efficiency and to be applicable to life safety reliability analysis. This Chapter also provides the necessary basics for the development of a new response surface method in the following Chapter. This response surface method based on interpolating moving least squares (IMLS) is derived and introduced in Chapter 6. It allows for the fast and accurate analysis of failure probabilities using advanced numerical simulation tools such as CFD fire simulation and thus for the quantification of risk using the latest and most accurate state-of-the-art tools in Fire Protection Engineering. Additional considerations are made to further improve the speed and accuracy of the algorithm by developing an importance-based design of experiment plan as well as parallelization and discretization strategies. Validation and benchmarking for accuracy and speed is performed at the end of the Chapter showing the high efficiency of the methodology developed.

The IMLS reliability method is used in Chapter 7 to quantify the risk to life for a typical multi-purpose assembly building. After the derivation of appropriate stochastic models and design scenarios for the particular building, a systematic analysis is performed to show the influence of the various parameters and scenarios on the quantified level of safety. Various further aspects of the analyses (such as correlation effects, coupled simulations etc.) are addressed in additional remarks. Also, system analysis is performed by modeling various fire protection barriers and their quantitative effect on the safety level—also considering their potential failure to "work as designed on demand". A full fire protection system analysis considering various installed barriers and their potential interaction effects with an additional system sensitivity analysis concludes the Chapter. The extensive results and insights gained in Chapter 8 are then summarized and appropriate conclusions are drawn for a risk-informed performance-based life safety code. Required elements of such a code are shown and future research possibilities are outlined.

Chapter 2

Incorporation of risk in FPE

Many recent publications employ the term *risk* without providing a clear definition. This might be due to the fact that the term *risk* is usually associated with a wide range of meanings, interpretations, and methods by an even larger field of disciplines, such as engineering, economics, politics, philosophy, etc. Hence, it is inevitable to take a closer look at the term *risk* and the corresponding ideas, methodologies, and assumptions with a special focus on the utilization in Fire Protection Engineering (FPE). In the following sections, an introduction into *(fire) risk assessment* will be provided along with various definitions, methodologies and strategies used, and critical aspects that have to be considered, such as the acceptable risk in terms of probability.

2.1. Definition of risk

The term risk has many different definitions in various disciplines. Even in FPE, many different definitions implicitly exist. Many engineering firms offer "risk analyses" which often times simply means the identification of potential weak points within the fire safety concept or the construction of potentially relevant scenarios. In this case, the term risk is not clearly defined in mathematical terms. A very comprehensive introduction into understanding risk with respect to FPE is given by Meacham (2004). An interesting and quite amusing introduction to pitfalls and previous failures of risk management can be found in Hubbard (2009, part I).

The common (purely) mathematical or technical definition of risk found in many engineering publications (e.g. Yung, 2008, p.8) is a function of a probability of an event or scenario and the consequences thereof usually assumed to be a multiplicative function so that

$$\text{Risk of an event} = \text{Probability of an event} \cdot \text{Consequence of that event} \tag{2.1}$$

where the probability and consequences are assumed to be quantifiable variables so that the equation can be solved deterministically. In terms of hostile building fires, the consequences are the effects of the fire (i.e. heat, toxic effluents) on the occupants, the assets in a building and the structural integrity. The probability is the overall probability of occurrence of the event causing the consequences. Therefore, the total risk is a simple summation of the risk emanating from various possible events which hereafter will be referred to as *scenarios*.

The mathematical definition of risk according to Equation 2.1 obviously does not allow for the consideration of the unknown and individual human response to risk exposure. Additionally, neither the two variables in Equation 2.1, probability and consequences, nor are the various scenarios easily assessable for particular cases. This will be discussed in the following.

2.1.1. Objective and subjective risk

Even though the mathematical function defined above is widely used in risk engineering, the public perception of risk is usually not accounted for as humans tend to be averse to risks and thus are not risk-neutral. Hubbard (2009, p.87) shows this in a very simple but comprehensible example. The reader is asked to take one of the following options:

- A payment of 5,000 dollars without a coin flip or
- a coin flip which pays 20,000 dollars on heads but costs 10,000 dollars on tails.

A risk-neutral person would consider both options equally, as they both have the expected value of a 5,000 dollar payment. Yet a very high percentage of people would decide for option one or, as Hubbard states, would even be willing to pay for the coin flip to avoid the potential loss of 10,000 dollars. People usually tend to avoid the possibility of a potential loss in favor of security–even if the potential benefit is disproportionately low. This behavior can also be observed in the financial sector (i.e. stocks vs. savings account).

Another bias to risk is the perception of scenarios with very large consequences which usually have high media presence while some events frequently occur with a lower magnitude of damage. Examples are The Station Fire leaving 100 people dead (Belluck and von Zielbauer, 2003) or the Düsseldorf Airport Fire with 17 casualties (von Züthpen, 1996). In the aftermath of these events extensive discussions about fire safety arose. On the other hand, many people still do not have home smoke detectors installed–even though the (neutral) risk of a fatal fire at home is dramatically higher. This might be due to the fact that domestic fires with up to one or two casualties can rarely be found in nation-wide news, therefore the *risk awareness* remains low.

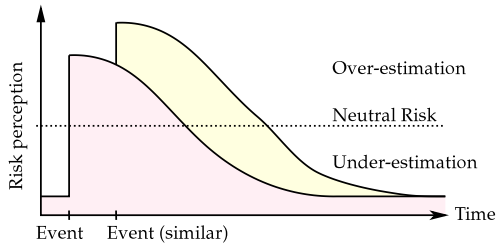

Figure 2.1.: Subjective awareness and perception of risk over time. An event usually causes the awareness to change abruptly from under- to over-estimation and then declines over time. In case of a similar event (even of lower magnitude) the awareness can be amplified further. Adopted from Proske (2004, p.174).

Not only the magnitude of an event, but also the time plays a major role in risk perception. As stated above, tragic events (i.e. fires with high number of casualties) caused discussions and even political decisions right after the event, which might even imply over-estimation or amplification of the risk (Meacham, 2004, p.218). This phenomenon can even be amplified further if a similar event happens in close temporal proximity to the initial event. Yet after a period of time after the event, the *risk awareness* declines and people tend to under-estimate the risk again. A qualitative comparison of subjective and objective (neutral) risk is shown in Figure 2.1.

2.1.2. Individual and collective risk

The risk awareness and perception described above leads to a categorization of risk into collective/societal risk or individual risk. Both have to be regarded separately as they contribute to the understanding of the subjective risk awareness/perception.

Individual risk only considers the risk of one individual person within a society. This person acts more or less independent of other people. As this approach only considers one person, the individual is the decision maker based on the individual value system. Usually, this decision only affects the individual and is subjected to human error (Starr, 1969). Hence, individual risk is normally not much of a concern within the society as i.e. accidents are attributed to those (individual) human errors. An example is the cigarette in bed leading to a fire with subsequent death of the smoker. This is commonly regarded as the individual's fault and not as a societal problem. In many codes, regulations, and guidelines this is accounted for with terms like "Protection of occupants not intimate with the initial fire development" (NFPA 101, 2008, p.45,Section 4.1.1).

Societal risk on the other hand is usually defined as a risk that potentially affects more than one person and usually happens without the influence of human error of the victims. Hence, a societal risk often describes one or multiple events that affect a large fraction of the population of a society and, therefore, has the highest priorities in the codes, regulations, and standards. Consequently, building regulations all over the world—such as NFPA 101 (2008) or MBO (2002)—contain protection goals and requirements for the protection of life safety of all other "occupants not intimate with the initial fire development" (NFPA 101, 2008, see above).

According to Proske (2004, p.45), an event (and thus the societal risk) is not only dependent on the magnitude but also on the source of the risk. He distinguishes between four categories of risk (Proske, 2004, p.34), namely

- natural risk,
- technical risk,
- risk to (physical and mental) health, and
- social risk

which all have interactions in some way. Yet it should be noted that the tolerance of events due to human error and/or the failure of technical systems with an impact on the life quality of a random individual as a part of a society is very low (Proske, 2004, Chapter 7). In terms of the example above, this means that it is not (at least to a certain degree) acceptable that the neighbor (as a random member of the society) of the smoker is harmed by the fire. Individual and societal risk are closely connected to voluntary and involuntary risk.

2.1.3. Voluntary and involuntary risk

Risk is commonly referred to as something negative, but the example by Hubbard stated above implies that risk can also incorporate a benefit—in this case an estimated payment of 5,000 dollars (also see Hubbard, 2009, p.88). According to Starr (1969), the action of people is a constant *risk-optimization* between potential cost and benefit of an event.

In terms of the example above this would be the maximal safety of the neighbor with minimal cost. Starr also distinguishes between *voluntary* and *involuntary* risk with respect to that optimization process which is obviously linked to the potential benefit. Proske (2004, p.167) finds that people always consider the potential consequences and are mainly aware if a risk is voluntary or involuntary and if the positive consequences outweigh the negative consequences. Starr (1969, p.1237) states that the voluntary risk of an individual person is roughly 1000 times greater than involuntary risks if that person has ultimate control over the actions taken.

This phenomenon explains why people are likely to demand higher safety standards in public buildings, whereas mandatory home smoke detectors are usually less likely to be accepted or enforced.

2.1.4. Risk treatment

Due to the very complex assessment of risk described above, the regulatory treatment of risk is similarly versatile. Pliefke et al. (2007) describe an attempt to remove the large ambiguities connected with risk and propose a standardized methodology for disaster risk management. Herein, risk can be treated with four different approaches:

Risk acceptance is a very simple approach where the risk imposed is simply accepted "as-is." This approach is usually a voluntary approach when the potential benefit is high enough to outweigh the negative consequences. Examples can range from something as simple as paragliding to something as complex as settlement in an earthquake region.

Risk rejection is the complementary approach of risk acceptance and is usually taken when the potential negative consequences significantly outweigh the potential benefits. A rejection of a loan is an example since the risk of money loss outweighs the benefits coming from the interest.

Risk transfer denotes the transfer of risk to a third party. The risk is accepted "as-is" with the constraint that the potential consequences are (partly) mitigated by i.e. insurances or the government. A home-owners insurance is an example of risk transfer. The transfer is compensated by the premiums for the insurance.

Risk mitigation is, unlike the transfer where the risk is usually accepted, the direct approach to reduce the magnitude of the potential consequences and/or the probability of the harmful events. The reduction of consequences and probabilities is the task of risk engineering.

It is evident that the four categories should not be seen independently of each other as the risk transfer will usually not work without some kind of mitigation measures. Additionally, it is impossible to account for all risks and magnitudes of events, so that some kind of risk acceptance is incorporated into transfer and mitigation. The engineering task is, therefore, to mitigate the risk to a level that is generally acceptable. This acceptance level is usually agreed upon by the Authorities Having Jurisdiction (AHJ). Further reading on risk mitigation and management can be found in Pliefke et al. (2007) and Sperbeck (2009, Chapter 2).

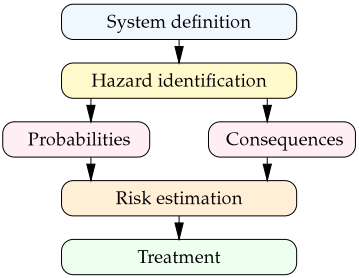

Figure 2.2.: Flowchart of risk analysis. Probabilities and consequences are the variables used to assess the quantitive risk. As consequences are usually very complex to assess, many risk-informed approaches are based on the risk on the probabilites, which are easier to assess (given that sufficient information is availbale). Adopted from Frantzich (1998, p.63).

A critical review of risk management and potential pitfalls can be found in Hubbard (2009). The general concept of risk analysis is shown in Figure 2.2. In this thesis, the focus lies on the mitigation aspect. In order to assess risk properly, a closer look has to be taken at the probability of occurrence of an event and the connected consequences of that event.

2.2. Consequences and acceptable risk

Fire statistics reveal a total of more than 3,300 fatalities, over 16,000 injuries and a total direct loss of approximately 15.4 billion US dollars due to fires in the United States in 2008 (Karter, 2009). Similar numbers can be found for many industrialized countries. Yet in many risk assessment models, the consequences of an event are usually treated stepmotherly as the assessment for the particular case is very difficult (Ramachandran, 1998, Chapter 9). Even though it seems easy to assess the initial monetary damage of a fire, it is nearly impossible to account for medium- or long-term impacts, such as business interruption or late effects of injuries, i.e. cancer due to inhalation of toxic substances. Even more complex is the assessment of the value of human life and health which is also afflicted with political, ethical, and philosophical arguments (Ramachandran, 1998, Chapter 10). Yet in life safety analysis, this consideration is inevitable to derive acceptance criteria. Some methods to assess this problem have been proposed and will be briefly described in the following. An extensive review of these approaches can be found in Proske (2004) and Ramachandran (1998).

2.2.1. Qualitative assessment (risk matrix)

A method often utilized in qualitative approaches is the establishment of a risk matrix with the dimensions defined as (unquantified) probabilities and (unquantified) consequences. This is done so that the qualitative risk can be quickly derived by combination as shown in Yung (2008, p.34). Acceptance criteria (risk bins) can be established easily by only allowing low or moderate risk combinations. For example, consequences can be estimated using a (relative) consequence ranking as proposed in Rosenbaum et al. (2007).

2.2.2. Mortality rates

The most simple approach to assess the overall consequences and the acceptable risk is a frequentistic approach as described by Yung (2008, Chapter 3). It is assumed that the current fire protection codes are acceptable ("deemed-to-satisfy") and sufficient since no significant efforts are undertaken by the AHJ to change the regulations. It is also assumed that the occurrence frequency of fires and the number of casualties per fire remain nearly constant in the future. Hence, a "casualty-per-fire" acceptance criteria can be derived by simply dividing the number of casualties by the number of fires. This can be further refined by distinguishing between occupancies, number of casualties per fire etc. The criteria found is based on the probability of the event. A very similar approach is also used in Tanaka (2008) and Tanaka et al. (2010). The extensive data on fire events and casualty numbers compiled by Holborn et al. (2004) can also be used to derive mortality rates.

2.2.3. As low as reasonably practicable (ALARP)

The ALARP approach is basically a combination of the previous two approaches. The fire statistics are taken and categorized by magnitude with regard to the safety objective. I.e. in order to derive acceptance criteria for life safety, the fire statistics are categorized by number of casualties and the respective number of events, and is then divided by the number of total number of incidents in order to derive the (annual) frequency. The number of casualties is then plotted against the frequency as shown in Figure 2.3. This type of representation is usually referred to as $F-N$ or $F-D$ diagram, where F is the frequency of occurrence and N or D are the number of casualties or the monetary damage, respectively.

If sufficient data is available, usually a scatter is visible for statistical reasons. Enveloping the area at the standard deviations denotes the acceptable area. The other two areas are low risk and high risk, respectively. Design curves for acceptable risk can be modeled around the envelopes and are usually slightly more conservative. A compilation of design ALARP-curves can be found in Proske (2004, Chapter 5.3).

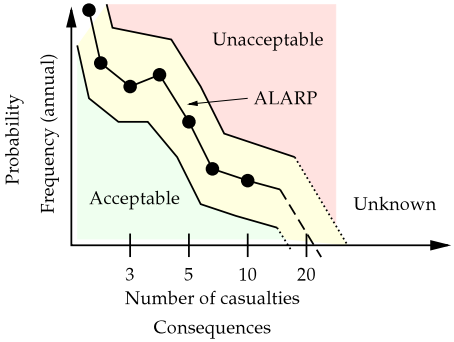

Figure 2.3.: Derivation of an ALARP acceptable risk based on an F-N diagram. Incident data is plotted against relative frequency of the incident's magnitude of consequences. The envelope around this area denotes the ALARP space. Designs falling into that area are assumed acceptable.

Looking at the design ALARP curves, it becomes obvious that the subjective risk perception is incorporated into the acceptable risks since the allowable probability of failure decreases disproportionately high with respect to the number of casualties or damage. A risk-neutral acceptable design requirement would, in this case, be a straight line (Proske, 2004, see Figure 53,p.204). This demonstrates that the acceptable risk criteria is based on limiting the maximum probability of occurrence.

2.2.4. Lost life years

The lost life years approach accounts for the life-time lost due to an event which can be events such as diseases or accidents likewise. The approach by Hofstetter and Hammitt (2001) accounts for the time in life (age), where the event is likely to happen and the magnitude of impact thereof. The years of life-time lost are expressed by the difference of the average expected life-times of the population with and without the event. Additionally, the years of life-time can be corrected for non-fatal diseases or disabilities of consequences of accidents by reducing the life quality. Hofstetter and Hammitt (2001) denote these correction factors which range from 0 to 1 as QALYs (quality adjusted life years) or DALYs (disability adjusted life years), respectively. Further information and examples on this approach are found in the report (Hofstetter and Hammitt, 2001).

Proske (2004, Chapter 6) provides further examples on this methodology and finds that the potential loss of expected life-time due to fire risk in general is approx. 20 days. Acceptable values can be derived based on this methodology.

2.2.5. Life quality index

A similar development of the concept described above is the life quality index (LQI) concept (Rackwitz and Streicher, 2002). This concept not only considers the expected life-time e but also incorporates the welfare in a society using the gross domestic product (GDP) and the required life-time utilized to earn the GDP (w) so that

$$LQI = GDP^{w} \cdot e^{1-w} \,. \tag{2.2}$$

The variables are considered the basic factors influencing life quality which are wealth, life expectancy and quality time besides work. Based on the formulation, the quality of life is an optimization task of Equation 2.2. Hence, the investment of resources into risk mitigation measures is also an optimization between the benefit of the measure and cost of the measure and the potential loss if the measure fails (Dehne, 2003, p.74) in order to maximize the LQI. Consequently, acceptance criteria can be derived from this optimization process. For example, a safety measure (costly but higher life expectancy) can be directly compared to the simple acceptance of that risk (no cost, lower life expectancy). Further considerations and details can be found in Rackwitz and Streicher (2002), Proske (2004, Chapter 7).

Dehne (2003, Chapter 8,p.76) utilizes the LQI method to establish reliability requirements for the structural fire protection because he finds the consequences to be very complex to assess. The required reliabilities ($1 - p_f$) or the maximum allowable failure probabilities (p_f) derived, respectively, are linked to so-called risk classes to allow for practical application of the concept. These risk classes imply the magnitude of severity of the consequences. Therefore, the reliability requirements should not solely be regarded as probabilities, but they also contain or (at least) imply the underlying risk. Hence, in mathematical terms Equation 2.1 is transposed for the probability, whereas the risk itself is categorized into classes with corresponding consequences.

Following this approach might be due to the fact that probabilities are "easier" to quantify than potential consequences (Dehne, 2003, p.76). Hence, this approach is widely and successfully used in risk engineering; however, this simplification should be kept in mind when applying probabilistic (quantitative) risk analysis (Hubbard, 2009, Chapter 9).

2.3. Probabilities

As described above, the acceptable risk is usually expressed in terms of a maximum allowed probability of occurrence of an event with a defined magnitude of consequences. If the probability of an event is below or equal to the acceptable probability, *safety* of the occupants is assured. In order to perform fire risk assessment, a look has to be taken at probabilities (the mathematical concept of probabilities is explained in Chapter 5). Faber (2009, p.2.2) states that the term *probability* can have two different definitions:

The frequentistic or aleatory definiton defines the probability as a result of multiple experiments that have been carried out. Hence, the probability is defined as the number of occurrences divided by the number of experiments. The exact probability can theoretically be derived if an infinite number of experiments is carried out. In practice, usually the number of occurrences is simply divided by a sufficient number of experiments. Hence, from a frequentistic point of view, the probability of tails from 1,000 coin flips with 563 times tails is 0.563 (Faber, 2009, p.2.3).

The subjective, epistemic or Bayesian definition, on the other hand, accounts for information about a system and defines the probability as a degree of belief that an event happens and is therefore subjective. For the example of the coin flips above, it is assumed that the coin is unbiased and it is known that only heads or tails are possible results. Hence, Faber (2009, p.2.4) states that in this case, the probability is found to be 0.5 based on this (subjective) information.

Utilizing frequentistic models is, in fact, an extrapolation of a limited number of previous experiments or occurrences into the future. On the other hand, the subjective models may be biased due to the subjectivity. For practical use, frequentistic information updated with knowledge seems to be the best possible approach (Hubbard, 2009, p.158ff) or more loosely formulated "because it has not happened yet (frequentistic) does not mean it will not happen at all (knowledge/belief)".

2.3.1. Referencing probabilities

When no or insufficient frequentistic information is available on certain probabilities of components, usually experts are being surveyed or educated guesses are made in order to derive an appropriate (subjective) probability. Unfortunately, this often leads to biased results as people are usually not trained ("uncalibrated") in estimating probabilities and also tend to be overconfident (Hubbard, 2009, Chapter 6). Proske (2004, p.167) states that the average car driver assumes that his driving skills are above average and Hubbard (2009, p.96) finds that people avoid guessing probabilities in favor of simpler scales (i.e. 1 to 10, or school grades). Additionally, the assumptions are often times biased by

current events and/or social trends for the reasons stated in Section 2.1.1. For that reason, Hubbard (2009, Chapter 6 & 10) proposes a "calibration" prior to the estimation of failure probabilities.

Risk (or a probability, respectively) always incorporates a reference dimension, such as "per year," "per event," or "per kilometer" which can also lead to a bias in the data. In structural engineering, the reference time is usually one year, as the loads and actions permanently act on the structure. When designing for life safety in a fire, the annual probability of a fire has to be considered in order to reach annual requirements or suggestions stated in various codes and standards, such as, for example, DIN EN 1990 (2002).

Additionally, it should be noted that design fire scenarios usually act as a conservative envelope for multiple similar scenarios and hence the according probability of the design fire scenario is an accumulation of the probabilities of all possible scenarios included (Rosenbaum et al., 2007, p.112).

2.3.2. Operational probability

All assumptions about probabilities and stochastic models, as well as the utilization of engineering assumptions and models (such as a fire scenario using CFD) leads to failure probabilities which do not exactly represent the "real" or "theoretical" probability. Due to the fact that stochastic models and failure probabilities of components are usually mathematical probability distributions fitted to the results of various experiments of a phenomenon, the convolution (rf. Section 5.2.4) of various distributions also has to be considered a model.

For that reason, Spaethe (1992, p.63) introduces the term *operational probability* (of failure) which is defined as follows (translated from German):

> "[...] That is why the term 'operational probability of failure' is introduced. It is a theoretical probability which serves the engineer as a comparative number and as a decision support for the quantification of statements about the safety and reliability. It is a conditional probability which is only valid under a compound of assumptions (i.e. the stochastic models). Hence, it is connected to the [underlying] theoretical model and cannot be separated [from this model] without further considerations. Operational probabilities should only be compared if the models are based on similar assumptions. [...]"

For structural integrity Spaethe states that the mechanical models are close to exact or, at least, conservative so that the operational probability of failure is usually higher than the theoretical failure probability. The numerical models (for evacuation and fire simulation) as well as the thresholds or fire scenarios in performance-based FPE are also not exact but unlike the mechanical models, they are not necessarily conservative (vfdb-Leitfaden, 2009; Münch, 2006).

Following Spaethe's argumentation, all stochastic models and fire scenarios and additional assumptions used in this work will be purposely chosen conservatively in order to achieve a higher operational than theoretical probability. Detailed scenarios, assumptions and stochastic models will be presented and described in the respective chapters. Hence, the use of model uncertainty factors is omitted herein.

2.4. Probabilistic design

All considerations above lead to the question of how accurate probabilistic design really is and how it can be used in order to verify an acceptable level of safety when used in a design approach. Generally, two different methods exist which both have been used within fire risk analyses (BS 7974, 2001, part 7,p.12).

2.4.1. Comparative probabilistic design

The first approach in utilizing probabilistic considerations in fire safety design is the so-called *comparative* approach and can be seen as a logical consequence of the model dependency introduced by Spaethe (1992, see above). Herein, the current regulatory body with deemed-to-satisfy and/or prescriptive regulations is used as the accepted level of safety, even though it is quantitatively unknown. For that reason, the quantitative safety level has to be derived by computing the probability of failure of an artificial building which complies with all current regulations. The resulting value p_f can be used as a benchmark. Now the actual quantitative safety value for the building to be designed is also computed using the same models and underlying assumptions to allow comparability. This is in absolute conjunction with the definition of "operational probabilities" as given by Spaethe (1992, see above). Thus, the actual reliability is considered a decision-support and relative indicator of safety for the fire protection engineer more so than an absolute number. A simple example of comparative probabilistic design is given in Belsham (2009). The drawback of this approach is the additional work that has to be performed analyzing the benchmark example which complies with the codes. In many cases, such as open atria and large buildings, a code compliant example simply does not exist. Belsham (2009, p.46) notes that possible shortcomings of the underlying data accuracy are canceled out due to the comparison.

2.4.2. Absolute probabilistic design

The other, more commonly used approach is the absolute probabilistic design. In this case, a failure probability is compared to an acceptable failure probability stated in the regulations, codes, or standards. Unlike the previous approach, the resulting failure probability is used as an absolute value and not merely as a decision-support. The acceptable reliability levels (with the corresponding maximum failure probabilities) are a substitute for the "risk" of that scenario as described in the previous section.

Acceptable probabilities of failure for structural engineering have been introduced in Germany based on a guideline called GruSiBau (1981). The levels proposed (GruSiBau, 1981, p.23) in that publication have widely been used in other regulatory documents, such as DIN EN 1990 (2002, Annex B and C) as basis for all structural building codes (including the fire parts). Additionally, semi-probabilistic safety concepts (Hosser et al., 2008; Dehne, 2003, for example) for structural fire safety design have been calibrated to meet these reliability requirements via partial safety factors.

Other reliability requirements, which are more or less in the same range as GruSiBau (1981), can be found in Rosenbaum et al. (2007, p.113f) who adopt values from the nuclear industry. Additional in-depth information on the acceptable risk criteria is given in Rasbash (1984) whose work led to the current acceptance criteria in the British Standard BS 7974 (2001, Part 7: Probabilistic risk assessment)—which are only valid if the stated failure probabilities are used.

In the absolute probabilistic design, the probability of failure is compared to a maximum allowed probability of failure. If the probability of failure is lower than the required p_f, the structure is considered "safe." In this approach, no distinction is made between different models or underlying data so that it cannot be assumed that shortcomings of the underlying data and models cancel out. For that reason, it is necessary to make sure that the models, data and scenarios used at least slightly underestimate the "real" reliability in oder to produce an operational probability that can be considered "safe" (see Section 2.3.2). This can be achieved in reliability engineering without significantly sacrificing system performance. Additionally, known uncertainties can also be accounted for by so-called *model uncertainty factors*, as demonstrated by Schnetgöke (2008, p.58) or Dehne (2003, Chapter 9.6).

2.5. Review of risk-informed approaches in FPE

Risk-informed (or probability-informed) approaches are not completely new to FPE and several different approaches can be found in the literature of the last two decades. A first full probabilistic approach is described in Magnusson et al. (1996) who utilize various probabilistic methods to assess the uncertainties for life-safety design. Based on an event tree analysis, the relevant scenarios are selected and probabilistic analyses using FOSM and Monte Carlo are performed to assess the probability of failure. The calculations utilize an analytic formulation based on various evaluations with zone fire models (response surface formulation) and a simple analytic exit door capacity model for the evacuation time. The authors find the failure probabilities to be rather high which might be due to conservative stochastic models (Magnusson et al., 1996, p.324) and the fact that neither the fire initiation probability nor any other barrier is incorporated into the calculations. Also, the fire scenarios are based on a t^2-fire which can be considered rather conservative for life safety (NFPA 101, 2008, Section A.5.5.3). All background details of the methods

used in the paper as well as further considerations and an exemplary application of risk-informed design to a hospital ward can be found in the (very comprehensive) dissertation by Frantzich (1998).

In their recent books, Hasofer et al. (2007) and Yung (2008) show examples of probabilistic life safety evaluations which are based on similar assumptions and considerations. Both books propose a wide range of probabilistic risk assessment tools and information is given on stochastic and uncertainty modeling. Fire, fire growth, and smoke spread models are given as well as models for human response and behavior. Additionally, models for the fire department intervention and the modeling of fire protection barriers are given in both books in order to provide a basis for a fully risk-informed fire protection design. The examples given are based on analytic problem formulations or assumptions and no probabilistic evacuation modeling using advanced models is performed. This is similar to the example given by Belsham (2009) who bases his risk analysis on the reliability of the fire protection barriers (doors, sprinklers, etc.). This methodology is also used by Tanaka (2008) who performs systematic, event-tree-based analyses for life safety utilizing available models and assumptions about failure probabilities. In a later paper (Tanaka et al., 2010) he also develops values for acceptable risk based on fire statistics (see Section 2.2.2).

A similar approach is given by Fitzgerald (2004, Chapter 18+19) who provides very detailed information on the decision-making process based on risk considerations. Yet he avoids the extensive use of quantitative probabilities due to concerns about the validity and applicability of these "numbers" (Fitzgerald, 2004, Appendix B).

Another risk-informed approach was chosen by Maag (2004) who evaluates the fire life safety of occupants using Bayesian networks. The extensive analyses performed are concentrated on domestic houses and not public or assembly buildings. Hence, no large numbers of occupants are expected (Maag, 2004, p.59) and, consequently, the evacuation simulation was omitted. The number of fatalities and the corresponding probabilities are assumed when certain conditions occur or requirements for successful evacuation fail (Maag, 2004, p.74).

Chu et al. (2007) calculates the expected risk to life based on scenarios derived from an event tree. ASET and RSET analyses are carried out using zone fire models and evacuation software tools to derive probability distributions for each. The convolution of the distributions found yields information about the failure probabilities and the expected risk to life of the occupants. The tail problematic of the underlying distributions is not considered.

In her dissertation, Notarianni (2000) evaluates uncertainties of domestic fires with respect to life safety performing survival analysis with numerical zone fire models. This approach was applied to assembly facilities in Albrecht and Hosser (2009). The variance

of the criteria is assessed with respect to the input parameters of the design fire. More information on the approach is found in Chapter 3.

A similar approach was used by Hostikka and Keski-Rahkonen (2003) who develop a probabilistic tool for the assessment of uncertainties. In his dissertation, Hostikka (2008, Chapter 2-3) also develops a method to refine probabilistic analysis using fast numerical models enhanced with point-wise evaluations of models with higher numerical cost. A first Monte Carlo based uncertainty analysis using CFD models is also presented by Hostikka (2009). Therein, 200 CFD simulations were carried out with very high overall computational cost (20 days on 5 nodes of a computing cluster).

Dehne (2003, Section 9.1) proposes a probabilistic method for smoke and heat control systems based on CFD calculations in order to design for life safety considering multiple fire protection barriers. As the main focus of his work is the structural fire protection, further calculations are omitted. He concludes that the very high computational cost requires the use of surrogate models (a.k.a. response surfaces) and is only applicable in special cases (Dehne, 2003, p.157).

Many other risk-informed approaches for structural fire protection exist, such as the semi-probabilistic safety concept based on the Eurocodes (Albrecht and Hosser, 2010a). An exemplary application therein shows the potential of cost-benefit optimization for fire protection barriers.

2.6. Conclusions for a risk informed life-safety approach

The previous sections have given a detailed introduction into risk, risk management, the variables, and problems involved. After an introductory definition of the term *risk*, the perception thereof is discussed on many different accounts such as collective vs. individual or objective vs. subjective risk. Risk is usually defined as a function of consequences and according probabilities.

It was found that the modeling of consequences is treated rather stepmotherly, especially for life safety. This is due to the fact that the value of human health and life is more of an ethical and philosophical question. Yet some (quantifying) approaches and models exist which are mainly based on statistics of previous events and are, therefore, a rather probabilistic approach. Additionally, other models to assess acceptable risk levels were presented as well as the four general possibilities to treat risk in society.

Furthermore, probabilities, their definition, and their origins were discussed. It was found that different approaches to assessing probabilities can lead to different results and findings. Probabilities can also be prone to subjective biases. Yet many risk analyses are based on the assessment of probabilities of occurrence of an event. Usually the

acceptable level of risk is modeled using a maximum probability of failure for an event with a corresponding magnitude. In order to use failure probabilities for later analyses, the term *operational probability* was introduced to provide a distinction between "exact" probabilities and calculated, model-dependent probabilities which can be used for risk analyses.

A literature review provides an overview to former and recent risk-informed assessment approaches of life safety in FPE. Many risk analyses have been performed on the life safety problem in FPE, yet few of them deal with the quantitative assessment of the probability of failure of egress design solutions based on state-of-the-art FPE engineering tools. Only one approach to uncertainty assessment using CFD-software and to probabilistic life safety analysis using evacuation software was found, whereas the demand for risk-informed life safety evaluations is higher than ever due to the advancement of optimized performance-based solutions in FPE.

In conclusion, objective risk acceptance criteria for human life and/or life safety are missing entirely at the moment. This is due to the manifold reasons, definitions, and forms of risk described above. Hence, operational, and thus model-dependent, failure probabilities derived from deemed-to-satisfy prescriptive codes herein are not final objective risk-acceptance criteria; but merely a status-quo evaluation of a biased risk measure which can be utilized for comparative design using the same or similar models, assumptions and scenarios. Hence, the reasonable utilization of state-of-the-art FPE engineering models in conjunction with reliability analyses will lead to operational probabilities which can be used as good estimators to assess the performance of egress design solutions and may can lead to risk-optimized solutions which can be considered to have the best reasonable cost-benefit ratio for expensive fire protection measures.

Chapter 3

Hierarchy for life safety design

As stated in Chapter 1, the fire safety design in Germany is traditionally satisfactory if the building complies with the requirements given in various prescriptive building fire codes. These building and fire codes are "deemed-to-satisfy," meaning that the accordance with the requirements leads to a "safe" building by definition. Many modern architecture buildings cannot necessarily comply with these codes. These codes are very constrictive to the layout and the material requirements so that the fire protection engineer has to find performance-based solutions which ensure that the same level of safety as in the codes is reached for the building.

After giving an overview of the traditional prescriptive codes (Section 3.1), the main focus of this Chapter is on the current utilization of the performance-based approach in Germany (and many other countries, such as the USA, GB, NZ etc.) using an empirical safety concept. In future safety concepts, distinctions will have to be made depending on the complexity of the underlying performance methods—which will be described in greater detail in Chapter 4—as models of higher complexity can yield more accurate results, and thus, will need to be treated differently regarding their consideration in safety concepts. For that reason, a hierarchy is proposed similar to the hierarchy implemented in the Eurocodes.

3.1. Prescriptive design–codes and standards

Prescriptive fire codes are mainly based on reason and—mostly tragic—experience and are easily applicable to standard buildings. The Swiss codes (VKF/AEAI, 2003) state that those codes will be satisfactorily applicable to approximately 90 % of the buildings. These codes contain requirements for escape route lengths, width, or specific requirements like emergency exit signage. Other requirements can be, for example, that no fire load may be stored within required hallways.

It becomes obvious that these requirements not only target the direct objectives of fire protection, but include requirements for the layout of the building, the fire resistance rating of structural components, the fire safety system (i.e. HVAC systems, sprinklers, smoke and heat exhausts etc.). The compliance with these—sometimes very complex—code environments leads to a "deemed-to-satisfy" solution, implying that accordance with the requirements will lead to a "safe" building per definition. The level of safety achieved by those codes is unquantified, and thus it is assumed that big differences occur between various occupancies. In Germany and other countries these codes are widely available and utilized since compliance can be easily shown and no further consideration has to be made. This is very advantageous on the one hand, since the fire protection design is relatively easy to fulfill, but it might not be risk-oriented and tailored to the performance of the particular building on the other hand. The advantages and disadvantages are shown in Table 3.1. Especially for large buildings with modern architecture, the limits of prescriptive design become obvious and performance-based solutions need to be found as open-space design and constrictive requirements are usually incompatible.

Nevertheless, some requirements of the prescriptive codes are quite useful to avoid rather dubious performance solutions, and thus should be retained even for performance codes. Such requirements could be, but are not limited to, that at least two independent egress paths should be existent (MBO, 2002, §33,p.28f) or requirements and standards for the signage of emergency exits. Another area of retained prescriptive requirements could be the design and maintenance of fire protection systems, as they are considered within the fire safety design with very low failure rates. Yet those rates can only be assumed if these systems have a certain standard they comply with. In a recent publication, Fleischmann (2011) bridges the gap between prescriptive and performance-based codes by prescribing certain parameters such as fire growth rates, etc. to be used in (performance-based) numerical simulations depending on the type of occupancy in order to retain some level of comparability. This seems to be quite conclusive even though it can be rather conservative to innovations in performance-based design. Yet momentarily it constitutes the best approach to allow for comparable design solutions. If these values are calibrated to fulfill the required safety level by using partial safety factors on the most relevant parameters, truly performance- and risk-optimized and comparable design solutions could be found using advanced fire engineering tools.

Table 3.1.: Prescriptive vs. performance-based codes, reproduced from Hadjisophocleous et al. (1998).

Code Type	Advantages	Disadvantages
Prescriptive Codes	• Straightforward evaluation of compliance with established requirements • No requirements for high level of engineering expertise	• Requirements specified without statements of objectives • Complexity of the structure of codes • No promotion of cost-effective designs • Very little flexibility for innovation • Presumption that there is only one way of providing the safety level
Performance Codes	• Establishment of clear safety goals and leaving the means of achieving those goals to the designer • Permit innovative design solutions that meet the performance requirements • Eliminate technical barriers to trade for a smooth flow of products • Facilitate harmonization of international regulation systems • Facilitate use of new knowledge when available • Allow for cost-effectiveness and flexibility in design • Non-complex documents • Permit the prompt introduction of new technologies to the market place	• Difficult to define quantitative levels of safety (performance criteria) • Need for education due to lack of understanding, especially during first stages of application • Difficult to evaluate compliance with established requirements • Need for computer models for evaluating performance

3.2. Performance-based approach

Performance-based design is often a possibility when a building cannot be build according to the specifications and requirements of the prescriptive codes. The deviations from the prescriptive design, or the complete design process, will target on fulfilling safety goals or safety objectives. The fire protection systems and measures are aligned to tackle particular problems by achieving the safety objectives which may arise. The solutions from performance-based design are not deemed-to-satisfy but prove achievement of the safety objectives by applying state-of-the-art engineering judgment and methods when considering of the impact of the fire effects heat, smoke and toxic effluents.

For the verification of the safe egress and life safety, performance-based design usually compares two time spans. The required safe egress time (RSET or $t_{\text{req.}}$) is either calculated by simulating the occupants' behavior and movement (see Section 4.3) or is assumed based on educated (best-guess) estimates. The latter can be found in the literature. Mehl (2004) proposes to cap this time to 2-3 minutes for rooms, 5-10 minutes for fire compartments and a maximum of 15 minutes for the entire building. The RSET values are compared to the available safe egress time (ASET or $t_{\text{avail.}}$), which is defined as the time until untenable conditions are reached. These untenable conditions are based on performance criteria that incorporate the various effects of the fire (mainly heat, smoke, and the toxic effluents) and will be discussed in detail in Section 4.2.5. The ASET times are usually determined from numerical fire simulation.

By comparing the ASET and the RSET times, a verification of the safe egress can be considered accomplished if

$$\text{ASET} \overset{!}{\geq} \text{RSET} \qquad \text{or} \qquad \frac{\text{ASET}}{\text{RSET}} \overset{!}{\geq} 1.0\,, \tag{3.1}$$

meaning that the ratio between the time available and the time required is greater than unity. Any value smaller than unity implies a failure of safe egress of all occupants, whereas a value greater than unity implies a safety margin. In addition to the input parameters for the evacuation and the fire simulation, the threshold values to determine untenability, as well as the fire scenario, are chosen to be (sometimes overly) conservative. For the evacuation simulation it is assumed that the occupancy limit is reached (or even exceeded) and that the exit choice of the occupants is very conservative. It is also sometimes required to verify life safety by assuming that at least one emergency exit fails due to locked doors or untenability. On the other side, the fire scenario as well as the fire parameters and the effluent rates (or yields, see Section 4.1.3) are also chosen conservatively for the fire simulation to account for the worst-case scenario (vfdb-Leitfaden, 2009). This leads to an unquantified and implicit—yet assumingly high—safety margin, as no probabilistic considerations have been done. On top of these conservative assumptions, an empirical safety concept is applied to the results for ASET and RSET.

3.2.1. Empirical safety concept

A common method to "quantify" the level of life safety is the application of an empirical safety concept. This concept simply adds a global, arbitrary, and empirical safety factor κ to Equation (3.1), so that

$$\text{ASET} \overset{!}{\geq} \kappa \cdot \text{RSET} \qquad \text{or} \qquad \frac{\text{ASET}}{\text{RSET}} \overset{!}{\geq} \kappa \,. \tag{3.2}$$

The safety factor quantifies the level of safety relatively between ASET and RSET. A safety factor of $\kappa \in 1, \ldots, n$ provides tenable conditions for $1, \ldots, n$ times as long as needed for egress. The absolute level of safety remains unknown but is very likely to be far higher because of the conservative input parameters, criteria thresholds and scenarios. Actual values for κ can be found in the literature: Mehl (2004) proposes safety factors in the range between 1.5-2.0 depending on the criteria chosen. A safety factor of 2.0 is also given in the BS 7974 (2001) and in Tubbs and Meacham (2007, p.290) who deduce this value to account for half of the exit doors being blocked during a fire. A similar consideration is taken into account in vfdb-Leitfaden (2009, p.381). Johnson and Timms (1995) and Deakin and Cooke (1994) even propose this factor to be between 2.0 and 3.0. It is assumed that the latter propose such high factors to account for the even higher uncertainty in numerical fire simulation in the mid-1990s compared to more recent CFD-based tools.

However, the absolute level of safety remains unknown and the questions may arise whether all assumptions and empirical safety factors really provide a sufficient achievement of the safety objectives or whether they lead to overly safe, and thus too expensive, solutions for life safety. Additionally, the comparability to the prescriptive design is not given or even possible (see Table 3.1), so it is unknown whether a deemed-to-satisfy building would meet the performance requirements.

3.3. Proposed verification levels and hierarchy

When designing for structural fire resistance in accordance with the Eurocodes, the designer can chose between three different approaches, namely the prescriptive approach, where values for certain structural members are tabulated (DIN 4102-4, 1994, for example) and the compensatory approach, where shortcomings are compensated for by installing fire protection systems—as well as the performance-oriented methods according to the simplified and the advanced calculation methods. This hierarchy is shown in Figure 3.1 and should be regarded as a basis for all other fire engineering standards, as the complexity of the methods should be in approximate accordance with the complexity of the problems.

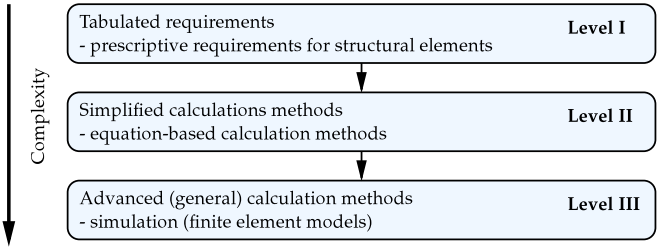

Figure 3.1.: Hierarchy of the Eurocodes, reproduced from Hosser et al. (2009).

Analogously, Tubbs and Meacham (2007) describe four different strategies for the tenability assessment based on the NFPA 101 (2008). These strategies are of different complexities and use different effects of the fire as tenability criteria. Consequently, they were categorized into three levels of approximately equal complexity yielding a hierarchy similar to the Eurocodes. The levels are described in detail in the following, leading to the comprehensive hierarchy shown in Table 3.2 and Figure 3.2.

3.3.1. Level Ia: Prescriptive design

The first verification level for life safety is the full compliance with all code requirements. The building and the safety of the occupants is then considered accomplished, since the codes are deemed-to-satisfy. Further information on this level is given in Section 3.1.

3.3.2. Level Ib: Compensation

The simplest performance-based approach is very similar to the prescriptive requirements. Through the installation of one or multiple appropriate fire or smoke protection systems, the safety objectives are qualitatively achieved. This procedure is usually used if material or geometrical requirements cannot be met, but the layout or the complexity of the building is rather close to the prescriptive codes. These compensation measures (i.e. installation of an automatic detection system if the required escape route lengths are exceeded) are very popular for simple problems, as they normally do not require advanced calculation methods and can be verified by conclusive argumentation of the planner. In Germany, as well as in many countries, this approach needs approval by the authorities having jurisdiction (AHJs) on a case-by-case basis and hence does not necessarily have a legal basis.

The big disadvantage of this method is that no quantitative assessment of the safety level is possible. Installing a fire protection system to compensate for shortcomings of the prescriptive requirements seems to be a reasonable method, but only a qualitative conclusion can be drawn, as the quantitative safety level remains unknown, i.e. how many meters of an overlong escape route can be compensated for with an automatic fire detection system.

In conclusion, this performance-oriented strategy can be considered rather conservative as the AHJs in Germany are constrictive and cautious with these compensation measures and demand a more detailed verification of the anticipated compensation if any doubt may arise.

3.3.3. Level IIa: Maintaining visibility and tenability

In this level, a smokeless layer of a chosen height may not be under-run until the evacuation of the hazard area is completed. The fire has to be simulated to a degree where it is possible to predict the height of the smokeless layer or other visibility criteria. Zone models (Section 4.1.2) can be utilized as well as CFD-simulations (Section 4.1.3) for more complex geometries in order to assess either the height of the smoke layer, or in some cases, the optical density (Section 4.2.1), if no clear layering can be achieved. The threshold heights or values for the optical density are discussed in Section 4.2.

This approach is extensively used in the standard DIN 18 232-2 (2007). Therein, a simulation of the evacuation is not performed, as the threshold may not be under-run during the whole fire scenario. A similar strategy, which can be considered to follow the same approach, is to conservatively cap the evacuation time. It is simply assumed that the evacuation has to be successfully completed within a certain amount of time, depending on the size and the complexity of the building. The chosen layer height or threshold value for chosen performance criterion must not be under-run for that period of time, allowing to continue the scenario (i.e. for structural fire design) without maintaining the criteria any longer.

This level does allow the quantification of the safety to a certain degree and can be considered to be rather conservative, as the direct effects of the fire on the occupants are not considered. Per definition, the smokeless layer is free of any toxic substances. As this is not necessarily true in reality, the minimum layer heights are often chosen to be significantly higher than the tallest occupant to allow for a safety margin. The threshold values are also chosen to be rather conservative.

3.3.4. Level IIb: Simplified timed egress

This level is very similar to the previous approach, except that in this case a calculation of the required egress time is performed, depending on the degree of complexity. For this approach, the simplyfied evacuation models are used, such as the capacity models or the hydraulic models (rf. Section 4.3.1) which can be performed by hand or with a simple spreadsheet software.

The approach can be regarded as a simplified performance-based approach, as the verification scheme is the same as in the advanced performance-based approach, but the models and the input parameters, as well as the tenability criteria are chosen to be simple and conservative. Additionally, the empirical safety concept can be applied here with κ-values according to Equation (3.2) to allow for the direct calibration of the safety level. Extensive probabilistic analyses of the Level IIb methods for a similar example as in Chapter 7 were carried out by Siemon (2011) under the supervision of the author in the context of this thesis. The benchmark example in Section 6.7.2 (page 115ff) shows the applicability of the method.

3.3.5. Level III: Advanced timed egress

In advanced timed egress approaches, tenability is assessed by considering the various direct effects of the fire on the occupants, which are described in Section 4.2. In this case, all criteria—heat, smoke and other toxic or other harmful effects—are considered and analyzed for severity of impact. In this context, the use of the FED values (Section 4.2.5) is highly recommended to account for momentary high doses and time-integrated effects of lower concentrations. The time until the threshold values are reached is considered the time available (ASET or $t_{avail.}$) for the occupants to evacuate safely from the hazardous compartment. As the modeling and simulation of and the various effects from the fire have to be done as accurately as possible, advanced simulations methods, such as CFD-models, are usually utilized, especially for the assessment of the toxic effects and for complex geometries.

This level is considered the most performance-oriented approach because it directly considers the interaction between the scenario and the fire effects and the behavior of and physical impacts on the occupants (vfdb-Leitfaden, 2009). The empirical safety concept can be applied using the safety factor κ from Equation (3.2) for a direct calibration of the safety level.

Table 3.2.: Overview of the three levels of design for life safety, the required skills or tools for utilization and complexity and accuracy of the methods.

	Level	Tools/Expertise	Complexity	Accuracy
Ia	Prescriptive Design	none	o -	--
Ib	Compensation	Negotiating skills	o	--
IIa	Maintaining tenability	zone models	+	o
IIb	Simplified timed egress	zone models (rarely CFD), simple evacuation tools	++	+
III	Advanced timed egress	CFD models, advanced evacuation tools	+++	++

3.3.6. Hierarchical classification and required competencies

Table 3.2 and Figure 3.2 give an overview of the three levels proposed with regard to complexity and degree of accuracy. These levels are similar to the verification levels of the Eurocode fire parts (Figure 3.1), which also provide three levels with increasing complexity and accuracy.

Such a flexible multi-level system has the advantage of allowing for the utilization of performance-based methods for complex and non-standard buildings, as well as providing tabulated requirements for standard-buildings, buildings that only slightly deviate from the prescriptive requirements, and any building in between without sacrificing or loosening the safety standards. Additionally, such a system can be used if it is desired to regulate the competencies for the fire life safety design. A Level I design can be virtually done by anybody involved in the design process since only tabulated requirements have to be adopted. This could be done by the structural engineer or the architect for simple designs. Level II designs require a portion of in-depth knowledge about fire protection engineering and hence should only be prepared by certified engineers, etc. Level III designs require the most knowledge about fire protection engineering, especially in the areas of fire dynamics, CFD- and evacuation simulation, and egress design. Here, accredited and certified individuals and/or engineering consultancies should be involved.

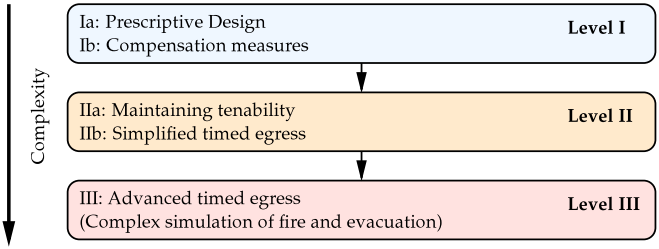

Figure 3.2.: Proposed hierarchy of the life safety approaches.

Such a hierarchy of three different complexity levels can be developed for all types of safety objective verifications and would constitute a simple and effective system for fire protection engineering and beyond. Further information about the knowledge required by fire protection professionals and the various interactions of fire protection engineering with other disciplines during a design process can be found in Lataille (2003, especially Chapters 1, 3 and 5).

3.4. Conclusions

In this Chapter the general approach of prescriptive and performance-based life safety designs were outlined. After a short summary of the prescriptive design method, an introduction was given into the performance-based approaches which are widely used around the world to either tackle deviations from the prescriptive codes or to provide a more cost-efficient and performance-oriented solution on a case-by-case basis using state-of-the-art engineering expertise. To add a margin of safety, usually an empirical safety concept is applied. Despite being easy to use, the big drawback of this concept is the empirical nature so that the real safety level remains unknown, providing room for interpretation and hence too conservative or too optimistic solutions.

As many different tools and models exist, it can sometimes be difficult for the AHJs or the certifying engineers to verify the complex matrix of input parameters and the interpretation of the results. Hence, a hierarchy was proposed (Figure 3.2) which is similar to the hierarchy in the Eurocodes. Based on that hierarchy, qualification profiles were recommended to perform life safety analyses depending on the complexity of the models.

Chapter 4

FPE models for life safety analysis

After the general introduction and classification of performance-based life safety design in the context of Fire Protection Engineering in the previous chapter, it is essential to understand the background of the tools for fire and evacuation simulation, the threshold models to determine untenability, as well as the input parameters in detail. In this Chapter, a short overview of some of the models is given with emphasis on the use in life safety design. This includes the various harmful effects of the fire on the building occupants as well as proposed threshold values and incapacitation models. The latter will be analyzed with regard to severity of impact and superposition with other fire effects and is described in greater detail. The existing models will be modified in order to provide a holistic, easy-to-use criterion for the practical application. A closer look will also be taken at the design fire scenarios and the underlying design fires. Various modifications are introduced to provide realistic, representative, and not overly conservative fire scenarios with their according design fires using prescribed heat release rate (HRR) curves.

4.1. Fire modeling

In order to accurately assess a fire scenario for the criteria and thresholds presented in Section 4.2, the fire itself, as well as the transport of the heat and byproducts of the combustion (i.e. soot and toxic substances), need to be simulated. The most common method to obtain this information is to utilize numerical simulation tools of varying accuracy, complexity, and numerical effort as shown in Figure 4.1. Some of the numerical methods will be briefly presented in the following with an emphasis on the CFD simulation.

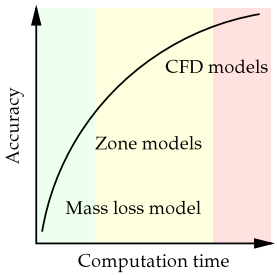

Figure 4.1.: Fire simulation accuracy vs. computational effort of the models described in the following.

4.1.1. Mass loss model

A very simple approach for the assessment of toxicity is the *mass loss model* proposed in ISO 13571 (2007). A certain amount of fire load mass (Δm) is consumed by the fire per unit time (Δt) producing byproducts which are released into the known volume (V) of the fire compartment. The mass loss rate as well as the byproduct yields are derived from experimental tests of various materials and products.

The mass loss model is based on the simple assumption that the byproducts will evenly and homogeneously distribute within the compartment so that the concentration of the byproduct i per unit volume V (in m^3) can be given as

$$C_i = \frac{\Delta m}{V} \,. \tag{4.1}$$

Based on these "average concentrations", the toxicity (and subsequently the ASET) can be evaluated using the toxic FED model. A further simplification is allowed in ISO 13571 (2007) if the yields are unkown. It this case, threshold concentrations are given which are based on toxic potency of common smoke composition. These thresholds for human incapacitation (assumed 50 % of the lethal concentration LCt_{50}) are given for well-ventilated fires ($450\ g \cdot min/m^3$) and for vitiated post-flashover fires ($220\ g \cdot min/m^3$).

This model is very simple and requires almost no numerical effort when being implemented into computer code. As the concentration is assumed to be homogeneous within the volume of the compartment, the mass loss model has to be considered rather inaccurate and, thus, cannot be utilized for large and complex geometries. Considering the underlying conservative assumptions of the threshold concentration, the model might be used to obtain a first estimate of the toxic potency within smaller compartments and single rooms.

4.1.2. Zone models

A more accurate numerical fire simulation method incorporating basic principals of thermodynamics and mass transport are the *zone fire model*s, which usually require computation times of less than one minute. This is due to the fact that the compartment is essentially subdivided into two "zones," the upper hot gas layer and the lower ambient air layer. Both layers are assumed to have homogeneous temperatures and mass concentrations, which limits the model applicability to simple compartment geometries, such as rectangular rooms (Schneider, 2002, p.39).

Within the model, the fire scenario is usually prescribed by a defined mass loss rate ($\dot{m}_P$) or heat release rate ($\dot{Q}, HRR$). Hence, a pyrolysis model is not incorporated and the rates have to be chosen based on conservative design fire scenarios (CFast 6.1, 2009, p.18). Above the source of the defined burning object, a plume model is utilized acting as a "pump" for mass and enthalpy transfer from the lower to the upper layer. The plume model contains an empirical correlation to predict the amount of mass and enthalpy transferred.

Based on the assumption of two heterogeneous layers, the change in the zone temperatures and the layer height (h_L) can be computed numerically by time-stepwise solution of the equations for conservation of mass ($\dot{m}$) and conservation of energy ($\dot{E}$) for each zone as schematically shown in Figure 4.2. The underlying equations are shown in detail in Schneider (2002, p.44f) and CFast 6.1 (2009, p.13f). State-of-the art zone models, such as CFast or MRFC (Max, 1990), are capable of computing multiple compartments and contain simple combustion models. CFast, for example, contains an algorithm to limit the heat release due to oxygen constraints and calculates effluents based on a reaction model utilizing stoichiometric coefficients (yields, ν_i).

Due to the low computational cost, the zone model CFast was used for the many required (Monte Carlo-) simulations for probabilistic studies, such as Notarianni (2000), Albrecht and Hosser (2009), and for the validation of the IMLS response surface method, described in Section 6.7.2. The disadvantage of the zone fire models is obviously the assumption of homogeneity in the zones and the constraint that complex geometries, such as modern architecture buildings or atria, cannot be assessed accurately with respect to the local dispersion of heat and toxic effluents.

Yet zone models have been successfully used in FPE for determining smoke volumes and smoke layer heights rather than toxicity modeling (vfdb-Leitfaden, 2009, p.110ff). A normative standard based on zone models to determine smoke layer heights is the German standard DIN 18 232-2 (2007) for the design of smoke and heat control systems. This code is based on maintaining a certain smoke layer height (see Section 4.2.1). Zone models can, therefore, be used for simple geometries and for simplified timed egress verification (Level II, Section 3.3).

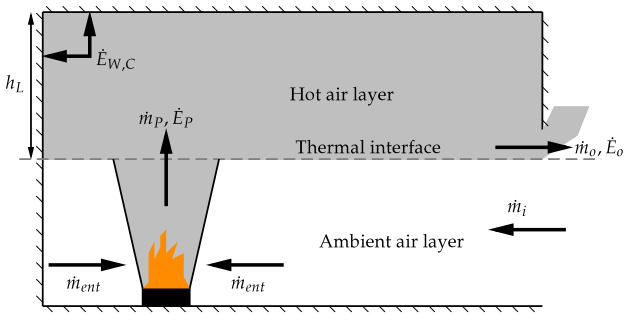

Figure 4.2.: Schematic representation of the assumptions used in zone models. $\dot{m}$ represents the mass transfer and $\dot{E}$ represents the energy transfer as derivatives with respect to time. The indices denote: W,C - wall, ceiling, o - out, i - in, ent - entrainment, and P - plume. h_L is the height of the upper layer. Adopted from Yeoh and Yuen (2009, p.3).

4.1.3. CFD (field) models

Currently, the most accurate approach to simulate a fire is the use of computational fluid dynamics (CFD). CFD is a very broad area of research and combustion, and pyrolysis modeling add additional challenges. Hence, the following paragraphs will merely give an overview of the basic principles and provide literature recommendations for further information. A focus will be placed on the underlying assumptions, approximations, and the discretization used in the state-of-the-art CFD-software Fire Dynamics Simulator (FDS 5.3, 2009) as these are most relevant for the life safety assessment.

Like the zone models, CFD programs solve a system of differential equations. Additionally to the transportation of mass and energy in the zone model, the transportation of momentum and the equation of state are solved for the Newtonian fluid[1] air. Details of the mathematical formulation and solution strategies can be found in Yeoh and Yuen (2009, Chapter 2). The solution of the equations mentioned above is performed numerically on a computational mesh, which is by far finer than the assumption of two zones in the zone models. The computational mesh describes the domain by a (large) number of control volumes (mesh cells) in which the differential equations are solved by utilizing numerical algorithms to approximate the solutions which cannot be found analytically. The shape of the volumes can be chosen arbitrarily. FDS uses a uniform, rectangular mesh with equally sized cubic cells, each with the edge length δx, as described in McGrattan

[1] A Newtonian fluid is a fluid where the shear stress is (linear) proportional to the strain rate, so that $\tau = \mu \cdot \frac{du}{dy}$, with τ denoting the shear stress, μ the viscosity, and $\frac{du}{dy}$ the strain rate.

et al. (2009, Section 3.3). Turbulence is modeled using the large eddy simulation (LES) which directly solves the large scale turbulent eddies with sufficient accuracy. Small scale (sub-grid size, $\leq \delta x$) eddies are approximated using appropriate formulations (Yeoh and Yuen, 2009, p.374ff).

All the considerations above allow for an accurate solution of the transport equations so that local information on all relevant parameters, such as temperature, pressure, velocity, or species concentrations, can be obtained. This allows for the modeling of complex geometries and the consideration of local effects and is mainly the reason why CFD simulations have recently become increasingly popular in FPE. Even though being very accurate compared to the mass loss model or zone models, it should be noted that CFD simulations are *not* a perfect representation of reality, since the following assumptions and approximations are underlying:

- Differential equation systems are solved numerically and not analytically. FDS, for example, uses a second order finite differences method (FDM)
- The computational domain is approximated by a finite number of control volumes (mesh cells) which, in FDS, are cubic and thus do not allow for exact representation of arbitrarily shaped objects.
- The state variables obtained by the numerical solution (such as temperature, pressure, etc.) are averaged within the cells and the accuracy therefore depends highly on the number of cells chosen.
- The temporal discretization is finite and depends on the time-step Δt.
- Initial and boundary conditions have to be chosen by the user. The initial velocity, for example, is usually assumed to be zero. This assumption does not hold for larger compartments in which a micro-climate or external influences (due to atmospheric winds or HVAC) may exist. The effects vary in their significance and should therefore be considered carefully.
- Various properties of the air have to be known, such as the density, specific heat, thermal conductivity, and viscosity. These values are functions of thermodynamic properties, such as temperature and pressure, and are determined experimentally (Knaust, 2009, p.39).
- In oder to account for radiative heat, additional properties, such the absorption coefficient, have to be known.
- The mixture fraction combustion model (McGrattan et al., 2009, Chapter 6) uses constant yields for CO_2, H_2O, CO, and soot which have to be defined by the user. Values are determined experimentally. A summary as well as numerical values can be found in Mulholland (2002); Purser (2002); vfdb-Leitfaden (2009). This approach leads to fixed amounts of these products being formed per unit time which persist indefinitely without further reaction.

- In under-ventilated fires, FDS uses a two-step reaction model to account for higher soot and CO production rates and local extinction due to the absence of oxygen. Further information on numerical combustion modeling can be found in Yeoh and Yuen (2009, Chapter 3).

The list is not to be considered exhaustive and shows that FDS—even though it is the most accurate tool available in FPE—incorporates various uncertainties. McGrattan et al. (2009, Chapter 4 of Volume 3) describe the various uncertainty effects based on the work by Hill et al. (2007) and attempt to provide some numerical values to quantify the uncertainties for various state variables.

Another drawback of the utilization of CFD is the high computational cost[2]. The equations above have to be solved for every time-step and in every cell of the computational mesh. Consequently, this leads to an increase of the computational effort by several magnitudes compared to the zone models. Generally, the accuracy of CFD models increases with a finer discretization. As FDS uses second order accuracy in space and time, a reduction of 50 % of the cell size reduces the discretization error by a factor of 4. Yet McGrattan et al. (2009, Volume 2,p.5) note that this does not necessarily reduce the output quantity errors due to the non-linearity of the equations. Additionally, a 50 % cell size reduction would increase the computational time by a factor of 16 as three space dimensions and the time dimension ($2^3 \cdot 2^1$) have to be considered. Therefore, it is highly advisable to perform a sensitivity study in order to find a compromise between accuracy and runtime. Usually, the mesh is gradually refined until the output values stabilize within a certain margin. Within this work, this is implicitly done with the refinement between the surrogate support point iterations as described in Section 6.6. A rule of thumb to find a sufficient cell edge length δx is based on the characteristic fire diameter D^* presented in Hill et al. (2007). Herein, D^* is dependent on the heat release rate $\dot{Q}$, so that

$$D^* = \left(\frac{\dot{Q}}{\rho_\infty c_p T_\infty \sqrt{g}} \right)^{\frac{2}{5}} \tag{4.2}$$

where ρ_∞ is the density (usually 1.204 kg/m^3), c_p the specific heat (1.005 $kJ/kg \cdot K$), and T_∞ the temperature (293 K) of the ambient air. g is the gravity (9.81 m/s^2). Values in the range $D^*/\delta x = 4 \ldots 16$ have been found to be appropriate for the discretization. The D^*-method implies that the discretization should be chosen proportional to the heat release rate. Further information can be found in Section 6.6.

[2]The CFD simulations constitute the bottleneck in the life safety analyses carried out herein.

4.2. Criteria and thresholds to determine ASET

In order to compute the time available for a safe egress, criteria and thresholds have to be defined. These thresholds are used for analysis of the outcomes of the numerical fire simulation and the point in time when the thresholds are underrun or overrun, respectively, is considered the available safe egress time (ASET). These criteria can be very manifold as a hostile fire has multiple effects on the occupants. Due to the smoke and heat released from the fire, the safe egress of the occupants can be delayed or detained–obviously with different levels of severity. As these threshold levels are usually based on various assumptions and limited data, it is essential for the designer to understand in detail how the data was derived and what implicit safety margins are involved. This also needs to be considered when calibrating a potential safety concept. The criteria, their origin, assumptions and backgrounds—which are sometimes rather empirical—are explained in detail in the following sections. As a conclusion, a new holistic measure will be derived which will be used for the examples in Chapter 7.

4.2.1. Implicit hazard criteria

The smoke generated by the fire is distributed throughout the fire compartment (and even further) by the buoyant convective currents of the fire and by naturally occurring air-currents (Drysdale, 1998; vfdb-Leitfaden, 2009). By definition from Mulholland (2002), smoke is "an aerosol containing a collection of liquid particles and gases from a combustion or pyrolysis process and the air that is entrained or mixed into the mass." The gases in the smoke can have asphyxiant or toxic/irritant effects when inhaled by the occupants or when settling onto mucous membranes (i.e. eyes).

Therefore, a common criterion is that the occupants shall not be affected by the smoke during the egress process. As the smoke is transported through the convective currents, a stratified flow will ideally be reached in simple geometries, where the upper layer is the smoke-filled layer and the lower layer is considered smoke free, or at least smoke-depleted, so that abidance in the lower layer is considered safe. This stratification is implemented in the zone models (see Section 4.1) and can also be observed in CFD simulation. Hence, a criterion is maintaining a given layer height for safe egress. This criterion is considered rather conservative, as the occupants are not exposed to any of the direct effects of the fire. In Germany, often times 2.5 m is used as threshold layer height (MVStättV, 2005), allowing the occupants to stand and walk upright and with the ability to see the emergency signs placed above the emergency exits—plus a safety margin. The ICC (2006) even requires 10ft ($\sim$3 m) for assembly facilities whereas Notarianni (2000) uses a lower height of 1.6 m to account for the face height of an average person and also analyzes for a layer height of 0.91 m (3ft) to consider a minimum crawl height as an ultimate limit for domestic buildings. The time available for safe egress is reached,

when the smoke layer descends below the chosen threshold value for the first time in the numerical simulation. If the threshold height is underrun, the safe egress can be considered delayed, as the people have to duck down or are already partly immersed in the smoke. At this point the smoke might have an impact on the occupants, such as different exit choice decisions and decreased movement speed or way-finding abilities (Purser, 2002).

Similar criteria which may delay the safe egress are decreased visibility or increased optical density; particles and droplets in the smoke obscure the visible light and thus the visibility to a certain degree. A visibility model for practical use in fire protection engineering is proposed by Jin (1978), who derives a model based on a threshold value for the human eye. To allow for a safe egress, the visibility of exit signs or of other elements of egress (doors, windows, etc.) has to be greater than the visibility threshold δ_c of the human eye. In his model, Jin (2002) assumes δ_c to be approximately between 0.01 and 0.05 and takes other parameters into account, so that his general formulation for the visibility leads to

$$V \approx \frac{1}{C_s} \ln\left(\frac{B_{EO}}{\delta_c k L}\right) \tag{4.3}$$

where C_s is the smoke density expressed by the extinction coefficient (1/m), B_{EO} is the brightness of the signs, k is a ratio between a scattering coefficient and the sum of the scattering and an absorption coefficient, and $L = 1/\pi$ is the mean illuminance of light from all directions in smoke. For reflective signs, Jin (2002) finds the visibility (in m) to be

$$V = \frac{(2 \sim 4)}{C_s} \tag{4.4}$$

and for light emitting signs

$$V = \frac{(5 \sim 10)}{C_s} \,. \tag{4.5}$$

Hence, a linear relationship is shown between the visibility and the extinction coefficient as $C_s \cdot V \cong$ const. for non-irritant smoke (Jin, 2002) and optical densities in the interval $0.1 \leq C_s < 0.25$, so that

$$V_1 = \frac{C}{C_s} \,. \tag{4.6}$$

Herein, the constant C is mostly chosen to be 6.0 as this has the best accordance with the experimental data from Jin (2002).

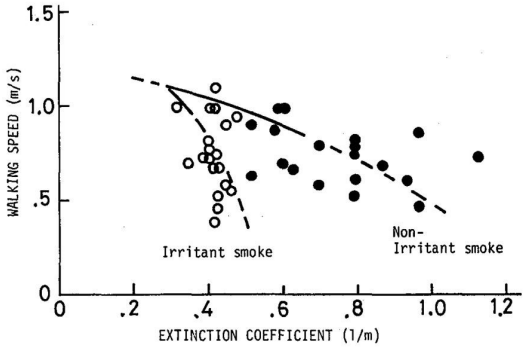

Figure 4.3.: Walking speed in smoke from Jin and Yamada (1985).

For irritant smoke and $C_s \geq 0.25$, Jin (2002) proposes to incorporate another term to account for the irritation of the mucous membranes and hence an overly proportional decrease of visibility for increasing extinction coefficients. Hence, the visibility can be computed to

$$V_1 = \left(\frac{C}{C_s}\right) \cdot (0.133 - 1.47 \log C_s) \,. \tag{4.7}$$

Jin (2002) observes a similar relationship between the walking speed and the extinction coefficient (shown in Figure 4.3) based on his experiments. This is backed by many other studies (Tubbs and Meacham, 2007; Purser, 2002; Bryan, 2002; Proulx, 2002; Nelson and Mowrer, 2002).

It should be noted that all the assumptions above are for homogeneous smoke. In reality, the smoke concentration, and hence the extinction coefficient and the visibility, can be subjected to local effects. When using CFD-simulations, the local visibility is based on the local extinction coefficient and is extrapolated. So the visibility in the homogeneous single cell might have a certain value but cannot be realistically extrapolated to adjacent cells. Forell (2010) proposes a methodology to assess inhomogeneous smoke based on CFD-simulations by additively using the single cell values of the extinction coefficient in the line of sight.

Various threshold values for a minimum visibility or a maximum extinction coefficient can be found in the literature. Jin (2002) states that extinction coefficients less than 0.1 will not have any effect on the occupants and the smoke will not contain any harmful toxic or irritant concentrations of fire effluents and therefore can be used as tenability limit. Values of 0.1 are also suggested in vfdb-Leitfaden (2009), while other sources use

Table 4.1.: Proposed threshold values for extinction coefficient and visibility from Jin (2002) and Purser (2002).

Familiarity/size	Extinction coefficient	Corresponding visibility
Unfamiliar	0.15 /m	13 m
Familiar	0.5 /m	4 m
Small travel distances	0.2 /m	5 m
Large travel distances	0.08 /m	10 m

a C_s of 0.2 (visibility 10-30 m) as the maximum tolerable extinction coefficient (Purser, 2002). Further values can be found in Jin (2002); Purser (2002). The latter also provide threshold values depending on familiarity and size of the compartment, as shown in Table 4.1. Purser (2002) proposes his thresholds to be used as fractional effective concentration

$$\mathrm{FEC}_{\mathrm{smoke}} = \frac{C_s}{\text{threshold } C_s} \overset{!}{\leq} 1.0\,, \tag{4.8}$$

so that the tenability limit is unity for easier application.

In summary, the tenability limits based on layer height or visibility can be considered rather conservative as the occupants are not exposed to potentially harmful concentrations of fire effluents. When reaching these tenability limits, the safe egress might be delayed and detained but might still be possible for the remaining occupants. In terms of a safety concept, these thresholds can be compared with a *serviceability limit* in structural design and not as an *ultimate limit* which would prevent a safe egress of the remaining occupants.

4.2.2. Asphyxiant gases

The effect of the inhalation of asphyxiant gases is usually twofold: either the oxygen level in the blood is decreased or the oxygen uptake capabilities of the blood are decreased leading to anemic hypoxia. The effects are similar to severe alcohol intoxication for lower doses and lead to lethargy or even euphoria before inducing unconsciousness. This may lead to incapacitation of safe egress (Purser, 2002). The major fraction of fire deaths can be traced back to asphyxiation by carbon monoxide (CO) and hydrogen cyanide (HCN). Further, CO_2 (over 5 %) and low oxygen concentrations (<15 %) can lead to asphyxiant effects.

Carbon monoxide (CO)

CO is the dominant byproduct of a fire and is considered the main reason for fire casualties. Gases with a potentially higher toxicity like HCN are released in lower concentration and therefore usually have a less severe impact. CO itself is flavorless and can not be sensed by olfactory cells when inhaled. Inhalation of CO combines with the hemoglobin in the blood and forms carboxyhemglobin (COHb), whereas the oxygen uptake capabilities are reduced and leads to anemic hypoxia as the affinity of the hemoglobin to CO is 250 times higher than to oxygen (O_2). Hence the CO intoxication is strongly correlated to increased COHb levels. Purser (2002) states that COHb levels of less than 30 % usually do not cause death while around 40 % cause incapacitation and 50-70 % are lethal for the majority of the population. The correlation between CO and COHb levels in humans is described by the Coburn-Forster-Kane (CFK) model which was modified by Steward (1975) for short term exposures based on experiments and simplified as a near-linear relationship. In his model, the COHb concentration can be calculated to

$$\%\text{COHb} = (3.317 \cdot 10^{-5})(\text{ppm CO})^{1.036}(\text{RMV})(t)\,, \tag{4.9}$$

where RMV is the volume of air breathed per minute (L/min) and t is the duration of exposure in minutes. RMV can be assumed to be around 25 L/min for an average adult in motion or 8.5 L/min for a resting adult. Based on this model, Purser (2002) develops an incapacitation model which uses unity for a conservative tenability limit so that

$$F_{I,CO} = \frac{(3.317 \cdot 10^{-5})(\text{ppm CO})^{1.036}(\text{RMV})(t)}{30\%\text{COHb}} \overset{!}{\leq} 1\,. \tag{4.10}$$

An overview of various threshold concentrations and their effects can be found in Bansemer (2004). Long term effects due to CO intoxication are presented in Christian (2001) but are not accounted for in the model above.

Hydrogen Cyanide (HCN)

The toxic potential of HCN is 20 times higher than that of CO. The effect bases on the cytotoxic hypoxia, meaning that the intra-cellular oxygen transport is blocked. In contrast to CO intoxication, HCN intoxications occur very quickly after exposure and enhance the respiratory frequency causing even more HCN to be inhaled during exposure. The effect of HCN is highly dependent on the concentration inhaled and increases exponentially over time. Based on multiple known concentrations that caused incapacita-

tion and the corresponding exposure time, Purser (2002) derives the time to incapacitation for HCN based on regression analysis and the corresponding exposure time to be

$$t_{I,HCN} = \exp(5.396 - 0.023 \cdot \text{ppm HCN}) \,, \tag{4.11}$$

so that the tenability limit based on unity yields

$$F_{I,HCN} = \frac{(\text{ppm HCN})(t)}{(\text{ppm HCN})(t_{I,HCN})} \overset{!}{\leq} 1.0 \,, \tag{4.12}$$

where t is the exposure time in minutes. An overview of various concentrations and their effects can be found in Bansemer (2004).

Carbon dioxide (CO_2)

Large amounts of CO_2 are usually released during a fire and its effect on the occupants must be considered also, even though the effects are less severe than those of the previously mentioned gases. Bansemer (2004) states that a concentration up to 5 % CO_2 can lead to increased respiratory frequency (hyperventilation), while larger concentrations may have an asphyxiant effect leading to incapacitation. Similar results are found by Purser (2002) who states that the respiratory mean volume (RMV) doubles at 3 % CO_2 and triples at 5 % CO_2. Based on his findings from multiple sources he deducts an equation for

$$\text{RMV}_{CO2}(\text{L/min}) = \exp(0.1903 \cdot \%\text{CO}_2 + 2.0004) \,, \tag{4.13}$$

and subsequently a hyperventilation factor

$$VCO_2 = \frac{\text{RMV}_{CO2}}{\text{RMV}} \,. \tag{4.14}$$

Herein, the reference RMV (the denominator in Equation 4.14) used by Purser (2002) is 7.1 L/min, accounting for a resting person. Hyperventilation factors for other RMVs are not given, so that 7.1 L/min will be used invariably.

For higher concentrations Purser (2002) also provides an incapacitation model in analogy to the CO model by using regression analysis between concentrations of incapacitation and the corresponding exposure time. The time to incapacitation from CO_2 can be calculated using

$$t_{I,CO2} = \exp(6.1623 - 0.5189 \cdot \%\,\text{CO}_2) \,, \tag{4.15}$$

so that the tenability limit based on unity yields

$$F_{I,CO2} = \frac{(\%\text{CO}_2)(t)}{(\%\text{CO}_2)(t_{I,CO2})} \overset{!}{\leq} 1.0 \,, \tag{4.16}$$

where t is the exposure time in minutes. An overview of various concentrations and their effects can be found in Bansemer (2004).

Oxygen (O_2)

O_2 is vital for the occupants to survive and therefore is not considered a toxic substance. Yet a lack of oxygen causes hypoxic hypoxia (Bansemer, 2004) and leads to incapacitation for low concentrations around 10-12 %, while the complete absence leads to death within several minutes. Based on studies of humans being exposed to low pressures to simulate high altitude from the 1970s, Purser (2002) developed a model to predict the time to unconsciousness based on regression analysis between the known points of oxygen vitiation to be

$$t_{I,O2} = \exp[8.13 - 0.54(20.9 - \%O_2)] \,, \tag{4.17}$$

where 20.9 is the percentage of oxygen under normal conditions at sea level. A tenability limit based on unity is defined as

$$F_{I,O2} = \frac{(20.9 - \%O_2)(t)}{(20.9 - \%O_2)(t_{I,O2})} \overset{!}{\leq} 1.0 \,, \tag{4.18}$$

where t is the exposure time in minutes. A more recent study about the incapacitation due to oxygen vitiation due to altitude, which confirms the findings from Purser's source, can be found in Asshauer (2006). An overview of various concentrations and their effects can be found in Bansemer (2004) and an overview of the times to incapacitation with the according concentration of the asphyxiant gases based on models shown previously can be seen in Figure 4.4.

4.2.3. Irritant gases

The current CFD model FDS 5.3 (2009) lacks appropriate pyrolysis and combustion models as well as transport equations for the manifold irritant gases that can occur during a fire. Additionally, source terms for those substances are rarely found and all effects on humans are not yet completely understood. Hence, herein the irritant substances have to be omitted in the simulations and thus will not be discussed in greater detail. To still account for their possible release, they were conservatively assumed to contribute with a total (lump-sum) of 0.3 in the FID model. This is obviously a very coarse approximation and only applicable to common scenarios without a known high release of these substances. For further information on the substances, the effects on humans, and the threshold modeling thereof, the reader is referred to the relevant literature, foremost Buff and Greim (1997) and Purser (2002).

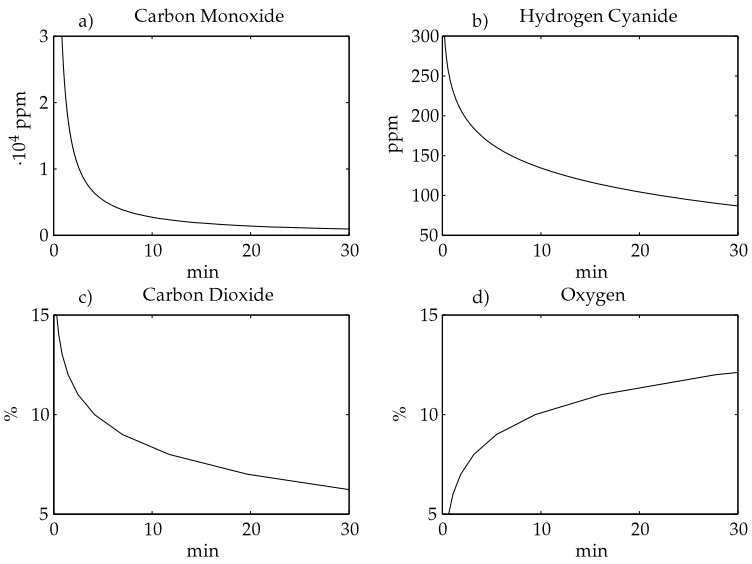

Figure 4.4.: Times to incapacitation for the asphyxiant gases based on the regression models from Purser (2002) for the defined time span up to 30 minutes.

4.2.4. Heat

Another direct hazard on the occupants is the heat generated by the fire. Occupants can be exposed to conducted, convected, and/or radiant heat. The effects of the heat can be separated into three different effects: hypothermia (heat stroke), skin burns, and thermal damage to the respiratory tract.

Hypothermia is a shock due to an increase of the body core temperature and normally needs a longer exposure to temperatures which do not cause skin burns. An increase of the core temperature to 40 °C causes unconsciousness and core temperatures over 42 °C are lethal. Hypothermia is rather unlikely to occur among occupants but can occur for firefighters who are exposed for longer times during fire fighting operation but wear protective clothing for peak heat exposure. According to Blockley (1973) hypothermia occurs for temperatures less than 120 °C for exposure times longer than 5 minutes. Notarianni (2000, Table 4-1, Chapter 4, Page 20) uses lower temperatures of 65 °C for incapacitation and 100 °C as lethal threshold and states the according references she compiled.

Skin burns are characterized by the degree of skin damage. Assuring a safe egress, it is anticipated that all occupants can leave the fire compartment without severe injuries. Hence, a threshold has to be set before severe burns can occur. Thermal damage to the respiratory tract occurs when hot gases are inhaled. The severity depends on the humidity of the gas and steam at 100 °C can cause severe damage down to the deep lung due to the high heat capacity of the water vapor. Respiratory tract damage is nearly always accompanied by severe burns of the facial skin. Thus, 120 °C can be used as a tenability limit for dry ($\leq$10 V-% H_2O) convective heat as this temperature causes pain for many people.

For radiant heat flux, 2.5 kW/m^2 is used as a tenability limit for pain (within approximately 5 minutes) in many codes and publications (vfdb-Leitfaden, 2009; BS 7974, 2001; ISO 13571, 2007; Purser, 2002). According to Purser (2002) this radiant flux is approximately reached if occupants pass underneath a hot gas layer of 200 °C. The direction of the radiant heat flux is neglected in this approach.

Based on various publications, Purser derives a regression model in order to estimate the time to incapacitation for convective heat. The model for radiant heat flux yields

$$t_{I,rad} = \frac{2.21}{q^{1.33}} \,, \tag{4.19}$$

and for convective heat

$$t_{I,conv} = 5 \cdot 10^7 T^{-3.4} \,, \tag{4.20}$$

where q is the radiant heat flux per unit area and T is the compartment temperature. It should be noted that $t_{I,rad}$ strongly tends to zero as $q > 2.5$ KW/m^2 (see Figure 4.5b). Slightly different threshold models can be found in ISO 13571 (2007) or vfdb-Leitfaden (2009) due to other regression models (Wieczorek and Dembsey, 2001). The various models are shown in Figure 4.5. The less conservative models could be used to assess tenability limits for fire fighting operation due to the protective clothing.

To account for both convective and radiant heat, a simplified additive model with unity as tenability limit is proposed so that

$$F_{I,H} = \left(\frac{1}{t_{I,rad}} + \frac{1}{t_{I,conv}} \right) (t) \overset{!}{\leq} 1.0 \,, \tag{4.21}$$

where t is the exposure time in minutes.

The criteria described in this section have a direct impact on the occupants and can cause incapacitation or can even be lethal, depending on the chosen threshold. When introducing his "barrier concept", Yung (2008) defines the ultimate barrier after a failure of safe egress as the rescue attempts of the fire department and, therefore, also considers lethal

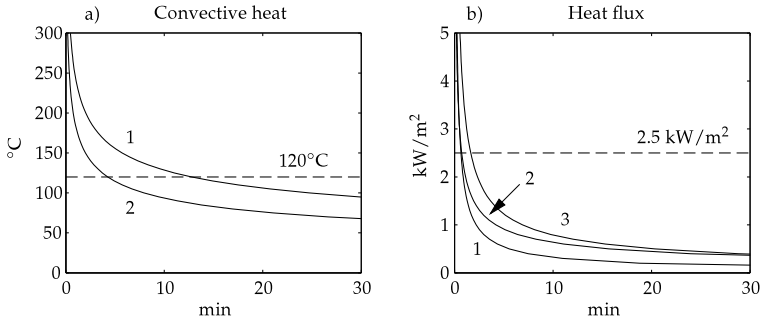

Figure 4.5.: Incapacitation times due to heat effects based on various regression models. a) convective heat (1 - heavy clothing, 2 - light clothing, bare skin). b) radiant heat (1 - Purser (2002), 2 - ISO 13571 (2007) for pain, 3 - ISO 13571 (2007) for burns)

doses as *ultimate limit*. In Germany, the codes for non-standard buildings (MVStättV, 2005, for example) explicitly do not allow this consideration (even though attempts to rescue incapacitated people would certainly be undertaken by German fire departments), so that the incapacitation thresholds implicitly consider a loss of life in this context. Hence, for the development of a safety concept, these incapacitation thresholds have to be compared with an *ultimate limit* in structural design as it prevents occupants from a safe egress by incapacitating them.

4.2.5. Threshold models

The criteria and the corresponding thresholds described above can be assessed in two different ways within numerical fire simulations. Either momentary threshold values can be considered, that is if a chosen threshold value or a tenability limit based on unity is reached for the first time. Another option is to integrate the effects over time to account for an accumulation effect which considers lower doses over time that can cause incapacitation even though the momentary threshold is not yet reached.

Momentary threshold models

Many simulation software tools calculate the values for the criteria (gas concentrations, temperature, flux etc.) at every time step so that these values can be analyzed for the chosen threshold value. The main problem here occurs with the sometimes very high oscillation within the data due to numerical effects, especially for small time steps. In reality,

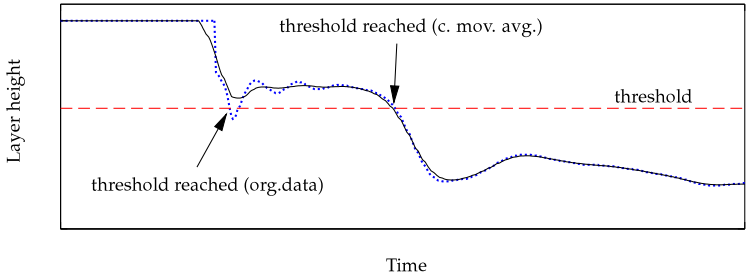

Figure 4.6.: Original data (dotted line) and central moving average smoothed data (solid line). It can be seen that the original data would produce a far more conservative result than the smoothed data.

oscillation effects at a fixed location also occur due to currents. Plain evaluation of the raw data for the time of transgression of a threshold can therefore lead to overly conservative results as shown in Figure 4.6. It is therefore recommended to apply a smoothing to the data. This corresponds very well to the doses-time relations which were discussed in the previous sections. It is proposed to use the central moving average smoothing (Mendenhall and Sincich, 1996) for the value $\bar{y}_t$ at time t based on n neighboring time steps so that

$$\bar{y}_t = \frac{y_{t-(n-1)/2} + \ldots + y_t + \ldots + y_{t+(n-1)/2}}{n}, n = 2k+1, k \in \mathbb{N}. \tag{4.22}$$

n should be chosen to represent the time span of the exposure which is used as threshold. The central moving average method can be regarded as a high-cut (low-pass) filter which filters high (unwanted) frequencies. The higher the number of neighboring points n is chosen, especially for large time steps Δt, the lower are the frequencies filtered, which can lead to unwanted filtering for long exposure times $(n \cdot \Delta t)$. Figure 4.6 shows the effect of the filter for a layer height evaluation. The original data produces an oscillation below the threshold which would lead to conservative results. The smoothed data filters this oscillation and leads to a better result. In reality a (slight) drop of the smoke layer below the threshold for a few seconds will not delay or detain the safe egress. Large drops for longer periods of time below the threshold would be accounted for if $(n \cdot \Delta t)$ is appropriately chosen. It should be noted that this procedure should not be applied to the ultimate thresholds, as, for example, a short burst of heat or radiant flux will cause instant incapacitation but is likely to be smoothed out. For the ultimate limits, a time-integrated model should be considered.

Integrated threshold models

Time-integrated threshold values should be used for heat and toxicity assessment to consider exposure to lower doses during a longer time-span which can also lead to incapacitation. The most well-known model for assessing criteria over time was developed by Purser (2002) incorporating the equations from the previous sections. Instead of looking at short term exposure times, the exposure is integrated over time (t) from the start of the fire so that

$$F_I = \int_t \frac{C(t)}{C(t) \cdot t_I[C(t)]} dt \,, \tag{4.23}$$

where $C(t)$ is the concentration or dose of the criteria which changes over the time during a fire and $t_I[C(t)]$ is the time to incapacitation at the concentration or dose $C(t)$. The numerical simulation gives concentrations or doses C_t for every time step Δt while they are constant in between. Hence, Equation 4.23 can be transformed to the discrete form

$$F_I = \sum_{t=0}^{t_n} \frac{C_t}{C_t \cdot t_I(C_t)} \cdot \Delta t \,, \tag{4.24a}$$

$$= \sum_{t=0}^{t_n} \frac{\Delta t}{t_I(C_t)} \overset{!}{\leq} 1.0 \,, \tag{4.24b}$$

where t_n is either the time until unity (tenability limit) is reached or the end of the simulation. With this approach, the dose is accumulated over the time of the fire so that the whole exposure history during the time needed for escape is accounted for. To be on the safe side, the physical absorption over time is disregarded in this model. Using this model, short time peaks are not filtered to remain on the safe side, but are buffered as the short time span of the peak is also considered within. F_I has a continuous growth over time and the steepness of the slope denotes the concentration.

4.2.6. Considering multiple criteria

The threshold models described in the previous sections can be used with the criteria presented to assess the time of incapacitation (ASET). The selection of the appropriate criterion can be difficult as it is unknown which one will be reached first. For an analysis they all have to be evaluated and the criterion with the shortest time to incapacitation has to be regarded. Assessment and comparison of various criteria and threshold values was done by Notarianni (2000) for domestic dwellings and by Albrecht and Hosser (2009) for an assembly hall. Both studies state the importance to consider all fire effects as the relevant criteria differs depending on many parameters.

Purser (2002) presents a simple additive model for the asphyxiants, which is similar to the additive heat model and also incorporates irritant gases contribution to hypoxia

(FLD_{irr}). He states that interaction effects are negligible and are not considered on the safe side. Additionally, the hyperventilation effect of CO_2 from Equation 4.14 is taken into account, so that the fractional effective dose model (FED) for asphyxiant gases yields

$$F_{I,\text{asphyx.}} = \max \begin{cases} (F_{I,CO} + F_{I,HCN} + FLD_{irr}) \cdot V_{CO2} + F_{I,O2} \text{ ,} \\ F_{I,CO2} \text{ .} \end{cases} \tag{4.25}$$

This model was simplified and generalized in ISO 13571 (2007) where all asphyxiant gases are simply added up. Yung (2008) bases his FID-threshold (fractional incapacitating dose) on unity, but only incorporates CO and the hyperventilation effects of CO_2. A more general formulation of the FED can be found in Speitel (1996) to also account for the heat effects $F_I = F_{I,\text{Gases}} + F_{I,\text{Heat}}$ so that only *one* value has to be smaller than unity for a verification of a safe egress.

To incorporate a safety margin, often times F_I-values far less than unity are chosen to determine the time of incapacitation. Notarianni (2000) and vfdb-Leitfaden (2009) propose 0.1 or 0.3 for incapacitation depending on the occupancy. NFPA 101 (2008) proposes the FED to be 0.3 for incapacitation and 0.8 as lethality limit. Similar values can be found in other codes and standards while only few use unity as a threshold to stay conservative.

4.3. Evacuation modeling

Besides the assessment of the time to untenability (ASET, $t_{avail.}$) using fire simulation tools, the "other side" also has to be regarded, which is the time needed for safe egress into a place of relative safety (RSET, $t_{req.}$) in a performance-based life safety assessment. The analysis of the required safe egress time to evacuate all occupants to a place of relative safety usually consists of various phases which are visualized in Figure 4.7. It becomes obvious that the actual crowd movement simulation can only be considered a part of the overall time needed. RSET or $t_{req.}$, respectively, is usually defined as

$$t_{req.} = \Delta t_{\text{warning}} + \Delta t_{\text{pre-movement}} + \Delta t_{\text{movement}} \text{ .} \tag{4.26}$$

Warning time usually includes the time until the fire is detected by either an automatic alarm system or the occupants. Fire detector actuation times usually range from 1-3 minutes. Further details including citations are given in Tubbs and Meacham (2007, p.292) or vfdb-Leitfaden (2009, Chapter 7.2). Additional time after the initial detection is required

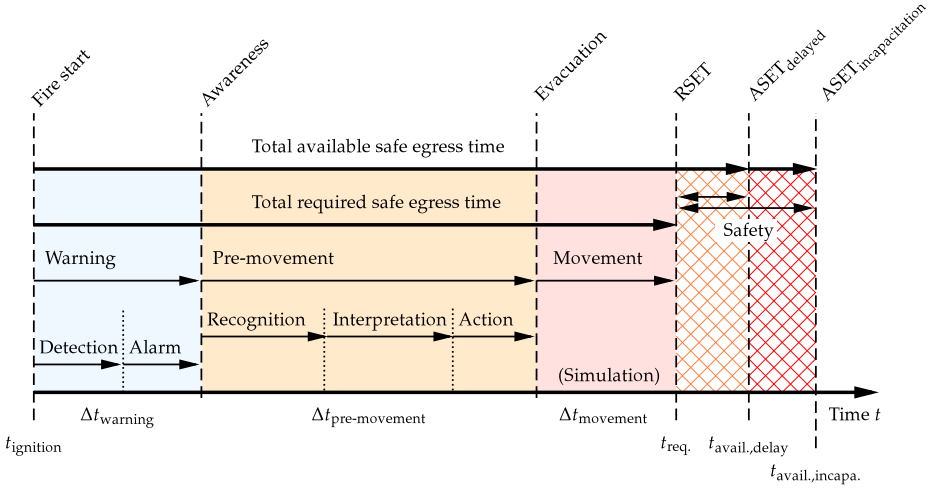

Figure 4.7.: Phases and time spans of evacuation in chronological order. It can be seen that the simulation of the occupants' movement is only one of many input parameters. The time (if exists) between REST and ASET can be considered a safety margin.

to alarm other occupants. This can be, for example, the processing time of the fire alarm system (NFPA 72, 2002) or the time for the occupants to become aware of the dangerous situation until first action is taken. Bryan (2002) gives an overview on the perception and interpretation of alarm cues.

The pre-movement time can also be sub-divided into several phases, namely the recognition phase, where the occupants become aware of the cue; the interpretation phase, where the signal is interpreted by the occupants; and the action phase, where attempts of fire fighting, acquisition of further information, or collection of personal items are undertaken. Obviously, all these times are individual for every occupant and are highly dependent on several factors, such as the building and occupancy type, the fire alarm system specifications, alertness, and familiarity of the occupants with the premises, etc. Extensive studies on the pre-movement time by analyzing previous fire events were carried out by Proulx (2002) who gives numerical values for the pre-movement time in the range from less than 1 minute until greater than 15 minutes. Purser (2002) uses such information to develop a model to assess the pre-movement time based on occupancy-specific information. A related model can be found in vfdb-Leitfaden (2009, Section 9.3). Pre-movement times can be estimated based on the several aspects shown above. The method provides two values which are considered the 1-percentile and the 99-percentile of the pre-movement time assuming an underlying right-skewed distribution. The values are empirically determined based on assessment of fire incidents and evacuation drills, and range from less than 1 minute to greater than 25 minutes. Especially the larger values do not have a sufficient statistical basis and thus have to be used carefully. A similar table can be found in Tubbs and Meacham (2007, p.294).

4.3.1. Crowd movement simulation

The actual egress process can be simulated numerically by finding appropriate mathematical models to describe the crowd behavior. This can be done in different levels of complexity. The accuracy of the models is usually verified by comparing the results to either evacuation drills or other verified egress simulation tools. State-of-the-art tools can even consider the interaction of smoke and the occupant movement. The following sections should be merely an introduction in the modeling approaches and assumptions within the models. A very comprehensive compilation of the currently available models can be found in Kuligowski (2002).

Hydraulic models

The idea of this approach is to consider the occupants as a virtual homogeneous fluid that flows out the exits. Hence, the term *hydraulic* model was established. The parameters, such as pre-movement time, speed, etc. are not assigned individually. A very simple approach is the model underlying the German assembly code (MVStättV, 2005). Therein, the exit doors are assumed to have a certain outflow rate given in occupants per meter door width and unit time ($\frac{P}{m \cdot s}$). This yields a first idea of the magnitude of the required egress times and exit capacities.

An advanced hydraulic model was developed by Predtechenskii and Milinskii (1978) who use empirical correlation between the occupant density and the speed of movement in various situations (normal, danger, stairs, bottlenecks, etc.). The model is scalable from simple rectangular rooms to complex geometries and even considers individual parameters via body sizes. The exit selection has to be done by the user. So-called network models are an advancement of hydraulic models which may have algorithms for individual behavior, such as exit selection, due to the underlying "network" on which the occupants move.

Individual models

The more advanced models consider all occupants individually and thus are called *individual* models. Various algorithmic approaches exist and are described and compared in Kuligowski (2002). The model used for the examples herein is the FDS+evac "social force" model developed by Korhonen and Hostikka (2009) which treats the occupants (named "agents") individually by solving the two-dimensional equation of motion

$$m_i \frac{d^2 \mathbf{x}_i(t)}{dt^2} = \mathbf{f}_i(t) + \boldsymbol{\xi}_i(t) \tag{4.27}$$

for each occupant i. In this equation, $\mathbf{x}_i(t)$ denotes the position and $\boldsymbol{\xi}_i(t)$ is a random fluctuation at the time t of the agent i. $\mathbf{f}_i(t)$ is a combined directional force on the agent as shown in Figure 4.8 which consists of the various forces acting on the agent so that

$$\mathbf{f}_i = \underbrace{\frac{m_i}{\tau_i}(\mathbf{v}_i^0 - \mathbf{v}_i)}_{\text{movement force}} + \underbrace{\sum_{j \neq i}(\mathbf{f}_{ij}^{soc} + \mathbf{f}_{ij}^{c} + \mathbf{f}_{ij}^{att})}_{\text{agent-agent (social)}} + \underbrace{\sum_{w}(\mathbf{f}_{iw}^{soc}\mathbf{f}_{iw}^{c})}_{\text{agent-wall}} + \underbrace{\sum_{k} \mathbf{f}_{ik}^{att}}_{\text{agent-environ.}} , \tag{4.28}$$

where the first term is the movement force with the agent's mass m and a relaxation parameter τ. The first sum describes the agent-agent interaction forces, namely social, contact, and attraction forces based on an empirical model, such as Helbing and Molnar (1995). The second sum are the agent-wall interactions, again sub-divided into social

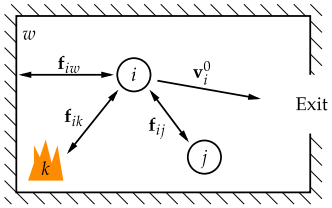

Figure 4.8.: Schematic representation of the forces acting on agent i in Equation 4.28. The vectors are not to scale.

and contact forces. The last sum describes additional forces, for example for agent-fire interaction. $\mathbf{v}^0$ is a vectorial flow field (hence $|\mathbf{v}^0|$ is the occupant's desired speed towards an exit). FDS+evac uses the algorithm from FDS to calculate this two-dimensional flow field assuming a highly viscous liquid. For more detailed information on the model and assumed numerical values for the variables introduced above, the reader is referred to the appropriate references, such as Korhonen and Hostikka (2009, Chapter 3), Helbing and Molnar (1995), Korhonen et al. (2008) etc.

The numerical cost of the FDS+evac is rather low compared to the CFD fire simulation. This is mainly due to the fact that the problem is only two-dimensional. Yet as the Equations 4.27 and 4.28 and the sub-models have to be solved for every agent and every time-step the numerical effort is dependent on the chosen number time-steps and the number of occupants as well as the complexity of the model (number of walls etc.).

Behavior in the fire

The models described are mathematical formulations of human behavior and thus are subjected to uncertainties. Additionally, humans have a tendency to be non-predictable and occasionally irrational behavior when exposed to high stress levels from unknown, unpredictable, and dangerous situations. Examples of this behavior can be found in Bryan (2002). The model described above also requires various input parameters, which are either completely unknown or based on empirical studies, mainly evacuation drills where no immediate hazard occurred so that the values derived can not be applied to real incidents without further considerations. This has to be accounted for in the scenarios assumed.

4.4. Design scenarios

All the methods, assumptions, and models described above for both—fire and egress simulation—are state-of-the-art approaches used in FPE. Considering the high and sometimes not quantifiable uncertainties involved in the process of life safety design, the fire protection engineer is obliged to use conservative assumptions and scenarios, namely the design scenarios which can be considered as an envelope around possible events, each with a probability of occurrence and a magnitude of impact. This allows for direct risk assessment as described in Chapter 2.

In order to find relevant design scenarios for life safety analysis, it is most suitable to compile all possible events and the corresponding probabilities into a so-called event tree as described i.e. by Yung (2008, p.55ff). This allows for a calculation of system failure probabilities as described in Section 5.5.5. Consequences of each branch in the event tree can be compiled in an absolute or relative manner so that numerical risk analysis can be performed. A simplified event tree can be seen in Figure 4.9. In that example three scenarios have to be analyzed using the IMLS response surface method described in Chapter 6 in order to calculate the probability of harming the health or life of *at least one of the occupants*. The threshold criterion has to be chosen carefully. To obtain fully comparable risk information, it is advised to use one criterion for all scenarios. A gradual approach is also possible (i.e. optical density for the desired scenario 1 and FED for the undesired yet possible scenarios 2 and 3) which rudimentary allows for the consideration of the likelihood of the scenario (compare Section 3.3).

Correlation effects (i.e. between occurrence of a fire and occupancy) are usually neglected in event tree analyses. For many problems, this assumption may be sufficient. Yet a critical review of possible interactions between events, etc. has to be performed when compiling an event tree (see Section 5.5.5).

It is evident that a nearly infinite number of branches can be found theoretically. In order to avoid overly complicated systems, the branches are chosen as envelopes for further sub-scenarios and thus contain conservative assumptions to some degree. This could, for example, mean that the occupancy-level is assumed to be rather high in order to account for all possible events even with fewer occupants present. The assumptions made herein will be described in the following sections. Further examples for enveloping design scenarios are the eight required design fires described in Table 4.2 and NFPA 101 (2008, Section A5.5.3,p.89f). More information on the development of performance-based design scenarios can be found in Rosenbaum et al. (2007, Chapter 8).

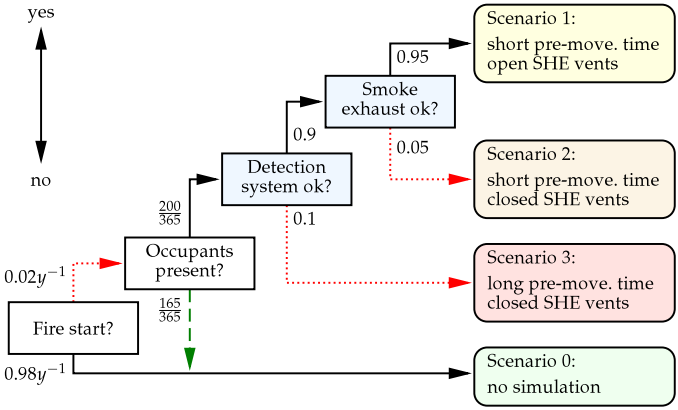

Figure 4.9.: Exemplary event tree for a life safety problem in an assembly building which hosts events on 200 days per year with two fire protection barriers installed (detection system and smoke and heat exhaust). The dotted red arrows denote the undesired paths, the solid black arrows denote the desired or planned paths, and the dashed green arrow implies fortune circumstances. The event tree yields the yearly probability of at least one occupant to be harmed or incapacitated.

4.4.1. Design fires

The definition of the fire scenarios to be investigated with the methods described above is the most crucial part in performance-based design. The fire has to be chosen in a way that the results produced envelop potential fire scenarios on the safe side. Yet overly conservative and thus unlikely scenarios can lead to very costly solutions in order to comply with the protection goals. NFPA 101 (2008, Section A5.5.3,p.89f) describes eight design fire scenarios that have to be considered in order to provide for life safety. Scenarios can be omitted if sufficient evidence is given that they cannot occur. Additionally, the omitted scenarios have to be briefly evaluated for potential consequences. This could be done within event trees: if a scenario is unlikely to a certain level, it can be omitted if the assumed consequences are also low. Otherwise, detailed analysis has to be performed. The eight scenarios are summarized in table 4.2. NFPA 101 (2008, Section A5.5.3, p.89f) explicitly states that the so-called t-squared fires are not required as they are considered too conservative for life safety purposes, leaving the engineer to select suitable fires or to utilize pyrolysis models to directly simulate the possible fire development, if applicable.

Table 4.2.: Design scenarios for life safety required in NFPA 101, adopted from Tubbs and Meacham (2007, Table 7-1, p.278).

Scenario	Purpose
1	*Occupancy-specific fire*. Addresses occupant activities, number and location of rooms, size, furnishings and contents of rooms, fuel properties and ignition sources, ventilation conditions, and first item ignited and its location.
2	*Ultrafast-developing fire* within the primary means of egress.
3	*Ignition in a normally unoccupied room* adjacent to a room with a large number of occupants. Addresses unoccupied ignition.
4	*Ignition in a concealed wall or ceiling space* adjacent to a large, occupied room.
5	*Slowly developing fire* shielded from fire protection systems near high-occupancy area.
6	*Largest fuel possible* in a given occupancy during normal operations with severe-case fuel types, geometries, and configurations. Addresses rapidly developing fires with occupants present.
7	*Exterior exposure fire*. Addresses external fire spread into or blocking egress from an area of concern, or developing untenable conditions.
8	*Ignition in ordinary combustibles with ineffective passive or active fire protection systems* in the room of origin. Addresses unavailability of systems.

The t-squared fire, modified for life safety applications

The t-squared fire is the most commonly chosen design fire. In this scenario, the rate of heat release (HRR, $\dot{Q}$) is prescribed assuming that a fire will spread exponentially until a maximum HRR is reached. When reaching the maximum HRR, the fire burns steady until 70 % of the fire load is consumed. This phase is often called "plateau". After 70 % of the fire load is consumed, the HRR decays linearly until all the fire load is completely consumed. This approach is based on the work of Heskestad (1984) who analyzed the heat release of fire plumes and found the quadratic increase after an *incubation period*. The growth rate is usually expressed by α or the time t_g to reach 1 MW, respectively. In order to design for structural resistance, sprinkler effectiveness, etc., the incubation phase is usually omitted since no significant heat release rates and thus temperatures are reached in that phase, which can be in the magnitude of several ten minutes as the examples in Peacock et al. (1999) show. The plateau and decay phases can be seen as the envelope described above and are shown in Figure 4.11.

This design fire is also often applied to life safety problems leading to very short ASET values. Considering the empirical safety factors, as described in Section 3.2.1, it can be very difficult to provide for life safety in performance-based approaches using such conservative assumptions. Yet tragedies such as "The Station Fire" (Tubbs and Meacham, 2007, p.83) sadly show that such scenarios are not impossible—but rather improbable.

On the other hand, the incubation phase of the fire might not have an influence on the structural integrity, but it might significantly impact the course of events in life safety, such as the reduction of the pre-movement time due to occupant reactions to fire cues (visible smoke, smell, etc.) or the activation of smoke detectors (vfdb-Leitfaden, 2009, p.55) and connected systems such as smoke and heat exhaustion systems as shown in Figure 4.9. Brein and Hegger (2005) account for the incubation time by qualitatively assuming a linear increase of the heat release rate until enough energy is released to start the quadratic fire growth phase with the *t*-squared approach.

Based on the considerations above, a new life safety design scenario is introduced, which combines the incubation and growth phases in order to provide for a reasonable and yet conservative design. In order to make the scenario compatible with current state-of-the-art the quadratic growth phase is retained along with the time t_g (or α, respectively) in seconds to reach a heat release of 1 MW. To account for the incubation phase mentioned by Brein and Hegger (2005), a linear phase is prefixed. Analyzing the heat release curves of the experimental data in Peacock et al. (1999), the incubation phase is, on average, slightly longer than the quadratic growth phase to 1 MW as shown in Figure 4.10. This can also be seen in Yung (2008, Figure 7.3,p.75). For the sake of simplicity and conservativeness, a full correlation between the incubation time t_i and the time to 1 MW t_g is presumed, so that $t_i = t_g$. This allows for an easy applicability and accounts for the fire growth rates of the assumed fire load. The applicability and conservativeness of this approach is shown in Figure 4.10 in comparison to the traditional *t*-squared fires and the heat release of an actual full-scale fire test. The course of the heat release rate of the new design fire is qualitatively shown in Figure 4.11.

Further assumptions have to be made regarding the heat release rate $\dot{Q}(t_i)$ at the time t_i. The value of $\dot{Q}(t_i)$ must have the energetic potential to initialize the exponential fire growth without being too conservative at the same time. For that reason, current standards for the ignitability and flammability of materials and structural elements were analyzed, such as the single burning item (SBI) test for building products (DIN EN 13 823, 2009) or the "room corner" test described in DIN EN 14 390 (2007, similar to ISO 9 705). In these tests, the building products are exposed to the thermal attack of a burning item, which is simulated by a defined burner. This is in perfect analogy with the interpretation of the incubation time in the literature, such as vfdb-Leitfaden (2009). The burner output ranges between 30 kW (SBI) and 100 kW (room corner). This is in the range of the incubation phase heat release rates measured by Peacock et al. (1999). As the maximum heat

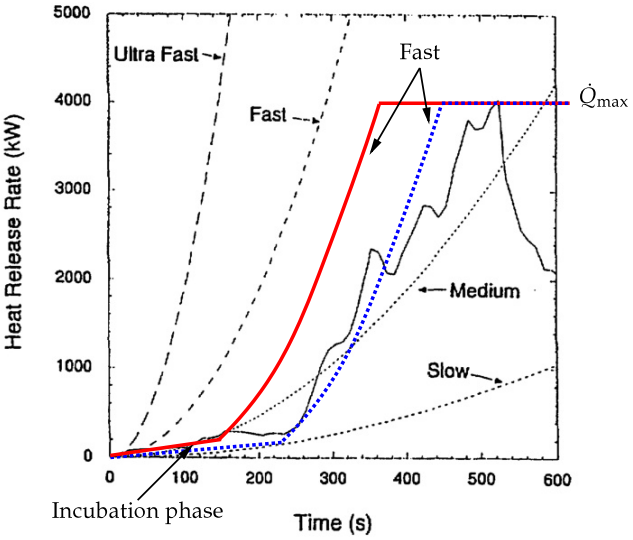

Figure 4.10.: Derivation of the modified t-squared fire based on the findings by Madrzykowski (1996). The comparison shows a full-scale fire of an office work station and the new and traditional t-squared design fires. The solid red line shows the modified t-squared design fire ($t_i = t_g$) which can still be considered to envelope the fire conservatively. The dotted blue line shows the best fit modified t-squared fire with $t_i > t_g$ based on an incubation time of 230 s and a "fast" fire growth thereafter. Adopted from Madrzykowski (1996).

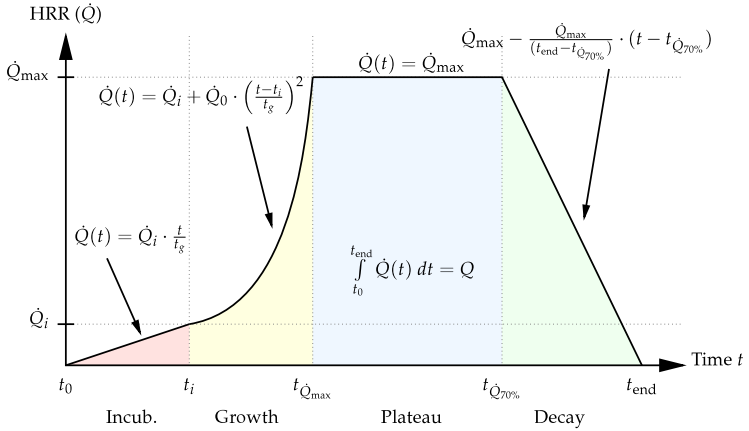

Figure 4.11.: Schematic course of the heat release rate of the modified t-squared fire along with the mathematical formulation of the HRR with respect to time. $\dot{Q}_i$ denotes the maximum HRR in the incubation phase and is defined as $0.02 \cdot \dot{Q}_{max}$. Not to scale.

release rates of local natural fires for life safety design are usually chosen in the range of 3-5 MW and under the simplifying assumption that $\dot{Q}_{max}$ and $\dot{Q}(t_i)$ are fully correlated, it will be presumed that $\dot{Q}(t_i) = 0.02 \cdot \dot{Q}_{max}$. This leads to $\dot{Q}(t_i)$-values of 60-100 kW for the common range.

In mathematical terms, the heat release rate from Figure 4.11 can be expressed as the piecewise function

$$\dot{Q}(t) = \begin{cases} 0 < t \leq t_i\,, & 0.02 \cdot \dot{Q}_{max} \cdot \frac{t}{t_g}\,, \\ t_i < t \leq t_{\dot{Q}_{max}}\,, & 0.02 \cdot \dot{Q}_{max} + \dot{Q}_0 \cdot \left(\frac{t-t_i}{t_g}\right)^2\,, \\ t_{\dot{Q}_{max}} < t \leq t_{\dot{Q}_{70\%}}, & \dot{Q}_{max}\,, \\ t_{\dot{Q}_{70\%}} < t \leq t_{end}, & \dot{Q}_{max} - \frac{\dot{Q}_{max}}{(t_{end}-t_{\dot{Q}_{70\%}})} \cdot (t - t_{\dot{Q}_{70\%}})\,, \\ t > t_{end}, & 0\,, \end{cases} \tag{4.29}$$

with $t_i = t_g$ and $t_{\dot{Q}_{70\%}}$ denoting the time at which 70 % of the fire load is consumed. $\dot{Q}_0$ is usually chosen to be 1 000 kW. All units are given in kilowatts (kW). This design fire—along with the appropriate modifications—can be used in the design scenarios 1,3, and 5-8 of NFPA 101 (2008, p.89f), see Table 4.2. The ultra-fast scenario 2 is tackled by omitting the incubation phase, while the concealed-space scenario needs more considerations due to space constraints. All design fires can be additionally modified to account for

the effect of active and passive fire protections system as described in Chapter 7 or in the relevant literature, such as Dehne (2003, Chapter 4), vfdb-Leitfaden (2009, p.79f), or Tanaka et al. (2010). If applicable, the effects can also be investigated within the CFD simulation (i.e. the effect of ventilation systems or sprinklers if the models are sufficiently validated).

For the probabilistic approach herein, the prevailing parameters to be treated stochastically are the time to 1 MW (t_g), the maximum heat release rate ($\dot{Q}_{\max}$) and the various yields for smoke and toxic effluents (CO, HCN, Soot). The fire load, which has a high sensitivity in structural fire design (Hosser et al., 2008), can be omitted herein as preliminary studies have shown that the parameter is irrelevant for the life safety analysis as it merely controls the length of the fire (Albrecht and Hosser, 2009; Albrecht et al., 2010).

4.4.2. Egress design

In deterministic performance-based approaches, usually the occupancy is chosen to full capacity in order to obtain conservative and enveloping results. Current codes provide values in the unit occupants per square meter, assuming that the entire floor area is homogeneously filled with people. Additional considerations are made for exit selection, walking velocities, pre-movement times, or percentages of adults, children, and disabled occupants based on the type of building, etc.

In a probabilistic approach, all the variables above can be assumed to follow statistical distributions. Many possible parameters have to be considered, making the probabilistic problem high-dimensional. Yet for some parameters, stochastic models do not exist or can only be assumed while others are irrelevant in the problem as their contribution to the total variance is very limited. The latter can be assessed with a preceding sensitivity analysis prior to the reliability analysis (rf. Section 6.1). This reduces the dimensionality and thus increases the performance of the reliability analysis.

For the analyses herein, the critical parameter distributions will be found on a single case basis. Conservatively, occupancy-levels are chosen to be rather high with possible overcrowding. This is important as catastrophic events, such as “The Station Fire,” have shown that overcrowding, and thus the number of occupants, can be a controlling variable. This effect was also shown in Albrecht et al. (2010) when performing sensitivity analyses for life safety analyses. The scenarios for the egress simulations chosen herein are dependent on the underlying fire scenarios as they might, for example, imply that some emergency exits become unavailable or influence the exit choice of the the occupants.

4.5. Conclusions

An introduction to the numerical models for fire and evacuation simulation at different levels of complexity was given in the previous sections along with the implicit uncertainties and simplifications of and within the models. Subsequently, criteria and threshold values are necessary to assess the tenability limit of a compartment. An overview of a broad variety of current models and the assumptions and considerations within are given based on a literature review of various international publications. It was found that many of the threshold models are based on animal experiments and subsequent extrapolation of the results (Purser, 2002) and hence incorporate some uncertainty. Assumed numerical values for the uncertainties can be found in ISO 13571 (2007). For ethical reasons, these uncertainties will be disregarded in the further work and the thresholds will be chosen conservatively–providing an unknown margin of safety. It is proposed to use the criteria that might delay egress as a serviceability limit while the criteria with direct effects on the occupants should be used as an ultimate limit. In addition to the overview, new threshold models for both categories are presented and the necessity of considering multiple criteria is discussed and mounted into the derivation of the fractional incapacitation model (FID), which includes asphyxiant, irritant and heat effects of smoke and heat generated by the fire.

A closer look was taken at the design fire scenarios and their corresponding design fire prescribed by HRR curves. Looking at various fatal fire events in assembly type buildings, various scenarios are proposed based mainly on the NFPA 101 (2008). An adaptable design fire based on the so-called t-squared fire considering the fire incubation phase was proposed based on a literature review of fire tests.

Chapter 5

Reliability analysis

In Chapter 2, an introduction to risk and risk assessment was given. As the consequences of loss for life safety are difficult to assess and might even lead to ethical problems, the focus herein is on the reliability evaluation in order to assess risk. In this Chapter, the mathematical background of the reliability methods used in Chapters 6 and 7 is given.

At first, randomness and random variables are defined and an introduction to the reliability problem and the current approaches is given along with remarks on data mining and especially sampling strategies, which can lead to a major increase in the speed and accuracy of reliability solvers. As computationally "expensive" CFD models should be utilized for the reliability assessment, the main idea of this Chapter is to identify potential optimization means for the derivation of the accurate and fast reliability algorithm with as few as possible solver runs (which will be introduced in Chapter 6).

As fire protection components can be regarded as "barriers" in a whole fire protection system, probabilistic system analysis has to be carried out. To avoid the high numerical effort of regarding all limit states at once—which also leads to nearly a incomputably complex limit-hyper-surface—some assumptions and simplifications for the system analysis herein are shown.

5.1. Univariate random models

In order to describe physical phenomena with random occurrences or magnitudes, often times random variables are utilized. These can be very manifold and versatile. In order to analyze random variables and to use them in probabilistic calculations they have to be based on values which are possible to be measured or assessed. Schneider (1994) names these variables "basic variables". Single occurrences of these basic variables are random

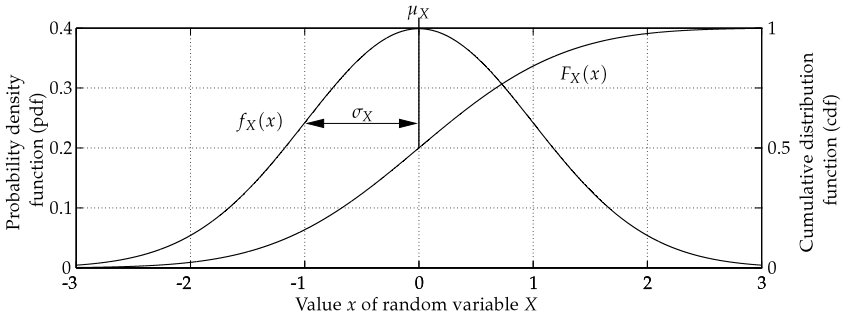

Figure 5.1.: Scheme of cumulative distribution function (cdf) and probability density function (pdf) for a standardized normal (Gaussian) distribution.

occurrences of the statistical population within a predefined interval. The basic variable can be described by a mathematical function

$$X : \omega \to X(\omega) \in \mathbb{R} \,, \tag{5.1}$$

where ω is a random occurrence of the entire population Ω. The variables and thus the describing functions can be either discrete or continuous and can have different properties. The describing functions $F_X(x)$ are called probability distribution functions (pdf) or cumulative distribution functions (cdf) and link the random event ω to a real number $x \in \mathbb{R}$. The probability of an event x yields

$$F_X(X) = P(X \leq x) = \int_{-\infty}^{x} f_X(u)\, du \,, \tag{5.2}$$

where $f(x)$ is the pdf and thus the derivative of the cdf (Bronstein et al., 2008). As real numbers have to be larger than $-\infty$ and smaller than $+\infty$, the limits of the cdf are

$$\lim_{x \to -\infty} F_X(x) = 0 \,; \quad \lim_{x \to +\infty} F_X(x) = 1 \,, \tag{5.3}$$

and accordingly

$$\int_{-\infty}^{+\infty} f_X(u)\, du = 1 \,. \tag{5.4}$$

Instead of describing a variable with a probability function, it can sometimes be useful to only characterize variables with the expected value (or mean value or ensemble average) and the variance which are considered the first and second statistical moments of a normal distribution as shown in Figure 5.1. For the continuous case, the expected value of X can be computed to

$$\mu_X = \mathrm{E}(X) = \int_{-\infty}^{\infty} x f_X(x)\, dx\,, \tag{5.5}$$

and the second statistical moment, the variance, yields

$$\sigma_X^2 = \mathrm{Var}(X) = \mathrm{E}[(X-\mu_X)^2] = \int_{-\infty}^{\infty} (x-\mu_X)^2 f_X(x)\, dx\,, \tag{5.6}$$

where σ_X is the standard deviation of X. Often times, a dimensionless coefficient of variation is used, which is defined $V_X = \frac{\sigma_X}{\mu_X}$. The definitions of the further statistical moments, such as skewness and kurtosis, can be found in Bronstein et al. (2008).

The most common statistical distribution, especially for application in physical and technical problems, is the normal or Gaussian distribution shown in Figure 5.1. A random variable is called normal distributed if the probability density function yields

$$f_X(x) = \frac{1}{\sqrt{2\pi}\sigma_X} \exp\left[-\frac{(x-\mu_X)^2}{2\sigma_X^2}\right]\,,\ -\infty < x < \infty\,. \tag{5.7}$$

The cumulative distribution function F_X can be found using the normal integral based on the standard $(0,1)$-normal distribution with a zero mean and unity variance (see Figure 5.1) so that

$$F_X(x) = \Phi\left(\frac{x-\mu_X}{\sigma_X}\right) \tag{5.8}$$

in which

$$\Phi(x) = \frac{1}{\sqrt{2\pi}} \int_{-\infty}^{x} \exp\left(-\frac{u^2}{2}\right)\, du\,. \tag{5.9}$$

This integral cannot be solved in closed form, but tabulated values and numerical approximation methods exist. The Gaussian distribution is considered the most "natural" distribution as, according to the central limit theorem, an additive superposition of independent random effects asymptotically tends to this distribution (Bucher, 2009). It should be noted that according to Chebyshev's inequality theorem (Bronstein et al., 2008; Bucher,

Table 5.1.: Probabilities for the σ_X-levels of a normal distribution. The probabilities describe the two-tailed values. Also see Figure 5.1.

Sigma level	Probability
$\pm 1\sigma_X$	3.17×10^{-1}
$\pm 2\sigma_X$	4.54×10^{-2}
$\pm 3\sigma_X$	2.7×10^{-3}
$\pm 4\sigma_X$	6.3×10^{-5}
$\pm 5\sigma_X$	5.7×10^{-7}
$\pm 6\sigma_X$	2.0×10^{-9}

2009) values x of the random variable X are unlikely to differ from the mean by a large multiple λ of the standard deviation due to

$$P(|X - \mu_X| \geq \lambda\sigma_X) \leq \frac{1}{\lambda^2} \,. \tag{5.10}$$

A more accurate compilation of the probabilities of $\lambda \cdot \sigma_X$ can be found in Table 5.1. Other statistical distributions to describe random variables can be found in the relevant literature such as Bronstein et al. (2008); Bucher (2009); Melchers (1999) and many more. A recapitulation of the distributions used within this work can be found in Annex C.

5.2. Multivariate random models

Normally, a probabilistic problem contains more than one random or basic variable, so that multiple statistical distributions have to be considered. Some of the random variables might even be correlated. In this section the background of multivariate models is briefly explained.

5.2.1. Joint probability functions

The mutual cumulative probability function of a n-dimensional multivariate random variable can be generally expressed by the joint probability function, or "copula," in analogy to Equation 5.2

$$F_{\mathbf{X}}(\mathbf{x}) = P\left[\bigcap_{i=1}^{n}(X_i \leq x_i)\right] = \int_{-\infty}^{x_n} \cdots \int_{-\infty}^{x_1} f_{\mathbf{X}}(\mathbf{u})\, d\mathbf{u} \,, \tag{5.11}$$

where $f_{\mathbf{X}}$ is the joint probability density function and vice versa $f_{\mathbf{X}}(\mathbf{x}) = \nabla F_{\mathbf{X}}(\mathbf{x})$. If all random elements X_i are statistically independent of each other, the joint probability function is simply the product of the element's functions so that

$$f_{\mathbf{X}}(\mathbf{x}) = \prod_{i=1}^{n} f_{X_i}(x_i) \,. \tag{5.12}$$

This allows for the simple multiplication of independent events i.e. in event trees (Hasofer et al., 2007; Bucher, 2009). If the variables are not independent, this simplification does not apply. In this case, the probability density function for each variable can be obtained by integrating over the other variables. This is called "marginal" probability density function and is formulated

$$f_{X_i}(x_i) = \int_{-\infty}^{\infty} \cdots \int_{-\infty}^{\infty} f_{\mathbf{X}} \, dx_1 \, \ldots \, dx_{i-1} \, dx_{i+1} \, \ldots \, dx_n \,. \tag{5.13}$$

With the marginal distributions computed it is now possible to also compute the conditional density functions by treating one of the variables as a fixed parameter. Bucher (2009) describes this as "slicing through the probability hill" of the joint probability density function as the equation yields

$$F_{X_j|X_i}(\mathbf{x}) = \frac{f_{\mathbf{X}}(\mathbf{x})}{f_{X_i}(x_i)} \,. \tag{5.14}$$

5.2.2. Random vectors

For a large number of random variables, they are compiled in vectorial form for better organization. A n-dimensional multivariate model $\mathbf{X}$ is described by

$$\mathbf{X} = [X_1, X_2, \ldots, X_n]^T \tag{5.15}$$

with a mean vector $\boldsymbol{\mu}_{\boldsymbol{X}}$ and a diagonal matrix of the standard deviations $\boldsymbol{\sigma}_{\boldsymbol{X}}$

$$\boldsymbol{\mu}_{\boldsymbol{X}} = [\mu_1, \mu_2, \ldots, \mu_n]^T \text{ and } \boldsymbol{\sigma}_{\boldsymbol{X}} = \operatorname{diag}[\sigma_1, \sigma_2, \ldots, \sigma_n] \,. \tag{5.16}$$

The coefficients of correlation ρ_{ij} describe the linear relationship between two random variables (Figure 5.2) and are defined by the quotient of the mutual variance (covariance) and the product of the standard deviations (Mendenhall and Sincich, 1996; Bronstein et al., 2008)

$$\rho_{ij} = \frac{\operatorname{Cov}(X_i X_j)}{\sqrt{\operatorname{Var}(X_i) \cdot \operatorname{Var}(X_j)}} = \frac{\sigma_{X_i X_j}}{\sigma_{X_i} \sigma_{X_j}} \,, \qquad \rho_{ij} \in [-1, 1] \tag{5.17}$$

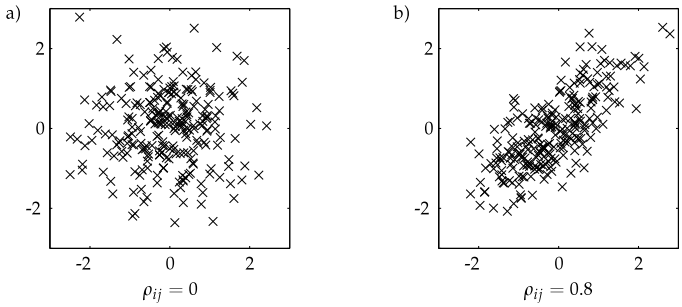

Figure 5.2.: Two possible correlations ρ_{12} for a bivariate standard normal distribution. a) 250 random samples with $\rho_{12} = 0.0$ and b) 250 random samples with $\rho_{12} = 0.8$.

with

$$\mathrm{Cov}(X_i X_j) = \mathrm{E}[(X_i - \mu_i)(X_j - \mu_j)] = \int_{-\infty}^{\infty}\int_{-\infty}^{\infty} (x_i - \mu_i)(x_j - \mu_j) f_{X_i X_j}(x_i, x_j)\, dx_i\, dx_j \quad (5.18)$$

in analogy to Equation 5.6. The coefficients of correlation can be assembled in the correlation matrix

$$\boldsymbol{\rho}_{XX} = \begin{bmatrix} 1 & \rho_{12} & \cdots & \rho_{1n} \\ \rho_{21} & 1 & \cdots & \rho_{2n} \\ \vdots & \vdots & \ddots & \vdots \\ \rho_{n1} & \rho_{n2} & \cdots & 1 \end{bmatrix} . \quad (5.19)$$

The covariance matrix can either be obtained by the general formulation

$$\mathbf{C}_{\mathbf{XX}} = \mathrm{E}[(\mathbf{X} - \boldsymbol{\mu}_X)(\mathbf{X} - \boldsymbol{\mu}_X)^T] \quad (5.20a)$$

or by matrix multiplication when the standard deviations and the correlation matrix are given separately

$$\mathbf{C}_{\mathbf{XX}} = \boldsymbol{\sigma}_X \boldsymbol{\rho}_{XX} \boldsymbol{\sigma}_X \quad (5.20b)$$

which is symmetrical and positive definite. This is important for sampling and the applicability of the principal component (PC) analysis in Section 6.4.1. For normal distributed multivariate variables Equation 5.7 can be generalized to

$$f_X(\mathbf{x}, \mathbf{C}_{\mathbf{XX}}) = \frac{1}{(2\pi)^{\frac{n}{2}} \sqrt{\det \mathbf{C}_{\mathbf{XX}}}} \exp\left[-\frac{1}{2}(\mathbf{x} - \boldsymbol{\mu}_X)^T \mathbf{C}_{\mathbf{XX}}^{-1} (\mathbf{x} - \boldsymbol{\mu}_X)\right] , \quad \mathbf{x} \in \mathbb{R}^n \quad (5.21)$$

while for copulas with other distributions this cannot be formulated as simple and requires special models, such as the Nataf-model.

5.2.3. The Nataf-model

The Nataf-model was first published in Nataf (1962) and uses the standardized probability density function of the previously introduced Gaussian copula

$$\phi_{\mathbf{U}}(\mathbf{u}, \mathbf{C_{UU}}) = \frac{1}{(2\pi)^{\frac{n}{2}}\sqrt{\det \mathbf{C_{UU}}}} \exp\left[-\frac{1}{2}\mathbf{u}^T\mathbf{C_{UU}^{-1}}\mathbf{u}\right] \quad , \quad \mathbf{u} \in \mathbb{R}^n \tag{5.22}$$

with zero means and unit standard deviations for every U_i. $\mathbf{C_{UU}}$ is the correlation matrix with the correlation coefficients ρ'_{ij} to approximate the given n-dimensional correlated random vector $\mathbf{X}$ by transformation into standard normal space by using $U_i = \Phi^{-1}[F_{X_i}(X_i)]$ (see Section 5.4.1 for inverse distribution functions) so that

$$f_{\mathbf{X}}(\mathbf{x}, \mathbf{C_{XX}}) = \phi_{\mathbf{U}}(\mathbf{u}, \mathbf{C_{UU}}) \cdot \mathbf{J} \, , \tag{5.23}$$

where $\mathbf{J} \equiv \frac{\partial(x_1,\ldots,x_n)}{\partial(u_1,\ldots,u_n)} = \frac{f_{X_1}(x_1)\cdot\ldots\cdot f_{X_n}(x_n)}{\phi_{U_1}(u_1)\cdot\ldots\cdot\phi_{U_n}(u_n)}$ is the Jacobian matrix. The remaining unknown is the correlation matrix $\mathbf{C_{UU}}$, whose elements ρ'_{ij} can be found by numerically solving the integrals from Equations 5.18 inserted in Equation 5.17 so that

$$\sigma_{x_i}\sigma x_j\rho_{ij} = \int_{-\infty}^{\infty}\int_{-\infty}^{\infty}(x_i - \mu_i)(x_j - \mu_j)\phi_2(u_i, u_j; \rho'_{ij})\, du_i\, du_j \, , \tag{5.24}$$

where ϕ_2 is a bivariate standard normal copula according to Equation 5.22. As the numerical solution of the integral can be very time-consuming, Liu and DerKiureghian (1986) proposed an empirical set of equations to approximate the ratio ρ'_{ij}/ρ_{ij}. Noh et al. (2008) find a deviation up 15 % in the midrange ($\rho_{ij} \approx 0.5$) and Melchers (1999) states that this ratio usually varies from approximately 0.9-1.1. He adds that for most problems the correlation coefficients are rarely known accurately enough so that it is mostly sufficient to use $\rho'_{ij} = \rho_{ij}$. This will be used for the analyses in Chapter 7.

5.2.4. Convolution of random variables

If two functions f and g are used within a mathematical operation, this operation $(f * g)$ also yields a function. This mathematical operation is called *convolution* (Bronstein et al., 2008, p.778). Hence in probability theory, the resulting function z of multiple distribution functions yields a new distribution function which is called the convolution of the input distribution functions. Since the distribution function defined in Equation 5.11 is an integral of the probability density function $f_{\mathbf{X}}$, the resulting distribution function F_Z of the function $G_Z(\mathbf{X})$ is—in perfect analogy—also an integral (convolution integral) with

$$F_Z(z) = P(Z \leq z) = P\left[G_Z(X_1, \ldots, X_n) \leq z\right] \tag{5.25a}$$

$$= \int_{G_Z(\mathbf{X})\leq z}\cdots\int f_{\mathbf{X}}(\mathbf{u})\, d\mathbf{u} \, , \tag{5.25b}$$

where $G_Z(\mathbf{X}) \leq z$ is the domain in which z is greater than the function of the random variables X_i. The convolution yields a new distribution function which does not necessarily have to be of the type of any of the distribution functions of the input variables. In case of only normal distributed and uncorrelated variables, the resulting function is also normal distributed (Six, 2001, p.26).

Schneider (1994, p.54) generalizes the resulting distributions under consideration of the Central Limit Theorem and shows that in case of a summation of distributions, the resulting distribution yields a normal distribution while multiplication yields log-normal distributed results.

5.3. Data mining

When random models are utilized numerically, they are usually based on a finite sample set. As these samples do not necessarily represent the whole statistical population and/or domain, they have to be treated with caution. In this section, an introduction is given to statistical data mining; yet only the essential information is given. For further details the reader is referred to the relevant literature, such as Bronstein et al. (2008); Melchers (1999); Bucher (2009); Mendenhall and Sincich (1996), and many more.

5.3.1. Estimating statistical moments

For a representative sample with n values of a basic variable X, the statistical moments mean and variance can be estimated by using the transformed Equations 5.5 and 5.6 (Bronstein et al., 2008, p.836) for a set of samples so that

$$\bar{x} = \frac{1}{n} \sum_{i=1}^{n} x_i \tag{5.26}$$

and

$$s^2 = \frac{1}{n-1} \sum_{i=1}^{n} (x_i - \bar{x})^2 \,. \tag{5.27}$$

The accuracy of the values found depends on the number of values n. Bronstein et al. (2008, p.842) provide a statistical test for the accuracy of the mean value based on an assumed normal distribution and find that only 49 values are needed to prove that $\bar{x}$ will not deviate more than 0.5σ from the statistical population mean μ in 99.95% of the cases. Mason et al. (2003) state that $n > 30$ is sufficient to fit a standard normal distribution according to the Lindeberg-Levy theorem.

The empirical variance and the linear correlation can be tested against the Student's distribution with the t-test (Mendenhall and Sincich, 1996, also see Section 6.1) and the goodness of fit of a normal distribution can be tested using the χ^2-test (Bronstein et al., 2008). The goodness of fit of other distributions can be evaluated with other tests, such as the Kolmogorov-Smirnov test or the Anderson-Darling test which can be found in Ushakov (1994). A summary can be found in Klinzmann (2008, Annex D).

5.3.2. Empirical distribution

Instead of fitting a distribution right away it can sometimes be sufficient to utilize an empirical distribution based on order statistics (Martinez and Martinez, 2002) for a preliminary analysis. The empirical cumulative distribution function is the step function

$$\hat{F}_n(x) = \frac{1}{n} \sum_{i=1}^{n} I(X_i \leq x) \,, \tag{5.28}$$

where $I(U)$ is an indicator function of the event U. The complementary distribution $\hat{S}_n(x) = 1 - \hat{F}_n(x)$ is called survivor function and was published by Kaplan and Meier (1958). It was successfully used for the evaluation of numerical samples in Notarianni (2000) and Albrecht and Hosser (2009). Due the central limit theorem by Lindeberg-Levy (Bronstein et al., 2008, p.830), $\hat{F}_n(x)$ yields $F(x)$ if $n \to \infty$.

5.3.3. Pitfalls

The most common problems in data mining and subsequent fitting of statistical distributions are located in the tail region (i.e. Figure 5.1 for $x < -2$ or $x > 2$), which is most relevant for reliability analyses.

Particularly, small sample sets often only provide information about the random space around the mean ($\pm 2\sigma$) as it is very unlikely to have extreme values in a small sample, as shown in Section 5.2, i.e. Equation 5.10 and Table 5.1.

This problem can be tackled with verified and reasonable fitting of extreme value distributions and extrapolation methods (Melchers, 1999; Klinzmann, 2008; Schneider, 1994) and/or by collecting the required amount of samples according to statistical requirements as described in Section 5.3.1 and in Mendenhall and Sincich (1996); Bronstein et al. (2008). For numerical samples, techniques such as Latin Hypercube sampling or quasi-random sequences (cf. Section 5.4) should be used for greater accuracy in the tail regions. A further remark on stochastic modeling is given in Section 7.3.2.

5.4. Sampling strategies

One of the biggest challenges of computational reliability analysis is the accurate and representative generation of samples from the basic variables and their distribution functions. As extensive literature exists on this topic, only the methods used within this work are briefly explained in the following sections.

5.4.1. Univariate sampling using the inverse transform method

Random numbers are normally generated by randomizer algorithms in the computing system. Various approaches for random and quasi-random or pseudo-random number generation exist and can be found in the literature such as Niederreiter (1992). For this work the pseudo-random number generator based on the Mersenne-Twister algorithm (Matsumoto and Nishimura, 1998) implemented into the Matlab 7.8.0 (2009) software is used among the methods explained below. This randomizer stream is "seeded" (initialized) by the current time-stamp and delivers sufficiently random numbers for the applications within.

In order to sample values from a probability distribution, the random numbers in the interval $[0, 1]$ can be regarded as a function $f_U(u)$ of the results of the function $F_X(x)$, so that $u = F_X(x)$. As the cumulative distribution functions of continuous distributions are strictly monotonic (Section 5.1) they can be inverted—proof omitted, see i.e. Rubinstein (1981, p.54)—so that

$$u = F_X(x) \rightarrow x = F_X^{-1}(u)\,, \tag{5.29}$$

where $f_U(u)$ is now the random generating function, which can be seen as the probability density function of a uniform distribution in the interval $[0, 1]$. This procedure is called inverse transform method (Fishman, 1995, Chapter 3.2) and is demonstratively shown in Figure 5.3. Even though Rubinstein (1981) states that this method is regarded as rather slow compared to other methods and inverse functions are extremely difficult or even impossible to find for some distributions it is very easy to implement this method numerically. The most time-critical part of the reliability analysis herein was found to be the solver runs and not the sampling.

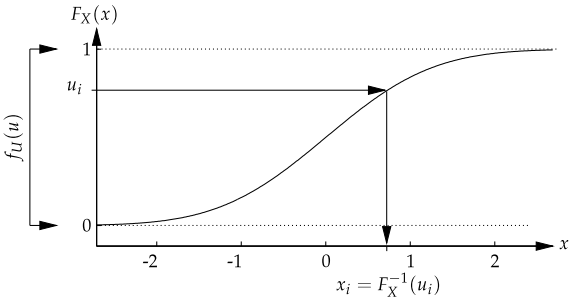

Figure 5.3.: Inverse transform method for the random sampling from a continuous cumulative distribution function $x_i = F_X^{-1}(u_i)$.

5.4.2. Multivariate sampling

For the case of a multivariate normal model, the sampling can be done independently according to the previous section if the variables are uncorrelated. Correlated sampling of k occurrences of the n-dimensional random vector $\mathbf{x}$ can be achieved by independent sampling in accordance to the previous section and subsequent rotation using a matrix $\mathbf{R}$ so that the random vector can be sampled

$$\mathbf{x}_k = \mathbf{U}_k\mathbf{R} + \boldsymbol{\mu}_{\mathbf{X}}^T, \quad \mathbf{x}_k \in \mathbb{R}^n \tag{5.30}$$

in which $\mathbf{U}$ is a $(n \times k)$-matrix with standard normal $\mathrm{N}(0,1)$ random numbers. The triangular matrix $\mathbf{R}$ can be obtained by decomposing the covariance matrix so that $\mathbf{R}^T\mathbf{R} = \mathbf{C}_{\mathbf{XX}}$ by using the Choleski (Fishman, 1995, p.223) or spectral decomposition (Martinez and Martinez, 2002, p.149). The sampling for the data in Figure 5.2 was done with this method.

This procedure is obviously only valid for normal distributed variables. For other distributions, the joint probability density function can be approximated by a Gaussian copula using the Nataf-model (Section 5.2.3) and subsequently, the sampling can be done using Equation 5.30.

5.4.3. Latin hypercube sampling

As stated in Section 5.3.3 and because of Equation 5.10, it is very unlikely to have samples in the tail regions, especially when the number of samples is low. Yet for reliability analyses, the tail regions of distributions can be most relevant. Hence, a method for better representation of the random space with only few samples is needed. An approach

to tackle this problem for the univariate case is the stratified sampling where the random space in divided into $1/N$ intervals for N samples. The actual sampling values are then randomly sampled within their interval according to the method previously described.

For the multivariate case the solution is slightly more complex as the number of samples would rise exponentially with the number of variables if sampling is done in each interval. Hence, Iman and Conover (1982) propose a method to represent the random (hyper-)space based on random permutations of the sampling sub-spaces (n-dimensional intervals) so that for a two-dimensional case, a Latin-Square-type ordering of the data would occur. Generalized to the n-dimensional case, this method yields n-dimensional hypercubes called *Latin Hypercubes*.

The sampling in matrix form can be done by creating a $N \times K$ matrix $\mathbf{P}$ where the columns represent the random permutations of the the sequence $1, \ldots, N$ and a $N \times K$ matrix $\mathbf{R}$ which is filled with random numbers in the interval $[0, 1]$ (Most, 2005, p.152). The sampling matrix $\mathbf{S}$ can then be obtained

$$\mathbf{S} = \frac{1}{N}(\mathbf{P} - \mathbf{R}) \tag{5.31}$$

and transformed into the random variables using the inverse transform method described above.

An exemplary sampling matrix according to the Latin Square scheme is shown below. It is apparent that a number does not appear twice in a row or a column. The circled ones denote a sampling of four values.

$$\begin{bmatrix} \textcircled{1} & 2 & 3 & 4 \\ 2 & 4 & \textcircled{1} & 3 \\ 3 & \textcircled{1} & 4 & 2 \\ 4 & 3 & 2 & \textcircled{1} \end{bmatrix} \tag{5.32}$$

It becomes evident that such a sampling can induce a spurious correlation into the data which has to be considered, especially for the correlated sampling case. Iman and Conover (1982) minimize the spurious correlation by incorporating it into an updated rotation matrix $\mathbf{R}'$ (see above) so that

$$\mathbf{R}' = \mathbf{R}\mathbf{Q}^{-1} \tag{5.33}$$

where $\mathbf{Q}$ is the Choleski lower triangular matrix of the sampling correlation matrix. Subsequent rearrangement of the original spuriously correlated sample is performed so that it has the same rank order as the rotated matrix. A source code example for the simple algorithm can be found in Forrester et al. (2008, p.17). More advanced methods for the reduction of spurious correlation and different optimized sampling methods can be found in the literature (Bucher, 2009; Fishman, 1995; Rubinstein, 1981; Niederreiter, 1992, etc.).

5.4.4. Quasi-random sampling

Another sampling approach, especially for numerical integration, is the utilization of mathematically deterministic algorithms that produce *quasi-random* numbers with very low discrepancy (Niederreiter, 1992, p.13). This means that the deterministic points appear to be random and are evenly distributed with very low correlation and clustering effects in the sampling space, and thus, allow for accurate numerical integration. The most commonly known formulations are the *Halton* and the *Sobol* sequence. The Halton sequence is a generalization of the one-dimensional sequence of van der Corput (1935) into n-dimensional space. A simple algorithm is described in his paper (Halton, 1960).

This sequence has good accuracy for a low dimensionality but has difficulties with a higher dimensionality as points in successive dimensions become correlated. Thus, the numerical effort increases as the sequence uses increasing prime numbers for every dimension. These effects are graphically shown in Krykova (2003, p.13f). For high dimensionality, the Sobol sequence is utilized with a base 2 for every dimension which avoids the correlation effects (Niederreiter, 1992, p.23f). A detailed algorithm can be found in Bratley and Fox (1988). Further quasi-random methods exist which are explained in detail in the literature cited, primarily Niederreiter (1992).

For the numerical integration problems in this thesis (see Chapter 7 and Section 6.3), which have a dimensionality $n < 10$, the Halton sequence is most suitable and converges faster than random sampling (Krykova, 2003, p.10). This sequence will only be applied for the numerical integration using the surrogate. Figure 5.4 shows the low discrepancy of a Halton point set compared to a Mersenne-Twister random point set.

5.4.5. Systematic Sampling (Design of Experiments)

Besides random or quasi-random sampling of the prescribed distributions, in many cases it might be useful to perform a systematic approach to identify critical parameters without having to consider the interaction with others. Also, for screening and surrogate construction, a systematic approach may have certain advantages over a completely random scheme. Systematic sampling is often called *design of experiments (DoE)* and is usually centered about the mean vector. The numerical effort (number of evaluations) is dependent on the dimensionality and the design chosen. Even though the selection of sampling plans should be targeted at the objective (i.e. surrogate construction, screening, sensitivity analysis), some systematic designs have proven to work for multiple purposes:

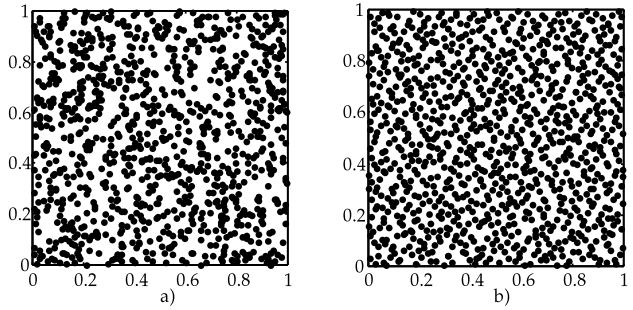

Figure 5.4.: 2-dimensional sampling of a) 1000 Mersenne-Twister random points and b) 1000 Halton points. It can be seen that the Halton points have no local clustering effects and thus have a lower discrepancy than the random points.

Axial Sensitive sampling plans are the simplest form of DoEs. One parameter is varied while all other parameters are kept fixed. The number of variations in every direction can be configured to the individual needs. For one variation in each direction, this methods needs $(n+1)$ evaluations where n is the number of dimensions.

(Full/Fractional) Factorial sampling plans can be pictured as a "grid" in the random space; m samples are generated in every dimension n including all interaction terms. This leads to a high number of (m^n) required evaluations. Within this work, this sampling plan is utilized using different numbers m based on the importance of the dimension instead of a fixed number for all dimensions. This is called leveled factorial design and can significantly reduce the required number of evaluations. For further details, see Section 6.4.2.

Central Composite sampling plans also incorporate interaction terms. These design plans are basically a superposition of a $(m = 2)$-fractional factorial design and an axial sensitive design plan. The layout is usually chosen to describe a radial hypersphere around the center so that the plan is fully rotatable and often times used for polynomial response surface modeling using interaction terms. The required number of evaluations is $(2^n + 2n + 1)$.

All the designs described above can be seen in Figure 5.5 for $\mathbb{R}^2$. Further design schemes exist but are omitted here as this would be beyond the scope of this work. Further details can be found in the relevant literature, such as Forrester et al. (2008, Chapter 1), Mason et al. (2003) or Antony (2003).

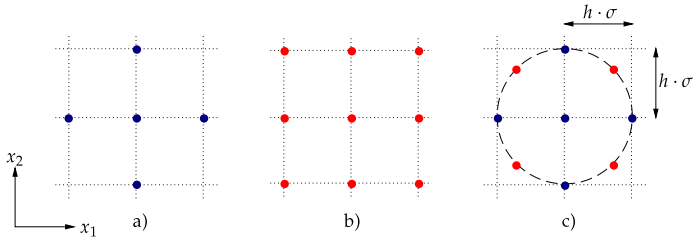

Figure 5.5.: Systematic sampling schemes in 2-D ($\mathbb{R}^2$). a) Axial sensitive sampling with 2 levels for each x_1 and x_2, b) full factorial design with $m = 2$ in both directions and c) central composite design. h is usually chosen depending on the expected probability of failure.

5.5. The reliability problem

Evaluating a design for reliability means to calculate the probability for the design to reach an undesired or unsafe state $\mathcal{F}$. For life safety analysis this unsafe state would be reaching untenable conditions in a compartment before the egress has been successfully completed, leaving people exposed to a hazardous environment. Hence, a *limit state* is reached when the available time for safe egress (ASET,A) is equal to the required safe egress time (RSET,R). This can be described mathematically in accordance with Equation 3.1 in Chapter 3.2, so that this limit state will be considered violated if the ASET is equal or smaller than the RSET

$$\mathcal{F} \equiv G(A,R) = A - R \leq 0 \tag{5.34}$$

where ASET (A) and RSET (R) can be arbitrarily distributed with a joint distribution function $F_{AR}(a,r)$. Subsequently, the probability p_f of the limit state to be violated can be derived from the solution of a convolution integral using Equation 5.25 so that

$$p_f = P[G(A,R) \leq 0] \tag{5.35a}$$

$$= \iint\limits_{\Omega_{\mathcal{F}}} f_{AR}(a,r)\, da\, dr \tag{5.35b}$$

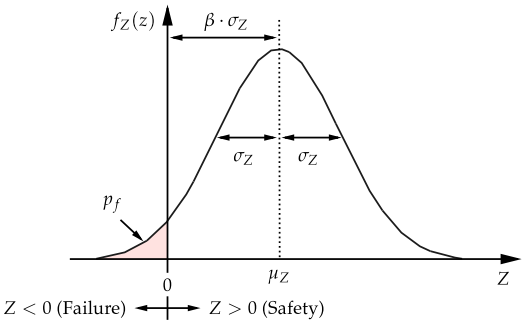

Figure 5.6.: Probability density of the convolution Z of A and R, and graphical representation of the reliability index β. Reproduced from Melchers (1999, p.19).

where $\Omega_{\mathcal{F}}$ denotes the failure domain $G(A, R \leq 0)$. For the special case of independent normal variables, Equation 5.35 can be transformed as shown in Schneider (1994, p.75), Melchers (1999, p.17) or Six (2001, p.30), so that

$$p_f = \int_{-\infty}^{\infty} \int_{-\infty}^{r \geq a} f_A(a) f_R(u)\, da\, du \tag{5.36a}$$

$$= \int_{-\infty}^{\infty} F_A(r) f_R(r)\, dr \tag{5.36b}$$

in which u is the control variable for the integration. For this particular case, the convolution Z between A and R yields a normal distributed variable F_Z (see Section 5.2.4) with mean and variance given by Melchers (1999, p.369) to be

$$\mu_Z = \mu_A - \mu_R \qquad \text{and} \qquad \sigma_Z^2 = \sigma_A^2 + \sigma_R^2 \tag{5.37}$$

so that $p_f = F_Z(z \leq 0)$. p_f is often expressed as *reliability index* β which describes the distance from $F_Z(z = 0)$ to the mean of F_Z in multiples of σ_Z so that

$$p_f = \Phi\left(\frac{0 - \mu_Z}{\sigma_Z}\right) = \Phi\left[\frac{0 - (\mu_A - \mu_R)}{\sqrt{\sigma_A^2 + \sigma_R^2}}\right] = \Phi(-\beta)\,, \tag{5.38}$$

and consequently $\beta = \frac{\mu_Z}{\sigma_Z}$ as shown in Figure 5.6.

5.5.1. The generalized reliability problem

For many problems more than two basic variables exist to assess a probabilistic problem which might also have a limit state function $G(\mathbf{X})$ that cannot be described analytically and is not differentiable. Additionally, the basic variables might be dependent and non-normal distributed so that the general formulation of the reliability problem can be found by considering Equation 5.35a and Equation 5.25b so that

$$p_f = P(\Omega_{\mathcal{F}}) \tag{5.39a}$$

$$= \int_{\Omega_{\mathcal{F}}} \cdots \int f_{\mathbf{X}}(\mathbf{u})\, d\mathbf{u} \tag{5.39b}$$

where $\Omega_{\mathcal{F}}$ is the failure domain of the limit state function $G(\mathbf{X})$. Obviously, the convolution integral is not necessarily solvable in closed from, meaning either approximation or numerical integration methods have to be utilized to calculate p_f. Some of the various existing methods will be briefly explained in the next sections.

5.5.2. Approximative methods

First order second moment (FOSM)

As the convolution of normal random variables yields a resulting normal distribution, the representation by the first two statistical moments, the mean and the variance, is sufficient for problems with only normal variables. The idea of computing the resulting distribution in this methodology is the linearization of a non-linear but differentiable limit state function $G(\mathbf{X})$ by using the first order Taylor series at the expansion point $\mathbf{x}_0$, so that

$$G(\mathbf{X}) = G(\mathbf{x}_0) + \nabla G(\mathbf{x}_0) \cdot (\mathbf{X}_i - \mathbf{X}_0) \tag{5.40a}$$

$$= G(\mathbf{x}_0) + \sum_{i=1}^{n} \left.\frac{\partial G}{\partial x_i}\right|_{\mathbf{x}=\mathbf{x}_0} (x_i - x_{i0})\,. \tag{5.40b}$$

Choosing the expansion point $\mathbf{x}_0$ to be the mean vector yields the expected value $\mathrm{E}(F_Z)$ and the variance can be calculated by inserting Equation 5.40 into Equation 5.6 so that

$$\sigma_z^2 = \mathrm{E}\left[\nabla G(\mathbf{x}_0) \mathbf{C}_{\mathbf{XX}} \nabla G^T(\mathbf{x}_0)\right] \tag{5.41a}$$

$$= \mathrm{E}\left[\left(\sum_{i=1}^{n} \frac{\partial G}{\partial x_i}(X_i - \mu_{X_i})\right)^2\right]\,. \tag{5.41b}$$

Equation 5.41 is known as the Gaussian Error Propagation Law (Bronstein et al., 2008, p.861). The resulting random variable Z is assumed to be normal distributed and thus the probability of failure p_f can be calculated according to Equation 5.39.

First order reliability method (FORM)

The first order reliability method (FORM) is an advancement of the FOSM method by Hasofer and Lind (1974) who transform the arbitrarily distributed random variables into standard normal (Gaussian) space $\mathbf{U}$. The objective of this iterative method is to find the point of the maximum joint probability density in the failure domain, the so-called design point $\mathbf{u}^*$.

The covariance matrix of the copula is calculated using the Nataf-model and is subsequently de-correlated by Cholesky or spectral decomposition. The limit state function is linearized by the Taylor series in the design point (shown above). The design point is not known and has to be found iteratively. If the point of maximum joint probability density of the failure domain $\mathbf{u}^*$ is found, the linearly approximated hyperplane touches the limit surface $G(\mathbf{X} = \mathbf{0})$ and is perpendicular to the minimum distance between the mean vector and the design point $\mathbf{u}^*$. Hence, $\mathbf{u}^*$ can be found iteratively using optimization algorithms. The algorithm can be found in detail in Melchers (1999, p.122) and a numerical example using the Rackwitz-Fiessler algorithm can be found in Bucher (2009, p.177).

Rarely, when the second order term of the Taylor series is used the method is called second order reliability method (SORM). This method requires that the limit state function is differentiable to the second order and the improvement in the results is usually not significant (Six, 2001, p.43) and does not justify the increased complexity and computational costs (Melchers, 1999, p.130).

Polynomial response surface method (RSM)

The two methods described above are only applicable for explicitly formulated limit state functions which have to be differentiable. In many cases, the limit state functions are only implicitly formulated when, for example, numerical models are utilized. In that case, a surrogate model for the implicit model or even the complete limit state function in explicit, differentiable form can be formulated using a polynomial (usually of second order)

$$\hat{f}(\mathbf{x}, \hat{\boldsymbol{\beta}}) = \mathbf{H}\hat{\boldsymbol{\beta}} + \boldsymbol{\varepsilon} \tag{5.42a}$$

$$= \hat{\beta}_0 + \sum_{i=1}^{n} \hat{\beta}_i x_i + \sum_{i=1}^{n} \sum_{j=1}^{n} \hat{\beta}_{ij} x_i x_j + \varepsilon \tag{5.42b}$$

where ε is the approximation error. The coefficient vector $\hat{\boldsymbol{\beta}}$ is fitted to a sufficient number of support points (so-called responses) which have been evaluated with the numerical model using least-square regression analysis (Box and Draper, 2007, p.17). Roos (2001, p.54) finds that this methodology has disadvantages as the approximation polynomial

has large model errors especially for highly non-linear and/or oscillating limit state functions. Moreover, the evaluated support points with the exact solution are only approximated due to the regression analysis (estimation error ε).

When a surrogate model in explicit form is found, FORM analysis can be utilized to calculate the probability of failure and the location of the design point. The design point found is usually evaluated with the numerical model to perform a check of accuracy. If the accuracy is not sufficient, a new surrogate model is found using new support points in the vicinity of the design point. The iterative approach along with an estimation algorithm for the design point based on linear interpolation was developed by Bucher and Bourgund (1990). For discontinuous limit state functions Most (2008) proposed an iterative response surface method based on support vector machines. Further remarks on response surface modeling are given in Chapter 6.

5.5.3. Integration methods

Instead of using approximative methods as shown above, the reliability problem can be solved directly by using direct analytical or numerical integration methods. Yet Six (2001, p.44) finds that the applicability is very limited to solve more complex reliability problems. Another option is the Monte Carlo integration method (and advancements thereof) which will be briefly explained in the following sections.

Monte Carlo simulation

The Monte Carlo method was first developed and published by Metropolis and Ulam (1949) to solve integrals using random numbers. Hence, this methodology is often used to solve the convolution integral from Equation 5.25b for implicit state functions. In order to utilize Monte Carlo simulation to only solve the integral in the failure domain $\Omega_{\mathcal{F}}$ from Equation 5.39, the indicator function[1] $I(\Omega_{\mathcal{F}})$ is introduced in order to distinguish between a failure or successful realization according to the limit state function so that

$$p_f = \int_{\Omega_{\mathcal{F}}} \cdots \int f_{\mathbf{X}}(\mathbf{u})\, d\mathbf{u} = \int_{\mathbf{X}} \cdots \int I(\Omega_{\mathcal{F}}) \cdot f_{\mathbf{X}}(\mathbf{u})\, d\mathbf{u}\,. \tag{5.43}$$

[1] Indicator function: $I(\Omega_{\mathcal{F}}) = \begin{cases} 1, & \text{for } G(\mathbf{X} \leq 0) \\ 0, & \text{for } G(\mathbf{X} > 0) \end{cases}$.

This resembles the generalized form of Equation 5.28 for the failure domain. Hence, for n random realizations (according to the input distributions) of the reliability problem, the probability of failure for a limit state function $G(\mathbf{X} \leq 0)$ can be calculated in discrete form to

$$\hat{p}_f = \frac{1}{n} \sum_{i=1}^{n} I[G(\mathbf{X} \leq 0)] \,. \tag{5.44}$$

For $n \to \infty$ the solution to $\hat{p}_f$ is exact due to the law of large numbers (LLN). This also means that a huge number of random realizations have to be calculated in order to find a sufficiently exact solution. Bucher (2009, p.179) gives a simplified equation to estimate the variance—and thus accuracy—of $\hat{p}_f$ to be $\sigma^2_{\hat{p}_f} \approx \frac{\hat{p}_f}{n}$.

Importance sampling

To tackle the problem of the high number of required samples (especially for very small p_f's), so-called weighted or importance sampling can be utilized to increase the frequency of failure realizations. This is achieved by introducing a weighting function into Equation 5.43 so that

$$p_f = \int_{\mathbf{x}} \cdots \int I(\Omega_{\mathcal{F}}) \cdot \frac{f_{\mathbf{X}}(\mathbf{u})}{h_{\mathbf{X}}(\mathbf{u})} \cdot h_{\mathbf{X}}(\mathbf{u}) \, d\mathbf{u} \tag{5.45}$$

and, thus, in accordance with Equation 5.44 the discrete form reads

$$\hat{p}_f = \frac{1}{n} \sum_{i=1}^{n} I[G(\mathbf{X} \leq 0)] \cdot \underbrace{\frac{f_{\mathbf{X}}(\mathbf{x})}{h_{\mathbf{X}}(\mathbf{x})}}_{\zeta_{\mathbf{X}}(\mathbf{x})} \,. \tag{5.46}$$

The fraction term in the equation is often referred to as likelihood ratio and will be denoted $\zeta_{\mathbf{X}}(\mathbf{u})$ in the following. $h_{\mathbf{X}}$ is chosen to minimize the variance of $\hat{p}_f$ (Rubinstein, 1981, p.122), so that a theoretical weighting function would only be defined in the failure domain yielding

$$h_{\mathbf{X}}(\mathbf{x}) = \frac{I(\Omega_{\mathcal{F}}) \cdot f_{\mathbf{X}}}{p_f} \,. \tag{5.47}$$

This is not practical as p_f is unknown a priori, so that $h_{\mathbf{X}}(\mathbf{x})$ is usually chosen to have a mean vector in—or, if unknown, in the vicinity of—the design point u^* as shown in Figure 5.7. This procedure is usually called importance sampling using design point (ISPUD, Six, 2001, p.44).

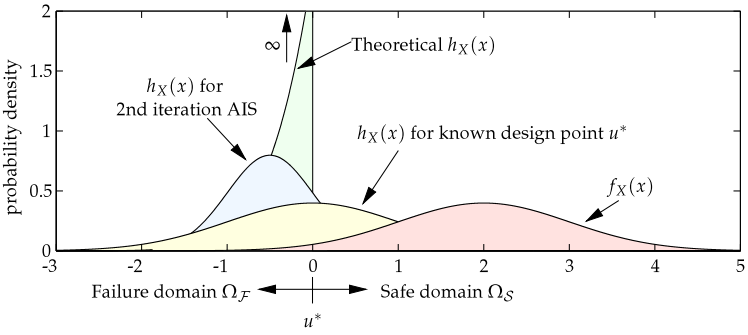

Figure 5.7.: Original probability density function $f_X(x)$ and weighting functions $h_X(x)$ for the theoretically optimal minimization of the variance of $\hat{p}_f$, if the design point u^* is known and for the 2nd iteration step in adaptive importance sampling.

An iterative approach, called adaptive importance sampling (AIS), is presented in Bucher (1988) who adapts the weighting function by considering the sampled points falling into the failure domain. This method will be used for exploitation of the surrogate within this work and hence is described in greater detail in Section 6.3. AIS has been enhanced, validated, and successfully applied in many studies, such as Six (2001, Chapter 7) or Schnetgöke (2008, Chapters 5 and 7). A possible realization of an adapted weighting function can be seen in Figure 5.7.

5.5.4. Limitations of the described reliability methods

All the methods described above have been used for various applications in practice and are considered state-of-the-art in reliability analysis. Nevertheless, the selection of the appropriate methods highly depends on the geometry of the boundary of the failure domain and on the accuracy needed.

In addition, the methods only work sufficiently accurate for reliability problems with one design point. For highly non-linear limit states yielding complex (and even oscillating) discontiguous boundary geometries (as exemplary shown for systems in Figure 5.8) of the failure domain, the methods described above can fail to converge properly. Multiple

design points cause a so-called "clustering" effect and thus a failure of the methods depending location of the design point. In practice, this problem especially occurs in system analyses of multiple limit states and is briefly described in the following section. Only the crude Monte Carlo simulation will always converge without further considerations, given that a sufficient number of evaluations of the limit state have been performed.

5.5.5. System analysis

Previously, it was only described how a reliability problem can be solved having one limit state function $G(\mathbf{X})$. Usually, a system contains multiple failure points with their own respective limit state functions. Hence, the reliability of a system is calculated based on an array of limit state functions $\mathbf{G}(\mathbf{X})$. The reliability problem can be solved holistically considering all limit states at once using the reliability methods above along with a failure domain

$$\Omega_{\mathcal{F}} = \bigcup_{i=1}^{n} \bigcap_{j=1}^{k_i} \Omega_{\mathcal{F},i} \,, \tag{5.48}$$

so that Equation 5.39 is universally valid. The solution of the integral in practice is rather complex as the superposition of the limit states functions yield a combined limit state that has a complex shape and might contain geometrical discontinuities as shown in Figure 5.8.

A second effect that can be seen is the the so-called "clustering effect", which occurs when the combined limit state function has two or more design points and/or if the failure domain is discontiguous. In this case, so-called cluster analysis can be performed. While usually methods such as the hierarchical clustering (Roos, 2011, p.198) are employed, especially the expectation-maximization (EM) algorithm (Gupta and Chen, 2010) is suitable since it yields distribution functions for each cluster which can subsequently be utilized in importance sampling, such as AIS. Generally, complex failure domains usually cause the approximation methods and the variance reducing methods to fail if no further considerations of the clusterin are made, so that only crude Monte Carlo simulation with a sufficient number of samples yields an accurate solution to the problem. Methods for general system analysis can be found in Melchers (1999, Chapter 5). Advanced response surface models for systems have been derived and tested by Roos (2001), Roos (2011).

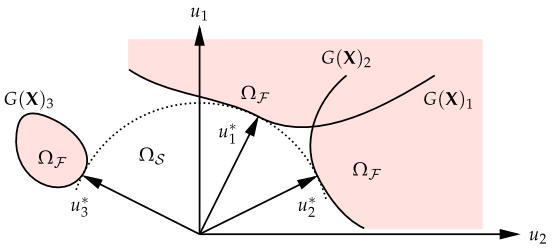

Figure 5.8.: Problems of system reliability analyses for discontiguous failure domain in U-space. It can be seen that all three design points u_i^* have the same distance to the origin. This usually causes the approximation models to fail. The variance reducing methods for the Monte Carlo simulation fail due to the clustering effect.

Nevertheless, when analyzing systems it is possible to decompose the system into different limit states (so-called *components*) and the causal connection between multiple components can be found to be either serial or parallel or a mixture to cause complete system failure, so that the system can be fully described using the theory of sets (Bronstein et al., 2008, p.327ff.). Hence, the general formulation of the reliability problem can be expanded for systems without loss of generality in accordance with Equation 5.39a to

$$p_f = P\left[\bigcup_{i=1}^{n}\bigcap_{j=1}^{k_i}(\Omega_{\mathcal{F},i})\right] \tag{5.49}$$

for so-called "k-out-of-n" systems. These can usually be described by multiple n parallel subsystems and k series subsystems. If a basic variable is used in two or more components of the system, correlation effects between the components will be induced into the system. As this might have a significant impact on the probability of failure (Melchers, 1999, p.167), it is suggestive to also calculate the bounds of p_f for an uncorrelated and a fully correlated case. Extensive information on first and second order (Ditlevsen bounds, Ditlevsen, 1979) bounds can be found in various publications, such as Melchers (1999, p.155), Klinzmann (2008, p.40).

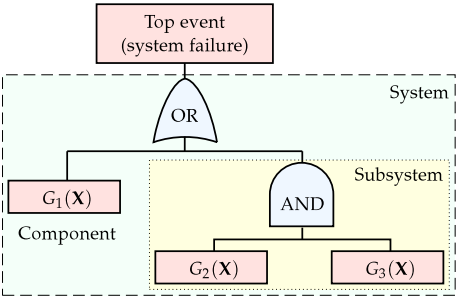

Figure 5.9.: Visualization of system using a fault tree with three components and a subsystem in international standard graphic notation.

Fault tree analysis

The system failure is usually the consequence of the failure of one or more components. A method for graphical and logical analysis is the so-called fault tree analysis, where the system failure is the top event. Starting from this top event the failure of the various subsystems and components to cause system failure is modeled by logically connecting the subsystems and components by AND or OR "gates" as described in Hasofer et al. (2007, p.71) and as shown in Figure 5.9.

After modeling the fault tree, the minimum cut set has to be found in order to identify the weakest links in the system. A cut set is considered minimal if it cannot be further reduced, but the top event can still occur. The complementary is the minimum path set, describing which subsystems and components have to function at the least in order to have the system operational. While small systems can be evaluated by visual inspection, more complex systems need to be evaluated numerically (using software tools) in order to find the minimum cut set. Hasofer et al. (2007, p.74) describe a method for evaluating cut sets using Boolean indicator functions. Assuming statistical independence between the limit states $G_i(\mathbf{X})$, the system reliability can be calculated using Boolean reduction as described, for example, in Hasofer et al. (2007, p.76).

An event tree is a different visualization of systems starting from an initial event (i.e. fire initiation) to evaluate possible (usually chronological) failure paths and scenarios due to the failure of function of single subsystems and components and is described in the following.

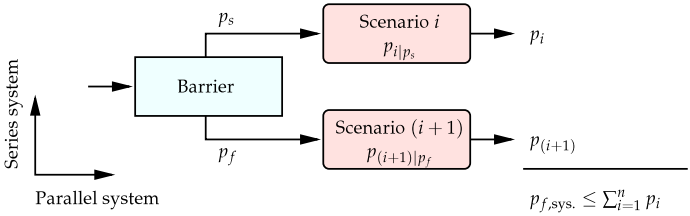

Figure 5.10.: Modeling of fire protection barriers within an event tree considering their possible failure to assess the overall impact on the safety level.

Event tree analysis

Event trees are used herein to model the various possible scenarios that potentially lead to failure. Event trees allow for an easy scenario generation and include the chronological order of events to occur. A very simplified example is shown in Figure 5.10. Usually, each branch of an event tree denotes a cut set of the system. This can be visualized by transforming the event tree to a fault tree.

Looking at Figure 5.10, the horizontal direction denotes roughly multiple parallel systems (each branch). Possible correlation effects or interaction effects between the barriers are modeled within the scenarios (see Chapter 7) and thus are approximately accounted for. In the vertical direction, an uncorrelated series system of the multiple scenarios can be assumed, as the possible function or malfunction of the barriers is purely stochastic[2] with the according probabilities.

Hence, it can be assumed that the upper first order bound of series systems

$$p_{f,\text{sys.}} \leq 1 - \prod_{i=1}^{n}(1 - p_i) \approx \sum_{i=1}^{n} p_i \tag{5.50}$$

constitutes a reasonable and conservative approximation of the system failure probability. This has been confirmed by a comparison to the results of a Monte Carlo simulation and the evaluation of the Ditlevsen bounds assuming uncorrelated events (shown in Table 5.2). Due to the accurate and yet conservative approximation and the simplicity of calculation compared to the more complex options, the upper first order bound $\sum_{i=1}^{n} p_i$ will be used herein for the system reliability assessment.

[2]The "way" or "route" through the event tree is a random process.

Table 5.2.: Comparison of system failure probabilities of the event tree in Section 7.5.2, page 144.

Method	$\hat{p}_{f,\text{sys.}}$
Upper first order bound ($\sum_{i=1}^{n} p_i$)	0.1206
Upper Ditlevsen bound	0.1203
MC-simulation (5,000,000 runs)	0.1169
Exact† ($1 - \prod_{i=1}^{n}[1 - p_i]$)	0.1167

†Assuming a perfectly uncorrelated series system.

5.6. Conclusions

In this Chapter, the mathematical background of reliability analysis and the corresponding problems thereof were introduced along with the various methods to compute the reliability of components and the system reliability. The convolution and computation of empirical failure probabilities of random parameters using numerically complex models is usually very computationally expensive. Hence, advanced algorithms were shown along with modifications and simplifications to optimize performance at low computational costs. A special remark was on the generation of sampling points and system analysis as well as the limitations of current algorithms to provide a solid basis for the development of the IMLS response surface method which is shown in great detail in Chapter 6.

Chapter 6

An IMLS response surface method

All the methods for reliability evaluation previously described either require a differentiable limit state function or a high number of solver evaluations which are quite *computationally expensive*. State-of-the-art CFD-models usually need a significant amount of time for one evaluation, depending on the complexity and the degree of discretization. Hence, the number of solver evaluations has to be reduced as far as possible while maintaining the same high accuracy. Some of the previously described reliability methods have been applied to practical problems, such as the reliability evaluation of FEM models by Schnetgöke (2008) using AIS. Despite the rather fast convergence of AIS (compared to crude MC), an extensive amount of solver evaluations were needed so that the discretization used had to be rather coarse.

Another approach, which will be followed herein, is the construction of a surrogate model for the limit state responses, assuming that the calculated responses of the CFD solver and the evacuation software can be decomposed in a way so that they yield a global trend, local effects, and local oscillation as shown in Figure 6.1. This means that, for example, the layer height within the simulation model will be generally underrun faster for, for example, higher heat release rates using large increments (in the HRR), but for small increments, it might even be underrun slightly slower because of a change in the scenario (i.e. opening of the smoke and heat exhaustion system, local trend effects) or due to physical and numerical effects (i.e. turbulence and turbulence modeling, local oscillation).

Hence, it is assumed that the response surface of the limit state function will *globally* have a contiguous failure domain and no significant discontinuities. *Locally*, the failure domain can be interrupted or irregular (patchy) and discontinuities might occur (Roos et al., 2007).

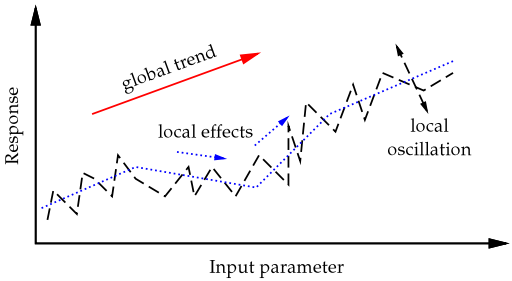

Figure 6.1.: Schematic decomposition of the responses for the one-dimensional case (not to scale). The dotted line represents the smoothed responses.

The validity of this assumption for global trends can be found in Albrecht and Hosser (2009) or Notarianni (2000) where sensitivity analyses have been performed using zone fire models. Hasofer and Qu (2002) and Magnusson et al. (1996) have shown the general applicability of the response surface methodology to numerical fire simulation.

In this approach, the local oscillation effects are smoothed out by the threshold models (see Section 4.2.5) as the stepwise temporal integration (FID values) and the central moving averages act as low-pass filters. The local effects will be accurately approximated with a surrogate model based on interpolating moving least squares (IMLS) so that no information from the solver responses is inaccurately represented due to global polynomial approximation (Roos, 2001, p.42). This also has the benefit over polynomial approximation that previous solver evaluations can be incorporated in further adaptations of the surrogate so that they act as marginal support points to stabilize and enhance the accuracy of the surrogate.

To further decrease the required number of numerical evaluations, a preceding sensitivity analysis yields information about the variance of the results and the relevance of the input parameters and hence helps to identify the *surrogate model of optimal prognosis*. The preliminary scan of the random space for the sensitivity analysis can also be used to obtain information about the approximate location of the design point so that further support points can be concentrated in this relevant area (compare to ISPUD, Section 5.5.3). Using this information for the subsequent reliability analysis leads to a significantly faster convergence. An overview over the developed reliability algorithm is given in Figure 6.2. The necessary processes are explained in detail in the following sections.

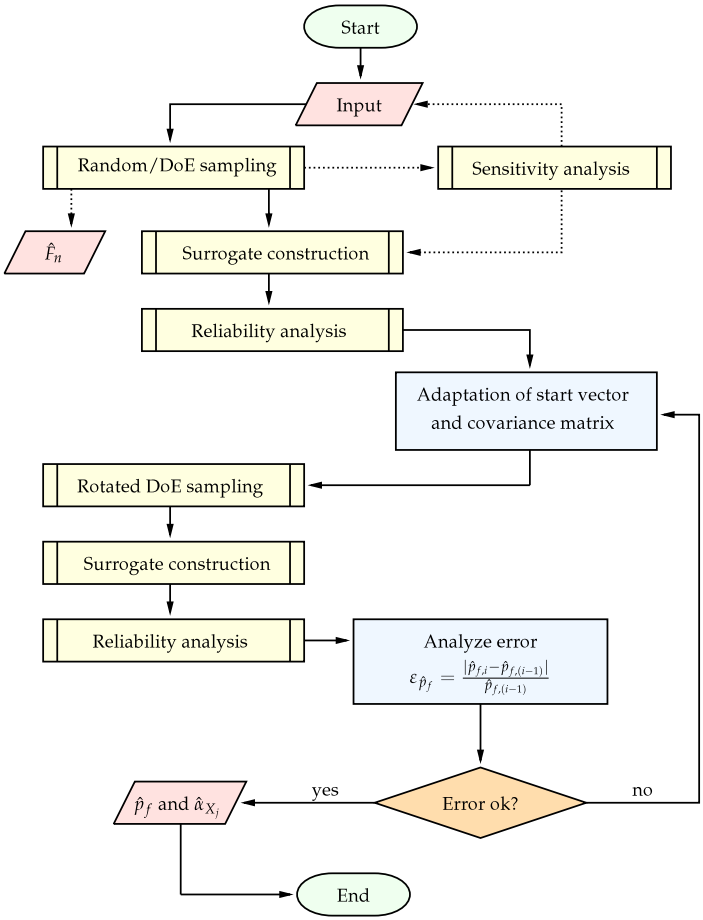

Figure 6.2.: Flowchart of the IMLS response surface algorithm. The preceding sensitivity analysis is optional but can lead to a reduction of the basic variables (dimensionality) and thus a decrease of the necessary solver evaluations.

6.1. Preceding sensitivity analysis

The main objective of the preceding sensitivity analysis is the reduction of the dimensionality of the problem as every random variable leads to a significant increase in the amount of necessary solver evaluations. Sensitivity analysis herein will be performed in two steps. The first step is a significance test for correlation between the input variables and the results. The second step is a stepwise test for the contribution of prediction accuracy (increase in model representation of the variance of the output) of the parameters to a linear or monotonic model. The latter test is used with regards to the assumption of a global trend for significant parameters as shown in Figure 6.1. Only the global trends are of particular interest for the sensitivity analysis as the local effects will be sufficiently modeled in the surrogate. Extensive work on sensitivity analysis was conducted by Saltelli and Homma (1992) and Saltelli et al. (2004). Hofer (1999) analyzes and identifies spurious correlation effects when small sample sets are being used due to high computational costs of the model.

The sampling dataset for the sensitivity analysis can either be based on Latin Hypercube sampling (see Section 5.4.3) according to the chosen stochastic models to provide a good representation of the random hyperspace ($\mathbb{R}^{(n_i+n_o)}$) where n_i and n_o are the number of input and output values, respectively. The user's manual of optiSLang 3.1.0 (2009, p.59) suggests at least $2(n_i+n_o)$ sample runs for LHS to get a decent representation.

The other option followed herein is the systematic sampling of the random space to verify that at least one unsafe-state response of the limit state function appears in the sample set. This is in order to obtain an approximate location of the design point and to stabilize the surrogate in that region. This sampling strategy also allows for sensitivity analyses and provides quasi-stable boundaries for the following surrogate iterations.

Generally, the parameter sensitivity can be divided into two classes. Either the parameter has no physically significant influence on the output, or the input range of the stochastic model is too small to cause a significant impact. Due to the "global" sampling and the high uncertainties in fire modeling, the latter case was rarely observed.

6.1.1. Significance of correlation

Not only input variables can be correlated (as described in Section 5.2.2) but also the input **X** and output **Y** parameters of an unknown "black boxed" model can be correlated to a certain degree so that Equation 5.17 becomes

$$\rho_{ij} = \frac{\mathrm{Cov}(X_i Y_j)}{\sqrt{\mathrm{Var}(X_i)\cdot\mathrm{Var}(Y_j)}} \quad \approx \quad \frac{SS_{X_i Y_i}}{\sqrt{SS_{X_i X_i} SS_{Y_i Y_i}}} = r_{ij}\,, \qquad \rho_{ij}, r_{ij} \in [-1,1] \tag{6.1}$$

where SS denotes the empirical variance from a sample dataset. Hence, r_{ij} is the empirical correlation ρ_{ij} for the dataset, called the *Pearson product moment coefficient of correlation* (Mendenhall and Sincich, 1996, p.127) and is unity for a perfectly linear model in accordance with the general case. Most and Will (2008) describe a correlation coefficient of greater than 0.7 as "generally strong" and less than 0.3 as "generally weak". Dehne (2003, p.125) uses a similar definition.

The statistical significance of the empirical correlation with respect to the correlation of the population can be tested with a hypothesis test against the t-(Student-)distribution. It is hypothesized that $H_0 : \rho_{ij} = 0$ while the alternative hypothesis states that $H_a : \rho_{ij} \neq 0$. A test statistic

$$t_{ij} = \frac{r_{ij}\sqrt{n-2}}{\sqrt{1-r_{ij}^2}} \tag{6.2}$$

is tested against a test value $t_{\alpha/2}$ with a chosen significance level α from the t-distribution with $(n-2)$ degrees of freedom (df) where n is the size of the sample dataset. H_0 is rejected in favor of H_a if the absolute value of the statistic is larger than the $t_{\alpha/2}$-value ($|t_{ij}| > t_{\alpha/2}$). The significance level α is usually chosen to be around 0.01 to 0.1 depending on the accuracy needed. Because of $F = t^2$ the t-test is a partial F-test for two variables (Draper and Smith, 1998, p.39).

The significance test described above only tests for *linear* correlation even though it is assumed that a globally rather *monotonic* trend with an unknown slope will occur instead. In order to utilize the test described above, the data is rank-transformed (Conover and Iman, 1981). The rank-transformation $\mathrm{Rk}(X_i)$ is graphically presented in Marino et al. (2008) and is described in greater detail in Schwieger (2005, p.25). The linear test described above can now be utilized for the rank-transformed data as a linear correlation of rank-transformed data describes a monotonic trend. The resulting r_{ij} is called *Spearman rank order correlation coefficient*.

The tests above can be used to identify linear and monotonic trends between input vs. output parameters. The algebraic sign of r_{ij} yields directional information. The square of r_{ij} yields the *coefficient of determination* R_{ij}^2 which is an indicator of the fraction of output variance that can be explained by the input variance. Schwieger (2005, p.23) describes R_{ij}^2 as an indicator criterion for linear trends if $R_{ij}^2 \approx 1$ and as a weak indicator for non-monotonic trends if $R_{ij}^2 \ll 1$. Consequently, the $R_{\mathrm{Rk}(ij)}^2$ of the rank-transformed data yields a sufficient (strong) indicator for monotonic trends if $R_{\mathrm{Rk}(ij)}^2 \approx 1$.

It should be noted that all these indicators do *not* imply causality. Hence, a qualitative evaluation of the parameters tested to be significant or insignificant, respectively, is highly advised. Methods for identifying spurious correlations are proposed in Hofer (1999).

6.1.2. Global contribution to prediction accuracy (stepwise regression)

After identifying the correlation effects between single input and output variables, suitable models for optimal prognosis incorporating multiple input parameters have to be identified and tested. A systematic approach for an additive variable testing model is the so-called stepwise regression (Draper and Smith, 1998, p.335). The stepwise algorithm starts by performing a significance test on all variables as described above. The input parameter yielding the highest t-value is selected (if the significance is higher than a predefined inclusion-threshold) and a simple linear or monotonic (using rank-transformed data) model is built using linear least square regression (see Section 6.2). Subsequently, the coefficient of determination R^2 (for two variables: r_{ij}^2) is calculated.

In a second step, two-variable regression is carried out for the previously included parameter and the parameters not yet included. The parameter yielding the highest increase in the *multiple coefficient of determination*

$$R^2 = 1 - \frac{\sum_{i=1}^{n}[\hat{y}(i) - \mu_y)^2]}{\sum_{i=1}^{n}[y(i) - \mu_y)^2]}, \quad R^2 \in [0,1] \tag{6.3}$$

is identified and included in the model ($\hat{y}$ is the approximated variance of the output and n the number of samples). Model validity of the bi-variate model is tested with the global F-test (Mendenhall and Sincich, 1996, p.195) and each included parameter is tested for significance with the partial F-test (t-test). If one of the included parameters underruns a predefined significance threshold, it is removed again. To avoid inclusion and subsequent removal, the remove-threshold is usually chosen to be less strict than the input-threshold. The latter step is sometimes omitted (Mendenhall and Sincich, 1996, p.243). This leads to a so-called *forward selection procedure* (Draper and Smith, 1998, p.336).

In the subsequent steps, the procedure is repeated for the other parameters until no further parameter meets the input-threshold criterion. The resulting significant parameters will be used to construct the surrogate, as their contribution gives the best representation of the output (highest R^2) with the lowest possible dimensionality. The algorithm has been successfully used and is visualized in tabular form in Albrecht (2008, Chapter 5).

Most and Will (2008) describe a similar stepwise method and utilize the change Δ in R^2 as a selection criterion for parameters. Hence, the ΔR^2 yields information about the contribution of an added variable. In the proposed method, the change in R^2 is used to determine whether a variable which tested significant also has a meaningful influence on the model accuracy. Bucher (2007) defines the ΔR^2 as *coefficient of importance* (CoI_i) for the variable i.

Herein, ΔR^2_{adj}, an *adjusted coefficient of determination*, will be used, since R^2 by definition (Eq. 6.3) increases with every parameter added. R^2_{adj} is defined

$$R^2_{adj} = 1 - \frac{n-1}{n-(k+1)}(1-R^2)\,, \quad R^2_{adj} \in [0,1] \tag{6.4}$$

which penalizes the coefficient of determination by the sample size n and the number of parameters k included; $(k+1)$ denotes the degrees of freedom (df) [1]. Most and Will (2008) recommend to use a threshold for $CoI_{i,min}(\equiv \Delta R^2_{adj})$ between 0.01 and 0.1. This, again, depends primarily on the desired accuracy and the number of variables in the initial problem.

Applying these methods usually yields a reduced number of input variables for the subsequent surrogate modeling and reliability analysis. It should be noted here that these *purely* mathematical tests do *not* substitute additional considerations (i.e. physical interpretation of included/removed variables) and engineering judgment, but rather provide a basis for decision making. All included or removed variables should, therefore, be qualitatively analyzed for importance as phenomena such as bifurcation effects, global oscillations, or heteroscedasticity (non-homogeneous variances of the approximation errors) are not accounted for in these tests. The most common regression pitfalls, and the treatment thereof, are described in detail in Mendenhall and Sincich (1996, Chapter 6).

6.2. Surrogate modeling

A *surrogate* model (also known as *regression* model or *response surface* in other disciplines) accurately represents the solver evaluations (support points) and the unresolved, and thus unknown, values in between. Mathematically, the original problem corresponds to a mapping $f : \mathbf{x} \rightarrow y$ where f is an implicit and potentially non-differentiable and/or discontinuous black box function[2] of the input vector $\mathbf{x}$ which is also computationally expensive (Box and Draper, 2007, Chapter 1). Thus, the surrogate is an attempt to build a substitute formulation $\hat{f}(\mathbf{x})$ based on a number of previously evaluated support points in order to bypass the high computational costs. This simplification is usually accompanied by approximation errors, so that the response mapping becomes

$$\hat{f} : \mathbf{x} \rightarrow \hat{y} + \epsilon \tag{6.5}$$

[1] $(k+1)$ to account for the intercept term.

[2] Fitting i.e. a linear model to a potentially harmonic response is obviously not useful. In this case, the approximation error ϵ will be strongly heteroscedastic so that the trend can be detected. Usually, preliminary considerations of the physical properties of the problem and the output such as in Figure 6.1 assist in the choice of the appropriate model (Forrester et al., 2008, p.75).

where ϵ is an undesired random and homoscedastic error component, which is usually normal distributed, so that the main objective of the surrogate is to minimize this error. In regression analysis, $\mathbf{x}$ are called predictor variables and y is the dependent or response variable. Many strategies and formulations of surrogate modeling exist depending on the physical properties of the problem and the underlying solvers or experiments[2] and can be found in the relevant literature about approximation theory and model building such as Forrester et al. (2008, polynomials, radial basis functions, spatial Kriging, support vectors), Draper and Smith (1998, linear and non-linear least square polynomials), Most (2008, support vector machines to map discontiguous functions), Kupper (1970, Fourier-based surfaces), or Dyken (2003, spline-based surfaces) along with many others.

The conventional polynomial response surface approach as described in Section 5.5.2 does not seem appropriate for the problem herein due to only providing a global approximation of the responses. Local effects can not be modeled. Adaptive concepts such those as described in Bucher and Bourgund (1990) disregard the computationally expensive support points from previous iterations for the design point search. It should also be mentioned that global polynomial approximation does not fulfill the interpolation and, thus, known and expensive information remains unused. In conjunction with the also approximative FORM algorithm, the error components increase and more iterations, and therefore expensive solver evaluations, are required.

In this work, the surrogate model will be based on moving least squares (MLS) which can be considered an enhancement of the least square polynomial fitting which has already been successfully used in numerical surface reconstruction (Alexa et al., 2003; Ahn et al., 2005), solving differential equations (Most, 2005; Netuzhylov, 2008; Kunle, 2001) and in response surface modeling for optimization (Breitkopf et al., 2005; Oudjene et al., 2009) and along with a few publications in reliability engineering (Proppe, 2008; Roos et al., 2007; Roos and Adam, 2006). The derivation of the method is described in detail in the following.

6.2.1. General linear least-squares

As stated in Equation 6.5 the aim is to find an approximation function $\hat{y} = \hat{f}(\mathbf{x})$ that accurately represents the behavior of the original, computationally expensive and implicit function $f(\mathbf{x})$ which has been evaluated for m support points. Using the linear independent polynomial ansatz, the approximation function yields (in matrix notation, see Equation 5.42 for the long form)

$$\hat{f}(\mathbf{x}, \hat{\boldsymbol{\beta}}) = \mathbf{y} = \mathbf{H}\hat{\boldsymbol{\beta}} + \boldsymbol{\varepsilon} \tag{6.6}$$

where $\mathbf{y}$ is a length m vector of the support point responses, $\mathbf{H}$ is a $(m \times n)$-matrix with n linear functions $h_i(\mathbf{x}_i)$ and $\hat{\boldsymbol{\beta}}$ a vector of length n of the free coefficients. The approxi-

mation error $\boldsymbol{\varepsilon}$ is a length m vector and can be minimized along the support points using Gaussian least squares. The vectors and matrices can be seen in full in Appendix A. In the previous Section is was assumed that ε_i is a random[3] error for every support point m_i which is defined

$$\varepsilon_i = f(\mathbf{x}_i) - \hat{f}(\mathbf{x}_i, \hat{\boldsymbol{\beta}}) \,. \tag{6.7}$$

Thus, for all support points the error vector $\boldsymbol{\varepsilon}$ has a mean $\mu_\varepsilon = 0$ and an unknown variance $\mathbf{I}\sigma_\varepsilon^2$ where $\mathbf{I}$ denotes the identity matrix to describe the randomness of the error. The variance σ_ε^2 can be minimized by adjusting the free coefficient vector $\hat{\boldsymbol{\beta}}$ so that

$$\sigma_\varepsilon^2 = \boldsymbol{\varepsilon}^T\boldsymbol{\varepsilon} = (\mathbf{y} - \mathbf{H}\hat{\boldsymbol{\beta}})^T(\mathbf{y} - \mathbf{H}\hat{\boldsymbol{\beta}}) \rightarrow \min_{\hat{\boldsymbol{\beta}}}! \tag{6.8a}$$

$$= \mathbf{y}^T\mathbf{y} - 2\hat{\boldsymbol{\beta}}^T\mathbf{H}^T\mathbf{y} + \hat{\boldsymbol{\beta}}^T\mathbf{H}^T\mathbf{H}\hat{\boldsymbol{\beta}} \,. \tag{6.8b}$$

The minimization can be achieved by differentiating with respect to the coefficients $\hat{\boldsymbol{\beta}}$ and setting the term to zero (Bronstein et al., 2008, p.991)

$$\frac{\partial\sigma_\varepsilon^2}{\partial\hat{\boldsymbol{\beta}}} = -2\mathbf{H}^T\mathbf{y} + 2(\mathbf{H}^T\mathbf{H})\hat{\boldsymbol{\beta}} \stackrel{!}{=} 0 \tag{6.9}$$

which leads to a system of normal equations

$$(\mathbf{H}^T\mathbf{H})\hat{\boldsymbol{\beta}} = \mathbf{H}^T\mathbf{y} \,. \tag{6.10}$$

In order to solve this equation system, at least $m = n$ support points are needed to find a non-singular solution (saturated sample set). To avoid overfitting, it is advised to have more support points than approximation terms so that $m > n$ (over-saturated sample set) or to perform a cross validation (Forrester et al., 2008, p.40). In case of non-singularity, the coefficients can be computed by transforming Equation 6.10 into

$$\hat{\boldsymbol{\beta}} = (\mathbf{H}^T\mathbf{H})^{-1}\mathbf{H}^T\mathbf{y} \tag{6.11}$$

using algorithms, i.e. the Gaussian elimination, Choleski, or others, to solve the equation system (Bronstein et al., 2008, Section 19.2, p.960). Figure 6.3 shows a linear and an overfitted least-square fits.

Sampling on the least-square surrogate is done by evaluating the polynomial with the coefficients found by inserting a set of input parameters so that

$$\hat{\mathbf{y}} = \mathbf{H}\hat{\boldsymbol{\beta}} \,. \tag{6.12}$$

[3]Non-systematic, no correlation.

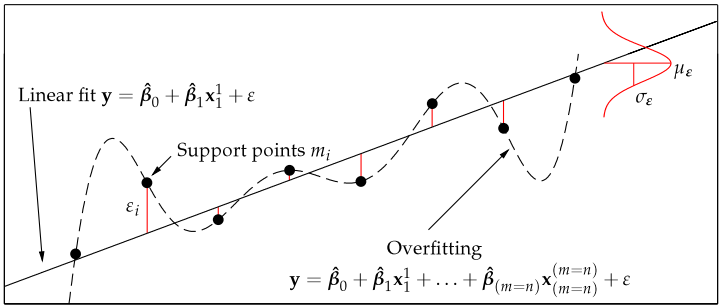

Figure 6.3.: Straight line model (solid line) and overfitted model (dashed line). Although the overfitted model accurately represents the support point values, the model is not suitable since values in between the support points are badly approximated.

6.2.2. Weighted least-squares

In the previously described case it was assumed that all support points contribute an equal amount of information to the construction of the surrogate model. Hence, the weighting of every support is equal to unity. This is not necessarily always the case; some support points might come from experiments and others from simulations, so that categorical or individual weights can be allocated to each support point in order to describe the importance of the error ε_i at support point m_i. This method is also used to stabilize the model variance or to limit the influence of outliers (Mendenhall and Sincich, 1996, p.465) i.e. by chosing $w_i = \frac{1}{\varepsilon_i^2}$.

The m weights w_i for every support point are assembled into a weighting matrix $\mathbf{W}$ which is a diagonal $(m \times m)$ matrix. In the conventional least-square fitting, $\mathbf{W}$ is an identity matrix and is, consequently, omitted. Inserting $\mathbf{W}$ into Equation 6.8 leads to a new optimization problem

$$\mathbf{W}\sigma_\varepsilon^2 = \boldsymbol{\varepsilon}^T \mathbf{W} \boldsymbol{\varepsilon} = (\mathbf{y} - \mathbf{H}\hat{\boldsymbol{\beta}})^T \mathbf{W} (\mathbf{y} - \mathbf{H}\hat{\boldsymbol{\beta}}) \rightarrow \min_{\hat{\boldsymbol{\beta}}}! \tag{6.13}$$

which can be solved in analogy to the Equations 6.9-6.11 so that

$$(\mathbf{H}^T \mathbf{W} \mathbf{H})\hat{\boldsymbol{\beta}} = \mathbf{H}^T \mathbf{W} \mathbf{y} \tag{6.14}$$

and subsequently

$$\hat{\boldsymbol{\beta}} = (\mathbf{H}^T \mathbf{W} \mathbf{H})^{-1} \mathbf{H}^T \mathbf{W} \mathbf{y}\,. \tag{6.15}$$

It tends to be rather complicated to find appropriate weights for all support points which are globally valid (Netuzhylov, 2008, p.15). This method is not applicable to sufficiently represent local trends accurately as only a global weighting of the support points is considered, therefore, yielding a global solution.

6.2.3. Moving least-squares

An enhancement of weighted least-squares was introduced by Lancaster and Salkauskas (1981) who also incorporate location information into the surrogate construction to have a locally and globally accurate approximation. This is achieved by choosing a weighting function that weighs the support points m_i according to the Euclidean distance[4] of their input parameters $\mathbf{x}_{m_i}$ to the evaluation point of the input parameters $\mathbf{x}$ so that

$$w_i(\mathbf{x}, \mathbf{x}_{m_i}) = w_i(||\mathbf{x} - \mathbf{x}_{m_i}||) \, . \tag{6.16}$$

Hence, the weighting matrix $\mathbf{W}(\mathbf{x})$ is dependent on the input parameters (location) and can be inserted into Equation 6.13 yielding

$$\mathbf{W}(\mathbf{x})\sigma_\varepsilon^2 = \boldsymbol{\varepsilon}^T\mathbf{W}(\mathbf{x})\boldsymbol{\varepsilon} = [\mathbf{y} - \mathbf{H}\hat{\boldsymbol{\beta}}(\mathbf{x})]^T\mathbf{W}(\mathbf{x})[\mathbf{y} - \mathbf{H}\hat{\boldsymbol{\beta}}(\mathbf{x})] \rightarrow \min_{\hat{\boldsymbol{\beta}}(\mathbf{x})}! \tag{6.17}$$

which—again—can be minimized using the general formulation from Equations 6.9-6.11, leading to

$$[\mathbf{H}^T\mathbf{W}(\mathbf{x})\mathbf{H}]\hat{\boldsymbol{\beta}}(\mathbf{x}) = \mathbf{H}^T\mathbf{W}(\mathbf{x})\mathbf{y} \tag{6.18}$$

so that the location-dependent coefficients can be computed to

$$\hat{\boldsymbol{\beta}}(\mathbf{x}) = [\mathbf{H}^T\mathbf{W}(\mathbf{x})\mathbf{H}]^{-1}\mathbf{H}^T\mathbf{W}(\mathbf{x})\mathbf{y} \, . \tag{6.19}$$

The difference to the globally weighted case is that the coefficients are now also dependent on the location, meaning they "move" along as the input parameters change. Thus, this approach is named *moving* least-squares (Netuzhylov, 2008, p.12).

Exploiting the surrogate involves a little more consideration, as the sampling in accordance with Equation 6.12 is now also location dependent

$$\hat{y}(\mathbf{x}) = \mathbf{h}(\mathbf{x})\hat{\boldsymbol{\beta}}(\mathbf{x}) \tag{6.20a}$$

$$= \mathbf{h}(\mathbf{x})[\mathbf{H}^T\mathbf{W}(\mathbf{x})\mathbf{H}]^{-1}\mathbf{H}^T\mathbf{W}(\mathbf{x})\mathbf{y} \tag{6.20b}$$

where $\mathbf{h}(\mathbf{x})$ is the polynomial ansatz for the input parameters $\mathbf{x}$. A numerical example is shown in Appendix A.

[4] As the input parameters are usually not on the same scale, the resulting distances are useless for further utilization if no scaling of the data is performed. Hence, all variables are standardized into the $\mathcal{N}(0,1)$-space before the surrogate is built and exploited. The resulting small distances have to be considered in the choice of the regularization parameter $\varepsilon_{\text{reg.}}$.

6.2.4. Weighting functions

The accuracy of the approximation from Equation 6.20 mainly depends on the choice of the weighting function $w_i(||\mathbf{x} - \mathbf{x}_{m_i}||)$. Generally, the weighting function must be symmetric around the support points, greater than zero, and monotonically decreasing within a defined influence radius D, which describes the support sub-space Ω_{m_i} of influence around a support point m_i (Kunle, 2001, p.19) so that

$$w_i(||\mathbf{x} - \mathbf{x}_{m_i}||) = \begin{cases} w_{d_i}(||\mathbf{x} - \mathbf{x}_{m_i}||) \,, & ||\mathbf{x} - \mathbf{x}_{m_i}|| \leq D \\ 0 \,, & ||\mathbf{x} - \mathbf{x}_{m_i}|| > D \,. \end{cases} \tag{6.21}$$

Often, a cubic (or higher order) polynomial (Kunle, 2001, p.19) (Netuzhylov, 2008, p.17) or a Gaussian curve (Most and Bucher, 2005) is chosen which leads to a smoothing of the data and thus to an undesired non-interpolation case for greater Ds while for smaller Ds the approximation is better. These phenomena are discussed in detail in Appendix B. Yet a minimum number of support points is required to solve the equation system (see above) so that small Ds can lead to ill-conditioned matrices.

An interpolation case is only achieved when the weight at the support points approaches infinity (Lancaster and Salkauskas, 1981)

$$\lim_{\mathbf{x} \to \mathbf{x}_{m_i}} w_i(||\mathbf{x} - \mathbf{x}_{m_i}||) = \infty \,, \tag{6.22}$$

so that a possible weighting function can be found to be

$$w_i(||\mathbf{x} - \mathbf{x}_{m_i}||) = \frac{1}{||\mathbf{x} - \mathbf{x}_{m_i}||^{\gamma}} \,, \quad \gamma = 2k \,, k \in \mathbb{N} \,. \tag{6.23}$$

Unfortunately, this leads to a singularity in the function and thus to numerical problems. An optimal interpolation function decreases the weight very quickly as the distance from the support point increases so that the weighting function nearly fulfills the so-called Kronecker-delta-property (Bronstein et al., 2008, p.276)

$$w_i(||\mathbf{x} - \mathbf{x}_{m_j}||) \approx \delta_{ij} = \begin{cases} 1 \,, & i = j \\ 0 \,, & i \neq j \,. \end{cases} \tag{6.24}$$

In order to consider both requirements from Equation 6.23 and 6.24, the weighting function is standardized to fulfill the Kronecker-delta-property and regularized to allow for the numerical evaluation at the support points by introducing a regularization parameter $\varepsilon_{\text{reg.}}$. Detailed information about the the incorporation of regularization parameters can be found in Netuzhylov (2008, Section 6.2.6) and Kunle (2001, Chapter 3).

Most and Bucher (2005) propose a suitable weighting function which enhances the approach by Shepard (1968) and nearly fulfills the interpolation requirements with sufficient accuracy based on Equation 6.23 with $\gamma = 2$:

$$w_R(||\mathbf{x} - \mathbf{x}_{m_i}||) = \frac{\tilde{w}_R(||\mathbf{x} - \mathbf{x}_{m_i}||)}{\sum_{j=1}^{m} \tilde{w}_R(||\mathbf{x} - \mathbf{x}_{m_i}||)} \tag{6.25}$$

with

$$\tilde{w}_R(||\mathbf{x} - \mathbf{x}_{m_i}||) = (||\mathbf{x} - \mathbf{x}_{m_i}||^2 + \varepsilon_{\text{reg.}})^{-2} , \quad \varepsilon_{\text{reg.}} \ll 1 . \tag{6.26}$$

When Equation 6.25 is inserted into Equation 6.20, the numerical effort can be significantly reduced (Most and Bucher, 2005) to

$$\hat{y}(\mathbf{x}) = \mathbf{h}(\mathbf{x})[\mathbf{H}^T\mathbf{W}(\mathbf{x})\mathbf{H}]^{-1}\mathbf{H}^T\mathbf{W}(\mathbf{x})\mathbf{y} \tag{6.27a}$$

$$= \mathbf{h}(\mathbf{x}) \left[\frac{1}{\sum_{j=1}^{m} \tilde{w}_R(||\mathbf{x} - \mathbf{x}_{m_i}||)} \mathbf{H}^T\tilde{\mathbf{W}}(\mathbf{x})\mathbf{H} \right]^{-1} \cdot \cdot \frac{1}{\sum_{j=1}^{m} \tilde{w}_R(||\mathbf{x} - \mathbf{x}_{m_i}||)} \mathbf{H}^T\tilde{\mathbf{W}}(\mathbf{x})\mathbf{y} \tag{6.27b}$$

$$= \mathbf{h}(\mathbf{x})[\mathbf{H}^T\tilde{\mathbf{W}}(\mathbf{x})\mathbf{H}]^{-1}\mathbf{H}^T\tilde{\mathbf{W}}(\mathbf{x})\mathbf{y} . \tag{6.27c}$$

$\tilde{\mathbf{W}}(\mathbf{x})$ can be constructed for infinite support ($D = \infty$) with the constraint that a minimum squared distance $||\mathbf{x} - \mathbf{x}_{m_i}||^2_{min} \gg \varepsilon_{\text{reg.}}$ is maintained to avoid the singularity. This is suitable as the formulation of the weighting function does not smooth the data and is nearly independent of the influence radius (Most and Will, 2008). The regularization parameter $\varepsilon_{\text{reg.}}$ has to be chosen to be greater than the square root of the machine precision so that a zero distance can be evaluated. Most and Bucher (2005) recommend $\varepsilon_{\text{reg.}} = 10^{-5}$. Figure 6.4 shows the approximation and interpolation power for the data from Figure 6.3. A 2-dimensional example is given in Figure 6.5. The corresponding matrices can be found in Appendix A.

6.3. Reliability analysis

As stated above, the exploitation of the IMLS surrogate has to be done point-wise and thus no closed-from expression is available to allow the use of, for example, FORM as in the classical RSM approach. Nevertheless, the point-wise exploitation allows the use of the numerical integration algorithms described in Section 5.5.3. Proppe (2008) and Roos and Adam (2006) recommend the use of the adaptive importance sampling (AIS) as described in the following, or in Bucher (1988), which reduces the necessary number of

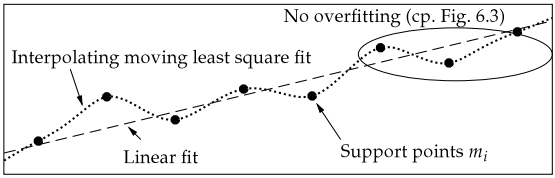

Figure 6.4.: Interpolating moving least square fit of the data from Figure 6.3. The interpolation condition is clearly fulfilled to a sufficient accuracy without the problems of overfitting (see encircled area). The line is purposely dotted to emphasize the point-wise sampling to construct the surrogate.

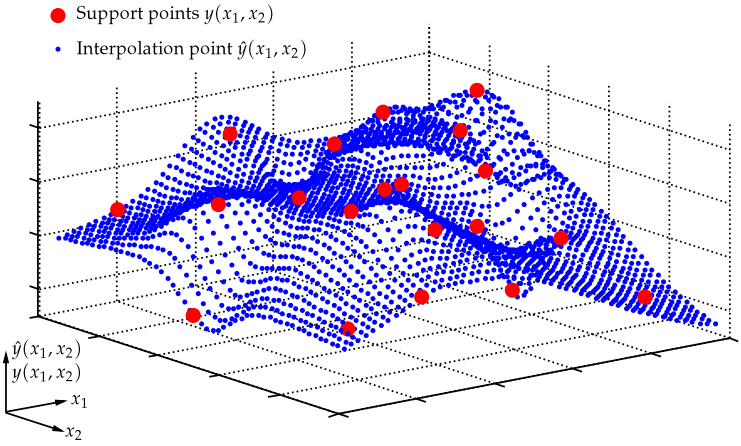

Figure 6.5.: Exemplary IMLS surface approximation to 20 support points with input parameters (x_1, x_2) and response values $y(x_1, x_2)$ using 2601 evaluation points $\hat{y}(x_1, x_2)$. Matlab 7.8.0 (2009) computation time on a 3.2 GHz machine was approximately 1.3 seconds (uncompiled).

evaluations but also yields additional information such as the approximate location of the design point and empirical sensitivity factors (Schnetgöke, 2008, p.76). In the following, the basic idea of the AIS and special considerations concerning the exploitation of the IMLS surrogate will be described. Further details on AIS can be found in Bucher (1988), Schnetgöke (2008, Section 5.5) and Six (2001, Section 7.2).

6.3.1. Basic methodology of AIS

The basic idea of the AIS methodology is to iteratively reduce the variance of the estimated probability of failure $\hat{p}_f$ by using a weighting function $h_{\mathbf{x}}$ as described in Section 5.5.3. $h_{\mathbf{x}}$ is adapted in AIS for every iteration step to converge towards the ideal weighting function (stated in Equation 5.47 and shown for the 1-D case in Figure 5.7). Six (2001, p.159) proposes a starting procedure for AIS in which the variances of the input parameters are multiplied by a factor of $2^2 \leq \psi^2 \leq 3^2$ to achieve a sufficient number of failure points[5] for the next iteration step. For the exploitation of the IMLS surrogate, this starting procedure should only be used with caution as the surrogate is extremely unstable for points outside the influence domains (Roos et al., 2007, Figures 11-17). Hence, ψ^2 should be chosen to assure that the resulting sampling points of $h_{\mathbf{x}}$ remain inside the domain represented by the surrogate. It is advisable to increase the number of surrogate evaluations rather than to increase ψ^2 as the numerical costs of a IMLS exploitation are very low ($\ll 1$ sec).

$\hat{p}_f$ can be calculated according to Equation 5.46 but is likely to be very inaccurate for the first iteration steps. The accuracy can be determined by the variance of $\hat{p}_f$ which can be calculated in continuous discrete form to

$$\hat{\sigma}^2_{\hat{p}_f} = \mathrm{E}\left\{\left[\hat{p}_f - \mathrm{E}(\hat{p}_f)\right]^2\right\} \rightarrow \min_{h_{\mathbf{X}}(\mathbf{u}_i)}! \tag{6.28a}$$

$$= \frac{1}{N}\sum_{i=1}^{N}\left[I(\Omega_{\mathcal{F},i}) \cdot \zeta_{\mathbf{X}}(\mathbf{x}_i) - \hat{p}_f\right]^2 \tag{6.28b}$$

where $\zeta_{\mathbf{X}}(\mathbf{u}_i)$ is the likelihood ratio as described in Section 5.5.3. In order to minimize the variance, a new weighting function $h_{\mathbf{x},2}$ has to be found which approximates the ideal weighting function (see Equation 5.47) more accurately and therefore yields better results.

The information from the first iteration is used to update $h_{\mathbf{x},2}$ for the second iteration by only considering those evaluations where the limit state was violated (failure points).

[5] $N_f \approx 10 \cdot n$ for n input parameters (Six, 2001, p.159).

The new weighting function yields a mean value for the j-th random variable based on N evaluations (continuous and discrete form)

$$\hat{\mu}_{X_j} = \frac{1}{p_f} \int_{\mathbf{X}} I(\Omega_{\mathcal{F}}) \cdot x_j \cdot \zeta_{\mathbf{X}}(\mathbf{u}) \cdot h_{\mathbf{x}}(\mathbf{u}) \, d\mathbf{u} \tag{6.29a}$$

$$= \frac{1}{\hat{p}_f \cdot N} \sum_{i=1}^{N} I(\Omega_{\mathcal{F},i}) \cdot x_{j,i} \cdot \zeta_{\mathbf{X}}(\mathbf{x}_i) \tag{6.29b}$$

and a covariance between the j-th and the k-th random variable (continuous and discrete form)

$$\hat{\sigma}^2_{X_j,X_k} = \frac{1}{p_f} \int_{\mathbf{X}} I(\Omega_{\mathcal{F}}) \cdot x_j \cdot x_k \cdot \zeta_{\mathbf{X}}(\mathbf{u}) \cdot h_{\mathbf{x}}(\mathbf{u}) \, d\mathbf{u} - \mu_{X_j} \cdot \mu_{X_k} \tag{6.30a}$$

$$= \frac{1}{\hat{p}_f \cdot N} \sum_{i=1}^{N} I(\Omega_{\mathcal{F},i}) \cdot x_{j,i} \cdot x_{k,i} \cdot \zeta_{\mathbf{X}}(\mathbf{x}_i) - \hat{\mu}_{X_j} \cdot \hat{\mu}_{X_k} \, . \tag{6.30b}$$

The adaptation of $h_{\mathbf{x}}$ using a mean and a variance uniquely determines a joint normal density. In this work, the Gaussian copula shown in Equation 5.22 and in Appendix C.5 is utilized for the weighting functions $h_{\mathbf{x},i}$ as proposed in Bucher (1988). The numerical integration of the discrete Equations 6.29b and 6.30b is herein performed using the quasi-random Halton points as described in Section 5.4.4.

For multiple iteration steps, the weighting function is improved and hence the updated mean ($\hat{\mu}_{\mathbf{X}}$) of the weighting function $h_{\mathbf{x}}$ converges towards the location of the actual design point while the covariance ($\hat{\sigma}^2_{\mathbf{X}}$) of $h_{\mathbf{x}}$, and thus the variance of $\hat{p}_f$, is significantly reduced (see Figures 5.7 and 6.6). The coefficient of variation of $\hat{p}_f$, which hereafter will be denoted ε_{AIS} ($= \sqrt{\hat{\sigma}^2_{\hat{p}_f}} / \hat{p}_f$), is usually chosen as a convergence criterion for the algorithm. Cabral and Katafygiotis (2001) propose 10 % to be sufficiently accurate while Six (2001, p.159) uses 5 % as convergence criterion.

An illustrated example of the algorithm with the first two iteration steps of a 2-dimensional reliability evaluation is given in Figure 6.6. A similar example and a detailed flowchart of the complete algorithm can be found in Six (2001, p.160,p.162). Schnetgöke (2008, p.77) provides a table of the minimum required number of evaluations depending on the assumed probability of failure. As the numerical cost exploitation of the IMLS surrogate is very low, a high number of evaluations of the surrogate for each iteration can be anticipated.

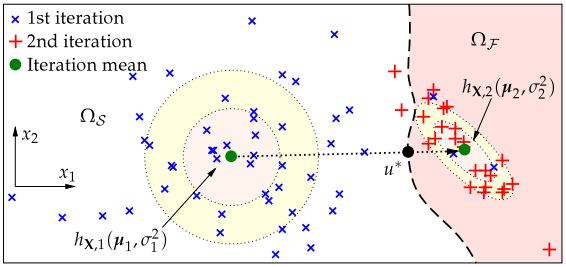

Figure 6.6.: The first two iteration steps of adaptive importance sampling (AIS). The shift of the mean vector towards the theoretical design point u^* and the reduction of the (co)variances can be clearly seen. The number of samples was purposely chosen to be very low for better illustration. In reality, many more samples would be used.

6.3.2. Empirical sensitivity factors

A very good approximation of the theoretical design point can be retrieved by choosing the mean vector ($\hat{\mu}_{\mathbf{X},fin}$) of the last iteration prior to convergence of the reliability problem and to then perform a linear interpolation between the defined mean and the mean vector of the last iteration. This method has been described by Bucher and Bourgund (1990) who use it for the update of a quadratic polynomial response surface.

Six (2001, p.158) proposes a method to derive empirical sensitivity factors $\hat{\alpha}_{X_j}$ based on the ratio of shift of the mean $\hat{\mu}_{X_j,fin}$ and the total shift of the mean vector (contribution to overall variance). To provide for equal weighting, the means are standardized to

$$\hat{\tilde{\mu}}_{X_j,fin} = \frac{\hat{\mu}_{X_j,fin} - \mu_{X_j}}{\sqrt{\sigma^2_{X_j}}} \tag{6.31}$$

where μ_{X_j} and $\sigma^2_{X_j}$ are the first two statistical moments of the initial random input variable X_j of the reliability problem. The sensitivity factor for the j-th of n random variables can then simply be calculated to

$$\hat{\alpha}_{X_j} = \frac{\hat{\tilde{\mu}}_{X_j,fin}}{\sqrt{\sum_{i=1}^{n} \hat{\tilde{\mu}}^2_{X_i,fin}}} \,. \tag{6.32}$$

In Figure 6.6 the sensitivity of X_1 is dominating ($\hat{\alpha}_{X_1} \gg \hat{\alpha}_{X_2}$) in the reliability problem as the shift of the mean vector is mainly in X_1-direction.

6.4. Surrogate adaptivity and convergence criteria

The adaptive importance sampling procedure described in the previous section was applied to the IMLS surrogate and not the underlying model. Hence the probability of failure and the sensitivity factors are, in fact, near-exact with respect to the surrogate—but only approximative to the underlying reliability problem, whereas the approximation quality of the surrogate is unknown in between the support points. Hence, criteria to determine convergence have to be defined in order to terminate the computation at a sufficient accuracy.

For this purpose, the number of support points is increased in order to create a higher information density in the vicinity of the real design point. A subsequent reliability analysis including the new support points yields the updated probability of failure. Comparing the failure probabilities from the previous iteration step $\hat{p}_{f,(i-1)}$ with the current one $\hat{p}_{f,i}$, a simple criterion can be established. If the error is acceptable within a certain error margin (i.e. 5 %) the algorithm is terminated as the probability of failure and the sensitivities are found with a sufficient accuracy. This means that the empirical failure probability has stabilized so that

$$\varepsilon_{\hat{p}_f} = \frac{|\hat{p}_{f,i} - \hat{p}_{f,(i-1)}|}{\hat{p}_{f,(i-1)}} \overset{!}{\leq} 0.05 \,. \tag{6.33}$$

In order to build the updated surrogate, a few more support points in the vicinity of the assumed design point location have to be evaluated. In order to keep the number of limit state evaluations as low as possible and to gain as much information as possible, the new DoE is centered around the mean vector of the last AIS iteration. The support points are sampled around that point according the systematic sampling schemes (described in Section 5.4.5). An approach followed herein is the utilization of the factorial sampling with varying levels.

6.4.1. Decomposition of the covariance

In order to maximize the information density gained from the additional support points, the sampling is performed according to the principal components (PC) of the covariance matrix of the previous AIS iteration on the surrogate. The principal components are orthogonal, uncorrelated combinations of the random variables which (in descending order) describe the highest variability in the data. Principal component analysis or spectral decomposition is applied in many fields. In image processing or random field theory, this decomposition is often referred to as Karhunen-Loéve transformation (Bucher, 2009, p.141).

The principal components can be found by decomposing ("de-correlating") the covariance matrix as described in Section 5.4.2. The methodology is described in great detail in Gentle (2009, p.549). Herein, only the most relevant parts are explained.

The covariance matrix obtained from the last AIS iteration is decomposed into the triangular matrices

$$\mathbf{R}^T\mathbf{R} = \mathbf{C}_{\mathbf{XX}} \tag{6.34}$$

so that the decomposed diagonal matrix $\mathbf{\Lambda}$ of the eigenvalues λ_i can be calculated[6]

$$\mathbf{\Lambda} = \mathbf{R}^T\mathbf{C}_{\mathbf{XX}}\mathbf{R}\,. \tag{6.35}$$

The matrix $\mathbf{R}$ can be found using Choleski or spectral decomposition (see Section 5.4.2). Herein, $\mathbf{R}$ is found by solving the eigenvalue problem

$$(\mathbf{C}_{\mathbf{XX}} - \lambda\mathbf{I})\mathbf{x} = \mathbf{0} \tag{6.36}$$

where $\mathbf{I}$ is the identity matrix and $\mathbf{0}$ a zero vector. The columns of $\mathbf{R}$ are, therefore, the eigenvectors. The percentage of total variability (the "importance") of the i-th principal component with regard to all n others can be calculated to $\lambda_i / \sum_{k=1}^{n} \lambda_k$.

6.4.2. Importance-based DoE

The importance of the principal components will be utilized to create an optimized layout of the new support points for the surrogate. If a factorial design of experiments (DoE) is used, the number of support points ("levels") in each PC direction is chosen in dependence of the importance of λ_i. The design is then centered around the previous AIS design point $\mathbf{u}^*_{k-1}$ and rotated using $\mathbf{R}$ according to Equation 6.34. The methodology is visualized for clarity in 2-D in Figure 6.7 using a $[5, 3]$-level factorial design. Another possibility is to use random or quasi-random sampling in the subspace around the design point which was not followed herein.

The support points from the previous iteration steps can be "recycled" in the new surrogate to accurately limit and stabilize the sampling and to avoid the extrapolation pitfalls. As the surrogate nearly fulfills the interpolation conditions, no further considerations have to be taken here. This methodology has the advantage that no information from previous expensive model evaluations is lost or omitted. For higher dimen-

[6] if $\det(\mathbf{C}_{\mathbf{XX}} - \lambda\mathbf{I})\mathbf{x} = 0$ (Bronstein et al., 2008, p.318)

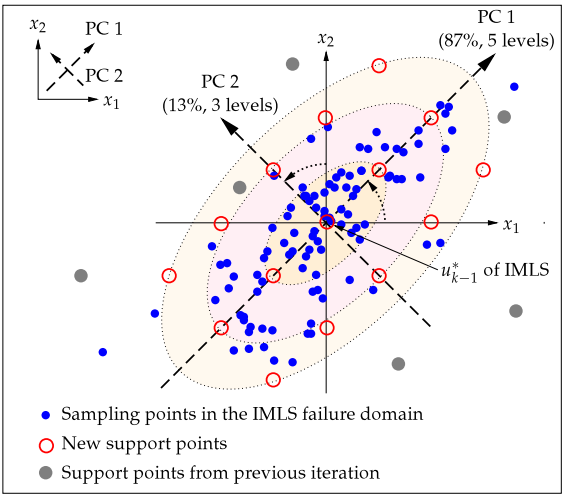

Figure 6.7.: Arrangement of the support points for the next iteration step. The density of information obtained from this strategy is superior to blind sampling. The first principal component (PC 1) contributes 87% to the total variability and hence five levels are used in that direction, while only three levels are used for the less important, second principal component (PC 2). Support points from previous iterations can be re-used to provide a stable boundary.

Table 6.1.: Proposed number of levels chosen depending on the importance of the PC.

$\lambda_i / \sum_{k=1}^{n} \lambda_k$	**# Levels in PC direction**
0.00-0.25	1-3[†]
0.25-0.75	3
0.75-1.00	5

[†] depending on the problem dimensionality

sional problems, the levels of the DoE are optimized to obtain a high information density from the additional model evaluations so that no unnecessary, yet (numerically) expensive evaluations are made. A strategy to omit PC directions if they underrun an importance threshold for λ_i is described in Gentle (2009, p.550). Herein, all PCs are used but the number of levels are adapted according to the contribution of the PC to the total variance (as shown in Table 6.1) so that the DoE is optimized for information density.

6.5. Parallelization

The algorithm described above significantly reduces the required computational cost due to the reduction in required solver evaluations. Yet a certain number[7] of evaluations is still required. Processing these evaluations sequentially on a single computer (or even CPU) can not only exceed the computational capacity of this computer but is also very inefficient with respect to time.

The algorithm proposed above provides the opportunity for a multi-layer parallelization which can be considered a mixture of *high-performance* (HPC) and *high-throughout computing* (HTC). HPC is mainly a massive parallelization of a single solver evaluation by utilizing a large number of computational resources (compute cluster) which are tightly connected to interchange data at high-speed. This parallelization is achieved within the program code of the solver using interfaces like MPI (Message Passing Interface) or openMP. Both methods are commonly used in CFD software and, thus, are both implemented in FDS 5.3 (2009).

As the DoE requires multiple solver evaluations which are non-interacting during the evaluation, HTC can be utilized for a further parallelization of the problem. Magoulès et al. (2009, p.1) define HTP, or "grid computing", as an attempt to increase the "amount of work per unit time". This is achieved by evaluating solver runs simultaneously on various machines. Usually this is done by loosely coupling multiple computers into a

[7] Depending on the dimensionality and the shape of the response hyper-surface.

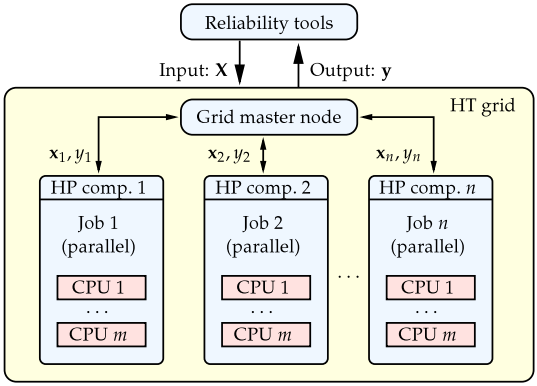

Figure 6.8.: Parallelization of the reliability algorithm. The n required support points are distributed onto n HP computers which are incorporated into a HT grid. Each computer has m CPUs to solve each support point parallelized (theoretical case).

so-called *grid*. A master node administers the available resources and assigns standalone jobs to the connected nodes (batch processing system). Further information on grid computing and the applicability to probabilistic (Monte Carlo) problems can be found in Magoulès et al. (2009, especially Chapter 7).

As shown in Figure 6.8, these considerations theoretically allow for the utilization of multiple high performance computers coupled into a grid. For the simple benchmark problems from Section 6.7, the iBMB simulation PCs were coupled into a grid using the Condor Version 7.5.2 (2010) grid software while the simulations were performed on one CPU each. The more complex examples in Chapter 7 were executed on the TU Braunschweig computing cluster[8] which allowed for both parallelization methods.

6.6. Adaptive discretization

For the analyses in this work the CFD solver FDS 5.3 (2009) by McGrattan et al. (2009) was used for the simulation of the fire scenarios and the evaluation of the times to untenability (ASET). As described in Section 4.1.3, FDS uses a uniform, rectangular mesh with equally sized cube mesh cells, each with the edge length δx. The optimum discretization (best accuracy/speed ratio), and thus the δx to be used, is a priori unknown.

[8] VVT-cluster: 556 CPUs (2.4GHz), 1.1 TeraBytes RAM

The user guide for FDS 5.3 (2009, p.74) generally advises to perform a "mesh sensitivity study" where the δx should be gradually refined until the results stabilize. Hill et al. (2007) find that values in the range of $D^*/\delta\, x \;=\; 4 \;\ldots\; 16$ usually yield reasonable results for common problems and thus give a "rule of thumb"-specification for the needed discretization. D^* is a characteristic fire diameter and is described in detail in Section 4.1.3.

As the cells describe a three-dimensional computational domain and all equations implemented into the CFD code have to be evaluated for each cell, choosing a smaller δx obviously leads to an exponential increase in the number of cells and computation time. The latter is limited, even though parallelization strategies were used as described above. In order to optimize the discretization, an adaptive approach was utilized as described in the following.

The algorithm starts with a preliminary scan of the random space in order to determine the globally most significant parameters (sensitivity analysis) and the approximate location of the design point for the reliability analysis. Naturally, highly accurate, and thus numerically expensive, solutions are not needed. Hence, the discretization is chosen to be rather coarse, with the constraint that the results produced are still acceptable, so that δx can be chosen to be $D^*/\delta x \approx 4 \ldots 6$.

After the first iteration step of the algorithm, the discretization is refined for the adaptation of the surrogate model in order to find more accurate support point values for the reliability assessment around the design point as described in the Sections 6.3 and 6.4. A further mesh refinement can be performed in the next iterations if required. As the convergence criteria (Section 6.4) of the algorithm is based on a comparison between the results of the previous and the current iteration, *a mesh sensitivity study is already implicitly performed*.

Herein, the mesh refinement was terminated at $D^*/\delta x \;\approx\; 12$ to reduce the computational effort. This is reasonable as the uncertainties introduced by the input parameters, assumptions about the fire scenario, tenability models, etc. are by far higher than the remaining model uncertainty.

As all support points are used in all iterations, it is possible to introduce further weighting ($\mathbf{W}_{\delta x}$) for the support points in the surrogate based on the (location independent) weighted least-squares described in Section 6.2.2. This reduces the influence of the support points with larger δx-values and increases the influence of support points based on finer meshes. This approach was not followed herein. As the reliability analyses only required 2-4 iterations, the initial discretization was already chosen to produce accurate results, and the results only varied slightly upon mesh refinement due to the space-time filtering and the FID model used. This gradual adaptive refinement method allows for an even faster convergence of the algorithm and requires less numerical effort without sacrificing accuracy since an implicit mesh sensitivity study is performed.

6.7. Validation and benchmarking

In the following, two simple examples will be shown to validate and benchmark the methodology. The first example is an analytical function that should represent the possible solver responses of numerically expensive simulations. In this example, only two random variables are used to provide a graphical representation of the random space. A second example using a zone fire model is presented to show the practical application of the method. As the simulation times of analytical functions and zone fire models are very short, Monte Carlo simulation can be used to validate the methodology.

6.7.1. Analytical function

In order to test and validate the methodology, an analytical, 3-dimensional test function ($\mathbb{R}^3$) was chosen to be

$$z = f(x_1, x_2, x_3) = x_1 - x_2 + \cos(x_2) + 0.1 \cdot x_1 \cdot x_2 + 5 + 1 \cdot 10^{-5} \cdot x_3 \tag{6.37}$$

with a failure domain

$$\Omega_{\mathcal{F}} \equiv f(x_1, x_2, x_3) \leq 0 \tag{6.38}$$

to provide a non-linear surface and a non-significant variable to test for the approximation and the sensitivity analysis. All three random variables were chosen to be uncorrelated and Gauss (standard) normal distributed $[\mathcal{N}(0,1)]$. For the sensitivity analysis and the initial surrogate construction, 9 samples were evaluated based on a 3-level full factorial design with $\psi^2 = 3$ (see 5.4.5). For higher dimensionality, other DoEs should be used, such as the central composite design.

Analyzing for linear and rank correlation between input and output showed (expectedly) that only x_1 and x_2 are significantly correlated, while $\rho_{x_3,z} \approx 0$. The stepwise regression methodology also showed that x_3 has no significant contribution to the output values, which is expected due to the small multiplier of x_3. The overall (adjusted) model accuracy of the linear model was already $R^2_{adj} = 0.918$. Hence, a stepwise regression of the rank-transformed data was omitted.

As a result of the sensitivity analysis, the surrogate is constructed based only on x_1 and x_2 (as x_3 has proven to have no significant influence on the limit state) so that the dimensionality is reduced ($\mathbb{R}^3 \rightarrow \mathbb{R}^2$) as shown in Figure 6.9. As the implemented algorithms are very fast, 50,000 sampling points based on the Halton sequence were generated with a covariance multiplier of $\psi^2 = 2$ for the first iteration of the reliability analysis with AIS, which is far more than the required number given in Schnetgöke (2008, p.77) so that convergence is already expected after 2-3 iteration steps. The 50,0000

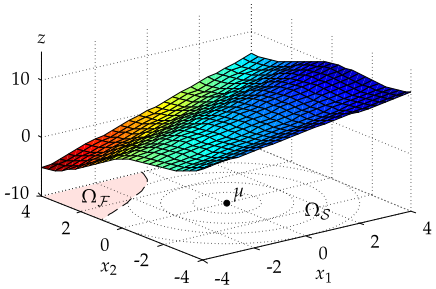

Figure 6.9.: 3D visualization of the reduced analytic function from Equation 6.37.

points were evaluated with the IMLS surrogate based on the 27 support points with the corresponding responses. The (uncompiled) IMLS algorithm realized in Matlab 7.8.0 (2009) required approximately 60 seconds of CPU-time on a single-core 3.2 GHz machine.

The results of the analyses are shown in Table 6.2 and are visualized in Figure 6.10. Only 25 evaluations of the actual limit state function were required to find a solution that is very close to the accuracy of 1,000,000 crude Monte Carlo runs. The sensitivity factors found are also very close those found by FORM and AIS using the limit state function directly. Further benchmark analyses can be found in Table 6.3.

Figure 6.10 shows that the initial DoE is merely a scan of the whole random space in order to find the approximate location of the limit state. The subsequently evaluated support points are already close to the real design point, resulting in a very fast convergence of the algorithm. Due to the very fast computation of the IMLS interpolation values it is possible to use an extremely high number of samples on the surrogate so that the AIS only requires very few iterations.

The analysis of the simple and verifiable benchmark problem constitutes the general applicability of the model. In a second example, a zone fire model will be utilized to verify the applicability to FSE-specific problems. Zone fire models have a very low computation time, so that a benchmark AIS-analysis is possible.

Table 6.2.: Iterations of the IMLS-AIS-response surface algorithm of the reliability problem from Equation 6.37.

Iteration	$\hat{p}_f$	ε_{AIS}	α_{x_1}	α_{x_2}	**CPU-time (IMLS)**	$\varepsilon_{\hat{p}_f} = \frac{\lvert\hat{p}_{f,i} - \hat{p}_{f,(i-1)}\rvert}{\hat{p}_{f,(i-1)}}$
1. Surrogate (9 evaluations [3×3]):						
1.1	0.00074	0.038	0.6198	-0.7848	56.8 sec	
1.2	0.00074	0.005	0.6168	-0.7872	57.0 sec	
2. Surrogate (8 evaluations [4×2]):						
2.1	0.00199	0.012	0.5984	-0.8012	57.3 sec	
2.2	0.00198	0.005	0.5999	-0.8001	57.5 sec	167.00 %
3. Surrogate (8 evaluations [4×2]):						
3.1	0.00196	0.006	0.5818	-0.8133	57.8 sec	
3.2	0.00196	0.005	0.5821	-0.8131	57.6 sec	**1.01 %**
Convergence after a total of 25 evaluations						

Table 6.3.: Comparative benchmarks of the reliability problem from Equation 6.37.

Benchmark	$\hat{p}_f$	ε_{AIS}	α_{x_1}	α_{x_2}	$\Delta = \frac{\lvert\hat{p}_f - p_{f,BM}\rvert}{p_{f,BM}}$
Adaptive Importance Sampling (total: 2 × 50,000 evaluations):					
B1.1	0.00191	0.040	0.5773	-0.8165	
B1.2	0.00191	0.005	0.5789	-0.8154	2.62 %
Crude Monte Carlo (total: 4 × 1,000,000 evaluations):					
B2.1	0.00189	Mersenne-Twister random sampling			3.70 %
B2.2	0.00192	Latin-Hypercube random sampling			2.08 %
B2.3	0.00191	Halton sequence quasi-random sampling			2.62 %
B2.4	0.00193	Sobol sequence quasi-random sampling			1.55 %
First order reliability method (Comrel 8.00, 2004) (total: 42 evaluations):					
B3.1	0.00233	–	0.5500	-0.8300	15.88 %

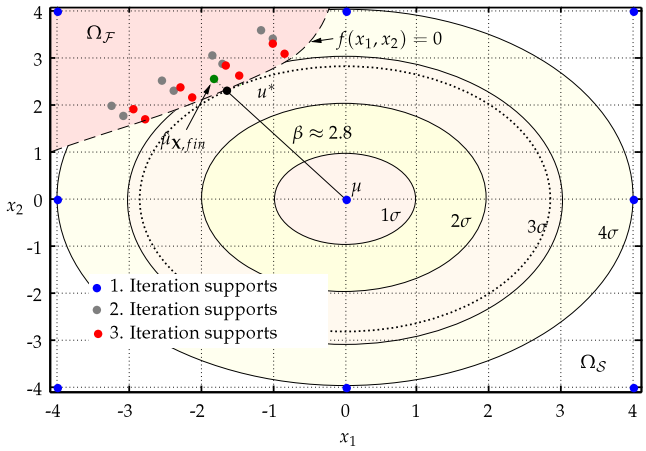

Figure 6.10.: Visualization of the benchmark function and locations of the support points for the iterations. The IMLS sampling points are not shown.

Table 6.4.: Stochastic model of the zone fire benchmark reliability problem.

Parameter	**Unit**	**Distribution**	μ	σ
Fire Load Q	MJ	Normal	5000	500
Growth rate t_g	s	Normal	300	50
Max. HRR	MW	Normal	3.5	0.5
All variables are considered to be uncorrelated.				

6.7.2. Zone fire model

In order to test, validate and benchmark the applicability of the IMLS-RSM method to FSE problems, the zone fire model CFast 6.1 (2009) was utilized to estimate the probability of having less than 140 seconds before a smoke layer height of 2.0 m is underrun considering a αt^2 fire scenario so that

$$\Omega_{\mathcal{F}} \equiv \text{ASET} \leq 140\ s. \tag{6.39}$$

The room geometry was chosen to be a 200 m^2 assembly room without smoke and heat exhaustion (SHE), which was already analyzed in Forell (2007a) and Albrecht and Hosser (2009). The stochastic model was changed and reduced for simplicity and is shown in Table 6.4.

A preliminary sensitivity analysis using the stepwise linear method showed that the fire load Q has no significant influence on this problem and hence will be modeled deterministically with the mean value for the further analysis. These results correspond with the findings in Albrecht and Hosser (2009) who also state that fire load has no influence for the given problem. This is due to the fact that the fire load determines the duration of the fire. Yet, the thresholds for life safety are mostly reached within the growth phase of the fire. The most significant variable was the fire growth rate t_g which is expressed as the time in seconds until 1 MW is reached[9]. This was expected as previous analysis (Albrecht and Hosser, 2009) showed similar results. As the R^2_{adj} of the linear model was very high (> 80 %), a stepwise rank regression was omitted herein. The iterations and results are shown in Table 6.5.

To validate the results, the reliability was also analyzed with direct adaptive importance sampling. One evaluation of CFast 6.1 (2009) including the automated threshold analysis of the output took approximately 1.3 seconds on a single-core 3.2 GHz machine. Validation benchmarks were performed with the implemented AIS code[10] (B2) in Matlab 7.8.0 (2009) as well as the AIS code (B1) implemented in optiSLang 3.1.0 (2009). A crude Monte Carlo simulation was also performed using Latin Hypercube sampling (B4) and Halton points (B5). The number of simulations had to be limited to 10,000 which was not enough for the failure probabilities to fully stabilize so that the deviation is slightly higher. The results of the analyses can be found in Table 6.6. It can be seen that the same accuracy as AIS can be achieved with only 36 evaluations of CFast 6.1 (2009). It should be noted that full factorial designs were chosen, as the numerical cost of a limit state evaluation is very low. For problems with a higher stochastic dimensionality and more complex numerical models, DoEs such as the central composite design should be preferred. The sensitivity analysis has proven to be a very helpful tool to reduce the dimensionality and thus the complexity of the problem. Figure 6.11 shows the random space and the support points used.

[9] α and t_g are related as: $\alpha = \dot{Q}_i + \frac{1000\ \text{kW}}{t_g^2}$.

[10] The implemented Matlab code (see Appendix D) uses either Halton quasi-random points, Latin Hypercube points, or Mersenne-Twister random points for the numerical integration. The example was computed using Halton points.

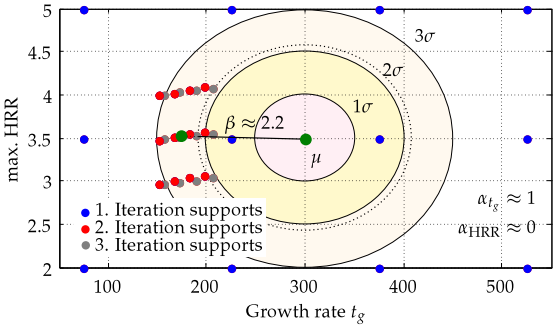

Figure 6.11.: Random space and support points of the CFast example. It is clearly visible that t_g is the controlling variable. This is in accordance with the findings of Forell (2007a) and Albrecht and Hosser (2009).

Table 6.5.: Results of the reliability analysis for the zone fire model reliability problem.

RS-Iteration	**Method**	$\hat{p}_f$	**Evaluations**	$\varepsilon_{\hat{p}_f} = \frac{\lvert\hat{p}_{f,i} - \hat{p}_{f,(i-1)}\rvert}{\hat{p}_{f,(i-1)}}$
1	IMLS-RSM	0.0216	12 [4 × 3]	–
2	IMLS-RSM	0.0152	12 [4 × 3]	29.63%
3	IMLS-RSM	0.0150	12 [4 × 3]	**1.32%**

Table 6.6.: Results of the benchmarks for the zone fire model reliability problem.

Benchmarks		$\hat{p}_f$	**Evaluations**	$\Delta = \frac{\lvert\hat{p}_f - p_{f,BM}\rvert}{p_{f,BM}}$
B1	AIS (optiSLang 3.1.0, 2009)	0.0155	4,000 [4 × 1,000]	3.23%
B2	AIS (Matlab 7.8.0, 2009)	0.0154	4,000 [4 × 1,000]	2.60%
B3	FORM (optiSLang 3.1.0, 2009)	0.01503	n/a	0.13%
B4	crude MC (optiSLang 3.1.0, 2009)	0.0161	10,000	6.83%
B5	crude MC (Matlab 7.8.0, 2009)	0.0158	10,000	5.06%

6.8. Conclusions

In this Chapter, a new and innovative response surface method was introduced based on interpolating moving least squares (IMLS). The methodology was derived in detail and enhanced with various features to further improve performance in terms of speed and accuracy. To keep the number of required support points as low as possible, additional considerations were made for the generation of importance-based design of experiment plan and adaptive discretization. To distribute the load on high throughput cluster computers, a crude parallelization was implemented. The methodology is validated and benchmarked using an analytical function and a zone fire model example. Both benchmark exercises were also analyzed with various conventional reliability algorithms to show the accuracy and speed of the new method. The validated method can now be utilized to calibrate the currently accepted safety levels by using code-compliant buildings and state-of-the-art fire engineering tools. This will be done among other considerations, such as the influence of barriers, in the next Chapter 7.

Chapter 7

Quantification of safety levels

The detailed example shown in this chapter is the analysis of a fully code-compliant medium-sized assembly building in order to determine the currently accepted operational safety levels using the state-of-the-art FPE methods introduced in Chapter 4. This rather small building was chosen instead of larger or atrium type buildings for various reasons: firstly, many of the most severe fires with high numbers of casualties during the last decade have happened in buildings of this size and occupancy, such as The Station Fire (Bryner et al., 2007), the Gothenburg Disco Fire (Wickström et al., 2004) or the Lame Horse Fire (Belosokhov et al., 2010). This type of building can be assumed as the most critical regarding occupant life safety, since the comparably low volume of this type of building due to, for example, rather low ceiling heights or small compartmentalization, leads to higher concentrations of smoke faster than in large atria with high ceilings. Secondly, it was found that all the effects of the various scenarios, influence of fire protection systems, etc. can be demonstrated in this exemplary application so that a larger sized example would not lead to significant additional information at exponentially higher numerical cost. Yet, for a later derivation of a safety concept it is inevitable to also include such scenarios. Additionally, fire codes usually require the escape routes to lead to a "place of relative safety" (Perry, 2003, p.79), which can also be a place in an adjacent compartment which is separated by fire-rated doors and walls. Thus, the building herein could also be regarded as one (critical) fire compartment within a larger complex building such as a shopping mall, a hotel, etc.

Stochastic models and design scenarios are derived from the literature specifically for medium-sized assembly buildings and are compiled into an event tree. The relevant identified scenarios are then evaluated using the IMLS response surface method in order to compute the scenario reliabilities. Additionally, the effect of fire protection barriers on the system reliability of life safety design is analyzed at the end of the Chapter along with appropriate methods of their consideration within the design process.

7.1. Multi-purpose community assembly building

The building for the analysis is a common multi-purpose community assembly building as shown in Figure 7.1. The layout was chosen so that various scenarios can be tested and state-of-the-art engineering tools can be utilized to their capabilities. The building has a vestibule which serves as a checkroom (for coats and jackets) and for security and ID checks. The main room consists of a dance floor with a DJ (turn-)table which is located in the lower middle of the room. A bar area with various tables is located in the upper right of the building, while the restrooms are located at the lower left.

In order to record the optical density and the toxic species for the tenability analyses in a structured and transparent way, control volumes were placed within the compartment. The three control volumes for the optical density are located centrally as shown in Figure 7.1, spanning an area of 4 m^2 at a height of 1.6-2.0 m to account for various body heights. For tenability analysis, the mean optical density of each control volume is analyzed for the threshold of 0.15 m^{-1}, allowing for a visibility of approximately 10m. ASET for visibility is assumed to be reached when any two of the three control volumes exceed the threshold. This is based on the preliminary analyses in Albrecht and Hosser (2009) where it was found that the visibility thresholds are usually reached before any toxic criteria. The occupants only need the visibility in order to locate the nearest available exit, but when they reach the vicinity of the exits, visibility is no longer relevant for a safe evacuation.

The toxicity criteria become important during a later phase of the evacuation, when the occupants are usually in the process of egress. Hence, the fractional incapacitating dose (FID) values will be recorded in close proximity to the exits. The control volumes span 2 m^2 at a height of 1.6-2.0 m. ASET is set to be reached if one of the five control volumes reaches an FID value of 1.0. This is assumed to be the ultimate threshold where people will be severely harmed by the fire.

The FID_{total} model used herein is a holistic overall FED-model based on Speitel (1996) as described in Section 4.2.6, including asphyxiant species[1] as well as flux and temperature criteria. As FDS in the current version does not allow for the accurate modeling of the release and transport of irritant substances, the initial FID value is set to a lump-sum of 0.3 to account for the potential release of these species. Hence, the complete incapacitation model used reads

$$FID_{\text{total}} = F_{I,\text{asphyx.}} + F_{I,\text{heat}} + F_{I,\text{irrit.}}(= 0.3) \overset{!}{\leq} 1\,. \tag{7.1}$$

[1] Lack of oxygen, hydrogen cyanide, carbon dioxide (including hyperventilation), and carbon monoxide.

This approach has the advantage that the threshold values are smoothed and stabilized due to the spatial and the temporal integration within the FID model, allowing for the generation of stable and continuous responses, which are an essential requirement for an accurate surrogate model. The analyses of the FDS output files, including the calculation of the FID-values and the determination of the ASET times are completely automated in the implemented software so that the results are consistent for every FDS simulation. RSET times are also automatically determined from the output files of the FDS+evac simulation as the times where the last occupant (id est simulation "agent") has left the compartment.

Both fire and evacuation simulation are terminated after 20 minutes, as this is set to be the maximum time in which the process of evacuation of a fire compartment has to be completed according to Mehl (2004). If threshold values are not reached, they will be conservatively chosen to be 1,201 seconds, which is one second after the termination of the simulations.

7.2. Fire scenarios on the basis of NFPA 101

To completely assess the current level of life of safety within a standard assembly building, various scenarios have to be taken into account along with their corresponding probability of occurrence which can be derived from fire statistics. Herein, the scenarios were chosen on the basis of NFPA 101 (2008) and are as follows:

1. *Standard design fire* on the basis of NFPA Scenario 1 where all models from Section 7.3.1 are used along with the design fire from Section 4.4.1. This scenario and the corresponding probability of failure of life safety will be regarded as the *baseline scenario*. Reliability evaluation will be performed for both visibility (optical density) and toxic/heat (FID) criteria. The fire will be located in the bar due to the high fire initiation potential.
2. A hidden slowly developing (smoldering) fire is assumed to develop in the storage room. Instant fire and smoke spread occurs when the door is opened or fails (burn-through). In order to account for the incomplete combustion (equivalence ratio[2] $\Phi > 1$), the yields will be conservatively doubled according to Hull et al. (2008). Evaluation is performed using visibility and toxic/heat (FID) criteria.

[2]The (global) equivalence ratio gives information about the ventilation conditions and is defined: $\Phi = \frac{\%\,\text{Oxygen required}}{\%\,\text{Oxygen supplied}}$, where $\Phi \ll 1$ describes a well-ventilated fire. More information can be found in Forell (2007b).

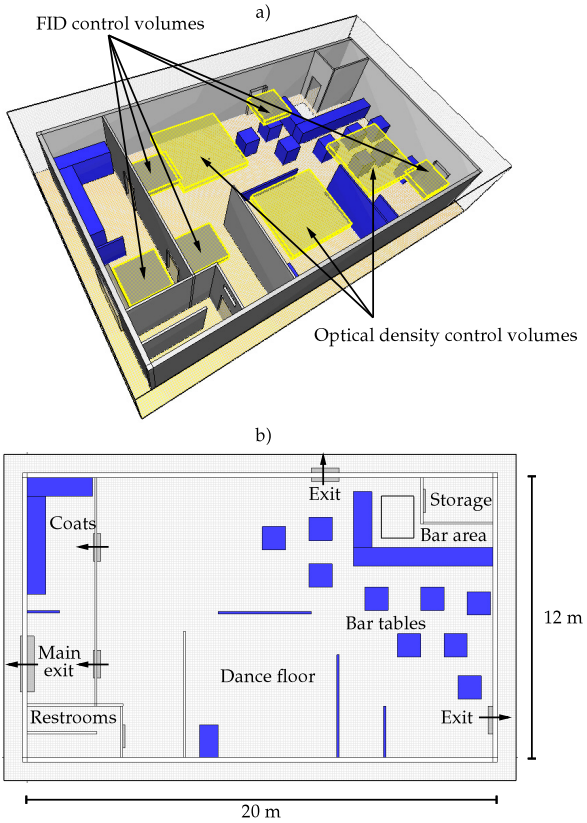

Figure 7.1.: Layout of the assembly building. The control volumes for optical density and FID, respectively, are shown in a). An overview over the exit situation is given in b). The ceiling height is 4 m.

3. Fire near the main entrance/exit (vestibule/checkroom) blocking the primary means of egress and thus leaving the occupants to use only the emergency exits. This scenario is roughly in accordance with the exit capacity calculation requirements given in the U.K. code Approved Document B (2006, Section 3.21,p.37), where the discount of the largest exit door is required. The analysis is based on optical density and FID criteria in proximity of the remaining usable exits.
4. An ultra-fast fire scenario will be considered omitting the linear growth phase (equates to the "classic" αt^2-scenario) in the design fire using visibility and toxic/heat (FID) criteria. The probability of this scenario to occur is considered rather low. The fire will be located in the vicinity of the DJ (turn-)table. This scenario could be flammable decoration as seen in The Station Fire or the Lame Horse Fire.

All fire scenarios described above are conservatively assumed to be based on a polyurethane (PUR, $CH_{1.46}O_{0.23}N_{0.08}$) reaction leading to rather high amounts of smoke and asphyxiant effluents, as can be seen in Table 7.3. These assumptions are reasonable considering the interior and decoration of such facilities and the aforementioned tragic fires.

Other scenarios are disregarded at first as the geometry is rather simple. Scenarios with function or malfunction of the fire protection barriers installed and the corresponding impact on the life safety levels are shown in Section 7.5. Analysis with the scenarios mentioned above gives some insight of the operational probabilities of failure of life safety and the risk of at least one casualty during a fire in a code compliant, standard, multi-purpose community assembly building. Additionally, the mean margin of safety can be quantitatively derived as the mean of the convolution distribution function of the reliability problem, which can be found by inserting the mean vector into the model. This "margin of safety"-approach was recently proposed by Babrauskas et al. (2010).

7.3. Stochastic models

Finding stochastic models for the various parameters for both fire and evacuation simulation is very difficult, because such data usually does not exist, or is very limited and only applicable on a case-by-case basis. Hence, the models introduced in the following sections are compiled from the cited literature and/or are based on best guess estimates incorporating some degree of conservativeness. Thus, the models ultimately included into the analysis are, considering the definition from Section 2.3, *best knowledge subjective probabilities enhanced with available frequentistic information*. As a result, the convolution and the corresponding probabilities of failure should be regarded the same way.

7.3.1. Models for fire simulation

The most predominant uncertain parameters that can be identified for a design fire in accordance with Equation 4.29 are the maximum heat release rate ($\dot{Q}_{max}$ or HRR_{max}) and the fire load (Q) for which models are widely available, such as in JCSS 2.20 (2001). Therein, a normal distribution is assumed for the fire load in assembly/office buildings with a mean of 600 MJ/m^2 and a of variation of 30 %. Previous analyses (Albrecht and Hosser, 2009; Albrecht et al., 2010) have shown that the fire load merely controls the length of the fire but has no significant impact on the time until any thresholds (optical density, FID) are reached. Therefore for further analysis, the fire load will be used deterministically with the mean value of 600 MJ/m^2.

For the maximum heat release rate, the values are estimated in BS DD 240 (1997) to be around 250 kW/m^2 (500 kW/m^2 for storage/warehouses), while vfdb-Leitfaden (2009, p.91) states up to 620 kW/m^2 for public buildings and at least 430 kW/m^2 for coatrooms. Hence, a mean of 500 kW/m^2 was conservatively chosen with a standard deviation of 100 kW/m^2 which is in accordance with Hosser et al. (2008) who chose a normal distribution with a variation of 20 %.

The fire growth rate for the t-squared fire is the most influential parameter as shown in Forell (2007a) and Albrecht et al. (2010). Various stochastic models can be found in the literature with different characteristics. Magnusson et al. (1996) use a uniform distribution for α ranging from 0.001 to 0.01 kW/s^2. Hasofer and Qu (2002) also use a uniform distribution for the fire spread rate ranging from 0.1 to 2.0 m/s. Notarianni (2000, Chapter 4, p35) gives discrete probabilities for the common classes of fire growth rates as shown in Table 7.1 for domestic houses and condominiums.

Holborn et al. (2004) analyzes data from London Fire Brigade reports. For "other" (than dwellings) buildings, he finds the probabilities as also shown in Table 7.1. Using distribution fitting, the fire growth rate α can be approximately considered to be log-normal distributed with a mean $\mu_\alpha = -6.5$ and a standard deviation of $\sigma_\alpha = 2.0$. The expected values of the distribution is, therefore, $E(\alpha) = 0.012$, which corresponds to a medium growth rate. The large discrepancies to the data by Notarianni may be due to the fact that Holborn's data for public buildings is based on estimations of fire investigators after actual fire events and thus also includes the smoldering phase until established burning occurs. Notarianni's data is based on controlled laboratory fire tests of furniture with a defined ignition source (Lawson et al., 1983) and is derived for domestic buildings. As the smoldering phase will be included in the chosen scenario (see Figure 4.11), the range of Notarianni's data seems more suitable here and will be considered in the distribution function for the model in Table 7.3. A left-skewed distribution, such as the Gumbel (min) seems appropriate as small t_gs become more likely.

Table 7.1.: Fire growth rate classes and probabilities by Holborn et al. (2004, for buildings other than dwellings) [1] and probabilities according to Notarianni (2000, Chapter 4, p35, for furniture) [2].

Fire growth class	α kW/s^2	$t_{1\,\mathrm{MW}}$ s	**Likelihood** [1]	[2]
Very slow	< 0.000412	< 1 600	0.27	–
Slow	0.000412-0.006594	400-1 600	0.54	0.20
Medium	0.006594-0.026375	200-400	0.10	0.50
Fast	0.026375-0.1055	100-200	0.07	0.25
Ultra fast	>0.1055	<100	0.03	0.50

Additional to the three above, further parameters are needed to represent uncertainty in the generation of byproducts in the fire, such as asphyxiant gases or visibility constraints due to smoke. In FDS this is usually accomplished by prescribing so-called yields (see Section 4.1.3), which are stoichiometric ratios of the release of combustion byproducts. Usually, the release of carbon monoxide (CO), carbon dioxide (CO_2), and hydrogen cyanide (HCN) are most relevant for tenability analysis (Section 4.2.2), while the soot yield is the controlling variable in the visibility threshold assessments (Albrecht et al., 2010). The yields are dependent on the burning material and no stochastic models could be found in the literature. Yet a number of possible CO, CO_2, and soot yields for various materials in well-ventilated conditions can be found, for example, in Tewarson (2008) or vfdb-Leitfaden (2009). Bansemer (2004) derives empirical models for the yields of polyamide and polycarbonate in dependence of heat flux and air supply. HCN yields are given in Purser and Purser (2008) based on experiments and depending on the equivalence ratio Φ. In order to derive sufficient and implicitly conservative stochastic models, the most common materials are compiled from the available data as shown in Table 7.2 and, subsequently, appropriate distributions are chosen accordingly. For the analysis herein, conservative normal distributions were chosen for the yields as shown in Table 7.3, as no other information about the possible distributions was found. The correlation between the yields is unknown but it is assumed to be dependent on the equivalence ratio. Yet for simplicity, it will be omitted herein. Further random parameters, such as wind, external influences, etc. are not considered within the analyses in order to keep the dimensionality reasonable. An addition for future considerations or specific problems is unproblematic if the stochastic model is known.

Table 7.2.: Subset of the material yields from Tewarson (2008, Table 3-4.16), vfdb-Leitfaden (2009, p.81), and Purser and Purser (2008) for well-ventilated conditions. Fluids were omitted.

Material	y_{CO_2}	y_{CO}	y_{Soot}	y_{HCN}
Wood (oak)	1.27	0.004	0.015	–
MDF Board	1.2	0.002	–	<0.0035
Cellulose	0.83	0.004-0.09	0.02-0.09	–
Polyester	1.65	0.070	0.091	–
Polyurethane (foam)	1.55	0.010	0.131	<0.007
PVC	0.46	0.063	0.172	–
Polyamide 6	–	–	0.011	<0.059
Plastics (general)	0.86-1.12	0.05-0.09	0.06-0.20	<0.01

7.3.2. Models for evacuation simulation

For the egress simulation only physical parameters were considered in order to retain model-independence to some degree as stated in Section 4.4.2. Albrecht et al. (2010) have shown that the most influential parameters for the egress simulation are pre-movement time and the occupancy level, which can either be expressed by the absolute number of occupants or by a number of occupants per unit area. The latter can usually be found in codes and standards for assembly buildings. The German code (MVStättV, 2005) assumes values of 2 occ./m^2 for general assembly buildings, while the compiled values in vfdb-Leitfaden (2009, p.272) range from 0.1-0.5 occ./m^2 for shopping centers up to 4.0 or 5.0 occ./m^2 for bars/dance clubs or stances in stadia. These values denote the maximum possible local densities. Such an occupancy for the entire building will not be reached (see i.e. restrooms, bar area, kitchen, storage, etc.). The Approved Document B (2006, Table C1) acknowledges this by giving maximum densities of 3.3 occ./m^2 for "standing spectator areas, bar areas (within 2 m of serving point)" and maximum 2 occ./m^2 for "venue for pop concerts and bar without fixed seating". "Area" is defined therein as gross floor area excluding fixed parts of the structure but including counters. Hence, gross floor space densities are very likely to be lower. It should also be noted that these are design values for a conservative design and not mean values. Looking at the "Station Fire" (Tubbs and Meacham, 2007, p.83ff) with approx. 460 occupants at 350m^2 (without offices), an averaged (over the gross floor space) density of 1.3 occ./m^2 can lead to a catastrophic outcome.

In conclusion, the occupancy level has a high influence on the egress time and has led to catastrophic events in the past. The stochastic model herein is chosen to be conservative and also to allow for overcrowding, even though the likelihood of a severe fire with concurrent high occupancy levels can be considered relatively low. Yet values of up to

4 occ./m^2 can be considered as local effects. Averaged density models for the gross floor space will be derived and used.

Assuming that a gross floor space-averaged occupant density of 3 occ./m^2 is approximately the 95th-percentile of a Gumbel (max) distribution, a (conservative) mean of 1.5 and standard deviation of 0.5 occ./m^2 is chosen for the general purpose assembly building. This density is used throughout the whole assembly room (gross floor space) so that on average the occupancy will be 360 (ca. 240 m^2). A theoretical number of 600 occupants (2.5 occ/m^2) is, therefore, not exceeded in 90 % of the time. This assumption is reasonable and yet can be considered conservative to a high degree. Local peaks and other effects are omitted in favor of the gross floor model.[3]

High influence on the limit state was also found for the warning and pre-movement times (Albrecht et al., 2010) which have been described in detail in Section 4.3. The warning time is composed of detection and alarm time and is chosen to be normal distributed with a mean of 60 seconds and a standard deviation of 15 seconds. This model can be updated[4] with actual site-specific simulation data after the initial fire simulations.

The pre-movement time, which consists of recognition, interpretation, and action of the occupants before starting the evacuation, is selected based on the data compiled in vfdb-Leitfaden (2009, Section 9.3) and Tubbs and Meacham (2007, p.294). As a skewed distribution is shown in vfdb-Leitfaden (2009, p.258), a Gumbel (max) distribution was chosen with a mean of 90 seconds with a standard deviation of 25 seconds for an operational alarm system with voice guidance (even though this is rarely used in Germany) and a mean of 180 seconds with a standard deviation of 45 seconds for a non-operating or non-existing voice guidance system. This can be deemed reasonable as it is assumed that all occupants start the movement at the same time, which leads to higher congestion at the exits and hence is conservative to a degree that justifies the choice of the distributions. Other models are derived and described for the specific scenarios considered.

Other parameters to be considered in the analysis are the occupant-specific parameters velocity and shoulder-width. While the former is the anticipated maximum speed towards an exit (if no other external forces apply, see Section 4.3), the latter controls the outflow through the exits. For example, if an exit is 1.2 m wide, two persons with shoul-

[3] Yet, local effects could easily be modeled by using multiple "&EVAC"-items in FDS+evac with varying densities or even random fields as described in Bucher (2009, Chapter 5) for other models.

[4] Updating of stochastic models can be performed using Bayesian updating as described by Papadimitriou and Katafygiotis (2005).

Table 7.3.: Stochastic model for the life safety reliability quantification problem for stoichiometric combustion.

Parameter	Unit	Distribution	Mean	Std.-Dev.	Cov.-Var.
$\mathrm{HRR}_{\max}$	$\mathrm{kW/m^2}$	Normal	500	100	20 %
t_g	s	Gumbel (min)	250	50	20 %
y_{CO}	g/g	Normal	0.090	0.030	33 %
y_{HCN}	g/g	Normal	0.006	0.002	33 %
y_{Soot}	g/g	Normal	0.120	0.040	33 %
Occ. density	$\mathrm{occ./m^2}$	Gumbel (max)	1.5	0.5	33 %
Warning time	s	Normal	60	15	25 %
Pre-move. time	s	Gumbel (max)	90/180	25/45	28/25 %
Velocity	m/s	Normal	1.25	0.3	24 %
Shoulder width	m	Normal	0.51	0.07	14 %

der width of 0.6 m could exit at the same time, while only one person with a shoulder width of 0.9 m is able to exit at once. Both parameters are given along with their variation in Korhonen and Hostikka (2009, p.20) for various groups of occupants. For the analysis herein, these values will be utilized and are assumed to be normal distributed with a standard deviation given in Table 7.3.

Further parameters, such as the stochastic treatment of social forces, etc. are omitted for simplicity, but could easily be added to the model. A complete overview of all (fire and egress simulation) stochastic parameters is given in Table 7.3, leading to a 10-dimensional reliability problem.

Explanatory remark I: Physical vs. mathematical boundaries of stochastic modeling

When assessing reliability problems, uncertain parameters are modeled using mathematical distribution functions (see Annex C) whose required parameters are adjusted to a sample set. Even assuming the sample set is representative and the fitting is done carefully using the appropriate mathematical tools (see Section 5.3), there will always be a discrepancy between the mathematical formulation of the distribution and the parameter for the simple fact that the distribution boundaries range from $-\infty$ to $+\infty$ for most continuous distributions or from 0 to $+\infty$, i.e. for the log-normal distribution. This implies—even though being highly improbable—that physically impossible parameter constellations can occur, such as for example a zero compressive strength for concrete or negative values for t_g, the time in seconds until 1 MW is reached. Naturally, all parameters do have more or less sharp defined boundaries which physically cannot be under-

or overrun. However, when reliability analysis is performed, these limits or boundaries are neglected as the convolution is performed using only the mathematical (unbounded) functions. Hence, in selected cases, the reliability algorithm converges to a design point on the joint probability density function, which is mathematically correct but constitutes a physically impossible parameter set, such as negative or very low[5] t_g-values or occupant densities above 8 m^{-2}. This shows once more the necessity of a clear distinction between *operational* vs. *mathematical probabilities* as mentioned in Section 2.3.2. In the aforementioned cases, these parameter sets with low mathematical failure probabilities imply a zero operational failure probability for the *particular scenario* and *particular input parameters*. Therefore, a conclusive qualitative check of the whole calculation is indispensable.

7.4. Reliability assessment

In the following Sections, the scenarios described are evaluated for their failure probabilities along with the stochastic models introduced previously. As each of the four chosen scenarios is a possible, but more or less likely scenario, they have to be assessed within a system approach with their corresponding probability of occurrence.

The reference period of the system is chosen to be one year in accordance with the structural codes (DIN EN 1990, 2002). As the arrival of fire events during the building lifetime ($t \geq 0$) is assumed to be a Poisson process[6], the time between fire is exponentially distributed with the rate parameter $\lambda > 0$ which denotes the expected number of fires per unit time (Bronstein et al., 2008, p.833), in this case one year. Hence, the annual probability of fire occurrence can be computed to

$$P(t = 1a) = 1 - e^{-\lambda \cdot 1} \approx \lambda \tag{7.2}$$

for small λs (< 0.1) so that in the following λ will be taken as a fire initiation probability to account for the reference period of one year. For more information see Annex C.4.

The probability of occupants being present as shown in Figure 4.9 had to be omitted since their correlation to the fire initiation cannot be ruled out for the scenarios considered.

[5] This would denote an explosion-like fire spread which cannot be modeled with FDS.
[6] Fires can occur at any time and are independent of one another.

7.4.1. System analysis

To assess the overall system reliability without any active fire protection barriers, the scenarios from Section 7.2 are compiled into an event tree and the corresponding probabilities of occurrence can be derived from the literature. Fire ignition frequencies are given in various publications and standards, such as Hosser et al. (2008) or BS 7974 (2001, Annex A). Herein, an overall annual probability of 2 % was chosen in accordance with the latter standard and the remark above (refer to Appendix C.4). In many cases, fire fighting action is undertaken by the occupants upon early detection of a fire. Holborn et al. (2004, Table 18) finds the probability of failure of an intervention attempt to be 75 %. In a successful attempt (25 %), the fire is considered extinguished or at least confined in a way so that a subsequent hazard to the occupants is prevented.

In the unlikely case of a fire and failure of manual intervention, the "standard scenario" (rf. Section 7.2) will have a probability of occurrence of 50 %. This assumption is based on Holborn's findings that fire damages from 1 up to 10 m^2 occur in 49 % of all fires. A fire with a HRR_{max} of 2.5 MW is in accordance with the assumptions used for the derivation of the design fire (Section 4.4.1). Fires with a damage size of less than 1 m^2 occur in 26 % of cases, so that the likelihood of the slow, smoldering fire is chosen to be 25 % as the (non-human) damage to the building structure will probably be rather low. The remaining 25 % are cases in which the ultra-fast fire (10 %) and the blocking of the primary means of egress (15 %) occur. The numbers are chosen arbitrarily but are likely to be conservative, both also with a HRR of 2.5 MW. An overview of the resulting event tree can be seen in Figure 7.2.

7.4.2. Scenario 1: Standard scenario

As described above, the standard scenario (fire in the bar area) was evaluated for both, optical density and FID criteria to derive baseline probabilities of failure. It should be noted here, that the limit state implies that the thresholds are reached at one of the control volumes before all occupants (agents) have left the compartment, which means that occupants may be—but not necessarily automatically are—exposed to the delaying or incapacitating effects of the fire. This fact, as well as the choice of rather conservative assumptions about the scenario and the variables lead to the high observed failure probabilities which are listed in Table 7.4. Yet the results have to be regarded as conditional probabilities of failure, as a fire start has to occur and all fire protection barriers have to fail before this scenario takes place. The failure probabilities are in good accordance with the findings for the optical density threshold reliability assessment performed in Albrecht and Hosser (2010b). Including hydrogen cyanide (HCN) yields and temperature criteria into the analysis leads to far higher failure probabilities for the FID threshold than in the paper. This can also be be seen when looking at the sensitivities for both criteria as shown

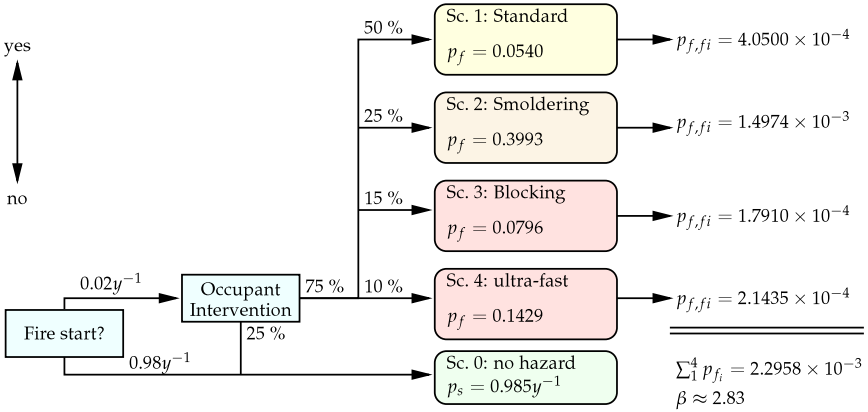

Figure 7.2.: Complete event tree of the reliability assessment of the code compliant multi-purpose assembly building, exemplary shown for the time-integrated FID criterion.

in Figure 7.3. For the optical density, the time to 1 MW (t_g) on the fire side and the occupant density or the resulting number of occupants, respectively, and the pre-movement time on the evacuation side have the highest influences. The soot yield has a statistically significant yet subordinate impact on the limit state. For the incapacitation, the influence of t_g is even larger while the influence of both number of occupants and pre-movement time decreases. Instead of the soot yield, the HCN yield now plays a statistically significant (yet also subordinate) rule. This is due to the fact that the FID is mainly controlled by the HCN intoxication, as also found by Purser (2002). It should be noted again that the HCN yield was chosen very conservative herein.

The mean margin of safety can be derived by looking at distance between the support point value at the mean vector and the zero-state of the limit state function. For the optical density, the mean safety margin is 12 seconds (implying a left-skewed convolution distribution), while it is 345.6 seconds (>5 minutes) for incapacitation.

Explanatory remark II: Coupled simulation

Recent state-of-the-art simulation tools such as FDS+evac allow for the coupling between fire and evacuation simulations. The agents react to the fire simulation by, for example, reducing walking speed, changing exit routing when walking through smoke, or

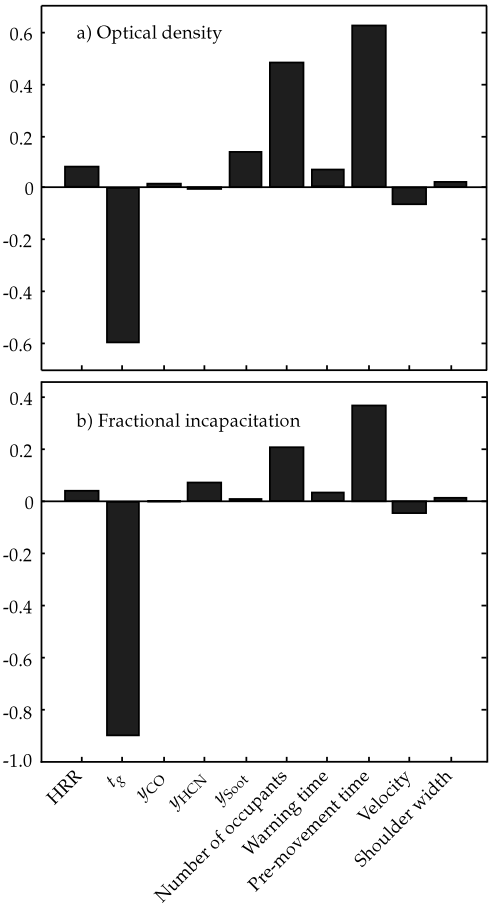

Figure 7.3.: Sensitivities of the standard scenario 1 for a) the optical density and b) the fractional incapacitation dose (FID). The highest influence on the overall variance is observed for the time to 1 MW (t_g), the number of occupants, and the pre-movement time.

Table 7.4.: Number of supports, convergence behavior, and results of the reliability analysis for the standard scenario for both optical density and FID thresholds.

Surrogate	**AIS**	ε_{AIS}	$\varepsilon_{\hat{p}_f} = \frac{\lvert\hat{p}_{f,i} - \hat{p}_{f,(i-1)}\rvert}{\hat{p}_{f,(i-1)}}$	$\hat{p}_f$
Optical density				
1	1	0.0231	–	65.19 %
1	2	0.0096	0.0522	68.59 %
2	1	0.0049	0.0058	68.19 %
Fractional incapacitation dose (FID)				
1	1	0.1647	–	4.05 %
1	2	0.0334	0.2494	5.06 %
2	1	0.0454	0.0850	5.49 %
2	2	0.0090	0.0164	5.40 %

becoming incapacitated when reaching an individual incapacitation dose. Herein, the methodology was used for the standard scenario to study the effects that are introduced by the coupling for the specific scenario. In this case, no visibility threshold exists (the agents are just slowed down), so that this criterion has to be omitted. The individual FED-values of the agents from the fire simulation are based only on the gas concentrations of carbon monoxide (CO) and dioxide (CO_2) and reduced oxygen (O_2) levels. Hydrogen cyanide (HCN) is omitted even though it greatly affects the incapacitation. Additionally, the temperature and flux criteria are not included either. This leads to very low FED-values (in the 1×10^{-4}-range) for the given stochastic models and thus no casualties (FED equals unity) were observed in any of the support point simulations performed. Hence, the results are very optimistic compared to the full fractional incapacitation (FID) model used herein and no reasonable further quantitative analysis could be performed.

A comparison between the evacuation times of the coupled simulation vs. the decoupled case showed little to no differences. This may be simply due to the fact that the visibility reducing the walking speed is not reached until nearly all the agents are near the exit doors where the walking speed is controlled by the outflow and not by visibility conditions. Hence, for this particular case, the coupling did not have any advantages over the traditional ASET/RSET approach, but a generalization cannot be made, especially for larger, more complex buildings. Also, as the coupled simulations are still in research and development, the traditional decoupled simulations will be utilized for further analyses.

Explanatory remark III: Jackknifing the surrogate

In order to assess the accuracy of the surrogate, so-called "statistical jackknifing" (leave-one-out cross validation) is performed (Mendenhall and Sincich, 1996, p.420). This means that one support point with the known result is omitted when generating the surrogate. The error between surrogate and the omitted known support point value gives an idea about the power and accuracy of the approximation. The jackknifing was performed on the mean of the FID evaluation. The difference $\Delta_{\epsilon_{\text{IMLS}}}$ between the support point value (345.6s) and the IMLS-surrogate value (346.7s) is 1.1 seconds, which implies *relative error of less than 1%*. This shows the approximative power of the IMLS algorithm as well as the validity of the assumptions in Figure 6.1. The same accuracy range was also reached in previous analyses, i.e. in Albrecht and Hosser (2010b).

Explanatory remark IV: Influence of distribution functions and correlations

In the previous analyses it was found that the variables which were chosen to be Gumbel-distributed (t_g, occupant density, pre-movement time) had the highest influence on the limit state. In order to assess the impact of the type of distribution function, those parameters were set to normal distributions with the same parameters given in Table 7.3. The resulting failure probability decreases to $\hat{p}_{f,\text{normals}} = 0.16$ % for the FID threshold. This probability is more than 30 times lower than the reference value of $\hat{p}_f = 5.4$ % utilizing the skewed Gumbel-distributions. Yet, t_g and the pre-movement time still have the highest sensitivities (-0.85 and 0.37, respectively), followed by the HCN yield (0.26). The sensitivity of the occupant density decreased to 0.14, as shown in Table 7.5.

Besides the choice of the distribution function, some of the input parameters might be correlated. In order to determine the influence, linear correlations were introduced into the stochastic model. A high correlation[7] of 0.75 was assumed between all yields, between the warning and pre-movement time and a negative correlation of -0.75 between occupant density and shoulder widths. The calculations were performed using the previous normal distributions to avoid the more complex Nataf transformations as the general trend remains the same. Compared to the previous analysis, the probability of failure increases to $\hat{p}_{f,\text{norm.,corr.}} = 0.24$ % which is 1.5 times higher than $\hat{p}_{f,\text{normals}}$ without the correlations. The dominant parameter sensitivities are t_g (-0.72), the pre-movement time (0.39) and the warning time (0.34) HCN yield (0.27), followed by the other yields. Obviously, the sensitivity of previously less influential parameters is increased due to the correlation.

Another informative evaluation was performed by correlating the three most influential parameters in a way so that they would produce higher failure probabilities. t_g is negatively correlated with a correlation of -0.8 to the occupant density and the pre-

[7] Definition according to Dehne (2003, p.125). Low correlation: ± 0.25, medium correlation: ± 0.50, high correlation: ± 0.75.

Table 7.5.: Influence of the distribution functions and correlation effects.

Criteria	$\hat{\alpha}_{t_g}$	$\hat{\alpha}_{\text{num. occ.}}$	$\hat{\alpha}_{\text{pre-move.}}$	$\hat{p}_f$
All normal distributions	-0.8493	0.1447	0.3682	0.16 %
Correlated normal dist.	-0.7378	0.1133	0.3926	0.24 %
Maxium correlation effect	-0.6063	0.5388	0.5590	1.33 %
Standard w/ skewed dist.	-0.8999	0.2107	0.3681	5.40 %

movement time, while the latter ones are correlated positively by 0.8. Even though this is unreasonable (as, for example, a faster fire spread would rather not be correlated to a longer pre-movement time), it shows the maximal theoretical impact of the correlation. The resulting failure probability of $\hat{p}_{f,\text{norm,corr.,unr.}} = 1.33$ % is eight times higher than without correlation. Yet it is far less than the impact of changing distribution types or even the distribution parameters. A comprehensive summary is given in Table 7.5.

The overall impact of the correlations on both failure probability and sensitivities is far lower than the impact of changing the distribution functions. Hence, for future data collection it might be more important to gain more accurate information about the distributions of the parameters—and of the statistical moments thereof as they will have the ultimate influence. It should be noted that correlations can have a far more significant impact for different cases so that the findings above cannot be fully generalized.

7.4.3. Scenario 2: Hidden smoldering fire

For the initially hidden smoldering fire scenario, some adjustments had to be made to both the stochastic model and the design fire in order to account for the specific risk of this scenario. The fire is assumed to start in the storage room, located in the upper right of the assembly building. The fire will start while the door is closed, leading to a ventilation controlled fire, most likely with $\Phi \gg 1.0$. To account for the incomplete combustion[8] in a rather conservative manner[9], the yields (means and standard deviations) were all multiplied by a factor of two in approximate accordance with the findings by Stec et al. (2009) for highly under-ventilated fires. The HRR(t) is assumed to linearly increase to 2 % in the time t_g and subsequently to increase linearly to 25 % of HRR$_{\text{max}}$ in another

[8]The simulation of low energy under-ventilated fires and the corresponding effluents is still state of research and development.

[9]One may also argue that this whole scenario is overly conservative and unlikely. Yet, hidden fires have lead to catastrophic events before, such as the Gothenburg discotheque fire in 1998 where 63 people died after a fire could develop hidden and undetected for at least 10-20 minutes with subsequent sudden spread into the main assembly premises (Wickström et al., 2004).

Table 7.6.: Results of the reliability analyses and sensitivities for the three predominant variables for the hidden scenario.

Criteria	$\hat{\alpha}_{t_g}$	$\hat{\alpha}_{\text{num. occ.}}$	$\hat{\alpha}_{\text{pre-move.}}$	$\hat{p}_f$
Optical Density	-0.5695	0.5783	0.5842	99.25 %
FID	-0.6542	0.3882	0.5087	39.93 %

timespan t_g, and thereafter remaining at a plateau. The door is assumed to be opened or to fail after a mean of 300 seconds (5 minutes) to instantly release the accumulated highly toxic effluents from the storage room into the assembly area without any prior warning. Hence, the 300 seconds are added to the mean of the warning time. This can be considered conservative.

The severity of impact of this scenario despite the low energy fire becomes obvious when looking at the failure probabilities. For the optical density, the failure probability is larger than 99 %, implying that in nearly every case at least one person will experience an optical density of less than 0.15/m before he or she can leave the compartment safely. For the combined FID model, the failure probability is about 40 % (0.3993), which is also considerably higher than in the standard scenario (more than 7 times). As many occupants would be significantly slowed down by the thick smoke, the actual percentage can be higher as a coupled simulation would reveal.

Looking at the actuation times, the potential impact of a smoke detection and alarm system on the safe escape becomes quite obvious. A smoke detector installed (simulated) in the storage rooms detected the heavy smoke at an average of approximately 40 seconds into the fire development, which is still far in the phase of the fire development where it could be manually extinct by the occupants and where a safe escape is highly probable. The quantitative impact of smoke detection systems is shown in Section 7.5.1.

7.4.4. Scenario 3: Blocking primary exit

This scenario is based on the requirement of Approved Document B (2006) to discount the primary means of egress, which in this case is the main exit on the left that is assumed to be blocked by a fire developing in the coat-/checkroom. As the FID threshold will be reached very quickly within that room, the control volume near the main door was disregarded for a second reliability analysis in this scenario. The sensitivities tend to shift slightly compared to the standard scenario 1, but the order of magnitude remains the same; the time to 1 MW t_g, the number of occupants, and the pre-movement time

Table 7.7.: Results of the reliability analyses and sensitivities for the three predominant variables for the blocking scenario.

Criteria	$\hat{\alpha}_{t_g}$	$\hat{\alpha}_{\text{num. occ.}}$	$\hat{\alpha}_{\text{pre-move.}}$	$\hat{p}_f$
Optical Density	-0.5811	0.5717	0.5605	68.27 %
FID with coatroom	-0.6889	0.5197	0.4892	42.80 %
FID w/o coatroom	-0.8293	0.3898	0.3540	7.96 %

are still the dominating variables. The velocity slightly gains influence for both criteria as longer distances have to be covered to reach the next exit. The probabilities of failure are shown in Table 7.7 along with the sensitivities of the three aforementioned most influential variables.

Comparing the FID probabilities with and without consideration of the coat room control volume backs the assumption that a fire in the coat room would block the main exit. The room fills up with toxic effluents rather quickly so that the FID thresholds are reached comparably fast. Yet, as people would use the opposite direction to evacuate, the omission of the coat room control volume is very reasonable. Comparing the failure probabilities for the optical density criteria and FID to the standard scenario (68 % and 5 %, respectively) leads to the conclusion that the failure of the primary means of egress is nearly irrelevant in *this particular case*. Even though, the RSET was on average about 100 seconds longer than in the standard scenario due to the blocked exit, the ASET until reaching the chosen criteria were also delayed by about 100 seconds due to the smoke retention in the coat room.

The wall between the coat room and the main area, therefore, acts like a smoke curtain and significantly delays the time to untenability (ASET). Hence, the discount requirement for the main egress path from Approved Document B (2006) does not imply a large additional margin of safety—*for this particular case*.

Analyzing all evaluated support point FDS-results for the activation of the smoke detectors yields an average detection time of 45 seconds for the detector located in the coat room. The detector positioned centrally in the compartment activates on average after 155 seconds.

Table 7.8.: Results of the reliability analyses and sensitivities for the three predominant variables for the ultra-fast scenario.

Criteria	$\hat{\alpha}_{t_g}$	$\hat{\alpha}_{\text{num. occ.}}$	$\hat{\alpha}_{\text{pre-move.}}$	$\hat{p}_f$
Optical Density	-0.5671	0.5794	0.5854	99.46 %
FID	-0.6910	0.3056	0.5971	14.29 %

7.4.5. Scenario 4: Ultra-fast fire

This scenario is considered important as (ultra-)fast developing fires have cost many lives, such as in the "Station Fire" in 2003 (Tubbs and Meacham, 2007, p.83ff), where flammable insulation material rapidly caught on fire after being ignited by fireworks. Another, similar tragic example is the "Lame Horse Fire" in Perm, Russia where decoration was also ignited by fireworks leading to a very fast fire development (Belosokhov et al., 2010).

For the ultra-fast fire herein, the HRR(t) is assumed to develop quadratically without prior linear fire incubation phase near the DJ table in the lower middle of the room. The cause could also be fireworks and flammable decorative material. Even though it seems rather unlikely that warning and pre-movement times are still as long as in the standard scenario, they will be used herein for the sake of comparability and because videos from both, the Station Fire and the Lame Horse Fire show that the pre-movement times can still be fairly long which ultimately contributed to the fatal outcomes. As in the hidden fire scenario, the failure probability in case of the ultra-fast scenario was larger than 99 % for the optical density criterion and about 14 % for the FID threshold. The highest sensitivities are found for the three parameters given in Table 7.8. The HCN yield also has a fairly high influence on the limit state with a sensitivity of 0.22. The smoke detector in the simulations actuated after an average of only approximately 30 s.

The failure probabilities of these analyses are a little higher but approximately in the same range as the values found by Forell (2007a), who uses lower yields and a different distribution function for t_g (proposed by Holborn et al., 2004, see Section 7.3.1).

7.4.6. Overall reliability

Considering the system shown in Figure 7.2, the overall system reliability or probability of failure, respectively, can now be assessed by inserting the calculated scenario failure probabilities and using the upper bound method shown in Section 5.5.5. For the optical density threshold, a $p_{f,\text{all,optd.}}$=1.19 % was found. Assuming a normal distributed con-

Table 7.9.: Quantitiative comparison of the scenarios with and without weighting by the scenario probability. The numbers denote factors to reach the same failure probability as the standard scenario. The higher the number, the more relevant is the scenario.

Scenario	**Optical density**		**FID**	
	Weighted	Unweighted	Weighted	Unweighted
Standard	1.00	1.00	1.00	1.00
Hidden	0.73	1.46	3.70	7.39
Blocking	0.30	1.00	0.44	1.47
Ultra-Fast	0.29	1.46	0.53	2.65

volution, this corresponds to a reliability index $\beta = 2.26$. For the FID threshold, the system failure is $p_{f,\text{all,FID}} = 0.23\ \%$ ($\beta = 2.83$). Compared to the structural reliability requirements, this number would be little lower, but well in a $\Delta\beta = \pm 0.5$ range of the serviceability requirements from DIN 1 055-100 (2001).

A comparison of the $p_{f,fi}$-values of each scenario allows for a sensitivity analysis to identify the most critical scenario for the particular case by baselininig each scenario to the standard scenario as shown in Table 7.9. That Table additionally shows these comparative values if the probability for each scenario is omitted (all scenarios are equally likely) to have unbiased values.

It is obvious that for the optical density threshold, the standard scenario is most relevant when looking at the weighted case. For the unweighted comparison, the hidden and the ultra-fast scenarios are the most relevant. For the FID criterion, the hidden scenario is the most relevant for both, the weighted and the unweighted case. This is due to the high toxic potential and the sudden impact.

7.5. Modeling and impact of fire protection barriers

According to Ramachandran (1998, p.12) the cost of meeting current (prescriptive) building fire safety regulations can generate costs as high as 1-9 % of the total building cost and additional high annual maintenance burdens. Keeping these numbers in mind, the quantitative impact on the life safety should be analyzed carefully in order to optimize and justify the costs. It should be noted that within this work, only the impact on life safety is considered. A system may also have impacts on other protection goals, such as structural fire resistance and, last but not least, the insurance premiums, so that the findings here can only be regarded as partial optimization/justification and are not generally transferable.

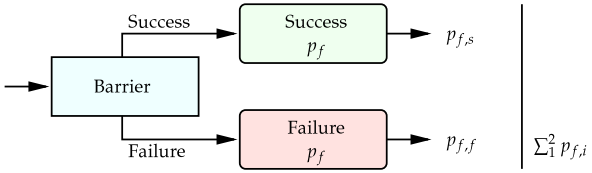

Figure 7.4.: Modeling of fire protection barriers within an event tree considering their possible failure to assess the overall impact on the safety level.

In the following sections, the modeling of the most common fire protection barriers is shown for the "standard fire" and for others if particular interest persists. As systems are always subject to failure with a corresponding failure rate or probability, the following analyses consider two scenarios each, as shown in Figure 7.4 and applied in Albrecht and Hosser (2010b). The reliabilities of the fire protection systems are taken from BS 7974 (2001, p.76).

7.5.1. Automatic detection system

The effect of an automatic detection system is the early notification of the occupants and thus yields reduced alarm/pre-movement times. In order to model the effect, the stochastic models from Section 7.3.2 for the pre-movement times are changed: the occupants will be guided by voice instructions directly after the alarm and thus the mean pre-movement time shortens to 90 s with a standard deviation of 25 s instead of the former 180/45 s assumption. Only inducing changes on the evacuation side of the equation has the big advantage that the fire simulations can be "recycled", saving large amounts of computational resources. To analyze the influence of a smoke detection and alarm system, the standard fire scenario was analyzed for the comparison with the other barriers.

Additionally, the hidden fire scenario was also analyzed as an early detection will have a very large effect on the reliability. Even though it was found in Section 7.4.3 that the smoke detectors actuate after around 40 s on average, only the stochastic model for the pre-movement time was adjusted to 90/25 s in order to remain conservative and to retain comparability. The reliability of a commercial smoke detection system is chosen to be 90 % according to previously cited sources. The results are summarized in Table 7.10.

Table 7.10.: Results of the reliability analyses and sensitivities for the three predominant variables for the smoke detection.

Scenario	$\hat{\alpha}_{t_g}$	$\hat{\alpha}_{\text{num. occ.}}$	$\hat{\alpha}_{\text{pre-move.}}$	$\hat{p}_f$
Standard with detection, Opt.	-0.6975	0.4221	0.5211	21.42 %
Standard w/o detection, Opt.	-0.5972	0.4785	0.6188	68.19 %
Standard with detection, FID	-0.9594	0.1779	0.2010	1.74 %
Standard w/o detection, FID	-0.8999	0.2107	0.3681	5.40 %
Hidden with detection, Opt.	-0.6008	0.4308	0.6450	3.92 %
Hidden w/o detection, Opt.	-0.5695	0.5783	0.5842	99.25 %
Hidden with detection, FID	-0.9098	0.1998	0.2282	1.01 %
Hidden w/o detection, FID	-0.6542	0.3882	0.5087	39.93 %

It should be noted that for the FID reliability analyses, the algorithm has to shift t_g to approximately 10 seconds to obtain the design point. Such short times for the fire growth phase may be mathematically correct but are unrealistic for the actual fire development as already mentioned in Section 7.3.2. Hence, the real values for the failure probabilities are likely to be far less. The formulation of other fire scenarios and more precise (stochastic) modeling—i.e. incorporation of boundaries and/or tail approximation for t_g—may be the subject of further research work.

Analyzing the calculated failure probabilities with the systematic approach shown in Figure 7.4 and assuming a 90 % reliability or a 10 % probability of failure, respectively, of the smoke detection and alarm system to *work as designed on demand* leads to $p_{f,s} =$ 19.3 % and $p_{f,f} =$ 6.8 % for the standard scenario using the optical density threshold and $p_{f,s} =$ 1.6 % and $p_{f,f} =$ 0.5 % for the FID criteria. Hence, the total probabilities of failure including the alarm system and its possible malfunction are 26 % for the optical density and 2 % for the FID criterion. Compared to the case without an alarm system, this is an improvement of the safety level by a factor of approximately 2.6 times in both cases.

A far greater impact can be observed for the hidden fire scenario: also considering the 90 % reliability, the $p_{f,f}$ becomes 3.5 % for the optical density threshold and 0.9 % for the FID criterion. The $p_{f,s}$'s are 10 % and 4 %, respectively. The total probabilities considering a 10 % failure of the alarm system yield 13.4 % for the optical density and 4.9 % for the FID. Comparing these values to the failure probabilities without an alarm system installed results into an improvement of the safety level by a factor of around *seven to eight times* for both criteria. All results are shown in Table 7.11.

Table 7.11.: Results of the system analysis for a detection system.

Detection system	$p_{s/f,\text{detec.sys.}}$	$\hat{p}_{f,\text{scenario}}$	$\hat{p}_{f,s} \mid \hat{p}_{f,f}$	$\hat{p}_{f,\text{sys.}}$
Standard scenario	90 %	21 %	19.3 %	
Optical density	10 %	68 %	6.8 %	26 %
Standard scenario	90 %	1.7 %	1.6 %	
FID criterion	10 %	5.4 %	0.5 %	2 %
Hidden scenario	90 %	3.9 %	3.5 %	
Optical density	10 %	99 %	9.9 %	13.4 %
Standard scenario	90 %	1 %	0.9 %	
FID criterion	10 %	40 %	4 %	4.9 %

Concluding, an alarm system is a very efficient way to shorten the alarm and pre-movement times which provides significantly more time to egress for the occupants until untenable conditions are reached. Being alarmed at an early stage of the fire also reduces the danger of impassable exit routes. The highest impact can be observed for fires that otherwise would grow to a fully developed stage undetected.

7.5.2. Smoke and heat exhaustion

Smoke and heat exhaustion systems (SHE) have the effect that the harmful impacts of the fire on the occupants are delayed and/or mitigated due to the extraction of smoke and heat. Hence, SHEs aim at the ASET part of the limit state. For the consideration in the analyses, the SHE system has to be included into the fire simulation as exemplary shown in Albrecht and Hosser (2010b). The reliability of an SHE system to *work as designed on demand* is given with also 90 % in BS 7974 (2001).

To show the effect, a total of eight 1 m^2 natural SHE vents were added to the simulations. This is far more than required by the codes, but as the building serves as a multi-purpose assembly room they might also be used for natural lighting during the daytime. The vents have an assumed opening time of 15 s after the first smoke detector actuates. The fire scenario was chosen to be the standard scenario while two cases were assumed. In the first case, the detection system is only installed to open the vents but not to alarm the occupants, whereas in the second case, a full alarm is issued upon actuation so that the pre-movement time is also reduced according to Table 7.3. The results for the optical density threshold are compiled in Table 7.12.

Table 7.12.: Results of the reliability analyses and sensitivities for the three predominant variables for the SHE cases using the optical density threshold.

Scenario	$\hat{\alpha}_{t_g}$	$\hat{\alpha}_{\text{num. occ.}}$	$\hat{\alpha}_{\text{pre-move.}}$	$\hat{p}_f$
SHE without alarm, Opt.	-0.8380	0.2767	0.4429	14.72 %
SHE with alarm, Opt.	-0.9334	0.2286	0.2496	5.35 %
Failure of SHE (standard), Opt.	-0.5972	0.4785	0.6188	68.19 %

Table 7.13.: Results of the system analysis for a SHE system.

SHE system	$p_{s/f,\text{detec.sys.}}$	$\hat{p}_{f,\text{scenario}}$	$\hat{p}_{f,s} \mid \hat{p}_{f,f}$	$\hat{p}_{f,\text{sys.}}$
Standard scenario	90 %	14.7 %	13.2 %	
Optical density	10 %	68 %	6.8 %	20 %

The FID criterion was not reached for any of the support points until the fire simulations were terminated at 1,200 seconds (20 minutes), which was defined as the absolute maximum time[10] in which a fire compartment has to be fully evacuated, regardless of the fire effects (Mehl, 2004). This means that the SHE system mitigates the threat of being severely harmed or incapacitated by toxic and heat effects scenario beyond simulation capability for the particular scenario, implying an unquantified, but implicitly very high actual level of safety.

Using the systematic approach previously shown in Figure 7.4 leads to $p_{f,s} = 13.2$ % and $p_{f,f} = 6.8$ %, adding up to a total of 20 % probability of failure if a SHE system with 10 % probability of failure and without alarm is installed as shown in Table 7.13. Compared to the case without SHE installed, which led to a probability of failure of 68 %, it can be concluded that the SHE system without alarm increased the safety for the optical density threshold by a factor of greater than three. If the occupants are also alarmed by an alarm system giving instructions, the pre-movement time is reduced which leads to $p_{f,s} = 4.9$ % and a total barrier probability of failure of 11.7 %, decreasing the failure probability by a factor of 5.8. Assuming that an audible alarm works as designed with proper instructions to the occupants (after fire detection and subsequent opening of the SHE vents)[11] with a reliability of 95 % leads to the event tree in Figure 7.5 and a total failure probability of 12 %.

[10] This may also constitute a serviceability limit for the normal use of the building.

[11] This is important to mention as these probabilities are conditional and the order cannot be interchanged within the event tree. More information can be found in the explanatory remark at the end of this Section (p. 149).

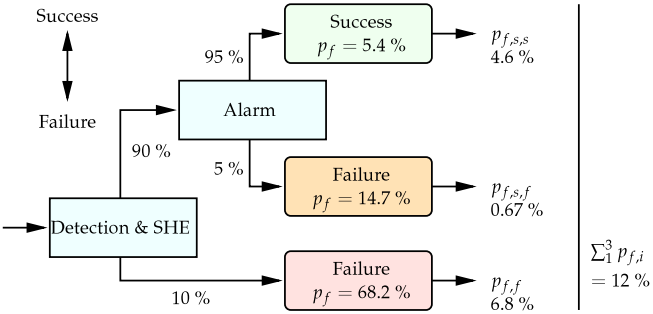

Figure 7.5.: Modeling of the smoke and heat exhaustion barrier with coupled alarm system within an event tree considering their possible failure to assess the overall impact on the safety level.

In conclusion, the SHE system has a very large effect on the life safety as it significantly reduces the possibility of reaching the optical density threshold during egress and nearly completely mitigates the toxic and heat effects of the fire. Even if the egress is delayed by reaching high optical densities, no immediate threat is imposed on the occupants (for this particular scenario).

7.5.3. Supression systems

Fire suppression systems, such as sprinklers, have an effect on both ASET and RSET. Usually, the effect on the fire is modeled within the HRR. Models, i.e. by Dehne (2003, p.17ff) or Rosenbaum et al. (2007, p.94) assume that upon sprinkler activation, the HRR is instantly retained at a steady level with subsequent decay as shown in Figure 7.6. The activation time is dependent on the fire parameters as well as the response time index (RTI) of the sprinklers. Upon activation, it is assumed herein that the HRR plateaus for 300 s and then linearly decays in another 300 s. This approach can be considered very conservative, as a study by Madrzykowski et al. (2006) shows that the activation time is faster and the effect of the sprinkler on the HRR is usually more effective (near-instant extinguishment of the fire).

Another option is the direct modeling of the interaction of sprinkler systems with the fire as i.e. done in Bryner et al. (2007) which could also account for various side-effects on the occupants of the fire-sprinkler interaction, such as generation of hot steam, disruption of the smoke/heat stratification, etc. Herein, the former approach was used, while the latter gives ideas for many further research topics.

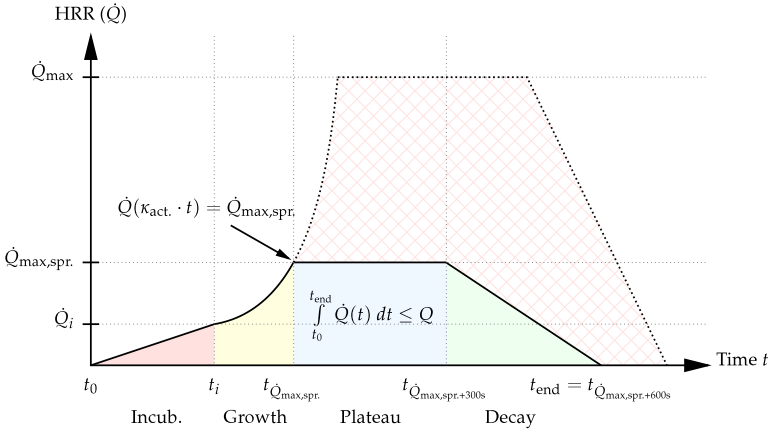

Figure 7.6.: Schematic course of the heat release rate of the sprinklered fire compared to the unsprinklered original scenario. Not to scale.

In order to find a simple and effective sprinkler activation model for the standard scenario, sprinklers were introduced into the fire simulation, being located right above the fire in the bar area. The sprinklers were chosen to have an activation temperature of 68 °C and a response time index (RTI) of 100 $m^{0.5}s^{0.5}$, which describes a commonly used sprinkler for office/assembly occupancy in Germany. A parameter study was performed varying t_g and HRR_{max} (or $\dot{Q}_{max}$) and correlating the activation time to those variables. The results showed a nearly perfect linear correlation between t_g and the activation time ($\rho_{t_g,Act.} > 0.98$), while the HRR_{max} was insignificant. Therefore, for the standard scenario the activation time was modeled as a factor $\kappa_{act.}$ of t_g. This $\kappa_{act.}$-factor was calculated to be 1.7, so that the sprinklers were modeled to activate at $1.7 \cdot t_g$ within the simulation. Considering the design fire proposed in Section 4.4.1, the sprinklers activate after the linear incubation phase, but long before the plateau or even before 1 MW is reached. After sprinkler activation, the $HRR_{max,spr.}$ (or $\dot{Q}_{max,spr.}$) is assumed to be constant for five minutes and then decay linearly in another five minutes. This is in approximate accordance with the assumptions by Dehne (2003, p.17ff) and Rosenbaum et al. (2007, p.94) but must be considered very conservative.

The reliability of sprinkler systems to *work as designed on demand* is given to 95 % (maximum value) in Great Britain (BS 7974, 2001) and even 98 % in Germany (DIN EN 1991-1-2/NA, 2010) if the system is planned, built, and maintained in compliance with VdS CEA 4001 (2008).

Table 7.14.: Results of the reliability analyses and sensitivities for the three predominant variables for the sprinklered standard scenario.

Scenario	$\hat{\alpha}_{t_g}$	$\hat{\alpha}_{\text{num. occ.}}$	$\hat{\alpha}_{\text{pre-move.}}$	$\hat{p}_f$
Sprinkler, Opt.	-0.5850	0.4895	0.6229	67.94 %
Standard w/o sprinkler, Opt.	-0.5972	0.4785	0.6188	68.19 %
Sprinkler, FID	-0.7816	0.1662	0.4687	0.014617 %
Standard w/o sprinkler, FID	-0.8999	0.2107	0.3681	5.40 %

The results of the analyses are shown in Table 7.14. It is evident that, the results for the optical density are nearly identical with the results from the un-sprinklered standard scenario. An in-depth analysis showed that this is suitable, as the optical density threshold is usually reached before $1.7 \cdot t_g$. Additionally, the optical density is a momentary threshold, so that the sprinkler has no significant influence on the reliability for this particular case[12]. Yet a large effect is observed for the FID criterion where the probability of failure is significantly lower than for the un-sprinklered scenario. As the threshold is reached later (after $1.7 \cdot t_g$) and is cumulative and time-integrated, the lower release of heat and asphyxiant gases directly affects the criterion. Looking closer at the results, one might even argue if the scenario is prone to failure at all, as the design point of the convolution pushes t_g near zero, which is mathematically correct but not necessarily physically realistic (refer to the remark on page 128). As for the sensitivities, t_g, the pre-movement time and the number of occupants have a high influence. Additionally, the HCN-yield has a significant impact on the results ($\alpha_{y_{\text{HCN}}}$=0.3444).

A system analysis was performed as shown in Figures 7.4 and 7.5 to demonstrate the impact of a sprinkler system, taking into account the possibility of a failure of 2 % thereof. There is no evident impact on the optical density for the reasons stated above. For the FID criterion, the total probability of failure is 0.12 % and thus about 44 times lower than the un-sprinklered scenario with a 5.4 % probability of failure as shown in Table 7.15. Considering the reason stated above, the relative level of safety will even be higher implicitly.

[12] In different setups and scenarios, the results may be different and the sprinklers may have a significant impact on the optical density, for example when it comes to smoke filling times of larger volumes etc.

Table 7.15.: Results of the system analysis for a sprinkler system.

Sprinkler system	$p_{s/f,\text{detec.sys.}}$	$\hat{p}_{f,\text{scenario}}$	$\hat{p}_{f,s} \mid \hat{p}_{f,f}$	$\hat{p}_{f,\text{sys.}}$
Standard scenario	98 %	0.014 %	0.014 %	
FID criterion	2 %	5.4 %	0.11 %	0.12 %

Table 7.16.: Results of the reliability analyses and sensitivities for the three predominant variables for the sprinklered ultra-fast scenario.

Scenario	$\hat{\alpha}_{t_g}$	$\hat{\alpha}_{\text{num. occ.}}$	$\hat{\alpha}_{\text{pre-move.}}$	$\hat{p}_f$
Sprinklered, ultra-fast, Opt.	-0.5671	0.5794	0.5854	99.46 %
Un-sprinklered, ultra-fast, Opt.	-0.5672	0.5793	0.5855	99.47 %
Sprinklered, ultra-fast, FID	-0.4195	0.2756	0.5992	0.92 %
Un-sprinklered, ultra-fast, FID	-0.6910	0.3056	0.5971	14.29 %

Influence of a sprinkler system on the ultra-fast fire

As mentioned above, the sprinklers did not have a large impact when assessing the standard fire, as they usually actuate later compared to the other measures. This is different for the ultra-fast fire where high temperatures are reached very early during the fire development. Madrzykowski et al. (2006) conclude from a comparison of sprinklered and unsprinklered experiments and simulations that a sprinkler would have prevented the Station Fire disaster where an ultra fast fire occurred. Hence, the ultra-fast scenario from above was re-evaluated with the sprinkler model introduced above. The results are compiled in Table 7.16. It can be seen that the sprinklers do not have any influence on the visibility (optical density threshold) as this criterion is reached shortly after the fire starts. Yet, a significant impact can be seen for the FID criterion, which is nearly completely mitigated due to the reduction of the maximum heat release rate and the early termination of the fire. It should be noted that herein, the fire was assumed to start at floor level which conservatively implies a comparatively late actuation. Also, the sprinkler model (plateau & linear decay) can be considered conservative compared to the direct simulation used by Madrzykowski et al. (2006).

In conclusion, the sprinkler system does have a very large effect, as the possibility of occupants being severely threatened of incapacitation is mitigated. Yet a risk of delaying the safe egress and thus inflicting injuries due to smoke inhalation could not be prevented according to the models utilized. A full system analysis using SHE vents is presented in Section 7.6. It should be noted that the results are very specific for the building and the fire scenarios considered and, therefore, cannot be generalized.

A far better effect for sprinklers should be observed for larger compartments with higher smoke filling volumes and better (direct, physical) modeling of the sprinkler effect, as the model used herein can be considered conservative compared to other detailed studies.

7.5.4. Organizational fire protection and trained personnel

Organizational fire protection and trained personnel may have the biggest impact on the system reliability as it can affect multiple scenarios and parameters within the fire protection and life safety system. Yet the effect is usually implicit and thus very hard to model or quantify as no data is currently available. Additionally, the organizational fire protection includes various aspects of which some may be complied with (i.e. presence of evacuation maps) while others are neglected completely (i.e. propping smoke doors open). Some of the imaginable effects of highly trained staff or even dedicated fireguard personnel within a holistic organizational fire protection concept include, but are not limited to:

- Effect on the scenarios:
  - Reduction of the fire initiation frequency due to proper maintenance of, for example, electric installations.
  - Lower failure probabilities due to well-maintained fire protection systems.
  - Higher probability of success of the manual intervention, as the staff is familiar with the use of fire extinguishers and responds more quickly to a fire.
  - Lower probability of severe scenarios like the ultra-fast fire due to the use of inflammable (temporary) decoration and the prohibition of firework usage.
  - Faster egress due to evacuation management (i.e. live voice communication instead of alarm sound or taped messages).
- Effect on the parameters used:
  - Reduction of fire load.
  - Use of inflammable materials or retardants to extend t_g.
  - Limiting the number of occupants by strictly enforcing maximum allowable capacities.
  - Reducing the warning and/or pre-movement times.

As absolutely no data is available to quantify the effects of well-trained personnel, no direct influences are considered herein. The detailed modeling of these effects constitutes an interesting topic for further research. Omitting the influence entirely penalizes those building operators who do invest into organizational fire protection. Hence, a very sim-

plistic approach is presented herein. If the organizational fire protection is considered appropriate within a building, the reliability of manual intervention is assumed to increase to, for example, 75 % instead of 25 % with low organizational consideration. This has a significant effect, as the manual intervention is a critical decision gate within the event tree as shown in Figures 7.2 and 7.8. This means that the success of the manual intervention ultimately leads to a safe state where no hazard is imposed on the occupants. Hence, $p_{f,s}$ (the upper branch in Figure 7.4) always leads to a zero probability of failure so that $p_{f,f}$ fully controls the sub-tree but is directly dependent on the barrier reliability, so that the failure probability of the barrier acts as a plain multiplier for $p_{f,f}$.

A simple example shows the influence of the organizational fire protection. Assuming a 75 % failure probability of the manual intervention for the standard scenario using the FID threshold ($p_f = 5.4$ %) leads to a total system probability of failure of 4 %, while a 25 % failure probability leads to only 1.35 % in a system analysis, implying that a good organizational fire protection increases the safety level by a factor of three for the particular case.

Explanatory remark V: Interchangeability of conditional event tree components

As previously mentioned, the probabilities calculated in Figure 7.5 are conditional probabilities and thus the components or barriers cannot be interchanged within the event trees due to interdependencies. The simple system example from Figure 7.5 has the underlying assumption that the audible alarm can only warn the occupants if the detection and the SHE worked as designed. To illustrate what happens if components are changed is shown in Figure 7.7. It is now assumed that the opening of the SHE vents is dependent on the detection, but the audible alarm is independent of the opening of the SHE vents and included into the detection reliability.

One can see that the second scenario changes to the scenario with an alarm from Section 7.5.1, as the fire is detected and the occupants are warned but no SHE vents are opened. This differs from the “SHE open but without alarm”-scenario. The total failure probabilities are only very similar due to the similar results of the two scenarios and the low influence thereof within the system. Yet it points out the necessity of the proper compilation of the event tree.

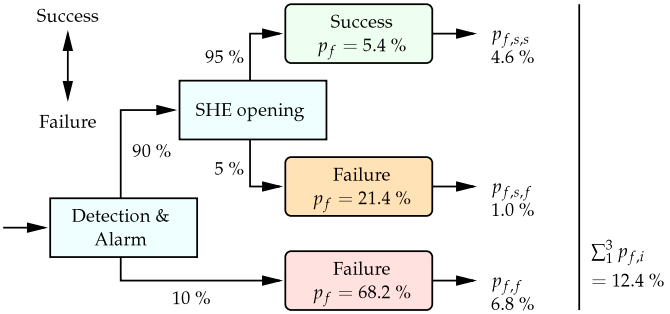

Figure 7.7.: Impact of interchanging conditionally dependent components in the system modeling process.

7.6. Full system analysis and barrier interaction effects

In order to assess the full system performance and to identify the most effective fire protection barriers, a complete system analysis is performed for the standard scenario assuming all barriers described above are installed. An overview of the system is given in the global event tree shown in Figure 7.8. All the scenarios within the event tree and their corresponding probability of failure can be found above. The only scenario that cannot be assessed directly is the combination of sprinklers and SHE system, as this scenario needs additional consideration due to the interdependency of both barriers (refer to Section 5.5.5): if the SHE system works as designed, a great share of the heat is removed directly through the vents which could cause a delay in the heat-dependent sprinkler actuation. Hence, a similar analysis as described in Section 7.5.3 was performed. Again, a very high correlation ($\rho_{t_g,\text{Act.}} > 0.98$) was found between t_g and the sprinkler actuation time, but the factor increases to 1.8, implying the aforementioned delay.

The result of the interaction case is shown in Table 7.17 for the optical density, along with some comparative values. Interestingly, an effect of the sprinkler is now significant despite having no effect without the SHE vents. This is most certainly due to the fact that the SHE system delays the smoke filling of the room by pushing the design point forward in time to a degree that the sprinkler system can now affect the optical density by cutting the HRR. This shows a significant interdependency of barrier systems (which might even be higher for different scenarios) and the necessity to model these effects. The FID threshold was not reached in any of the support point simulations. Hence, the toxic and heat effects are now completely mitigated beyond simulation capability for the standard scenario.

Table 7.17.: Results of the reliability analyses and sensitivities for the three predominant variables for the sprinkler-SHE-interaction standard scenario with alarm compared to the other cases.

Scenario	$\hat{\alpha}_{t_g}$	$\hat{\alpha}_{\text{num. occ.}}$	$\hat{\alpha}_{\text{pre-move.}}$	$\hat{p}_f$
Sprinkler-SHE-interaction	-0.9329	0.2011	0.2444	0.0308
SHE w/ alarm, Opt.	-0.9334	0.2286	0.2496	0.0535
Sprinkler, Opt.	-0.5850	0.4895	0.6229	0.6794
Standard w/o sprinkler or SHE, Opt.	-0.5972	0.4785	0.6188	0.6819

If all possible interactions are considered within the event tree, simple multiplication and addition can be used to evaluate the system; all branches are independent minimal cut-sets of the system and interaction (correlation) effects are modeled within the scenario. The results of the various branches are shown in Figure 7.8. The total probability of failure of the system for the standard fire scenario using the optical density threshold is $p_{f,\text{sys.}} = 0.00157$. Assuming a normal distribution of the system convolution, this corresponds to a reliability index $\beta_{\text{sys.}} = 2.95$, which is approximately the reliability requirement for serviceability of DIN 1 055-100 (2001).

Explanatory remark VI: Influence of barrier failure probabilities

When evaluating the influence of the fire protection barriers, a failure probability for each barrier is needed to assess the overall performance of the sub-system. The values stated above are compiled from the relevant cited literature but may vary depending on many factors. In order to assess the influence of the barrier reliability on the system reliability, a sensitivity analysis can be performed by varying the failure probabilities within a reasonable range. This is done herein by varying one barrier failure probability from the minimum to the maximum within the assumed range while holding all others constant (axial sensitive DoE, see Section 5.4.5). The resulting probability bands are then plotted in a so-called "tornado-diagram" to visualize the sensitivity of each barrier. The ranges are compiled in Table 7.18 and the resulting system reliability bands are plotted in Figure 7.9.

It becomes clear that the highest sensitivities can be found for the two primary gates, the fire start and the manual intervention, respectively. Unfortunately, these two parameters have the highest uncertainties and appropriate data is very hard to find as it is rarely recorded properly. Having such a large uncertainty range, these barriers will have the highest influence on a probabilistic design, for example, for the derivation of a safety concept, these values need to be chosen at a fixed, deterministic level–even though this may penalize premises with low fire initiation probabilities. Yet a designer could otherwise highly influence the resulting failure probability and thus "sugarcoat" his design. For future fire data acquisition, it is highly desirable to model and/or improve those probabilities.

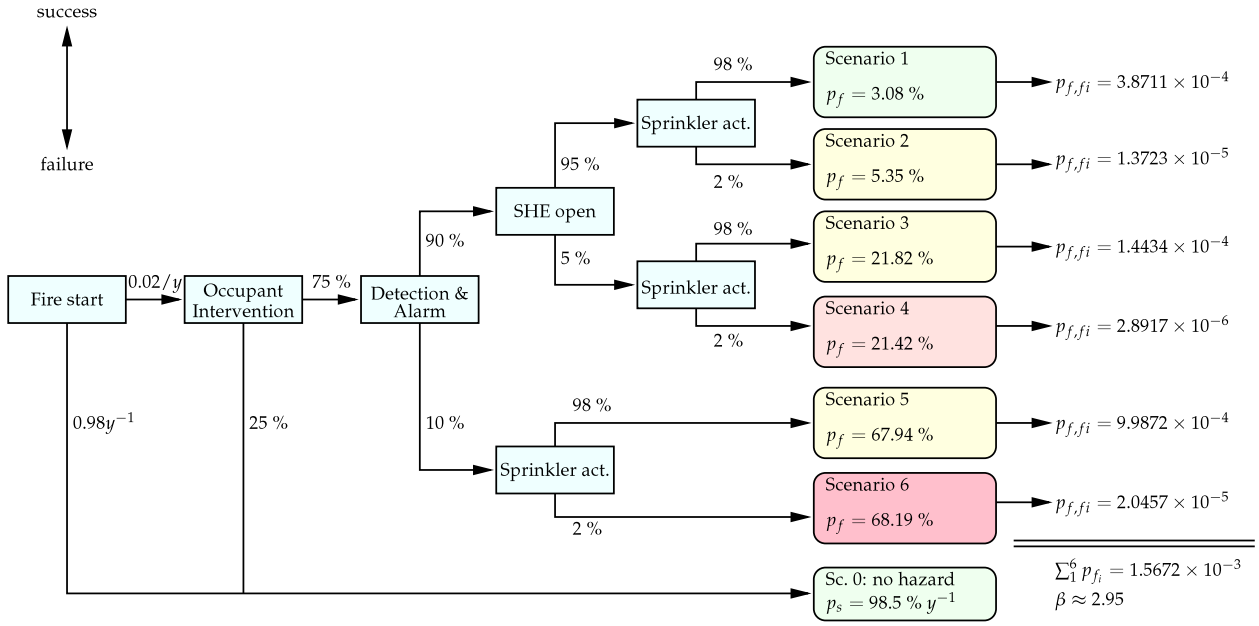

Figure 7.8.: Full fire protection system event tree for all aforementioned barriers, exemplary shown for the optical density threshold.

Table 7.18.: Min-max ranges for the various barrier failures and according system failure probabilities for the optical density compiled from the aforementioned literature.

	Barrier		**System**	
	min p_f	max p_f	$p_{f,\text{sys.,min}}$	$p_{f,\text{sys.,max}}$
Fire start (per annum)	0.5 %	12 %	0.04 %	0.94 %
Manual intervention	25 %	100 %	0.05 %	0.21 %
Detection & alarm	5 %	25 %	0.11 %	0.30 %
SHE	5 %	20 %	0.16 %	0.19 %
Sprinkler	2 %	20 %	0.16 %	0.16 %

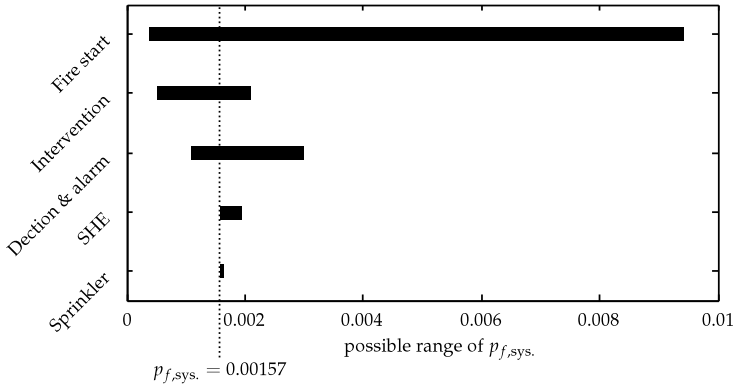

Figure 7.9.: Tornado system sensitivity diagram.

7.7. Conclusions

After the necessary stochastic models and fire scenarios along with their design fires are derived form various literature sources, reliability analyses were carried out for the multi-purpose assembly building. It can be seen that the failure probabilities are rather high when looking at the "per-hostile-fire probabilities". After converting those probabilities to per annum failure probabilities by incorporating the annual fire ignition frequencies, it was found that they were in a reasonable range. To see the impact of fire protection systems, they were modeled within a system approach, also accounting for their potential failure. The analysis and their results were outlined along with some remarks on common issues in life safety or reliability analysis.

It was also found that the results are highly dependent on the parameters, scenarios and models used. Especially for the sprinkler system—which has a rather marginal impact on the results herein—a different model will lead to very different results, i.e. even a shorter actuation time would significantly increase the safety level. Hence, a lot of research needs to be done in that area in order to sufficiently account for the systems used. The examples shown herein can be regarded as a first step towards the explicit quantification of the currently implicit safety levels of the prescriptive codes which can subsequently be used to derive and calibrate a safety concept evolving from a large number of calculations with various examples.

Chapter 8

Summary and Conclusions

Life safety design is the prevailing task in Fire Protection Engineering and a lot of consideration and effort is usually required to find sufficient and cost-effective solutions, which also reduce the risk of life loss to an acceptable level. In order to optimize this process, this thesis shows new approaches and methods in both Reliability and Fire Protection Engineering. First, a closer look is taken at the term *risk*, which is usually interpreted in many different ways. In order to constitute a basis for further considerations, the characteristics of risk are shown along with the components involved. Additionally, the derivation of acceptable safety levels, the interpretation of results, and the possibilities of risk-informed design are outlined. Based on these findings, a *hierarchy* is proposed which categorizes the various methods and techniques of life safety engineering according to their level of complexity. Current safety concepts based on merely empirical safety factors are described and the shortcomings are outlined, showing the necessity for a quantifying risk-informed approach.

Advanced procedures in life safety design utilize advanced and highly complex numerical methods, such as CFD and egress simulations which are described in Chapter 4. So-called *threshold models* implying the effect of fire effluents on the occupants ultimately determine the time available for a safe egress so that they had to be reviewed in greater detail to understand their origins and potential advantages and disadvantages. This leads to a *combined fractional incapacitation dose* model which accounts for all effects in a rather conservative manner. A remark was also given on design fires and design fire scenarios which are used to describe an estimated fire course conservatively. Shortcomings of the traditional t-squared design fire were identified and a new, *modified design fire* was introduced which accounts for the fire incubation phase which has a high influence on the life safety. This design fire is based on the t-squared approach and, thus, is compatible with the traditional approaches for structural fire safety.

In order to introduce a quantitative and risk-informed design, reliability theory is utilized to compute failure probabilities of life safety designs. For a better understanding of the advancements, a general introduction is provided in Chapter 5. Herein, the utilized mathematical formulations are shown along with solution algorithms for the *reliability problem*. Special consideration is given to the *generation of systematic, random, and quasi-random samples* which determine quality and speed for the algorithm developed. In order to allow for the probabilistic consideration of highly complex and numerically expensive models, a new *response surface method* is introduced based on *interpolating moving least squares* with a *preceding sensitivity analysis* to minimize the dimensionality and the number of support points. The derivation of the methods is presented in full detail along with considerations of *convergence criteria, adaptivity, parallelization, and adaptive discretization* to reduce the required run-time and the numerical costs even further. Two benchmark examples are generated in order to demonstrate the power and accuracy of the developed method.

In Chapter 7 the new response surface method is applied to an exemplary multi-purpose assembly building in order to test for the practical application of the methodology and to gain insight about the safety levels of a contemporary code-compliant building. For this building, various scenarios are tested for their potential *probability of failure of a safe egress* using visibility and incapacitation thresholds. Furthermore, the influences of *fire protection systems* on the probability of failure are modeled, evaluated, and compared to the case without such a system, providing valuable information of the potential benefit. Additionally, a *full probabilistic system analysis* is performed and the subsequent *system sensitivity analysis* yield the most influential parameters and barriers within the system.

8.1. Conclusions for a risk-informed life safety code

Introducing quantitative risk analysis into life safety analysis using advanced and numerically complex tools of fire protection engineering is a consequent step towards a (more) *risk-oriented* and *cost-benefit optimized* life safety design. Within this thesis, the basis for a future *holistic and objective life safety concept* is given along with the various considerations that should be taken. It was shown that the term risk with all related characteristics, such as i.e. *acceptable risk*, needs further consideration and that a direct adoption of accepted risk levels in other areas (i.e. structural fire design) is not advisable due a high model-dependency of the resulting failure probabilities. In order to derive a *risk measure* for life safety, the *failure probabilities* of current deemed-to-satisfy prescriptive life safety designs have to be analyzed and compared in order to find the *model-dependent safety levels*[1] throughout various occupancies where life safety is an issue.

[1] Comparing model-dependent safety levels allows for neglecting model uncertainty factors, as these are near impossible to find for the various life safety models.

An important role in the process of life safety design plys the accuracy and the complexity of the various models used. With a focus on developing a future safety concept, consideration is given to the hierarchy of models which can be categorized in levels of similar complexity in analogy to to the *three-step-approach* in the structural Eurocodes. This hierarchy is proposed along with required *levels of competencies* as inadequate utilization of models can greatly influence the quality of the results[2], especially for highly complex models, such as CFD. Hence, it is also inevitable to take a closer look at the models to understand the underlying procedures, methods, and assumptions, and to allude all shortcomings, simplifications, and (unquantifiable) model uncertainties therein. This leads to *various improvements* such as the definition of the *new FID model* or the derivation of design *fire scenarios* along with the development of a *new design fire* HRR curve which is compatible with those used for structural fire design.

As most complex buildings will indeed be evaluated for life safety using the complex models (Level 3), these will have to be considered in a risk-informed probabilistic life safety concept. Until now this was not deemed possible due to the very high numerical costs of the models in probabilistic analyses, such as the Monte Carlo method. Hence, a new *adaptive response surface method* is derived which allows for a fast and effective reliability analysis using the highly complex numerical methods. Additional features, such as the *preceding sensitivity analysis, entropy-optimized structured and quasi-random sampling*, as well as the *dual-layer parallelization* further reduce the numerical costs. This methodology is *not limited to life safety* models but can be applied to nearly all reliability problems. The surrogate formulation could also be utilized for optimization problems by simply exchanging the reliability solver with an optimization solver.

An important first step towards a risk-informed probabilistic safety concept is performed by applying the methods to a code-compliant assembly building in order to *derive the quantitative safety levels* and to test for the sensitivities of the input parameters as well as the influence of various fire protection systems or barriers. Even though the results are only valid for the particular building, some general conclusions can be drawn.

8.1.1. Code elements

The numerous considerations above show that a risk-informed life safety code will consist of numerous definitions, elements etc., which include but are not limited to:

- Detailed objective statement, identification of goals, prioritization, and limitations:
  - General definitions and terminology.
  - Objective: Providing for safe egress to an acceptable level of safety.

[2] Even magnitudes higher than the actual model error/uncertainty.

  - Goal: Minimize fire- and egress-related injuries and loss of life to an acceptable level.
  - Prioritization: Loss of life, injuries.
  - Limitations of the code.
- Hierarchy of the underlying FPE tools and clarification of competencies:
  - Verification levels and corresponding educational requirements for the designer (refer to Chapter 3).
  - Clear definition of the competencies of the fire protection designer, the AHJs and other stakeholders.
  - Definition of the acceptance process of the design (Who verifies? How is it verified?)
  - Statement of accredited FPE tools and/or validation examples to ensure applicability similar to DIN EN 1991-1-2/NA (2010, Appendix CC).
- Performance criteria and input parameters:
  - Acceptable performance criteria for the objective (i.e. optical density, FID), corresponding defined threshold values, and defined requirements where and how to determine those values within the fire simulation, for example "at a height of 2 m centrally located within the main fire compartment".
  - Acceptable levels of safety, i.e. reliability requirements similar to those given in DIN EN 1991-1-2/NA (2010, Appendix BB).
  - Required fire scenarios to verify for safe egress (refer to Chapter 4.4).
  - Specified (and possibly scenario dependent) input parameters, for example as proposed by Fleischmann (2011).
  - Safety format: Consideration of fire protection barriers and their possible failure within a probabilistic framework and
  - Partial safety factors to be applied to certain parameters in dependence of the occupancy, size etc. similar to the safety concept in DIN EN 1991-1-2/NA (2010, Appendix BB). In order to calibrate the system components and safety factors as shown in Chapter 7, the first three points in this section are very important.
- Retained prescriptive elements:
  - Basic requirements which cannot be substituted by performance-based methods, such as the requirement to have two independent exits or sufficient exit signage.

- Definition of qualitative criteria, such as avoiding bottlenecks within the egress design.
- Additional occupancy-specific criteria, for example means of horizontal evacuation for health care facilities or strategies within correctional or high-security facilities, as given in NFPA 101 (2008).
- Basic requirements for the configuration of the interior design and furnishing as well as electrical installations (non-flammable etc.).
- Definition and reference of applicable codes and standards. For example, a sprinkler system has to be planned, installed, and maintained according to VdS CEA 4001 (2008) or NFPA 13 (2010) in order to be considered at a 2 % failure probability to work as designed on demand in the safety format.

All the elements stated above—and possibly more—are needed to be extensively covered in order to provide a holistic and risk-informed life safety design using state-of-the-art performance-based engineering tools. Some of the elements which are identified as currently inconsistent are addressed in this work. Especially the structured approach to quantify safety levels as well as various improvements and preliminary requirements within the design process are essential in order to derive a risk-informed safety format and concept. Yet many parts still need to be calibrated and agreed upon.

8.1.2. Proposed safety format

If all the previous code elements are considered and the minimum required reliability levels $p_{f,\text{req.}}$ of the prescriptive codes are derived, it is straightforward to derive a safety format based on semi-probabilistic partial safety factors γ_i analogous to the safety format in DIN EN 1991-1-2/NA (2010). This allows for a semi-probabilistic design of life safety, which implicitly fulfills the required $p_{f,\text{req.}}$.

In the example in Chapter 7 it is found that the fire growth rate t_g, the number of occupants and the pre-movement time have the highest sensitivities (see Figure 7.3 on page 132). Combined, those three input parameters along with their according variances explain around 90 % of the overall resulting variance, making them most suitable for a safety format.

Choosing the 90-percentiles of the underlying distributions to be the characteristic values of those three parameters, the partial safety factors can be found

$$\gamma_i = \frac{1 + \alpha_i \cdot \Phi^{-1}(p_{f,\text{req.}}) \cdot V_i}{1 + 1.28 \cdot V_i} \tag{8.1}$$

for normal distributed parameters or

$$\gamma_i = \frac{1 - V_i \cdot \sqrt{6}/\pi \cdot \left[\Gamma + \ln\left(-\ln\left(\Phi\left(\alpha_i \cdot \Phi^{-1}\left(p_{f,\text{req.}}\right)\right)\right)\right)\right]}{1 - V_i \cdot \sqrt{6}/\pi \cdot \left[\Gamma + \ln\left(-\ln\left(0.9\right)\right)\right]} \tag{8.2}$$

for Gumbel distributed parameters. α_i is the sensitivity and V_i the coefficient of variance of the parameter i. $\Phi(\cdot)$ is the normal distribution function and Γ the Euler-Mascheroni constant.

Multiplying the derived safety factor with the chosen characteristic value of the underlying distribution yields the so-called "design value", for example for the fire growth rate t_g:

$$t_{g_d} = \gamma_{t_g} \cdot t_{g_k} \tag{8.3}$$

which can subsequently be used in deterministic calculations.

Using this approach, the reliability level is implicitly fulfilled without the need for extensive probabilistic analysis. This approach not only allows for a risk-optimized design without over- or undershooting the required safety, but also for a simple practical application in state-of-the-art performance-based life safety analyses as it is fully compatible to the safety format for the structural fire design in DIN EN 1991-1-2/NA (2010).

8.2. Further research possibilities

An application to similar buildings using the same models, scenarios, and assumptions cancel out any model uncertainty and are consequently comparable. A safety concept could, therefore, be derived if various model and scenario requirements are met and a *sufficient amount of exemplary applications* exists. This corresponds approximately to the derivation of the reliability requirements constituted in GruSiBau (1981). Hence, the biggest task towards a probabilistic safety concept will be the *extensive number of applications to various buildings and occupancies* with a subsequent *derivation of the safety format* based on those parameters with the highest sensitivities as it was done for the structural safety concept for the Eurocodes.

A very large area of *improvement are the underlying data and parameters*. As shown in the system sensitivity analysis, it is vital to have accurate data on fire initiation frequencies, barrier failure probabilities etc. Currently, these numbers are often based on sparse frequentistic data enriched with subjective and biased expert judgment as explained in Chapter 2.1.1 which strongly influences the overall reliability. In addition, obtaining better data and parameters, a focus should also be on the physical boundaries of parameters within the simulations as well as the derivation of *more accurate stochastic models* for the input parameters—especially for those with high sensitivities. The errors introduced by the input parameters are usually by far higher than the model errors/uncertainties. Nevertheless, the models used for life safety analysis should undergo constant *improvements*

to advance the accuracy and quality of the results. For example, the possible large potential of sprinkler systems for life safety is insufficiently modeled herein, as various publications show an instant fire suppression by such systems based on fire tests instead of the overly conservative HRR-model used. *Advanced sprinkler models* could yield far better results—as could better models for all life safety system components. Additionally, models have to be found for the intervention of trained personnel to be able *to reward for good organizational fire protection* in a safety concept.

Potential for improvement can also be found in the complex numerical models. To *predict concentrations of toxicants and smoke more accurately* it will be inevitable to develop, introduce and improve *pyrolysis and combustion models*, and *enhanced transport equations* into the CFD simulations to also account for the irritant species and ultimately allow for direct fire simulation instead of prescribed HRR-curves. The incapacitation models can be improved as many of them are based on clinical studies on animals with one isolated asphyxiant each. *Interaction effects* between the effluents are not modeled herein; the effects are simply added—the validity of this approach is admittedly assumed to be optimistic (Purser, 2002). Egress models need to be improved for *better representation of individual behavior* including *panic* and *congestion/bottleneck* behavior. Not until the agents can accurately simulate individual human behavior with all the necessary characteristics, it will be possible to *assess individual risk* of every person compared to the collective risk of all occupants within a fire compartment.

In conclusion, some of the findings in this thesis may pave a way towards

A RISK-INFORMED AND PERFORMANCE-BASED LIFE SAFETY CONCEPT IN CASE OF FIRE

using complex numerical models and state-of-the-art Fire Protection Engineering in order to allow more *risk- and cost-optimized life safety designs*. This way now needs to be walked upon—including all the remaining bumps and curves...

Bibliography

Soon-Jeong Ahn, Jaechil Yoo, Byung-Gook Lee, and Joon-Jae Lee. 3D Surface Reconstruction from Scattered Data Using Moving Least Square Method. In *Image Analysis and Processing - ICIAP 2005, 13th International Conference, Cagliari, Italy, September 6-8, 2005, Proceedings*, 2005. 96

Cornelius Albrecht. Development of a Multiple Truck Presence Model. Master's thesis, University of Rhode Island, 2008. 94

Cornelius Albrecht and Dietmar Hosser. Probabilistic Assessment of Performance Criteria for Egress Design. In Van Gelder, Prokse, and Vrijling, editors, *Proceedings of the 7th International Probabilistic Workshop*, 2009. 18, 33, 48, 60, 71, 90, 115, 116, 117, 120, 124

Cornelius Albrecht and Dietmar Hosser. A risk-informed framework for performance-based structural fire protection according to the Eurocode fire parts. In *Proceedings of the 12th International Conference on Fire Science and Engineering (InterFlam9)*, 2010a. 19

Cornelius Albrecht and Dietmar Hosser. A Response Surface Methodology for Probabilistic Life Safety Analysis using Advanced Fire Engineering Tools. Proceedings of the 10th International Fire Safety Symposium (IAFSS10), Maryland, 2011, September 2010b. 130, 134, 140, 142

Cornelius Albrecht, Matthias Siemon, and Dietmar Hosser. Application of sensitivity analysis to specific problems in Fire Protection Engineering to identify the most critical parameters and to reduce dimensionality. In Lucjan Gucma, Dirk Proske, and Pieter van Gelder, editors, *Proceedings of the 8th International Probabilistic Workshop in Szczecin*, pages 13–26, November 2010. 60, 124, 125, 126, 127

Marc Alexa, Johannes Behr, Daniel Cohen-Or, Shachar Fleishman, David Levin, and Claudio T. Silva. Computing and Rendering Point Set Surfaces. *IEEE Transactions on Visulaization and Computer Graphics*, 9(1):3–15, 2003. 96

Jiju Antony. *Design of Experiments for Engineers and Scientists*. Elsevier Science & Technology Books, 2003. 76

Approved Document B. Approved Document B – Volume 2: Buildings other than dwellingshouses (2006 Edition). Technical report, Communities and Local Government of the United Kingdom, 2006. 123, 126, 136, 137

Hartwig Asshauer. Hypoxia - An invisible enemy - Cabin depressurization effects on human physiology. *FAST - Airbus Technical Magazine*, 38:20–25, 2006. 43

Vytenis Babrauskas, Joseph M. Fleming, and B. Don Russell. REST/ASET, a flawed concept for fire safety assessment. *Fire and Materials*, 34:341–355, 2010. 123

Björn Bansemer. *Ein Modell zur szeanrioabhängigen Beurteilung der Rauchgastoxizität*. PhD thesis, Bergische Universität Wuppertal, Fachbereich D, Abteilung Sicherheitstechnik, 2004. 41, 42, 43, 125

Pam Belluck and Paul von Zielbauer. 96 Dead in Fire Ignited at Rhode Island Club. *The New York Times*, February 22:1, 2003. 6

I. P. Belosokhov, D. A. Samoshin adn B. B. Serkov, and V. V. Kholshevnikov. The Lame Horse Night-Club Fire: Disaster Timing. In *Proceedings of the 5th International Conference on Pedestrian and Evacuation Dynamics*, 2010. 119, 138

Micheal Belsham. Probable cause. *Fire Risk Management*, -:41–46, February 2009. 16, 18

W. V. Blockley. *Biology data book*. Federation of American Socitities for Experimental Biology, 1973. 44

George E. P. Box and Norman R. Draper. *Response Surfaces, Mixtures, and Ridge Analysis*. John Wiley & Sons Inc., Hoboken, NJ, 2. edition, 2007. 80, 95

Paul Bratley and Bennet L. Fox. Algorithm 659: Implementing Sobol's Quasirandom Sequence Generator. *ACM Transactions on Mathematical Software*, 14:88–100, March 1988. 75

Dieter Brein and Thomas Hegger. Innenraumluftqualität im Brandfall. *Bauphysik*, 27(4): 234–240, 2005. 57

Piotr Breitkopf, Hakim Naceur, Alain Rassineux, and Pierre Villon. Moving least squares response surface approximation: Formulation and metal forming applications. *Computers and Structures*, 83:1411–1428, 2005. 96

I. N. Bronstein, K. A. Semendjajew, G. Musiol, and H. Mühlig. *Taschenbuch der Mathematik*. Wissenschatflicher Verlag Harri Deutsch GmbH, Frankfurt/Main, 7. edition, 2008. 64, 65, 66, 67, 69, 70, 71, 79, 85, 97, 100, 107, 129

John L. Bryan. *Behavioral Response to Fire and Smoke*, chapter 3-12, pages 3–315–3–341. Volume 1 of DiNenno et al. (2002), 3rd edition, 2002. 39, 51, 53

N. P. Bryner, D. Madrzykowski, and W. L. Grosshandler. Reconstructing the Station Nightclub Fire: Computer Modeling of the Fire Growth and Spread. In *Proccedings of the 11th International Interflam Conference (INTERFLAM 2007)*, volume 2, pages 1181–

1192. interScience Communications, September 2007. 119, 144

BS DD 240. BS DD 240: Fire Safety Engineering in Buildings. Technical report, British Standards Institution, London, 1997. 124

BS 7974. Application of fire safety engineering principles to the design of buildings. Code of practice. Technical report, British Standards Institution (BSI), 2001. 16, 17, 25, 45, 130, 140, 142, 145

Christian Bucher. Adaptive sampling–an iterative fast Monte Carlo procedure. *Structural Safety*, 5(2):119–126, 1988. 83, 101, 103, 104

Christian Bucher. Basic concepts for robustness evaluation using stochastic analysis. In K.-U. Bletzinger, editor, *Efficient Methods for Robust Design and Optimisation - Proceedings of the EUROMECH Colloquium 482*, 2007. 94

Christian Bucher. *Computational Analysis of Randomness in Structural Mechanics*. Taylor & Francis Group, London, UK, 2009. 65, 66, 67, 70, 74, 80, 82, 106, 127

Christian G. Bucher and U. Bourgund. A Fast and Efficient Response Surface Approach for Structural Reliability Analysis. *Structural Safety*, 7(1):57–66, 1990. 81, 96, 105

Klaus Buff and Helmut Greim. *Abschätzung der gesundheitlichen Folgen von Großbränden*. Number Band 25 in Schriftenreihe der Schutzkommission beim Bundesminister des Innern. Bundesamt für Zivilschutz, Bonn, Bonn, 1997. 43

S. V. S. Cabral and L. S. Katafygiotis. Improved adpative importance sampling procedure for reliability estimation. In G. I. Schueller and P. D. Spanos, editors, *Proceedings of the international conference on Monte Carlo Simulation, Monte Carlo, Monaco, 18-21 June 2000*, pages 63–70. Balkema, Rotterdam, NL, 2001. 104

CFast 6.1. *CFAST – Consolidated Model of Fire Growth and Smoke Transport (Version 6) – Technical Reference Guide*. NIST, Fire Research Division, Gaithersburg, MD, April 2009. NIST Special Publication 1026, April 2009 Revision, Walter W. Jones, Richard D. Peacock, Glenn P. Forney, Paul A. Reneke. 33, 115, 116

D. Christian. A study to identify the incidence in the United Kingdom of long-term sequelae following exposure to carbon monoxide. In *Proceedings of the 2nd International Symposium for Human Behaviour in Fire*, London, 2001. Massachusetts Institute of Technology (MIT), Inter-Science Communications Ltd. 41

G.Q. Chu, T. Chen, Z.H Sun, and J.H. Sun. Probabilistic Risk Assessment for Evacuees in Building Fires. *Building and Environment*, 42:1283–1290, 2007. 18

Comrel 8.00. *STRUREL, a Structural Reliability Analysis Program-System: COMREL & SYSREL*. RCP GmbH, München, 2004. 114

Condor Version 7.5.2. *Condor High Throughput Computing Version 7.5.2 – Manual*. Condor Team, University of Wisconsin at Madison, 2010. URL `http://www.cs.wisc.edu/`

condor/. 110

W. J. Conover and R. L. Iman. Rank transformations as bridge between parametric and nonparametric statistics. *American Statistician*, 35:124–129, 1981. 93

G. Deakin and G. Cooke. Future Codes for Fire Safety Design. *Fire Safety Journal*, 23(2): 193–218, 1994. 25

Michael Dehne. *Probabilistisches Sicehrheitskonzept für die brandschutztechnische Bemessung*. PhD thesis, Institut für Baustoffe, Massivbau und Brandschutz, TU Braunschweig, 2003. 13, 17, 19, 60, 93, 134, 144, 145

DIN 1 055-100. Actions on structures - Part 100: Basis of design, safety concept and design rules, German Version. Technical report, Deutsches Institut für Normung e.V., 2001. 139, 151

DIN 18 232-2. Smoke and heat control systems - Part 2: Natural smoke and heat exhaust ventilators; design, requirements and installation. Technical report, Deutsches Institut für Normung e.V., November 2007. 27, 33

DIN 4 102-4. Fire behaviour of building materials and building components; synopsis and application of classified building materials, components and special components. Technical report, Deutsches Institut für Normung e.V., March 1994. 25

DIN EN 13 823. DIN EN 13 823:2009: Reaction to fire tests for building products – Building products excluding floorings exposed to the thermal attack by a single burning item, German Version. Technical report, Deutsches Institut für Normung e.V., 2009. 57

DIN EN 14 390. DIN EN 14 390:2007: Fire test – Large-scale room reference test for surface products, German Version. Technical report, Deutsches Institut für Normung e.V., 2007. 57

DIN EN 1990. Eurocode: Grundlagen der Tragwerksplanung, German Edition. Technical report, Normenausschuss Bauwesen (NABau) im DIN Deutsches Institut für Normung e.V., 2002. 15, 17, 129

DIN EN 1991-1-2/NA. National Annex - Nationally determined parameters – Eurocode 1 - Actions on structures – Part 1-2/NA: General actions - Actions on structures exposed to fire. Technical report, Normenausschuss Bauwesen (NABau) im DIN Deutsches Institut für Normung e.V., 2010. 145, 158, 159, 160

Phillip DiNenno, Dougal Drysdale, Craig Beyler, Douglas Walton, Richard Custer, John Hall, and John Watts, editors. *The SFPE Handbook of Fire Protection Engineering–Third Edition*, volume 1. National Fire Protection Association (NFPA), Quincy, MA, 3rd edition, 2002. 164, 169, 170, 172, 173, 174

Ove Ditlevsen. Narrow Reliability Bounds for Structural Systems. *Mechanics Based Design of Structures and Machines*, 4:453–472, 1979. 85

Norman Richard Draper and Harry Smith. *Applied Regression Analysis*. John Wiley & Sons Inc., Hoboken, NJ, 3. edition, 1998. 93, 94, 96

Dougal Drysdale. *An Introduction to Fire Dynamics*. John Wiley & Sons Inc., Hoboken, NJ, 2 edition, November 1998. 37

Erik Christopher Dyken. *The Simplified Surface Spline*. PhD thesis, University of Oslo - Department of Informatics, January 2003. 96

Micheal H. Faber. Risk and Safety in Engineering. Lecture Notes, ETH Zürich, February 2009. 14

FDS 5.3. *Fire Dynamics Simulator (Version 5) – Technical Reference Guide – Volume 1: Mathematical Model*. NIST, Fire Research Division, Gaithersburg, MD, February 2009. NIST Special Publication 1018-5, Kevin McGrattan, Simo Hostikka, Jason Floyd, Howard Baum, Ronald Rehm, William Mell, Randall McDermott. 34, 43, 109, 110, 111

George S. Fishman. *Monte Carlo - Concepts, Algorithms and Applications*. Springer-Verlag New York, Inc., NY, 1995. 72, 73, 74

Robert W. Fitzgerald. *Building Fire Performance Analysis*. John Wiley & Sons Ltd., Chichester, UK, 2004. 18

Charles Fleischmann. Is Prescription the Future of Performance-based Design? In *Proceedings of the tenth International Symposium on Fire Safety Science (IAFSS)*, 2011. 2, 22, 158

Burkhard Forell. Niveau der Personensicherheit von Versammlungsstätten – Nachweis nach vfdb-Leitfaden. In *Tagungsband der 56. Jahresfachtagung der vfdb, Leipzig, 20.-23. Mai 2007*, pages 294–317. vfdb - Verein zur Förderung des deutschen Branschutzes e.V., Mai 2007a. 115, 117, 124, 138

Burkhard Forell. *A Methodology to assess Species Yields of Compartment Fires by means of an extended Global Equivalence Ratio Concept*. PhD thesis, iBMB at TU Braunschweig, 2007b. 121

Burkhard Forell. Modellierung der Erkennbarkeit von Sicherheitskennzeichen bei inhomogenem Rauch. unpublished, 2010. 39

Alexander I. J. Forrester, Andras Sobester, and Andy J. Keane. *Engineering Design via Surrogate Modelling*. John Wiley & Sons Ltd., Chichester, UK, 2008. 74, 76, 95, 96, 97

Hakan Frantzich. *Uncertainty and Risk Analysis in Fire Safety Engineering*. PhD thesis, Lund University Sweden, Department of Fire Safety Engineering, 1998. 10, 18

J. E. Gentle. *Computational Statistics*. Springer-Verlag New York, Inc., NY, 2009. 107, 109

GruSiBau. Grundlagen zur Festlegung von Sicherheitsanforderungen für bauliche Anlagen. Technical report, Beuth Verlag, Berlin, 1981. 17, 160

Maya R. Gupta and Yihua Chen. Theory and Use of the EM Algorithm. *Foundations and Trends in Signal Processing*, 4(3)(3):223–296, 2010. doi: 10.1561/2000000034. 84

George V. Hadjisophocleous, Noureddine Benichou, and Amal S. Tamim. Literature review of performance-based fire codes and design environment. *Journal of Fire Protection Engineering*, 9(1):12–40, 1998. 23

J. H. Halton. On the efficiency of certain quasi-random sequences of points in evaluating multi-dimensional integrals. *Numerische Mathematik*, 2:84–90, 1960. 75

A. M. Hasofer and N. C. Lind. Exact and invariate second-moment code format. *Journal of Engineering Mechanics Div., Proc. ASCE*, 100:EM1:111–121, 1974. 80

A. M. Hasofer and J. Qu. Response surface modelling of monte carlo fire data. *Fire Safety Journal*, 37:772–784, 2002. 90, 124

A. M. Hasofer, V. R. Beck, and I. D. Bennets. *Risk Analysis in Building Fire Safety Engineering*. Butterworth-Heinemann (Elsevier Science), Burlington, MA, 1. edition, 2007. 18, 67, 86

D. Helbing and P. Molnar. Social force model for pedestrian dynamics. *Physical Review*, E 51:4282–4286, 1995. 52, 53

Gunnar Heskestad. Engineering Relations for Fire Plumes. *Fire Safety Journal*, 7(1):25–32, 1984. 56

K. Hill, J. Dreisbach, F. Joglar, B. Najafi, K. McGrattan, R. Peacock, and A. Hamins. Verification and Validation of Selected Fire Models for Nuclear Power Plant Applications, NUREG 1824. Technical report, United States Nuclear Regulatory Commission (USNRC), Washington, DC, 2007. 36, 111

Eduard Hofer. Sensitivity analysis in the context of uncertainty analysis for computationally intensive models. *Computer Physics Communications*, 117:21–34, 1999. 92, 93

Patrick Hofstetter and James K. Hammitt. Human Health Metrics for Environmental Descision Support Tools: Lessons from Health Economics and Descision Analysis. Technical report, National Risk Management Research Laboratory, US Environmental Protection Agency, Ohio, USA, September 2001. 12

P. G. Holborn, P.F. Nolan, and J. Golt. An analysis of fire sizes, fire grwoth rates and times between events using data from fire investigations. *Fire Safety Journal*, 39:481–524, 2004. 11, 124, 125, 130, 138

Dietmar Hosser, Astrid Weilert, Christoph Klinzmann, Ralf Schnetgöke, and Cornelius Albrecht. Abschlussbericht zum Forschungsvorhaben "Erarbeitung eines Sicherheitskonzeptes für die brandschutztechnische Bemessung unter Anwendung von Ingenieurmethoden gemäß Eurocode 1 Teil 1-2 (Sicherheitskonzept zur Brandschutzbemessung)". Technical report, Institut für Baustoffe, Massivbau und Brandschutz (iBMB), TU Braunschweig, November 2008. 17, 60, 124, 130

Dietmar Hosser, Cornelius Albrecht, Christoph Klinzmann, Christian Mahlmann, and Astrid Weilert. Abschlussbericht zum Forschungsvorhaben "Umsetzung leistungsorientierter Brandschutzvorschriften". Technical report, Institut für Baustoffe, Massivbau und Brandschutz (iBMB), TU Braunschweig, März 2009. 26

Simo Hostikka. *Development of fire simulation models for radiative heat transfer and probabilistic risk assessment*. PhD thesis, VTT Technical Research Centre of Finland, 2008. 19

Simo Hostikka. FDS Monte Carlo simulation of PRS-SI-D1. Presentation at a Prisme project meeting, April 2009. 19

Simo Hostikka and Olavi Keski-Rahkonen. Probabilistic Simulation of Fire Scenarios. *Nuclear Engineering and Design*, 224:301–311, 2003. 19

Douglas W. Hubbard. *The Failure of Risk Management: Why It's Broken and How to fix It*. John Wiley & Sons Inc., Hoboken, NJ, 2009. 5, 6, 8, 10, 13, 14, 15

Richard Hull, Krzysztof Lebek, Maddalena Pezzani, and Silvio Messa. Comparison of toxic product yields of burning cables in bench and large-scale experiments. *Fire Safety Journal*, 43:140–150, 2008. 121

ICC. International Code Council Performance Code for Buildings and Facilities. Technical report, International Code Council (ICC), Falls Chruch, VA, 2006. 37

Ronald L. Iman and W. J. Conover. A distribtuion-free approach to induce rank correlation among input variables. *Communications in Statistics - Simulation and Computation*, 11:311–334, 1982. 74

ISO 13571. Life-threatening components of fire - Guidelines for the estimation of time available for escape using fire date. Technical Report ISO 13571:2007(E), International Standardization Organization (ISO), 2007. 32, 45, 46, 49, 61

JCSS 2.20. JCSS Probabilistic Model Code – Part 2: Load models, Section 2.20: Fire. Technical report, Joint Committee on Structural Safety, 2001. 124

Tadahisa Jin. Visibility through Fire Smoke. *Journal of Fire & Flammability*, 9:135–157, 1978. 38

Tadahisa Jin. *Visibility and Human Behavior in Fire Smoke*, chapter 2-6, pages 2–42–2–53. Volume 1 of DiNenno et al. (2002), 3rd edition, 2002. 38, 39, 40

Tadahisa Jin and Tokiyoshi Yamada. Irritating Effects of Fire Smoke on Visibility. *Fire Science and Technology*, 5:79–90, 1985. 39

R. Johnson and G. Timms. Performance-based Design of Shopping Center Fire Safety. In *Proceedings of the First International ASIAFLAM Conference 1995*, Hong-Kong, March 1995. Inter-Science Communications Ltd. 25

E. L. Kaplan and P. Meier. Nonparametric Estimation from Incomplete Observations. *Journal of the American Statistical Society*, 53:457–481, 1958. 71

Michael J. Karter. Fire Loss in the United States 2008. Technical report, National Fire Protection Association (NFPA), August 2009. 10

Christoph Klinzmann. *Methodik zur computergestützten, probabilistischen Bauwerksbewertung unter Einbeziehung von Bauwerksmonitoring*. PhD thesis, Institute of Building Materials, Concrete Construction and Fire Protection (iBMB), TU Braunschweig, 2008. 71, 85

Christian Knaust. *Modellierung von Brandszenarien in Gebäuden*. PhD thesis, Deparment of Civil Engineering, Technische Universität Wien, 2009. 35

T. Korhonen, S. Hostikka, S. Heliövaara, and H. Ehtamo. Modelling Social Force Interactions in Fire Evacuation. In *Procceedings of the 7th International Conference on Performance-Based Codes and Fire Safety Design Methods*, Auckland, New Zealand, April 2008. SFPE. 53

Timo Korhonen and Simo Hostikka. *Fire Dynamics Simulator with Evacuation: FDS+Evac – Technical Reference and User's Guide*. VTT Technical Research Center of Finland, 2009. 52, 53, 128

Inna Krykova. Evaluating of path-dependent securities with low discrepancy methods. Master's thesis, Worcester Polytechnic Institute, 2003. 75

Erica D. Kuligowski. *Computer Evacuation Models for Buildings*, chapter Section Three, Chapter 17, pages 3–456–3–478. Volume 1 of DiNenno et al. (2002), 3rd edition, 2002. 51, 52

Matthias Kunle. *Entwicklung und Untersuchung von Moving Least Square Verfahren zur numerischen Simulation hydrodynamischer Gleichungen*. PhD thesis, Department of Physics, Eberhard-Karls-Universität zu Tübingen, 2001. 96, 100

Lawrence L. Kupper. *Optimal Response Surface Techniques using Fourier Series and Spherical Harmonics*. PhD thesis, University of North Carolina, Department of Statistics, April 1970. 96

P. Lancaster and K. Salkauskas. Surfaces generated by moving least squares methods. *Mathematics of Computation*, 37(155):141–158, 1981. 99, 100

Jane I. Lataille. *Fire Protection Engineering in Building Design*. Butterworth-Heinemann (Elsevier Science), 2003. 30

R. Lawson, W. Walton, and B. Twilley. Fire Performance of Furnishings Measured in the NBS Furniture Calorimeter, Part 1. Technical report, National Bureau of Standards, NBS, today: NIST, 1983. 124

P.-L. Liu and A. DerKiureghian. Multivariate distribution models with prescribed marginals and covariances. *Journal of Probabilistic Engineering Mechanics*, 1(2):105–112, 1986. 69

Trond Maag. *Risikobasierte Beurteilung der Personensicherheit von Wohnbauten im Brandfall unter Verwendung von Bayes'schen Netzen*. PhD thesis, Eidgenössische Technische Hochschule Zürich, 2004. 18

D. Madrzykowski, N.P.Bryner, and S. Kerber. The NIST Station Nightclub Fire Investigation: Physical Simulation of the Fire. *Fire Protection Engineering*, 31:34–46, 2006. 144, 147

Daniel Madrzykowski. Office work station hear release rate study: full scale vs. bench scale. In C. A. Franks and S. Grayson, editors, *Proceedings of the 7th International Interflam Conference in Cambride, UK*, pages 47–55. Inter-Science Communications Ltd., March 1996. 58

Sven Erik Magnusson, Hakan Frantzich, and Kazunori Harada. Fire Safety Design Based on Calculations: Uncertainty Analysis and Safety Verfication. *Fire Safety Journal*, 27: 305–334, 1996. 17, 90, 124

Frédéric Magoulès, Jie Pan, Kiat-An Tan, and Abhinit Kumar. *Introduction to Grid Computing*. CRC Press, Taylor and Francis Group, Boca Raton, FL, 2009. 109, 110

Simeone Marino, Ian B. Hogue, Christian J. Ray, and Denise E. Kirschner. A methodology for performing global uncertainty and sensitivity analysis in systems biology. *Journal of Theoretical Biology*, 254:178–196, 2008. 93

Wendy L. Martinez and Angel R. Martinez. *Computational Statistics with Matlab*. Chapman & Hall/CRC, Boca Raton, FL, 2002. 71, 73

Robert L. Mason, Richard F. Gunst, and James L. Hess. *Statistical Design and Analysis of Experiments - With Applications to Engineering and Science*. John Wiley & Sons, Inc., Hoboken, NJ, 2. edition, 2003. 70, 76

Matlab 7.8.0. *User's Manual for Matlab R2009a (7.8.0) - The Language of Technical Computing*. The Mathworks, Inc., Natick, MA, 2009. 72, 102, 113, 116, 117, 179, 191

M. Matsumoto and T. Nishimura. Mersenne Twister: A 623-Dimensionally Equidistributed Uniform Pseudo-Random Number Generator. *ACM Transactions on Modeling and Computer Simulation*, 8:3–30, January 1998. 72

U. Max. *Zur Berechnung der Ausbreitung von Feuer und Rauch in komplexen Gebäuden*. PhD thesis, Universität Kassel, 1990. 33

MBO. Musterbauordnung (MBO). Technical report, IS-Argebau, 2002. Zuletzt geändert durch Beschluss der Bauministerkonferenz vom Oktober 2008. 8, 22

Kevin McGrattan, Simo Hostikka, Jason Floyd, Howard Baum, Ronald Rehm, William Mell, and Randall McDermott. Fire Dynamics Simulator (Version 5) – Technical Reference Guide. Technical report, NIST, Fire Research Division, Gaithersburg, MD, February 2009. NIST Special Publication 1018-5. 34, 35, 36, 110

Brian J. Meacham. Understanding Risk: Quantification, Perception, and Characterization. *Journal of Fire Protection Engineering*, 14:199–227, August 2004. 5, 7

Friedrich Mehl. Richtlinien für die Erstellung und Prüfung von Brandschutzkonzepten. In Dietmar Hosser, editor, *Praxisseminar Brandschutz bei Sonderbauten*, volume 178. Institut für Baustoffe, Massivbau und Brandschutz, TU Braunschweig, 2004. 24, 25, 121, 143

Robert E. Melchers. *Structural Reliability Analysis and Prediction*. John Wiley & Sons Ltd., Chichester, UK, 2. edition, 1999. 66, 69, 70, 71, 78, 80, 84, 85

William Mendenhall and Terry Sincich. *A second course in statistics - Regression Analysis*. Prentice-Hall, Inc., Upper Saddle River, NJ, 5. edition, 1996. 47, 67, 70, 71, 93, 94, 95, 98, 134

N. Metropolis and S. Ulam. The Monte Carlo method. *Journal of the American Statistical Association*, 44:335–341, 1949. 81

Matthias Münch. Kritische numerische Aspekte bei der Anwendung von Feldmodellen. In *Tagungsband der 55. vfdb-Jahresfachtagung*, pages 256–288, May 2006. 15

Thomas Most. *Stochastic crack growth simulation in reinforced concrete structures by means of coupled finite element and meshless methods*. PhD thesis, Institute for Structural Dynamics, Bauhaus-Universität Weimar, 2005. 74, 96

Thomas Most. An adaptive response surface appproach for reliability analyses of discontinuous limit state functions. In Grauber, Schmidt, and Proske, editors, *Proceedings of the 6th International Probabilistic Workshop*, pages 381–396. Institut für Massivbau, Technische Universität Darmstadt, November 2008. 81, 96

Thomas Most and Christian Bucher. A Moving Least Squares weighting function for the Element-free Galerkin Method which almost fulfills the essential boundary conditions. *Structural Engineering and Mechanics*, 21(3):315–332, 2005. 100, 101

Thomas Most and Christian Bucher. New concepts for Moving least squares: An interpolating non-singular weighting function and weighted nodal least squares. *Engineering Analysis with Boundary Elements*, 32:461–470, 2008. 183

Thomas Most and Johannes Will. Meta-model of Optimal Prognosis - An automatic approach for variable reduction and optimal meta-model selection. In *Proceedings of the Weimar Optimization and Stochastic Days 5.0*. Dynardo Software and Engineering GmbH, November 2008. 93, 94, 95, 101

George W. Mulholland. *Smoke Production and Properties*, chapter 2-13, pages 2–258–2–268. Volume 1 of DiNenno et al. (2002), 3rd edition, 2002. 35, 37

MVStättV. Musterverordnung über den Bau und Betrieb von Versammlungsstätten (Muster-Versammlungsstättenverordnung - MVStättV). Technical report, IS-Argebau, 2005. 1, 37, 46, 52, 126

A. Nataf. Détermination des distributions de probabilités dont les marges sont donnés. *Computes rendus de l'Académie des sciences*, 225:42–43, 1962. 69

Harold E. Nelson and Frederick W. Mowrer. *Emergency Movement*, chapter 3-13, pages 3–367–3–380. Volume 1 of DiNenno et al. (2002), 3rd edition, 2002. 39

Hennadiy Netuzhylov. *A Space-Time Meshfree Collocation Method for Coupled Problems on Irregularly-Shaped Domains*. PhD thesis, Technische Universität Braunschweig, November 2008. 96, 99, 100, 185

NFPA 101. *NFPA 101: Life Safety Code*. National Fire Protection Association (NFPA), 2008. 1, 7, 8, 17, 26, 49, 54, 55, 59, 61, 121, 159

NFPA 13. *NFPA 13:Standard for the Installation of Sprinkler Systems*. National Fire Protection Association (NFPA), 2010. 159

NFPA 72. *NFPA 72: National Fire Alarm Code*. National Fire Protection Association (NFPA), 2002. 51

Harald Niederreiter. *Random Number Generation and Quasi-Monte Carlo Methods*. Society for Industrial and Applied Mathematics, Philadelphia, PA, 1. edition, 1992. 72, 74, 75

Yoojeong Noh, K. K. Choi, and Liu Du. Reliability-based design optimization of problems with correlated input variables using a Gaussian Copula. *Structural and Multidisciplinary Optimization*, 38:1–16, 2008. 69

Kathy A. Notarianni. *The Role of Uncertainty in Improving Fire Protection Regulation*. PhD thesis, Carnegie Mellon University, Pennsylvania, 2000. 18, 33, 37, 44, 48, 49, 71, 90, 124, 125

optiSLang 3.1.0. *User's Manual for OptiSLang - The Optimizing Structural Language, Nightly Build Version 3.1.0* . Dynardo Software and Engineering GmbH, Luthergasse 1D, Weimar, Germany, December 2009. 92, 116, 117

M. Oudjene, L. Ben-Ayed, A. Delameziere, and J.-L. Batoz. Shape optiomization of clinching tools using the response surface methodology with Moving Least-Square approximation. *Journal of Materials Processing Technology*, 209:289–296, 2009. 96

Costas Papadimitriou and Lambros S. Katafygiotis. *Bayesian Modeling and Updating*, volume 1, chapter 22, pages 509–528. CRC Press, Taylor and Francis Group, Boca Raton, FL, 2005. 127

R. Peacock, R. Portier, and P. Reneke. FastDATA 1.0, NIST Standard Reference Database Number 75, Online Preview Release, January 1999. URL `http://fire.nist.gov/fastdata/`. accessed Oct 28, 2010. 56, 57

Pat Perry. *Fire Safety–Questions and Answers: A Practical Approach*. Thomas Telford Publishing Ltd., London, 2003. 119

T. Pliefke, S. Sperbeck, M. Urban, U. Peil, and H. Budelmann. A standardized methodology for managing desaster risk – an attempt to remove ambiguity. In Luc Taerwe and Dirk Proske, editors, *Proceeding of the 5th International Probabilistic Workshop at Ghent*, 2007. 9

V. M. Predtechenskii and A. I. Milinskii. *Planning for Foot Traffic Flow in Buildings*. Amerind, New Dehli, 1978. 52

C. Proppe. Estimation of failure probabilities by local approximation of the limit state function. *Structural Safety*, 30:277–290, 2008. 96, 101

Dirk Proske. *Katalog der Risiken – Risiken und ihre Darstellung*. Eigenverlag Dirk Proske, 2004. 7, 8, 10, 11, 12, 13, 14

Guylene Proulx. *Movement of people: The Evacuation Timing*, chapter 3-13, pages 3–342–3–366. Volume 1 of DiNenno et al. (2002), 3rd edition, 2002. 39, 51

David Purser and Jenny Purser. HCN Yields and Fate of Fuel Nitrogen for Materials under Different Combustion Conditions in the ISO 19 700 Tube Furnace and Large-scale Fires. In *Fire Safety Science–Proceedings of the Ninth International Symposium*. International Association for Fire Safety Science (IAFSS), 2008. 125, 126

David A. Purser. *Toxicity Assessment of Combustion Products*, chapter Section Two, Chapter 6, pages 2–83–2–171. Volume 1 of DiNenno et al. (2002), 3rd edition, 2002. 35, 38, 39, 40, 41, 42, 43, 44, 45, 46, 48, 51, 61, 131, 161

Rüdiger Rackwitz and Hermann Streicher. Optimization and Target Reliabilities. In *Proceedings of the JCSS Workshop on Reliability Based Code Calibration*, 2002. 13

Ganapathy Ramachandran. *The economics of Fire Protection*. E & FN Spon, London, UK and Routledge, New York, NY, 1998. 2, 10, 139

D.J. Rasbash. Criteria for Acceptability for Use with Quantitative Approaches to Fire Safety. *Fire Safety Journal*, 8:141–158, 1984. 17

Dirk Roos. *Approximation und Interpolation von Grenzzustandsfunktionen zur Sicherheitsbewertung nichtlinearer Finite-Elemente-Strukturen*. PhD thesis, Institute for Structural Dynamics, Bauhaus-Universität Weimar, 2001. 80, 84, 90

Dirk Roos. Multi-doman Adaptive Surrogate Models for Reliability Analysis. In Harald Budelmann, Alexander Holst, and Dirk Proske, editors, *Proceedings of the 9th International Probabilistic Workshop*, pages 191–208. TU Braunschweig, November 2011. 84

Dirk Roos and Ulrike Adam. Adaptive Moving Least Square Approximation for the Design Reliability Analysis. In *Proceedings of the Weimar Optimization and Stochastic Days 3.0*, November 2006. 96, 101

Dirk Roos, Thomas Most, Jörg Unger, and Johannes Will. Advanced surrogate models within the robustness evaluation. In *Proceedings of the Weimar Optimization and Stochas-*

tic Days 4.0, November 2007. 89, 96, 103

Eric Rosenbaum et al. *SFPE Engineering Guide to Performance-Based Fire Protection*. National Fire Protection Association (NFPA) and Society of Fire Protection Engineers (SFPE), 2nd edition, 2007. 11, 15, 17, 54, 144, 145

Reuven Y. Rubinstein. *Simulation and the Monte Carlo Method*. John Wiley & Sons, Inc., Hoboken, NJ, 1981. 72, 74, 82

Andrea Saltelli and T. Homma. Sensitivity analysis for model output - Performance of black box techniques on three international benchmar exercises. *Computational Statistics & Data Analysis*, 13:73–94, 1992. 92

Andrea Saltelli, Stefani Tarantola, Francesca Campolongo, and Marco Ratto. *Sensitivity Analysis in Practice - A Guide to Assessing Scientific Models*. John Wiley & Sons Ltd., Chichester, UK, 2004. 92

Jörg Schneider. *Sicherheit und Zuverlässigkeit im Bauwesen - Grundwissen für Ingenieure*. Verlag der Fachvereine (vdf), Zürich, 1994. 63, 70, 71, 78

Ulrich Schneider. *Grundlagen der Ingenieurmethoden im Brandschutz*. Werner Verlag, Düsseldorf, 1 edition, 2002. 33

Ralf Schnetgöke. *Zuverlässigkeitsorientierte Systembewertung von Massivbauwerken als Grundlage für die Bauüberwachung*. PhD thesis, Institute of Building Materials, Concrete Construction and Fire Protection (iBMB), TU Braunschweig, 2008. 17, 83, 89, 103, 104, 112

Volker Schwieger. *Nicht-lineare Sensitivitätsanalyse gezeigt an Beispielen zu bewegten Objekten*. Verlag der Bayerischen Akademie der Wissenschaften in Kommision beim Verlag C. H. Beck, 2005. Habilitationsschrift an der Fakultät für Bau- und Umweltingenieurwissenschaften der Universität Stuttgart. 93

Donald Shepard. A two-dimensional interpolation function for irregularly-spaced data. In *Proceedings – 1968 ACM National Conference*, pages 517–524, 1968. 101

Matthias Siemon. Zuervlässigkeitsorientierte Bewertung der sicheren Entfluchtung im Brandfall mit Hilfe von Ingenieurmethoden. Master's thesis, Diplomarbeit, iBMB TU, Braunschweig, 2011. 28

Michael Six. *Sicherheitskonzept für nichtlineare Traglastverfahren im Betonbau*. PhD thesis, Institut für Massivbau, Technische Universität Darmstadt, 2001. 70, 78, 80, 81, 82, 83, 103, 104, 105

Gerhard Spaethe. *Die Sicherheit tragender Baukonstruktionen*. Springer-Verlag, Vienna, Austria, 2. edition, 1992. 15, 16

Louise C. Speitel. Fractional effective dose model for post-crash aircraft survivability. *Toxicology*, 115:167–177, 1996. 49, 120

Silvio T. Sperbeck. *Seismic Risk Assessment of Masonry Walls and Risk Reduction by Means of Prestressing*. PhD thesis, Technische Universität Braunschweig, 2009. 9

Chauncey Starr. Social Benefit versus Technological Risk – What is our society willing to pay for safety? *Science*, 19:1232–1238, 1969. 7, 8

A. A. Stec, T. R. Hull, J. A. Purser, and D. A. Purser. Comparison of toxic product yields from bench-scale to ISO room. *Fire Safety Journal*, 44:62–70, 2009. 135

Richard D. Steward. The effect of carbon monxide on humans. *Annual Review of Pharmacology*, 15:409–423, 1975. 41

T. Tanaka, D. Nii, J. Yamaguchi, H. Notake, and Y. Ikehata. A Study on Risk-Based Evacuation Safety Design Method in Fire for Office Buildings. In *Proceedings of the 12th International Conference on Fire Science and Engineering (InterFlam9)*, pages 849–860, 2010. 11, 18, 60

Takeyoshi Tanaka. Risk-Based Selection of Design Fires to Ensure an Acceptable Level of Evacuation Safety. In Björn Karlsson, editor, *Fire Safety Science – Proceedings of the ninth international symposium*, pages 49–62, 2008. 11, 18

Archibald Tewarson. *Generation of Heat and Gaseous, Liquid, and Solid Products in Fires*, volume 1, chapter Section Three, Chapter 4, pages 3–109–3–194. National Fire Protection Association (NFPA), Quincy, MA, 4th edition, 2008. 125, 126

Jeffrey S. Tubbs and Brian J. Meacham. *Egress Design Solutions – A guide to Evacuation and Crowd Management Planning*. John Wiley & Sons, Inc., Hoboken, NJ, 1. edition, 2007. 25, 26, 39, 49, 51, 56, 57, 126, 127, 138

Igor A. Ushakov. *Handbook of Reliability Engineering*. John Wiley & Sons, Inc., Hoboken, NJ, 1. American edition, 1994. 71

J. C. van der Corput. Verteilungsfunktionen. *Proceedings of the Nederlandse Akademie von Wetenschappen*, 38:813–821, 1935. 75

VdS CEA 4001. Spinkleranlagen, Planung und Einbau. Technical report, VdS Schadensverhütung GmbH, November 2008. 145, 159

vfdb-Leitfaden. Leitfaden Ingenieurmethoden des Brandschutzes, Technischer Bericht TB 04/01, 2. Auflage. Dietmar Hosser (Hrsg.), Verein zur Förderung des deutschen Brandschutzes e.V. (vfdb), Altenberge, Braunschweig, Mai 2009. 15, 24, 25, 28, 33, 35, 37, 39, 45, 49, 51, 57, 60, 124, 125, 126, 127

VKF/AEAI. (Schweizer) Brandschutznorm. Technical report, Vereinigung kantonaler Feuerversicherungen (VKF), November 2003. 21

Thomas von Züthpen. In der Feuerfalle. *Focus*, 16:20–25, 1996. 6

Ulf Wickström, Haukur Ingason, and Patrick Van Hees. The SP Investigation of the Discotheque Fire in Göteborg 1998. In *Proceedings of the tenth Interflam*, pages 965–976,

2004. 119, 135

Christopher J. Wieczorek and Nicholas A. Dembsey. Human Variability Correction Factors for Use with Simplified Engineering Tools for Predicting Pain and Second Degree Skin Burns. *Journal of Fire Protection Engineering*, 2:88–111, 2001. 45

Guan Heng Yeoh and Kwok Kit Yuen. *Computational Fluid Dynamics in Fire Engineering – Theory, Modelling, and Practice*. Butterworth-Heinemann (Elsevier Science), Burlington, MA, 2009. 34, 35, 36

David Yung. *Principles of Fire Risk Assessment in Buildings*. John Wiley & Sons, Ltd., West Sussex (UK), 2008. 5, 11, 18, 45, 49, 54, 57

Appendix **A**

Matrices of the example in Section 6.2

In this Appendix, the matrices and vectors of the example from Section 6.2 (pages 95ff) are shown in full to give the reader a better understanding of the matrix and vector operations performed. As the IMLS methodology is completely representable in matrix-vector-form, Matlab 7.8.0 (2009) was chosen as underlying programming language as matrices are handled without further consideration and at very good performance (for uncompiled code).

A.1. Least squares

The starting vectors and matrices from Equation 6.6 (page 96) for the linear case and the data points shown in Figure 6.3[1] (page 98) are as follows:

$$\mathbf{x} = [1, 2, 3, 4, 5, 6, 7, 8, 9, 10]^T \,, \tag{A.1a}$$

$$\mathbf{y} = [0.7380, 1.9967, 3.4195, 2.6808, 3.6705, 3.4476, 5.0025, 4.5102, 5.5119, 6.3982]^T \,, \tag{A.1b}$$

$$\mathbf{H} = \begin{bmatrix} 1 & x_1 \\ 1 & x_2 \\ \vdots & \vdots \\ 1 & x_{10} \end{bmatrix} = \begin{bmatrix} 1 & 1 \\ 1 & 2 \\ \vdots & \vdots \\ 1 & 10 \end{bmatrix} \,. \tag{A.1c}$$

[1] The Figure only shows eight out of the ten data points.

$\hat{\boldsymbol{\beta}}$ can then be computed according to Equation 6.11, so that

$$\hat{\boldsymbol{\beta}} = (\mathbf{H}^T\mathbf{H})^{-1}\mathbf{H}^T\mathbf{y} \tag{A.2a}$$

$$= \left(\begin{bmatrix} 1 & 1 & \dots & 1 \\ 1 & 2 & \dots & 10 \end{bmatrix} \cdot \begin{bmatrix} 1 & 1 \\ 1 & 2 \\ \vdots & \vdots \\ 1 & 10 \end{bmatrix} \right)^{-1} \cdot \begin{bmatrix} 1 & 1 & \dots & 1 \\ 1 & 2 & \dots & 10 \end{bmatrix} \cdot \begin{bmatrix} 0.7380 \\ 1.9967 \\ \vdots \\ 6.3982 \end{bmatrix} \tag{A.2b}$$

$$= [0.8128, 0.5318]^T . \tag{A.2c}$$

Hence, the least square solution for the linear model at $\mathbf{x}$ is

$$\hat{\mathbf{y}} = \mathbf{H}\hat{\boldsymbol{\beta}} \tag{A.3a}$$

$$= \begin{bmatrix} 1 & 1 \\ 1 & 2 \\ \vdots & \vdots \\ 1 & 10 \end{bmatrix} \cdot [0.8128, 0.5318]^T \tag{A.3b}$$

$$= [1.3446, 1.8764, 2.4081, 2.9399, 3.4717, \\ 4.0035, 4.5353, 5.0670, 5.5988, 6.1306]^T \tag{A.3c}$$

and the error vector yields

$$\boldsymbol{\varepsilon} = \mathbf{y} - \hat{\mathbf{y}} \tag{A.4a}$$

$$= [-0.6066, 0.1204, 1.0113, -0.2592, 0.1988, \\ -0.5559, 0.4673, -0.5569, -0.0869, 0.2676]^T . \tag{A.4b}$$

A.2. Interpolating moving least squares

For the interpolating moving least squares, the weighting matrix $\mathbf{W}(\mathbf{x})$ is introduced. The matrices are shown for $x_s = 2.8$. The matrices $\mathbf{x}$, $\mathbf{y}$, and $\mathbf{H}$ are the same as shown in Equation A.1.

Firstly, the weighting function $\mathbf{W}(\mathbf{x})$ is evaluated for the wanted location $x_s = 2.8$. In order to weight the input values, the distance needs to be obtained using the Eucledian distance d_i for every support point. For the simple, one-dimensional example, the distances are $d_i = |x_i - x_s|$ so that the distance vector becomes

$$\mathbf{d} = [1.8, 0.8, 0.2, 1.2, 2.2, 3.2, 4.2, 5.2, 6.2, 7.2]^T . \tag{A.5}$$

The distances can now be used to construct the diagonal weighting matrix based on the interpolating weighting function shown in Equation 6.25 for infinite support leading to

$$\mathbf{W}(x_s = 2.8) = \begin{bmatrix} 0.002 & 0 & 0 & \dots & 0 \\ 0 & 0.0039 & 0 & \dots & 0 \\ 0 & 0 & 0.9951 & \dots & 0 \\ \vdots & \vdots & \vdots & \ddots & \vdots \\ 0 & 0 & 0 & 0 & < 0.000 \end{bmatrix} . \tag{A.6}$$

One can see that the third entry on the diagonal trace is close to unity, denoting the high influence of the support point $(x, y) = (3, 3.4195)$ which has a close proximity to the evaluation location ($x_s = 2.8$). One can also see the steep gradient of the weighting function, as the influence of the support point $(x, y) = (2, 1.9967)$ is already fairly limited.

The weighting matrix can now be utilized to obtain the free coefficients $\hat{\boldsymbol{\beta}}(x_s = 2.8)$ using

$$\hat{\boldsymbol{\beta}}(\mathbf{x}) = [\mathbf{H}^T\mathbf{W}(\mathbf{x})\mathbf{H}]^{-1}\mathbf{H}^T\mathbf{W}(\mathbf{x})\mathbf{y} \tag{A.7a}$$

$$= \left(\begin{bmatrix} 1 & 1 & \dots & 1 \\ 1 & 2 & \dots & 10 \end{bmatrix} \cdot \begin{bmatrix} 0.002 & 0 & \dots & 0 \\ 0 & 0.0039 & \dots & 0 \\ \vdots & \vdots & \ddots & \vdots \\ 0 & 0 & 0 & 0.000 \end{bmatrix} \begin{bmatrix} 1 & 1 \\ 1 & 2 \\ \vdots & \vdots \\ 1 & 10 \end{bmatrix} \right)^{-1} \cdot$$

$$\cdot \begin{bmatrix} 1 & 1 & \dots & 1 \\ 1 & 2 & \dots & 10 \end{bmatrix} \cdot \begin{bmatrix} 0.002 & 0 & \dots & 0 \\ 0 & 0.0039 & \dots & 0 \\ \vdots & \vdots & \ddots & \vdots \\ 0 & 0 & 0 & 0.000 \end{bmatrix} \cdot \begin{bmatrix} 0.7380 \\ 1.9967 \\ \vdots \\ 6.3982 \end{bmatrix} \tag{A.7b}$$

$$= [0.4175, 0.9996]^T . \tag{A.7c}$$

Having determined the coefficients, the next step is to compute the $\hat{y}$-value with a linear model $\mathbf{h}(x_s)$ for $x_s = 2.8$, so that

$$\hat{y}(x_s = 2.8) = \mathbf{h}(\mathbf{x})\hat{\boldsymbol{\beta}}(\mathbf{x}) \tag{A.8a}$$

$$= [1.000, 2.8000] \cdot \begin{bmatrix} 0.4175 \\ 0.9996 \end{bmatrix} \tag{A.8b}$$

$$= 3.2163 . \tag{A.8c}$$

Obtaining values for the support points (i.e. $x_s = 3.0$) shows the approximation power of the interpolating moving least squares. The surrogate values yields $\hat{y}(x_s = 3.0) = 3.419487916799217$ while the support point value was chosen to $y(3.0) = 3.419487917032162$. The interpolation error, therefore, is only

$$\varepsilon_{\text{interp.}} = \frac{|3.419487916799217 - 3.419487917032162|}{3.419487917032162} \tag{A.9a}$$

$$= 6.8123 \times 10^{-11}\,, \tag{A.9b}$$

which is (definitely) sufficient for the evaluation of limit state functions.

Appendix **B**

Weighting functions

In Section 6.2.4 (page 100) other weighting functions besides the interpolating weighting function were mentioned. They will be evaluated for accuracy in the next sections. An overview over the weighting functions and their shape around the support point can be seen in Figure B.1.

B.1. Gaussian weighting

A Gaussian weighting function was given by Most and Bucher (2008)

$$w_i(||\mathbf{x} - \mathbf{x}_{m_i}||) = e^{-d^2/\alpha^2} \tag{B.1}$$

where $d = \frac{||\mathbf{x}-\mathbf{x}_{m_i}||}{D}$ and $d \leq 1$ for finite support. D is the influence radius and α is a shape parameter, usually chosen to be 0.4.

Using this weighting function for the data presented in Section 6.2 (page 95), the following results at the supports are obtained for an influence radius $D = 8$:

$$\begin{aligned}\hat{\mathbf{y}}(x_i) = [&1.1493, 1.8871, 2.4964, 3.0207, 3.5046,\\ &3.9830, 4.4790, 5.0073, 5.5795, 6.2071]^T\end{aligned} \tag{B.2}$$

compared to the "exact" solutions

$$\begin{aligned}\mathbf{y} = [&0.7380, 1.9967, 3.4195, 2.6808, 3.6705,\\ &3.4476, 5.0025, 4.5102, 5.5119, 6.3982]^T\end{aligned}, \tag{B.3}$$

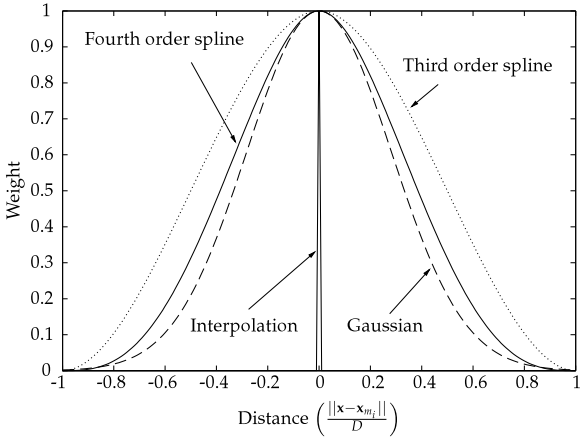

Figure B.1.: Comparison of the weighting function around the support (located at 0 distance). It is evident that the non-interpolation weighting functions can only approximate the support point value, whereas the quasi-interpolation function spikes only around the support, nearly fulfilling the Kronecker-delta-property δ_{ij} (see Equation 6.24 on page 100).

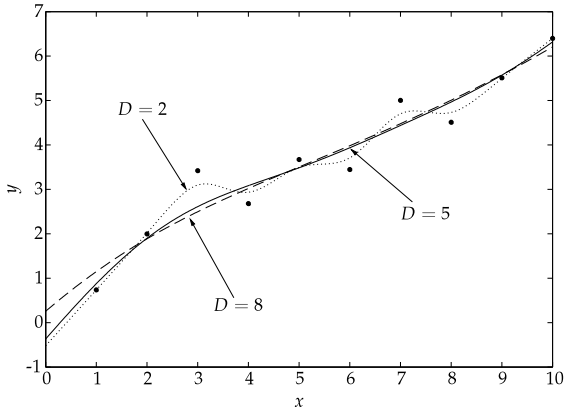

Figure B.2.: Comparison of the approximation using Gaussian weighting functions with different influence radii D.

the resulting error components are

$$\boldsymbol{\varepsilon} = \mathbf{y} - \hat{\mathbf{y}} \tag{B.4a}$$

$$= [-0.4113, 0.1096, 0.9231, -0.3399, 0.1659, \\ -0.5354, 0.5235, -0.4971, -0.0676, 0.1910]^T \tag{B.4b}$$

which lead to errors significantly larger than those obtained in Appendix A for the interpolating case (see Equation A.9b). Figure B.2 shows the approximation for three different influence radii D.

B.2. Spline weighting

Spline weighting functions were proposed by Netuzhylov (2008, p.17)

$$w_i(||\mathbf{x} - \mathbf{x}_{m_i}||) = \begin{cases} 1 - 3d^2 + 2d^3 & \text{Third order} \\ 1 - 6d^2 + 8d^3 - 3d^4 & \text{Fourth order} \end{cases} \tag{B.5}$$

where $d = \frac{||\mathbf{x}-\mathbf{x}_{m_i}||}{D}$ and $d \leq 1$. D is the influence radius.

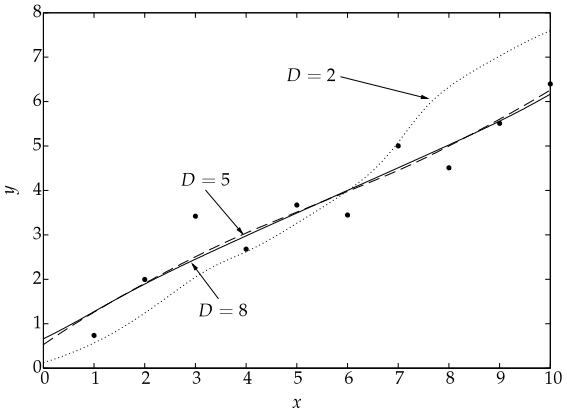

Figure B.3.: Comparison of the approximation using a cubic spline weighting function with different influence radii D..

Using this weighting function for the data presented in Section 6.2 (page 95), the following results at the supports are obtained for the third order spline and an influence radius $D = 8$:

$$\hat{\mathbf{y}}(x_i) = [1.2716, 1.8936, 2.4527, 2.9784, 3.4919, \\ 4.0012, 4.5105, 5.0242, 5.5609, 6.1676]^T \tag{B.6}$$

compared to the "exact" solutions

$$\mathbf{y} = [0.7380, 1.9967, 3.4195, 2.6808, 3.6705, \\ 3.4476, 5.0025, 4.5102, 5.5119, 6.3982]^T , \tag{B.7}$$

the resulting error components are

$$\boldsymbol{\varepsilon} = \mathbf{y} - \hat{\mathbf{y}} \tag{B.8a}$$

$$= [-0.5336, 0.1031, 0.9668, -0.2976, 0.1787, \\ -0.5535, 0.4920, -0.5140, -0.0490, 0.2305]^T \tag{B.8b}$$

which lead to errors significantly larger than those obtained in Appendix A for the interpolating case (see Equation A.9b). Figure B.3 shows the approximation for three different influence radii D.

Appendix C

Distribution functions

In the following, the distribution function utilized in this thesis are briefly described along with their mathematical formulation and parameters.

C.1. Normal distribution

The normal (or Gaussian) distribution is the most commonly known distribution function. It is continuously defined from $-\infty$ to $+\infty$. The distribution is symmetric about the mean and it is usually utilized to describe random fluctuations. Many random phenomena can be explained with the normal distribution.

The probability density function (PDF) of the random variable X is defined

$$f(x) = \frac{1}{\sigma\sqrt{2\pi}} \exp\left[-\frac{1}{2}\left(\frac{x-\mu}{\sigma}\right)^2\right], \quad x \in \mathbb{R}, \tag{C.1}$$

where μ is the mean value and σ^2 is the variance, so that σ is the standard deviation. Integration of the probability density function leads to the distribution function (CDF), which is defined

$$F(x) = \frac{1}{\sigma\sqrt{2\pi}} \int_{-\infty}^{x} \exp\left[-\frac{1}{2}\left(\frac{u-\mu}{\sigma}\right)^2\right] du. \tag{C.2}$$

A normal distributed variable X is usually denoted $X \sim \mathcal{N}(\mu, \sigma^2)$.

C.2. Log-normal distribution

The right skewed log-normal distribution is related to the normal distribution as a random variable X is log-normal distributed if $\ln(X)$ is normal distributed. It is continuously defined for all positive real numbers (including zero, $\mathbb{R}_{\geq 0}$) from 0 to $+\infty$ with a probability density function

$$f(x) = \frac{1}{\sigma x \sqrt{2\pi}} \exp\left[-\frac{(\ln x - \mu)^2}{2\sigma^2}\right], \quad x \in \mathbb{R}_{\geq 0} \tag{C.3}$$

with the location parameter μ and the squared scale parameter σ^2. Integration yields the distribution function

$$F(x) = \frac{1}{\sigma\sqrt{2\pi}} \int_0^x \frac{1}{u} \exp\left[-\frac{(\ln u - \mu)^2}{2\sigma^2}\right] du\,. \tag{C.4}$$

The log-normal distributed random variable X is usually denoted $X \sim \mathcal{LN}(\mu, \sigma^2)$ and is used to model income distributions and similar economic phenomena.

C.3. Gumbel distribution

The Gumbel distribution is one of the three commonly used distributions in extreme value theory named after the German mathematician Julius Gumbel and can either describe extreme minima (Gumbel-min) or maxima (Gumbel-max). The Gumbel distribution is continuously defined from $-\infty$ to $+\infty$ and either left or right skewed to describe the extreme values of the underlying data. The Gumbel-min distribution can be described by a location parameter α and a scale parameter β and a probability density function

$$f(x) = \frac{1}{\beta} \exp\left[\frac{x-\alpha}{\beta} - \exp\left(\frac{x-\alpha}{\beta}\right)\right], \quad x \in \mathbb{R}\,, \tag{C.5}$$

and the distribution function

$$F(x) = 1 - \exp\left[-\exp\left(\frac{x-\alpha}{\beta}\right)\right], \tag{C.6}$$

where $\alpha = \bar{x} + \Gamma \cdot \beta$ with $\beta = s \cdot \frac{\sqrt{6}}{\pi}$ and $\Gamma \approx 0.5772\ldots$ is the Euler-Mascheroni constant. $\bar{x}$ and s are the mean and standard deviation defined in Section 5.3.1 on page 70. The Gumbel-max distribution can be evaluated by inserting $-x$ into the Equations C.5 and C.6.

C.4. Exponential distribution

The Exponential distribution was used in this work to model the time between the (independent) occurrence of fire initiations, as the arrival thereof is assumed to be a Poisson process (Section 7.4.1, p.130). As time t is continuous, the distribution is also continuously defined from 0 to $+\infty$. The probability density function is given as

$$f(t) = \lambda \exp(-\lambda t)\,, \quad t \in \mathbb{R}_{\geq 0} \tag{C.7}$$

and the probability function reads

$$F(t) = 1 - \exp(-\lambda t)\,, \tag{C.8}$$

where $\lambda \in \mathbb{R}_{>0}$ is a rate parameter denoting the number of fires per unit time. Fire occurrence rates are usually given per year, so that the λs are usually very small. For the reference period of one year $t = 1$ and $\lambda < 0.1$, Equation C.8 can be simplified to $F(t) \approx \lambda$. An Exponential distributed variable T is usually denoted $T \sim \mathrm{Exp}(\lambda)$.

C.5. Multivariate normal distribution

The multi-variate normal distribution is a n-dimensional formulation of the normal distribution and is shown in detail in Section 5.2.2. For the sake of completeness, it is reproduced here. The probability density function reads

$$f_{\mathbf{X}}(\mathbf{x}, \mathbf{C_{XX}}) = \frac{1}{(2\pi)^{\frac{n}{2}}\sqrt{\det \mathbf{C_{XX}}}} \exp\left[-\frac{1}{2}(\mathbf{x}-\boldsymbol{\mu}_X)^T \mathbf{C_{XX}^{-1}}(\mathbf{x}-\boldsymbol{\mu}_X)\right]\,, \quad \mathbf{x} \in \mathbb{R}^n\,, \tag{C.9}$$

where $\boldsymbol{\mu}_{\mathbf{X}}$ denotes the mean vector and $\mathbf{C_{XX}}$ the covariance matrix. A closed-form distribution function does not exist so that the integrals have to be calculated numerically. This model is used for the weighting functions $h_{\mathbf{x}}$ to avoid the repeated complex evaluation of the Nataf-model. The notation of a n-dimensional multivariate normal variable $\mathbf{X}$ is usually $\mathbf{X} \sim \mathcal{N}_n(\boldsymbol{\mu}_{\mathbf{X}}, \mathbf{C_{XX}})$. Figure C.1 exemplary shows the probability density "hill" for $\mathbf{X} \sim \mathcal{N}_2([0,0]^T, [1, 0.8; 0.8, 1])$.

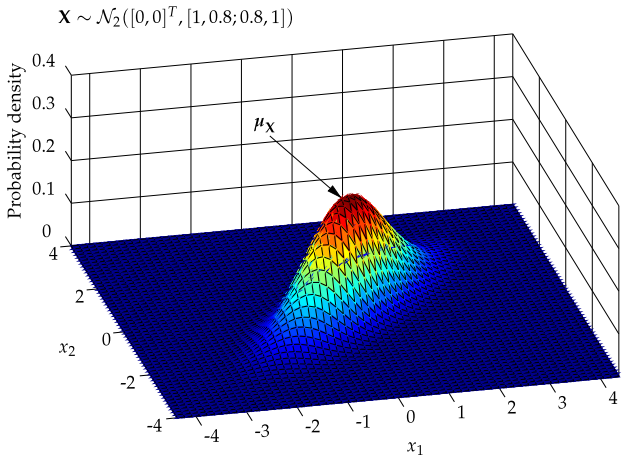

Figure C.1.: Probability density plot of a two-dimensional multivariate normal model.

Appendix D

MATLAB Toolbox for automated analysis

In order to fully automate the complex work-flow processes from Chapter 6 in order to perform the reliability analysis in Chapter 7, a toolbox was programmed in Matlab 7.8.0 (2009). In the following sections, the capabilities and selected solutions will be shown for the various packages.

D.1. File and I/O handling

The file and I/O handling for FDS and FDS+evac is a very specific package capable of

- generating the input files based on the input data sets for the DoE data for both, FDS and FDS+evac,
- generate batch files to run the simulations parallelized on the high performance/high throughput machines, and
- analyze the outputs of the simulations for threshold values in order to be able to evaluate the limit state.

The variable replacement within the input files is done by using "regular expressions". The pattern to be recognized is `#var_name#`, where `var_name` can be the name of the parameter to be replaced, while the #s are important for the proper recognition of the regular expressions.

D.2. Sensitivity analysis

The sensitivity analysis package is used for the preceding sensitivity analysis according to Section 6.1 and

- analyzes the correlation between the various input parameters and the results,
- rank-transforms the data,
- tests for significance of linear and rank correlation, and
- evaluates the global contribution to prediction accuracy by using stepwise regression.

D.3. Surrogate construction

The surrogate construction uses the responses of the support points to interpolate the limit state. In detail, the package

- transforms the inputs to normalize the input parameter dimensions,
- converts the predictors to the design matrix,
- evaluates for the Eucledian distance between the wanted point $\mathbf{x}$ and the support points $\mathbf{x}_{m_i}$,
- weights the distances according to the weighting function from Annex B to generate the weighting matrix $\mathbf{W}(\mathbf{x})$, and
- returns the surrogate model.

D.4. Reliability analysis

The reliability package was used for the evaluation of the failure probabilities and the sensitivities using Adaptive Importance Sampling. This package takes care of

- evaluation of the limit state function,
- generation of random number using either the Mersenne Twister, Latin-Hypercube sampling or the pseudo-random Sobol or Halton sequences for low discrepancy numerical integration,
- generation of the design of experiments for the primary scan and/or sensitivity analysis,
- generation of the appropriate stochastic model from the random numbers using the inverse transform methods,

- introducing either preset or adapted correlations into the stochastic model by using the Nataf transformation,
- computation of the likelihood ratio $\zeta_{\mathbf{X}}(\mathbf{u})$,
- adaptation of the wighting functions $h_{\mathbf{X}}(\mathbf{x})$ for every iteration, and
- computation of the failure probabilities and sensitivities.

D.5. Interaction

The aforementioned packages interact as shown in Figure D.1 to evaluate the reliability fully automated. The user needs to provide the stochastic models for the input parameter and FDS and FDS+evac input files prepared as stated above.

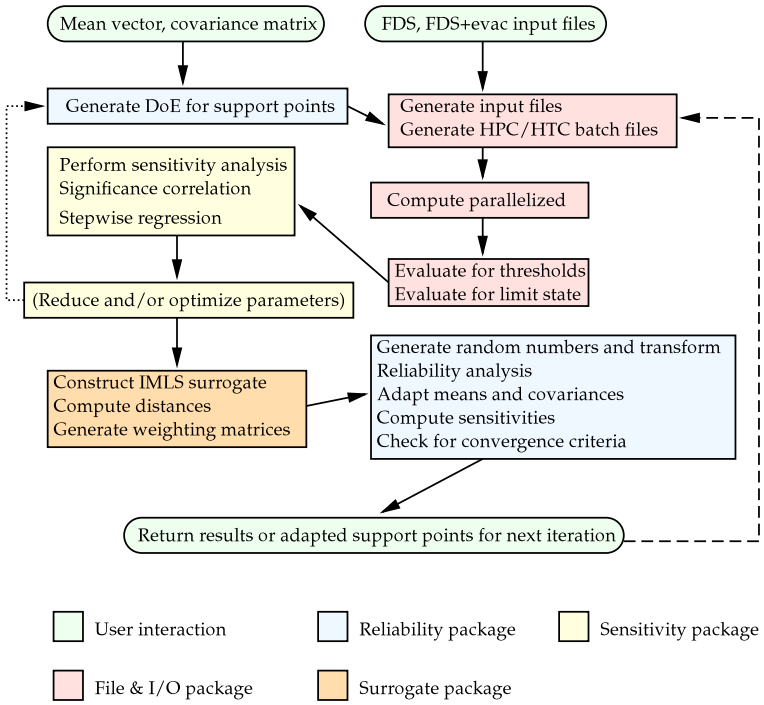

Figure D.1.: Interaction of the toolboxes during a scenario realiability analysis.

VERZEICHNIS DER BISHER IN DER SCHRIFTENREIHE DES IBMB ERSCHIENENEN HEFTE (ISSN 1439-3875)

In der Schriftenreihe "Institut für Baustoffe, Massivbau und Brandschutz der Technischen Universität Braunschweig - ISSN 0178-5796 (Heft 1 bis 16 als "Institut für Baustoffkunde und Stahlbetonbau der Technischen Hochschule Braunschweig", Heft 17 bis 39 als "Institut für Baustoffkunde und Stahlbetonbau der Technischen Universität Braunschweig") sind bisher die nachfolgend aufgeführten Hefte erschienen.

Sie können bezogen werden von:

Institut für Baustoffe,
Massivbau und Brandschutz
der Technischen Universität Braunschweig
Bibliothek
Beethovenstraße 52
38106 Braunschweig

Tel. (05 31) 3 91-54 54
Fax (05 31) 3 91-5900
E-Mail o.dienelt@tu-bs.de

oder über jede Buchhandlung.

Kosten:
Je nach Umfang zwischen € 7 und € 30
(zuzüglich Versandkosten)

Das aktuelle Verzeichnis unter:
www.ibmb.tu-bs.de (→ Bibliothek)

Vergriffene Hefte können als Kopien gegen Erstattung der Kopierkosten bezogen werden.

Heft 1:
Deters, R.: Über das Verdunstungsverhalten und den Nachweis öliger Holzschutzmittel. Institut für Baustoffkunde und Stahlbetonbau der Technischen Hochschule Braunschweig, 1962; Zugl.: Dissertation, Technische Hochschule Braunschweig, 1962

Heft 2:
Kordina, K.: Das Verhalten von Stahlbeton- und Spannbetonbauteilen unter Feuerangriff. Institut für Baustoffkunde und Stahlbetonbau der Technischen Hochschule Braunschweig, 1963; Sonderdruck aus: Beton 13(1962), S. 11-18, 81-84

Heft 3:
Eibl, J.: Zur Stabilitätsfrage des Zweigelenkbogens mit biegeweichem Zugband und schlaffen Hängestangen. Institut für Baustoffkunde und Stahlbetonbau der Technischen Hochschule Braunschweig, 1963; Zugl.: Dissertation, Technische Hochschule Braunschweig, 1963

Heft 4:
Kordina, K.; Eibl, J.: Ein Verfahren zur Bestimmung des Vorspannverlustes infolge Schlupf in der Verankerung. Zur Frage der Temperaturbeanspruchung von kreiszylindrischen Stahlbetonsilos. Institut für Baustoffkunde und Stahlbetonbau der Technischen Hochschule Braunschweig, 1964; Sonderdruck aus: Beton- und Stahlbetonbau 58(1963), S. 265-268; 59(1964), S. 1-11

Heft 5:
Ertingshausen, H.: Über den Schalungsdruck von Frischbeton. Institut für Baustoffkunde und Stahlbetonbau der Technischen Hochschule Braunschweig, 1965; Zugl.: Dissertation, Technische Hochschule Hannover, 1965

Heft 6:
Waubke, N.V.: Transportphänomene in Betonporen. Institut für Baustoffkunde und Stahlbetonbau der Technischen Hochschule Braunschweig, 1966; Zugl.: Dissertation, Technische Hochschule Braunschweig, 1968

Heft 7:
Ehm, H.: Ein Beitrag zur rechnerischen Bemessung von brandbeanspruchten balkenartigen Stahlbetonbauteilen. Institut für Baustoffkunde und Stahlbetonbau der Technischen Hochschule Braunschweig, 1967; Zugl.: Dissertation, Technische Hochschule Braunschweig, 1967

Heft 8:
Steinert, J.: Möglichkeiten der Bestimmung der kritischen Last von Stab- und Flächentragwerken mit Hilfe ihrer Eigenfrequenz. Institut für Baustoffkunde und Stahlbetonbau der Technischen Hochschule Braunschweig, 1967; Zugl.: Dissertation, Technische Hochschule Braunschweig, 1967

Heft 9:
Lämmke, A.: Untersuchungen an dämmschichtbildenden Feuerschutzmitteln. Institut für Baustoffkunde und Stahlbetonbau der Technischen Hochschule Braunschweig, 1967; Zugl.: Dissertation, Technische Hochschule Braunschweig, 1967

Heft 10:
Rafla, K.: Beitrag zur Frage der Kippstabilität aufgehängter Träger. Institut für Baustoffkunde und Stahlbetonbau der Technischen Hochschule Braunschweig, 1968; Zugl.: Dissertation, Technische Hochschule Braunschweig, 1968

Heft 11:
Ivanyi, G.: Die Traglast von offenen, kreisförmigen Stahlbetonquerschnitten: Brazier-Effekt. Institut für Baustoffkunde und Stahlbetonbau der Technischen Hochschule Braunschweig, 1968; Zugl.: Dissertation, Technische Hochschule Braunschweig, 1968

Heft 12:
Meyer-Ottens, C.: Brandverhalten verschiedener Bauplatten aus Baustoffen der Klassen A und B. Institut für Baustoffkunde und Stahlbetonbau der Technischen Hochschule Braunschweig, 1969

Heft 13:
Fuchs, G.: Zum Tragverhalten von kreisförmigen Doppelsilos unter Berücksichtigung der Eigensteifigkeit des Füllgutes. Institut für Baustoffkunde und Stahlbetonbau der Technischen Hochschule Braunschweig, 1968; Zugl.: Dissertation, Technische Hochschule Braunschweig, 1968

Heft 14:
Meyer-Ottens, C.: Wände aus Holz und Holzwerkstoffen unter Feuerangriff. Institut für Baustoffkunde und Stahlbetonbau der Technischen Hochschule Braunschweig, 1970; Sonderdruck aus: Mitteilungen der Deutschen Gesellschaft für Holzforschung, H.56(1969)

Heft 15:
Lewandowski, R.: Beurteilung von Bauwerksfestigkeiten anhand von Betongütewürfeln und -bohrproben. Institut für Baustoffkunde und Stahlbetonbau der Technischen Hochschule Braunschweig, 1970; Zugl.: Dissertation, Technische Hochschule Braunschweig, 1970

Heft 16:
Neubauer, F.-J.: Untersuchungen zur Frage der Rissesicherung von leichten Trennwänden aus Gips-Wandbauplatten. Institut für Baustoffkunde und Stahlbetonbau der Technischen Hochschule Braunschweig, 1970; Zugl.: Dissertation, Technische Hochschule Braunschweig, 1969

Heft 17:
Meyer-Ottens, C.; Kordina, K.: Gutachten über das Brandverhalten von Bauteilen aus dampfgehärtetem Gasbeton: aufgestellt für den Fachverband Gasbetonindustrie. Institut für Baustoffkunde und Stahlbetonbau der Technischen Universität Braunschweig, 1970

Heft 17:
Meyer-Ottens, C.; Kordina, K.: Gutachten über das Brandverhalten von Bauteilen aus dampfgehärtetem Gasbeton. Erw. Neuaufl. Institut für Baustoffkunde und Stahlbetonbau der Technischen Universität Braunschweig, 1974

Heft 18:
Bödeker, W.: Die Stahlblech-Holz-Nagelverbindung und ihre Anwendung: Grundlagen und Bemessungsvorschläge. Braunschweig. Institut für Baustoffkunde und Stahlbetonbau der Technischen Universität Braunschweig, 1971; Zugl.: Dissertation, Technische Hochschule Braunschweig, 1971, ISBN 3-89288-057-3

Heft 19:
Meyer-Ottens, C.: Bauaufsichtliche Brandschutzvorschriften: Beispiele für ihre Erfüllung bei Wänden, Brandwänden und Dekken. Institut für Baustoffkunde und Stahlbetonbau der Technischen Universität Braunschweig, 1971

Heft 20:
Liermann, K.: Das Trag- und Verformungsverhalten von Stahlbetonbrückenpfeilern mit Rollenlagern. Institut für Baustoffkunde und Stahlbetonbau der Technischen Universität Braunschweig, 1972; Zugl.: Dissertation, Technische Universität Braunschweig, 1972, ISBN 3-89288-056-5

Heft 22:
Nürnberger, U.: Zur Frage des Spannungsrißkorrosionsverhaltens kohlenstoffarmer Betonstähle in Nitratlösungen unter Berücksichtigung praxisnaher Verhältnisse. Institut für Baustoffkunde und Stahlbetonbau der Technischen Universität Braunschweig, 1972; Zugl.: Dissertation, Technische Universität Braunschweig, 1972, ISBN 3-89288-054-9

Heft 23:
Meyer-Ottens, C.: Zur Frage der Abplatzungen an Betonbauteilen aus Normalbeton bei Brandbeanspruchung. Institut für Baustoffkunde und Stahlbetonbau der Technischen Unversität Braunschweig, 1972; Zugl.: Dissertation, Technische Universität Braunschweig, 1972

Heft 24:
El-Arousy, T.H.: Über die Steinkohlenflugasche und ihre Wirkung auf die Eigenschaften von Leichtbeton mit geschlossenem Gefüge im frischen und festen Zustand. Institut für Baustoffkunde und Stahlbetonbau der Technischen Universität Braunschweig, 1973; Zugl.: Dissertation, Technische Universität Braunschweig, 1973, ISBN 3-89288-053-0

Heft 25:
Rieche, G.: Mechanismen der Spannungskorrosion von Spannstählen im Hinblick auf ihr Verhalten in Spannbetonkonstruktionen. Institut für Baustoffkunde und Stahlbetonbau der Technischen Universität Braunschweig, 1973; Zugl.: Dissertation, Technische Universität Braunschweig, 1973, ISBN 3-89288-052-2

Heft 26:
Tennstedt, E.: Beitrag zur rechnerischen Ermittlung von Zwangschnittgrößen unter Berücksichtigung des wirklichen Verformungsverhaltens des Stahlbetons. Institut für Baustoffkunde und Stahlbetonbau der Technischen Universität Braunschweig, 1974; Zugl.: Dissertation, Technische Universität Braunschweig, 1974, ISBN 3-89288-051-4

Heft 27:
Schneider, U.: Zur Kinetik festigkeitsmindernder Reaktionen in Normalbetonen bei hohen Temperaturen. Institut für Baustoffkunde und Stahlbetonbau der Technischen Universität Braunschweig, 1973; Zugl.: Dissertation, Technische Universität Braunschweig, 1973

Heft 28:
Neisecke, J.: Ein dreiparametriges, komplexes Ultraschall-Prüfverfahren für die zerstörungsfreie Materialprüfung im Bauwesen. Institut für Baustoffkunde und Stahlbetonbau der Technischen Universität Braunschweig, 1974; Zugl.: Dissertation, Technische Universität Braunschweig, 1974, ISBN 3-89288-050-6

Heft 29:
Kordina, K.; Maack, P.; Hjorth, O.: Traglastermittlung an Stahlbeton-Druckgliedern. Schlußbericht (AIF-Nr. 956). Institut für Baustoffkunde und Stahlbetonbau der Technischen Universität Braunschweig, 1974, ISBN 3-89288-048-4

Heft 30:
Eibl, J.; Ivanyi, G.: Berücksichtigung der Torsionssteifigkeit von Randbalken bei Stahlbetondecken. Schlußbericht, Institut für Baustoffkunde und Stahlbetonbau der Technischen Universität Braunschweig, 1974

Heft 31:
Kordina, K.; Janko, B.: Stabilitätsnachweise von Rahmensystemen im Stahlbetonbau. Schlußbericht (AIF-Nr. 1388), Institut für Baustoffkunde und Stahlbetonbau der Technischen Universität Braunschweig, 1974, ISBN 3-89288-049-2

Heft 32:
Hjorth, O.: Ein Beitrag zur Frage der Festigkeiten und des Verbundverhaltens von Stahl und Beton bei hohen Beanspruchungsgeschwindigkeiten. Institut für Baustoffkunde und Stahlbetonbau der Technischen Universität Braunschweig, 1976; Zugl.: Dissertation, Technische Universität Braunschweig, 1975

Heft 33:
Klingsch, W.: Traglastberechnung instationär thermisch belasteter schlanker Stahlbetondruckglieder mittels zwei- und dreidimensionaler Diskretisierung. Institut für Baustoffkunde und Stahlbetonbau der Technischen Universität Braunschweig, 1976; Zugl.: Dissertation, Technische Universität Braunschweig, 1976

Heft 34:
Djamous, F.: Thermische Zerstörung natürlicher Zuschlagstoffe im Beton. Institut für Baustoffkunde und Stahlbetonbau der Technischen Universität Braunschweig, 1977; Zugl.: Dissertation, Technische Universität Braunschweig, 1977

Heft 35:
Haksever, A.: Zur Frage des Trag- und Verformungsverhaltens ebener Stahlbetonrahmen im Brandfall. Braunschweig. Institut für Baustoffkunde und Stahlbetonbau der Technischen Universität Braunschweig, 1977; Zugl.: Dissertation, Technische Universität Braunschweig, 1977

Heft 36:
Storkebaum, K.-H.: Ein Beitrag zur Traglastermittlung von vierseitig gelagerten Stahlbetonwänden. Institut für Baustoffkunde und Stahlbetonbau der Technischen Universität Braunschweig, 1977; Zugl.: Dissertation, Technische Universität Braunschweig, 1977, ISBN 3-89288-045-X

Heft 37:
Bechtold, R.: Zur thermischen Beanspruchung von Außenstützen im Brandfall. Institut für Baustoffkunde und Stahlbetonbau der Technischen Universität Braunschweig, 1977; Zugl.: Dissertation, Technische Universität Braunschweig, 1977, ISBN 3-89288-046-8

Heft 38:
Steinert, J.: Bestimmung der Wasserdurchlässigkeit von Kiesbeton aus dem Wassereindringverhalten. Institut für Baustoffkunde und Stahlbetonbau der Technischen Universität Braunschweig, 1977; Unveränderter Nachdruck der Erstveröffentlichung Bad Honnef, Osang, 1977 (Zivilschutzforschung, Bd. 7)

Heft 39:
Weiß, R.: Ein haufwerkstheoretisches Modell der Restfestigkeit geschädigter Betone. Institut für Baustoffkunde und Stahlbetonbau der Technischen Universität Braunschweig, 1978; Zugl.: Dissertation, Technische Universität Braunschweig, 1978, ISBN 3-89288-047-6

Heft 40:
Alda, W.: Zum Schwingkriechen von Beton. Institut für Baustoffe, Massivbau und Brandschutz der Technischen Universität Braunschweig, 1978; Zugl.: Dissertation, Technische Universität Braunschweig, 1978, ISBN 3-89288-035-2

Heft 41:
Teutsch, M.: Trag- und Verformungsverhalten von Stahlbeton- und Spannbetonbalken mit rechteckigem Querschnitt unter kombinierter Beanspruchung aus Biegung, Querkraft und Torsion. Institut für Baustoffe, Massivbau und Brandschutz der Technischen Universität Braunschweig, 1979; Zugl.: Dissertation, Technische Universität Braunschweig, 1979, ISBN 3-89288-036-0

Heft 42:
Schneider, U.: Ein Beitrag zur Frage des Kriechens und der Relaxation von Beton unter hohen Temperaturen. Institut für Baustoffe, Massivbau und Brandschutz der Technischen Universität Braunschweig, 1979; Zugl.: Dissertation, Technische Universität Braunschweig, 1979

Heft 43:
Institut für Baustoffe, Massivbau und Brandschutz: Veröffentlichungen 1967 bis 1979. Institut für Baustoffe, Massivbau und Brandschutz der Technischen Universität Braunschweig, 1979, ISBN 3-89288-037-9

Heft 44:
Kordina, K.; Fröning, H.: Druckmessungen in Silozellen mit einer neu entwickelten Sonde. Abschlußbericht, Institut für Baustoffe, Massivbau und Brandschutz der Technischen Universität Braunschweig, 1979, ISBN 3-89288-038-7

Heft 45:
Henke, V.: Ein Beitrag zur Zuverlässigkeit frei gelagerter Stahlbetonstützen unter genormter Brandeinwirkung. Institut für Baustoffe, Massivbau und Brandschutz der Technischen Universität Braunschweig, 1980; Zugl.: Dissertation, Technische Universität Braunschweig, 1980

Heft 46:
Schneider, U.; Haksever, A.: Wärmebilanzrechnungen für Brandräume mit unterschiedlichen Randbedingungen (Teil 1). Institut für Baustoffe, Massivbau und Brandschutz der Technischen Universität Braunschweig, 1980

Heft 47:
Walter, R.: Partiell brandbeanspruchte Stahlbetondecken: Berechnung des inneren Zwanges mit einem Scheibenmodell. Institut für Baustoffe, Massivbau und Brandschutz der Technischen Universität Braunschweig, 1981; Zugl.: Dissertation, Technische Universität Braunschweig, 1981, ISBN 3-89288-039-5

Heft 48:
Svensvik, B.: Zum Verformungsverhalten gerissener Stahlbetonbalken unter Einschluß der Mitwirkung des Betons auf Zug in Abhängigkeit von Last und Zeit. Institut für Baustoffe, Massivbau und Brandschutz der Technischen Universität Braunschweig, 1981; Zugl.: Dissertation, Technische Universität Braunschweig, 1981, ISBN 3-89288-040-9

Heft 49:
Institut für Baustoffe, Massivbau und Brandschutz: Veröffentlichungen 1967 bis 1981. Institut für Baustoffe, Massivbau und Brandschutz der Technischen Universität Braunschweig, 1981, ISBN 3-89288-041-7

Heft 50:
Ojha, S.K.: Die Steifigkeit und das Verformungsverhalten von Stahlbeton- und Spannbetonbalken unter kombinierter Beanspruchung aus Torsion, Biegemoment, Querkraft und Axialkraft. Institut für Baustoffe, Massivbau und Brandschutz der Technischen Universität Braunschweig, 1982, ISBN 3-89288-042-5

Heft 51:
Henke, V.: Zusammenstellung und Anwendung Bayes'scher Verfahren bei der Stichprobenbeurteilung. Projekt D1 des SFB 148. Institut für Baustoffe, Massivbau und Brandschutz der Technischen Universität Braunschweig, 1982, ISBN 3-89288-043-3

Heft 52:
Haksever, A.: Stahlbetonstützen mit Rechteckquerschnitten bei natürlichen Bränden. Institut für Baustoffe, Massivbau und Brandschutz der Technischen Universität Braunschweig, 1982; Zugl.: Habil.-Schr., Technische Universität Istanbul, 1982, ISBN 3-89288-044-1

Heft 53:
Weber, V.: Untersuchung des Riß- und Verformungsverhaltens segmentärer Spannbetonbauteile. Braunschweig. Institut für Baustoffe, Massivbau und Brandschutz der Technischen Universität Braunschweig, 1982; Zugl.: Dissertation, Technische Universität Braunschweig, 1982, ISBN 3-89288-017-4

Heft 54:
Ranisch, E.-H.: Zur Tragfähigkeit von Verklebungen zwischen Baustahl und Beton: geklebte Bewehrung. Unveränderter Nachdruck der Ausgabe 1982. Institut für Baustoffe, Massivbau und Brandschutz der Technischen Universität Braunschweig, 1986; Zugl.: Dissertation, Technische Universität Braunschweig, 1982, ISBN 3-89288-010-7

Heft 55:
Wiedemann, G.: Zum Einfluß tiefer Temperaturen auf Festigkeit und Verformung von Beton. Institut für Baustoffe, Massivbau und Brandschutz der Technischen Universität Braunschweig, 1982; Zugl.: Dissertation, Technische Universität Braunschweig, 1982

Heft 56:
Timm, R.: Ein geometrisch und physikalisch nichtlineares Rechenmodell zur optimalen Biegebemessung ebener Stahlbetonrahmen. Institut für Baustoffe, Massivbau und Brandschutz der Technischen Universität Braunschweig, 1982; Zugl.: Dissertation, Technische Universität Braunschweig, 1982, ISBN 3-89288-018-2

Heft 57:
Diederichs, U.: Untersuchungen über den Verbund zwischen Stahl und Beton bei hohen Temperaturen. Institut für Baustoffe, Massivbau und Brandschutz der Technischen Universität Braunschweig, 1983; Zugl.: Dissertation, Technische Universität Braunschweig, 1983, ISBN 3-89288-019-0

Heft 58:
Schneider, U.: Wärmebilanzrechnungen in Verbindung mit Versuchen in Brand-räumen (Teil 2). Institut für Baustoffe, Massivbau und Brandschutz der Technischen Universität Braunschweig, 1983, ISBN 3-89288-020-4

Heft 59:
Dobbernack, R.: Wärmebilanzrechnungen in Brandräumen unter Berücksichtigung der Mehrzonenmodellbildung (Teil 3). Institut für Baustoffe, Massivbau und Brandschutz der Technischen Universität Braunschweig, 1983, ISBN 3-89288-021-2

Heft 60:
Hillger, W.: Verbesserungen und Erweiterungen von Ultraschallprüfverfahren zur zerstörungsfreien Fehlstellen- und Qualitätskontrolle von Betonbauteilen. Institut für Baustoffe, Massivbau und Brandschutz der Technischen Universität Braunschweig, 1983; Zugl.: Dissertation, Technische Universität Braunschweig, 1983, ISBN 3-89288-014-X

Heft 61:
Blume, F.: Zur Wirklichkeitsnähe der Lastannahmen in Silovorschriften für Zellen aus Stahlbeton und Spannbeton. Institut für Baustoffe, Massivbau und Brandschutz der Technischen Universität Braunschweig, 1984; Zugl.: Dissertation, Technische Universität Braunschweig, 1984, ISBN 3-89288-013-1

Heft 62:
Nölting, D.: Das Durchstanzen von Platten aus Stahlbeton : Tragverhalten, Berechnung, Bemessung. Institut für Baustoffe, Massivbau und Brandschutz der Technischen Universität Braunschweig, 1984; Zugl.: Dissertation, Technische Universität Braunschweig, 1984, ISBN 3-89288-012-3

Heft 63:
Wesche, J.: Brandverhalten von Stahlbetonplatten im baupraktischen Einbauzustand. Institut für Baustoffe, Massivbau und Brandschutz der Technischen Universität Braunschweig, 1985; Zugl.: Dissertation, Technische Universität Braunschweig, 1985, ISBN 3-89288-009-3

Heft 64:
Droese, S.: Untersuchungen zur Technologie des Gleitschalungsbaus. Institut für Baustoffe, Massivbau und Brandschutz der Technischen Universität Braunschweig, 1985; Zugl.: Dissertation, Technische Universität Braunschweig, 1985, ISBN 3-89288-000-X

Heft 65:
Institut für Baustoffe, Massivbau und Brandschutz: Forschungsarbeiten 1978 - 1983. Institut für Baustoffe, Massivbau und Brandschutz der Technischen Universität Braunschweig, 1984, ISBN 3-89288-001-8

Heft 66:
Hegger, J.: Einfluß der Verbundart auf die Grenztragfähigkeit von Spannbetonbalken. Institut für Baustoffe, Massivbau und Brandschutz der Technischen Universität Braunschweig, 1985; Zugl.: Dissertation, Technische Universität Braunschweig, 1985, ISBN 3-89288-002-6

Heft 67:
Kepp, B.: Zum Tragverhalten von Verankerungen für hochfeste Stäbe aus Glasfaserverbundwerkstoff als Bewehrung im Spannbetonbau. Institut für Baustoffe, Massivbau und Brandschutz der Technischen Universität Braunschweig, 1985; Zugl.: Dissertation, Technische Universität Braunschweig, 1985, ISBN 3-89288-003-4

Heft 68:
Sager, H.: Zum Einfluß hoher Temperaturen auf das Verbundverhalten von einbetonierten Bewehrungsstäben. Institut für Baustoffe, Massivbau und Brandschutz der Technischen Universität Braunschweig, 1985; Zugl.: Dissertation, Technische Universität Braunschweig, 1985, ISBN 3-89288-004-2

Heft 69:
Haß, R.: Zur praxisgerechten brandschutztechnischen Beurteilung von Stützen aus Stahl und Beton. Institut für Baustoffe, Massivbau und Brandschutz der Technischen Universität Braunschweig, 1986; Zugl.: Dissertation, Technische Universität Braunschweig, 1986, ISBN 3-89288-005-0

Heft 70:
Institut für Baustoffe, Massivbau und Brandschutz: 17. Forschungskolloquium des Deutschen Ausschusses für Stahlbeton, März 1986, Kurzfassungen der Beiträge. Institut für Baustoffe, Massivbau und Brandschutz der Technischen Universität Braunschweig, 1986, ISBN 3-89288-006-9

Heft 71:
Ehm, C.: Versuche zur Festigkeit und Verformung von Beton unter zweiaxialer Beanspruchung und hohen Temperaturen. Institut für Baustoffe, Massivbau und Brandschutz der Technischen Universität Braunschweig, 1986; Zugl.: Dissertation, Technische Universität Braunschweig, 1986, ISBN 3-89288-007-7

Heft 72:
Hartwich, K.: Zum Riß- und Verformungsverhalten von Stahlfaserverstärkten Stahlbetonstäben unter Längszug. Institut für Baustoffe, Massivbau und Brandschutz der Technischen Universität Braunschweig, 1986; Zugl.: Dissertation, Technische Universität Braunschweig, 1986, ISBN 3-89288-008-5

Heft 73:
Scheuermann, J.: Zum Einfluß tiefer Temperaturen auf Verbund und Rißbildung von Stahlbetonbauteilen. Institut für Baustoffe, Massivbau und Brandschutz der Technischen Universität Braunschweig, 1987; Zugl.: Dissertation, Technische Universität Braunschweig, 1987, ISBN 3-89288-011-5

Heft 74:
Hinrichsmeyer, K.: Strukturorientierte Analyse und Modellbeschreibung der thermischen Schädigung von Beton. Institut für Baustoffe, Massivbau und Brandschutz der Technischen Universität Braunschweig, 1987; Zugl.: Dissertation, Technische Universität Braunschweig, 1987, ISBN 3-89288-015-8

Heft 75:
Institut für Baustoffe, Massivbau und Brandschutz: Fachseminar Neue Bemessungsregeln durch Änderung der Stahlbeton- und Spannbetonvorschriften DIN 1045, DIN 4227, Juni 1986, Kurzfassungen der Beiträge. Institut für Baustoffe, Massivbau und Brandschutz der Technischen Universität Braun-schweig, 1986, ISBN 3-89288-022-0

Heft 76:
Budelmann, H.: Zum Einfluß erhöhter Temperaturen auf Festigkeit und Verformung von Beton mit unterschiedlichen Feuchtegehalten. Institut für Baustoffe, Massivbau und Brandschutz der Technischen Universität Braunschweig, 1987; Zugl.: Dissertation, Technische Universität Braunschweig, 1987, ISBN 3-89288-016-6

Heft 77:
Großmann, F.: Spannungen und bruchmechanische Vorgänge im Normelbeton unter Zugbeanspruchung. Institut für Baustoffe, Massivbau und Brandschutz der Technischen Universität Braunschweig, 1987; Zugl.: Dissertation, Technische Universität Braunschweig, 1987, ISBN 3-89288-023-9

Heft 78:
Rohling, A.: Zum Einfluß des Verbundkriechens auf die Rißbreitenentwicklung sowie auf die Mitwirkung des Betons zwischen den Rissen. Institut für Baustoffe, Massivbau und Brandschutz der Technischen Universität Braunschweig, 1987; Zugl.: Dissertation, Technische Universität Braunschweig, 1987, ISBN 3-89288-024-7

Heft 79:
Henning, W.: Zwangrißbildung und Bewehrung von Stahlbetonwänden auf steifen Unterbauten. Institut für Baustoffe, Massivbau und Brandschutz der Technischen Universität Braunschweig, 1987; Zugl.: Dissertation, Technische Universität Braunschweig, 1987, ISBN 3-89288-025-5

Heft 80:
Richter, E.: Zur Berechnung der Biegetragfähigkeit brandbeanspruchter Spann-betonbauteile unter Berücksichtigung geeigneter Vereinfachungen für die Materialgesetze. Institut für Baustoffe, Massivbau und Brandschutz der Technischen Universität Braunschweig, 1987; Zugl.: Dissertation, Technische Universität Braunschweig, 1987, ISBN 3-89288-026-3

Heft 81:
Kiel, M.: Nichtlineare Berechnung ebener Stahlbetonflächentragwerke unter Einschluß von Brandbeanspruchung. Institut für Baustoffe, Massivbau und Brandschutz der Technischen Universität Braunschweig, 1987; Zugl.: Dissertation, Technische Universität Braunschweig, 1987, ISBN 3-89288-027-1

Heft 82:
Konietzko, A.: Polymerspezifische Auswirkungen auf das Tragverhalten modifizierter zementgebundener Betone (PCC). Institut für Baustoffe, Massivbau und Brandschutz der Technischen Universität Braunschweig, 1988; Zugl.: Dissertation, Technische Universität Braunschweig, 1988, ISBN 3-89288-028-X

Heft 83:
Grzeschkowitz, R.: Zum Trag- und Verformungsverhalten schlanker Stahlbetonstützen unter besonderer Berücksichtigung der schiefen Biegung. Institut für Baustoffe, Massivbau und Brandschutz der Technischen Universität Braunschweig, 1988; Zugl.: Dissertation, Technische Universität Braunschweig, 1988, ISBN 3-89288-030-1

Heft 84:
Wiese, J.: Zum Trag- und Verformungsverhalten von Stahlbetonplatten unter partieller Brandbeanspruchung. Institut für Baustoffe, Massivbau und Brandschutz der Technischen Universität Braunschweig, 1988; Zugl.: Dissertation, Technische Universität Braunschweig, 1988, ISBN 3-89288-031-X

Heft 85:
Rudolph, K.: Traglastberechnung zweiachsig biegebeanspruchter Stahlbetonstützen unter Brandeinwirkung. Institut für Baustoffe, Massivbau und Brandschutz der Technischen Universität Braunschweig, 1988; Zugl.: Dissertation, Technische Universität Braunschweig, 1988, ISBN 3-89288-032-8

Heft 86:
Kordina, K.; Meyer-Ottens, C.; Noack, I.: Einfluß der Eigenbrandlast auf das Brandverhalten von Bauteilen aus brennbaren Baustoffen. Institut für Baustoffe, Massivbau und Brandschutz der Technischen Universität Braunschweig, 1989, in Vorbereitung, ISBN 3-89288-058-1

Heft 87:
Institut für Baustoffe, Massivbau und Brandschutz: Forschungsarbeiten 1984 - 1989. Institut für Baustoffe, Massivbau und Brandschutz der Technischen Universität Braunschweig, 1989, ISBN 3-89288-034-4

Heft 88:
Grossert, E.: Untersuchungen zum Tragverhalten von Massivbrücken mit zweizelligem Kastenquerschnitt. Institut für Baustoffe, Massivbau und Brandschutz der Technischen Universität Braunschweig, 1989; Zugl.: Dissertation, Technische Universität Braunschweig, 1989, ISBN 3-89288-059-X

Heft 89:
Falkner, H.; Teutsch, M. [Hrsg.]: Weiterbildungsseminar "Bauen in Europa", 15.-16. November 1990 in Braunschweig, Kurzreferate, ISBN 3-89288-063-8

Heft 90:
Falkner, H.; Teutsch, M.; Claußen, T.; Voß, K.-U.: Vorspannung im Hochbau. Institut für Baustoffe, Massivbau und Brandschutz der Technischen Universität Braunschweig, 1991, ISBN 3-89288-064-6

Heft 91:
Falkner, H.; Teutsch, M. [Hrsg.]: Fachtagung Spannbeton im Hoch- und Industriebau, Kurzreferate, 1991, ISBN 3-89288-065-4

Heft 92:
Heins, T.: Simulationsmodell zur sicherheitstechnischen Beurteilung der Rauchausbreitung in ausgedehnten Räumen. Institut für Baustoffe, Massivbau und Brandschutz der Technischen Universität Braunschweig, 1991; Zugl.: Dissertation, Technische Universität Braunschweig, ISBN 3-89288-066-2

Heft 93:
Hagen, E.: Zur Prognose des Gefährdungspotentials von Raumbränden. Institut für Baustoffe, Massivbau und Brandschutz der Technischen Universität Braunschweig, 1992; Zugl.: Dissertation, Technische Universität Braunschweig, 1991, ISBN 3-89288-072-7

Heft 94:
Falkner, H.; Teutsch, M. [Hrsg.]: Fachseminar "Instandsetzung und Ertüchtigung von Massivbauten", 14.-15. November 1991 in Braunschweig, Kurzreferate, ISBN 3-89288-068-9

Heft 95:
Qualitätssicherung im Bauwesen, VMPA-Tagung 1992, 25.-26.06.1992, Tagungsbericht, ISBN 3-89288-071-9

Heft 96:
Weiterbildungsseminar "Brandschutz im Industriebau", 30.09.1992 in Braunschweig, Kurzreferate, ISBN 3-89288-070-0

Heft 97:
Falkner, H.; Teutsch, M. [Hrsg.]: Fachseminar "Neue Technologien im Bauwesen", 12.-13.11.1992 in Braunschweig, Kurzreferate, ISBN 3-89288-073-5

Heft 98:
Gunkler, E.: Verstärkung biegebeanspruchter Mauerwerkswände durch bewehrte Ergänzungsschichten. Institut für Baustoffe, Massivbau und Brandschutz der Technischen Universität Braunschweig, 1993; Zugl.: Dissertation, Technische Universität Braunschweig, 1992, ISBN 3-89288-074-3

Heft 99:
Dorn, T.: Zur Berechnung des Tragverhaltens brandbeanspruchter Tragwerke in Verbundbauweise unter besonderer Berücksichtigung der Träger-Stützen-Anschlüsse. Institut für Baustoffe, Massivbau und Brandschutz der Technischen Universität Braunschweig, 1993; Zugl.: Dissertation, Technische Universität Braunschweig, 1992, ISBN 3-89288-075-1

Heft 100:
Falkner, H.; Teutsch, M. [Hrsg.]: Fachseminar "Stahlfaserbeton", 04.03.1993 in Braunschweig, Kurzreferate, ISBN 3-89288-076-X

Heft 101:
Falkner, H.; Teutsch, M.: Vergleichende Untersuchungen an unbewehrten und stahlfaserbewehrten Industriefußböden. Forschungsbericht, Institut für Baustoffe, Massivbau und Brandschutz der Technischen Universität Braunschweig, 1993, ISBN 3-89288-077-8

Heft 102:
Falkner, H.; Teutsch, M.: Comperative studies of plain and steel fiber reinforced concrete industrial ground slabs. Forschungsbericht, Institut für Baustoffe, Massivbau und Brandschutz der Technischen Universität Braunschweig, 1993, ISBN 3-89288-078-6

Heft 103:
Braunschweiger Brandschutz-Tage 1993: Fachseminar Brandschutz - Forschung und Praxis. 06.-07.10.1993, Kurzreferate, ISBN 3-89288-079-4

Heft 104:
Thienel, K.-C.: Festigkeit und Verformung von Beton bei hoher Temperatur und biaxialer Beanspruchung. Institut für Baustoffe, Massivbau und Brandschutz der Technischen Universität Braunschweig, 1993
Zugl.: Dissertation, Technische Universität Braunschweig, 1993, ISBN 3-89288-080-8

Heft 105:
Falkner, H.; Teutsch, M. [Hrsg.]: Braunschweiger Bauseminar 1993 "Dauerhafte Bauwerke aus Faserbeton", 11.-12.11.1993 in Braunschweig, Kurzreferate, ISBN 3-89288-081-6

Heft 106:
Neuentwicklungen im baulichen Brandschutz. Dr. Meyer-Ottens 60 Jahre; Fachseminar 18.03.1994 in Braunschweig, ISBN 3-89288-085-9

Heft 107:
Bunte, D.: Zum karbonatisierungsbedingten Verlust der Dauerhaftigkeit von Außenbauteilen aus Stahlbeton. Institut für Baustoffe, Massivbau und Brandschutz der Technischen Universität Braunschweig, 1994
Zugl.: Dissertation, Technische Universität Braunschweig, 1993, ISBN 3-89288-086-7

Heft 108:
Holzenkämpfer, P.: Ingenieurmodell des Verbundes geklebter Bewehrung für Betonbauteile. Institut für Baustoffe, Massivbau und Brandschutz der Technischen Universität Braunschweig, 1994
Zugl.: Dissertation, Technische Universität Braunschweig, 1994, ISBN 3-89288-087-5

Heft 109:
Forschungsarbeiten 1990 - 1994. Institut für Baustoffe, Massivbau und Brandschutz der Technischen Universität Braunschweig, 1994, ISBN 3-89288-088-3

Heft 110:
Falkner, H.; Teutsch, M.; Rohde, S.: Untersuchung der Schubtragfähigkeit und der Wasserundurchlässigkeit von Arbeitsfugen unter Verwendung von Stremaform-Abschalelementen.
Falkner, H.; Teutsch, M.; Claußen, T.: Schubtragfähigkeit des Vergußbetons zwischen Köcher-, Block oder Hülsenfundamenten und Stützenfuß bei unterschiedlich profilierten Betonoberflächen.
Institut für Baustoffe, Massivbau und Brandschutz der Technischen Universität Braunschweig, 1994, ISBN 3-89288-089-1

Heft 111:
Voß, K.-U.: Zum Trag- und Verformungsverhalten bei Schwellbeanspruchung. Institut für Baustoffe, Massivbau und Brandschutz der Technischen Universität Braunschweig, 1994
Zugl.: Dissertation, Technische Universität Braunschweig, 1993, ISBN 3-89288-090-5

Heft 112:
Weiterbildungsseminar Brandschutz bei Sonderbauten: 05./06.10.1994 in Braunschweig; Kurzreferate, 1994, ISBN 3-89288-092-1

Heft 113:
Falkner, H.; Teutsch, M. [Hrsg.]: Aus der Forschung in die Praxis: 10./11.11.1994; Braunschweiger Bauseminar 1994, ISBN 3-89288-091-3

Heft 114:
Warnecke, P.: Tragverhalten und Konsolidierung von historischem Natursteinmauerwerk, 1995
Zugl.: Dissertation, Technische Universität Braunschweig, 1995, ISBN 3-89288-094-8

Heft 115:
Braunschweiger Brandschutz-Tage 1995: 6. Fachseminar Brandschutz - Forschung und Praxis: 04.-05.10.1995, Kurzreferate, ISBN 3-89288-093-X

Heft 116:
Huang, Z.: Grenzbeanspruchung gebetteter Stahlfaserbetonplatten, 1995
Zugl.: Dissertation, Technische Universität Braunschweig, 1995, ISBN 3-89288-095-6

Heft 117:
Falkner, H.; Teutsch, M.; Huang, Z.: Untersuchung des Trag- und Verformungsverhaltens von Industriefußböden aus Stahlfaserbeton. Institut für Baustoffe, Massivbau und Brandschutz der Technischen Universität Braunschweig, 1995, ISBN 3-89288-096-4

Heft 118:
Kubat, B.: Durchstanzverhalten von vorgespannten, punktförmig gestützten Platten aus Stahlfaserbeton, 1995
Zugl.: Dissertation, Technische Universität Braunschweig, 1995, ISBN 3-89288-097-2

Heft 119:
Falkner, H.; Teutsch, M. [Hrsg.]: Dichte Bauwerke: 09./10.11.1995; Braunschweiger Bauseminar 1995, ISBN 3-89288-091-3

Heft 120:
Steinert, C.: Bestimmung der Wärmeübergangsbedingungen auf Bauteile im Brandfall, Abschlußbericht, 1995, ISBN 3-89288-099-9

Heft 121:
Schütte, J.; Teutsch, M.; Falkner, H.: Fugenlose Betonbodenplatten, Forschungsbericht, 1996, ISBN 3-89288-100-6

Heft 122:
Weiterbildungsseminar Brandschutz bei Sonderbauten: 24./25.09.1996 in Braunschweig, Kurzreferate, 1996, ISBN 3-89288-101-4

Heft 123:
Droese, S.; Riese, A.: Belastungsversu-che an zwei Durchlauf-Plattenstreifen aus Elementplatten mit Aufbeton aus Stahlfaserbeton, 1996, ISBN 3-89288-102-4

Heft 124:
Hankers, C.: Zum Verbundtragverhalten laschenverstärkter Betonbauteile unter nicht vorwiegend ruhender Beanspruchung, 1996
Zugl.: Dissertation, Technische Universität Braunschweig, 1996, ISBN 3-89288-103-0

Heft 125:
Schmidt-Döhl, F.: Ein Modell zur Berechnung von kombinierten chemischen Reaktions- und Transportprozessen und seine Anwendung auf die Korrosion mineralischer Baustoffe, 1996
Zugl.: Dissertation, Technische Universität Braunschweig, 1996, ISBN 3-89288-104-9

Heft 126:
Falkner, H.; Teutsch, M. [Hrsg.]: Ingenieurbauwerke mit neuen Konzepten: 14./15.11.1996, Braunschweiger Bauseminar 1996, ISBN 3-89288-105-7

Heft 127:
Forschung über Baudenkmalpflege - Arbeitsberichte: 1990 - 1993, 1996, ISBN 3-89288-106-5

Heft 128:
Festschrift zum 65. Geburtstag von Prof. Dr.-Ing. F. S. Rostásy: Baustoffe in Praxis, Lehre und Forschung, 1997, ISBN 3-89288-107-3

Heft 129:
Forschung über Baudenkmalpflege - Arbeitsberichte: 1994, 1997, ISBN 3-89288-108-1

Heft 130:
Forschung über Baudenkmalpflege - Arbeitsberichte: 1995, 1997,
ISBN 3-89288-109-X

Heft 131:
Falkner, H.; Teutsch, M.; Klinkert H.: Trag- und Verformungsverhalten dynamisch beanspruchter Fahrbahnen aus Beton- und Stahlfaserbeton, Forschungsbericht, 1997, ISBN 3-89288-110-3

Heft 132:
Schütte, J.: Einfluß der Lagerungsbedingungen auf Zwang in Betonbodenplatten, 1997
Zugl.: Dissertation, Technische Universität Braunschweig, 1997, ISBN 3-89288-111-1

Heft 133:
Braunschweiger Brandschutz-Tage 1997: 7. Fachseminar Brandschutz - Forschung und Praxis: 01.-02.10.1997, Kurzreferate,
ISBN 3-89288-112-X

Heft 134:
Ameler, J.: Betonverhalten bei hohen Temperaturen und triaxialer Beanspruchung - FE-Modell auf der Basis der Betonstruktur, 1997
Zugl.: Dissertation, Technische Universität Braunschweig, 1997, ISBN 3-89288-113-8

Heft 135:
Tagung Konsolidierung von historischem Natursteinmauerwerk: 06./07.11.1997 in Braunschweig, ISBN 3-89288-114-6

Heft 136:
Falkner, H.; Teutsch, M. [Hrsg.]: Innovatives Bauen: 13./14.11.1997, Braunschweiger Bauseminar 1997, ISBN 3-89288-115-4

Heft 137:
Forschung über Baudenkmalpflege - Arbeitsberichte: 1996 - 1997. 1998.
ISBN 3-89288-116-2

Heft 138:
Scheibe, M.: Vorhersage des Zeitstandverhaltens unidirektionaler Aramidfaserverbundstäbe in alkalischer Umgebung. 1998.
Zugl.: Braunschweig, TU, Diss., 1998.
ISBN 3-89288-117-0

Heft 139:
Weiterbildungsseminar Brandschutz bei Sonderbauten : 29./30.9.1998 in Braunschweig ; Kurzreferate. 1998.
ISBN 3-89288-118-9

Heft 140:
Gutsch, A.: Stoffeigenschaften jungen Betons - Versuche und Modelle. 1998. Zugl.: Braunschweig, TU, Diss.
ISBN 3-89288-119-7

Heft 141:
Falkner, H. ; Teutsch, M. [Hrsg.]
Beton auf neuen Wegen : 12.-13.11.1998 ; Braunschweiger Bauseminar 1998.
ISBN 3-89288-120-0

Heft 142:
Betonbau - Forschung, Entwicklung und Anwendung : Festschrift zum 60. Geburtstag von Univ.-Prof. Dr.-Ing Horst Falkner am 20.4.1999. 1999.
ISBN 3-89288-121-9

Heft 143:
Teutsch, M ; Klinkert, H.
Leistungsklassen von Stahlfaserbeton. 1999.
ISBN 3-89288-122-7

Heft 144:
Forschungsarbeiten 1995 - 1999. 1999.
ISBN 3-89288-123-5

Heft 145:
Braunschweiger Brandschutztage 1999: 8. Fachseminar Brandschutz - Forschung und Praxis ; 4.-5. Oktober 1999 in Braunschweig., Kurzreferate. 1999.
ISBN 3-89288-124-3

Heft 146:
Falkner, H. ; Teutsch, M. [Hrsg.]
Bauen im nächsten Jahrtausend : 11.11.-12.11.1999 ; Braunschweiger Bauseminar 1999.
ISBN 3-89288-125-1

Heft 147:
Weiterbildungsseminar Brandschutz bei Sonderbauten: 28./29.3.2000 in Braunschweig; Kurzreferate, 2000.
ISBN 3-89288-126-X

Heft 148:
Hariri, K.: Bruchmechanisches Verhalten jungen Betons - Laser-Speckle-Interferometrie und Modellierung der Rißprozeßzone. 2000.
Zugl.: Braunschweig, TU, Diss., 2000.
ISBN 3-89288-127-8

Heft 149:
Wigger, H.: Rissbildung in historischem Natursteinmauerwerk : Beobachtung, Versuche und Berechnungsmodelle. 2000.
Zugl.: Braunschweig, TU, Diss., 2000.
ISBN 3-89288-128-6

Heft 150:
Neubauer, U.: Verbundtragverhalten geklebter Lamellen aus Kohlenstoffaser – Verbundwerkstoff zur Verstärkung von Betonbauteilen. 2000
Zugl.: Braunschweig, TU, Diss., 2000.
ISBN 3-89288-129-4.

Heft 151:
Brandschutz in Chemikalienlagern. 2000.
ISBN 3-89288-130-8

Heft 152:
Falkner, H. ; Teutsch, M. [Hrsg.]
Trends und Entwicklungen im Bauwesen : 9.-10.11.2000 ; Braunschweiger Bauseminar 2000.
ISBN 3-89288-131-6

Heft 153:
Rostásy, F.S. ; Budelmann, H. [Hrsg.]
Rissbeherrschung massiger Betonbauteile : Bauwerk, Werkstoff, Simulation ; Braunschweig, 20.3.2001.
ISBN 3-89288-132-4

Heft 154:
Krauß, M. ; Hariri, K. ; Rostásy, F.S.
Hydratationsgrad, Ultraschall-Technik zur Beschreibung der Erhärtung, bruchmechanisches Verhalten jungen Betons : Berichte ; Forschungsprojekt der EU (Brite Euram BE96-3843), IPACS. 2001.
ISBN 3-89288-135-9.

Heft 155:
Gutsch, A. ; Rostásy, F.S.
Spannungs-Dehnungslinie, viskoelastisches Verhalten und autogenes Schwinden jungen Betons : Berichte ; Forschungsprojekt der EU (Brite Euram BE96-3843), IPACS. 2001.
ISBN 3-89288-136-7

Heft 156:
Rostásy, F.S. ; Krauß, M. ; Gutsch, A.
Spannungsberechnung und Risskriterien für jungen Beton – Methoden des iBMB : Bericht ; Forschungsprojekt der EU (Brite Euram BE96-3843), IPACS. 2001.
ISBN 3-89288-137-5

Heft 157:
Rostásy, F.S. ; Krauß, M. ; Gutsch, A.
Früher Zwang in massigen Sohlplatten : Bericht ; Forschungsprojekt der EU (Brite Euram BE96-3843), IPACS. 2001.
ISBN 4-89288-138-3

Heft 158:
Braunschweiger Brandschutztage 2001: 9. Fachseminar Brandschutz - Forschung und Praxis ; 1.-2. Oktober 2001 in Braunschweig., Kurzreferate. 2001.
ISBN 3-89288-139-1

Heft 159:
Falkner, H. ; Teutsch, M. [Hrsg.]
Bauen im Wandel der Zeit : 8.-9.11.2001 ; Braunschweiger Bauseminar 2001. 2001.
ISBN 3-89288-140-5.

Heft 160:
Beiträge zum 40. Forschungskolloquium des Deutschen Ausschusses für Stahlbeton : 11.-12.10.2001 in Braunschweig. 2001.
ISBN 3-89288-141-3

Heft 161:
Dora, B.: Hydraulisch erhärtende Baustoffe aus Betonbrechsand – Phasenveränderungen durch Temperaturbehandlung und Einsatzmöglichkeiten.
Zugl.: Braunschweig, TU, Diss., 2001.
ISBN 3-89288-142-1.

Heft 162:
RO 70 : 50 Jahre Forschung und 25 Dissertationen ; Prof. Dr.-Ing. Dr.-Ing. E. h. zum 70 Geburtstag gewidmet. 2002.
ISBN 3-89288-143-X.

Heft 163:
Praxisseminar Brandschutz bei Sonderbauten : 1. und 2. Oktober 2002 in Braunschweig ; Kurzreferate.
2002.
ISBN 3-89288-144-8

Heft 164:
Stahlfaserbeton : Ein unberechenbares Material? ; 14.-15. November - Braunschweiger Bauseminar 2002.
ISBN 3-89288-145-6

Heft 165:
Niemann, P.
Gebrauchsverhalten von Bodenplatten aus Beton unter Einwirkungen infolge Last und Zwang. Zugl.: Braunschweig, TU, Diss., 2002.
ISBN 3-89288-146-4

Heft 166:
Budelmann ; H. ; Falkner, H. [Hrsg.]
Bauen im Bestand : 25. März 2003.
ISBN 3-89288-147-2

H. 167:
Blume, G.W.: Ingenieurmodell zur brandschutztechnischen Bemessung von Bauteilen auf der Basis von experimentell ermittelten Verbrennungseffektivitäten. 2003.
Zugl.: Braunschweig, TU, Diss., 2002.
ISBN 3-89288-148-0

H. 168:
Braunschweiger Brandschutztage 2003: 10. Fachseminar Brandschutz - Forschung und Praxis ; 30.9. - 1.10.2003 in Braunschweig., Kurzreferate. 2003.
ISBN 3-89288-149-9

H. 169:
Falkner, H. ; Teutsch, M. [Hrsg.]
Bauforschung und –praxis in schwierigen Zeiten : 13. und 14. November ; Braunschweiger Bauseminar 2003.
ISBN 3-89288-150-2

H 170:
Hemmy, O.: Zum Gebrauchs- und Tragverhalten von Tunnelschalen aus Stahlfaserbeton und stahlfaserverstärktem Stahlbeton.
Zugl.: Braunschweig, TU, Diss., 2003.
ISBN 3-89288-151-0

H. 171:
Dehne, M.: Probabilistisches Sicherheitskonzept für die brandschutztechnische Bemessung. 2003.
Zugl.: Braunschweig, TU, Diss., 2003.
ISBN 3-89288-153-7

H. 172:
Paliga, K.: Entstehung und Vermeidung von Betonabplatzungen bei Tunnelbränden. 2003.
Zugl.: Braunschweig, TU, Diss., 2003.
ISBN 3-89288-154-5

Heft 173:
Festschrift zum 60 Geburtstag von Univ.-Prof. Dr.-Ing. Dietmar Hosser : Brandschutz und mehr...
2003.
ISBN 3-89288-152-9

Heft 174:
Timm, M.: Verbundwirkung des Betons im Bereich von STREMAFORM - Abschalelementen : Untersuchungsbericht ; Okt. 2000. 2004.
ISBN 3-89288-156-1

Heft 175:
Zehfuß, J.: Bemessung von Tragsystemen mehrgeschossiger Gebäude in Stahlbauweise für realistische Brandbeanspruchung.
Zugl.: Braunschweig, TU, Diss., 2004.
ISBN 3-89288-155-3

Heft 176:
Nause, P.: Berechnungsgrundlagen für das Brandverhalten von Druckgliedern aus hochfestem Beton. 2004.
Zugl.: Braunschweig, TU, Diss., 2004.
ISBN 3-89288-157-X
Nicht in der Schriftenreihe erschienen.

Heft 177:
Budelmann ; H. ; Falkner, H. [Hrsg.]
Bauen im Bestand : 23. März 2004.
ISBN 3-89288-158-8

H. 178:
Praxisseminar Brandschutz bei Sonderbauten : 29. – 30.9.2004 in Braunschweig ; Kurzreferate. 2004.
ISBN 3-89288-159-6

H. 179:
Krauß, M.: Probabilistischer Nachweis der Wirksamkeit von Maßnahmen gegen frühe Trennrisse in massigen Betonbauteilen. 2004.
Zugl.: Braunschweig, TU, Diss., 2004.
ISBN 3-89288-160-X.

H. 180:
Weiske, R.
Durchleitung hoher Stützlasten bei Stahlbetonflachdecken. 2004.
Zugl.: Braunschweig, TU, Diss., 2004.
ISBN 3-89288-161-8.

H. 181:
Falkner, H. ; Teutsch, M. [Hrsg.]
Qualität im Bauwesen : 11. und 12. Nov. ; Braunschweiger Bauseminar 2004.
ISBN 3-89288-162-6

H. 182:
Festschrift zum 60. Geburtstag von Univ.-Prof. Dr.-Ing. Klaus Peter Großkurth : Struktur und Anwendung der Baustoffe.
2005.
ISBN 3-89288-163-4

H. 183:
Budelmann, H. ; Laube, M. ; Hinrichs, W. [Hrsg.]
Bauen im Bestand : 23. Februar 2005.
ISBN 3-89288-164-2

H. 184:
Hinrichs, W.
Charakterisierung einer einheitlichen Messmethodik und Validierung ausgewählter Verfahren für die Bestimmung der Maschenweiten von Stahldrahtgeweben : Das Forschungsvorhaben wurde von der Stiftung Stahlanwendungsforschung im Stifterverband für die Deutsche Wissenschaft e.V. gefördert (Az: A 182/S24/10036/02. 2005).
ISBN 3-89288-166-9.

H. 185:
Braunschweiger Brandschutz-Tage ´05 : 11. Fachseminar Brandschutz – Forschung und Praxis, 28. und 29. Sept. 2005 in Braunschweig, Tagungsbericht.
ISBN 3-89288-167-7.

H. 186:
Will, J.: Entwicklung eines sauerstoffkalorimetrischen Verfahrens zur Bestimmung von Brandparametern bei unterschiedlich ventilierten Bränden. 2005.
Zugl.: Braunschweig, TU, Diss., 2005.
ISBN 3-89288-168-5.

H. 187:
Rigo, E.M.: Ein probabilistisches Konzept zur Beurteilung der Korrosion zementgebundener Baustoffe durch lösenden und treibenden Angriff. 2005.
Zugl.: Braunschweig, TU, Diss., 2005.
ISBN 3-89288-169-3.

H. 188:
Budelmann, H. ; Gutsch, A.-W. [Hrsg.]
Bauen im Bestand : Beton in der Abwassertechnik ; 6. Sept. 2005.
ISBN 3-89288-170-7.

H. 189:
Gerritzen, D.P.
Zur Frage der Nachnutzbarkeit verbundlos vorgespannter Stahlbetondecken nach Brandeinwirkung. 2005.
Zugl.: Braunschweig, TU, Diss., 2005.
ISBN 3-89288-171-5.

H. 190:
Falkner, H. ; Teutsch, M. [Hrsg.]
Bewe(ä)rter Betonbau : 10. und 11. November ; Braunschweiger Bauseminar 2005.
ISBN 3-89288-172-3

H. 191:
Kurzberichte aus der Forschung 2005.
2006.
ISBN 3-89288-173-1

H. 192:
Praxisseminar Brandschutz bei Sonderbauten : 26.-27. Sept. 2006 ; Kurzreferate.
ISBN-10: 3-89288-174-X
ISBN-13: 978-3-89288-174-2.

H. 193:
Sperling, D.
Eine Methode zur automatisierten Überwachung von Spannbetonfahrwegträgern. 2006.
Zugl.: Braunschweig, TU, Diss., 2006.
ISBN-10: 3-89288-175-8
ISBN-13: 978-3-89288-175-9.

H. 194:
Grunert, J.P.
Zum Tragverhalten von Spannbetonfertigteilbalken aus Stahlfaserbeton ohne Betonstahlbewehrung. 2006.
Zugl.: Braunschweig, TU, Diss., 2006.
ISBN-10: 3-89288-176-6
ISBN-13: 978-3-89288-176-6.

H. 195:
Budelmann, H. ; Gutsch, A.-W. [Hrsg.]
Bau Symposium Braunschweig (BSB 2007) : Stand und Entwicklung des Trockenbaus ; 8. März. 2007.
ISBN 978-3-89288-177-3.

H. 196:
Bruder, S.
Adaptive Modellierung der Dauerhaftigkeit im Zuge der Überwachung von Betonbauwerken. 2007.
Zugl.: Braunschweig, TU, Diss., 1996.
ISBN 978-3-89288-178-0.

H. 197:
Holst, A.
Korrosionsmonitoring und Bruchortung vorgespannter Zugglieder in Bauwerken. 2007.
Zugl.: Braunschweig, TU, Diss.
ISBN 978-3-89288-179-7.

H. 198:
Forell, B.
A Methodology to assess Species Yields of Compartment Fires by means of an extended Global Equivalence Ratio Concept. 2007.
Zugl.: Braunschweig, TU, Diss.
ISBN 978-3-89288-180-3.

H. 199:
Braunschweiger Brandschutz-Tage ´07 : 21. Fachseminar Brandschutz – Forschung und Praxis, 26. und 27. Sept. 2007 in Braunschweig, Tagungsband.
ISBN 978-3-89288-181-0.

H. 200:
Nothnagel, R.
Hydratations- und Strukturmodell für Zementstein. 2007.
Zugl.: Braunschweig, TU, Diss.
ISBN 978-3-89288-182-7

H. 201:
Riese, O.
Ein Brandausbreitungsmodell für Kabel. 2007.
Zugl.: Braunschweig, TU, Diss.
ISBN 978-3-89288-183-4

H. 202:
Braunschweiger Brandschutz-Tage ´08 : 22. Fachtagung ; Brandschutz bei Sonderbauten , 30.9. – 1.10.2008 – Tagungsband.
ISBN 978-3-89288-185-8

H. 203:
Klinzmann, C.
Methodik zur computergestützten, probabilistischen Bauwerksbewertung unter Einbeziehung von Bauwerksmonitoring. 2008.
Zugl.: Braunschweig, TU, Diss.
ISBN 978-3-89288-186-5.

H. 204:
Schnetgöke, R.
Zuverlässigkeitsorientierte Systembewertung von Massivbauwerken als Grundlage für die Bauwerksüberwachung. 2008.
Zugl.: Braunschweig, TU, Diss.
ISBN 978-3-89288-187-2.

H. 205:
Budelmann, H. ; Gutsch, A.-W. [Hrsg.]
Bau Symposium Braunschweig (BSB 2008): Konstruktiver Holzbau ; 4. November 2008.
ISBN 978-3-89288-188-9.

H. 206:
Kampmeier, B.
Risikogerechte Brandschutzlösungen für den mehrgeschossigen Holzbau. 2008.
Zugl.: Braunschweig, TU, Diss., 2008.
ISBN 978-3-89288-189-6.

H. 207:
Husemann, U.
Erhöhung der Verbundtragfähigkeit von nachträglich aufgeklebten Lamellen durch Bügelumschließungen.
Zugl.: Braunschweig, TU, Diss., 2009.
ISBN 978-3-89288-190-2

H. 208:
Braunschweiger Brandschutz-Tage ´09 : 23. Fachtagung Brandschutz – Forschung und Praxis, 29.9.2008 – 30.9.2009 ; Tagungsband.
ISBN 978-3-89288-191-9

H. 209:
Sperbeck, S.T.
Seismic Risk Assessment of Masonry Walls and Risk Reduction by Means of Prestressing. 2009.
Zugl.: Braunschweig, TU, Diss., 2009.
ISBN 978-3-89288-192-6

H. 210:
Braunschweiger Brandschutz-Tage 2010 : : 24. Fachtagung ; Brandschutz bei Sonderbauten , 21. und 22.9.2010 – Tagungsband.
ISBN 978-3-89288-194-0

H. 211:
Hohm, V.
Wärmetransportmodell für gekoppelte Prozesse in der Brandsimulation. 2010.
Zugl.: Braunschweig, TU, Diss.
ISBN 978-3-89288-195-7.

H. 212:
Kruse, D.
Entwicklung von Hochleistungsbrandschutzbeschichtungen zum Entzündungsschutz von Holz unter Vollbrandbedingungen. 2011.
Zugl.: Braunschweig, TU, Diss., 2010.
ISBN 978-3-89288-196-4.

H. 213:
Twelmeier, H.
Dauerhaftigkeitsprognose der Verfugung von gipshaltigem historischem Mauerwerk. 2011.
Zugl.: Braunschweig, TU, Diss., 2010.
ISBN 978-3-89288-197-1.

H. 214:
Braunschweiger Brandschutz-Tage 2011 : : 25. Fachtagung Brandschutz – Forschung und Praxis, 27. und 28.9.2011 – Tagungsband.
ISBN 978-3-89288-198-8

H. 215:
Hollmann, D.W.
Grundlagen und Ingenieurmodell für den Nachweis von Holzbauteilen mit Hochleistungsbrandschutzbeschichtungen. 2011.
Zugl.: Braunschweig, TU, Diss., 2011.
ISBN 978-3-89288-199-5

H. 216:
Rostásy, F.S.
Assessment of Mechanical Properties of Structural Materials for Cryogenic Application (June 1988). 2011.
ISBN 978-3-89288-200-8

H. 217:
Albrecht, C.
A risk-informed and performance-based life safety concept. 2012.
Zugl.: Braunschweig, TU, Diss., 2012.
ISBN 978-3-89288-202-2.

H. 218:
Braunschweiger Brandschutz-Tage 2012 : : 26. Fachtagung Brandschutz bei Sonderbauten, 19. und 20.9.2012 – Tagungsband.
ISBN 978-3-89288-203-9.